General Disclaimer

One or more of the Following Statements may affect this Document

- This document has been reproduced from the best copy furnished by the organizational source. It is being released in the interest of making available as much information as possible.

- This document may contain data, which exceeds the sheet parameters. It was furnished in this condition by the organizational source and is the best copy available.

- This document may contain tone-on-tone or color graphs, charts and/or pictures, which have been reproduced in black and white.

- This document is paginated as submitted by the original source.

- Portions of this document are not fully legible due to the historical nature of some of the material. However, it is the best reproduction available from the original submission.

Produced by the NASA Center for Aerospace Information (CASI)

GER - 14303

ADVANCED PASSIVE COMMUNICATION SATELLITE SYSTEMS COMPARISON STUDIES

April 1969

VOLUME III - APPENDICES

Contract No. NAS5-10295

N69-26435
(ACCESSION NUMBER) (THRU) 1
(PAGES) (CODE) 07
(NASA CR OR TMX OR AD NUMBER) (CATEGORY)
FACILITY FORM 602

Prepared by

GOODYEAR AEROSPACE CORPORATION

Akron, Ohio

for

NATIONAL AERONAUTICS AND SPACE ADMINISTRATION

GODDARD SPACE FLIGHT CENTER

Greenbelt, Maryland

CODE IDENT NO. 25500

GOODYEAR AEROSPACE
CORPORATION

AKRON 15, OHIO

ADVANCED PASSIVE COMMUNICATION

SATELLITE SYSTEMS COMPARISON STUDIES

Volume III- Appendices

April 1969

FINAL REPORT

Contract No. NAS 5-10295

Prepared for

NATIONAL AERONAUTICS AND SPACE ADMINISTRATION
GODDARD SPACE FLIGHT CENTER
Greenbelt, Maryland

E-ID-26(7-64)218-52
REF: ENGINEERING PROCEDURE S-017

FOREWORD

This report was prepared by prime contractor Goodyear Aerospace Corporation and subcontractor Stanford Research Institute under NASA Contract NAS-5-10295.

The work was administrated by Goddard Space Flight Center. Mr. W. Nyberg, Code 733, was the NASA Technical Officer throughout the program.

This report covers work that was started November 1966 and completed August 1968. J. Roth was the Goodyear Aerospace Project Engineer with B. R. Stack of Stanford Research Institute serving as Project Engineer on the subcontract.

The work reported hwerein is the result of a cooperative effort by a number of persons from Goodyear Aerospace Corporation and Stanford Research Institute. Volumes I and II were prepared by:

J. Roth	Goodyear Aerospace Corporation
R. D. Ray	Goodyear Aerospace Corporation
E. J. Roth	Goodyear Aerospace Corporation
B. R. Stack	Stanford Research Institute

The appendixes, (Volume III), were written by the following GAC and SRI personnel.

APPENDIX

A. Marketos, J.D., Raff, B.W.; Goodyear Aerospace Corporation; "Saddle Reflector Design and Preliminary Structural Analysis."

B. Roth, J., Ray, R.D., Telew, W.; Goodyear Aerospace Corporation; "Saddle Gain and Reflection Characteristics."

C. Schneider, L.,Nedelk, J.; Goodyear Aerospace Corporation; "Position Keeping, Attitude Control, and Fuel Requirements for Large Area-to-Mass Ratio Satellites."

D. Stack, B.R.; Stanford Research Institute; "Study of the Capabilities of Parabolic Antenna Systems with Large Equivalent Apertures."

E. McNaul, J.P.; Stanford Research Institute; "Alternate Antenna Designs."

F. Stack, B.R.; Stanford Research Institute, " An Approximate Expression for the Cost-Gain Relationship in Large Parabolic Antennas."

G. McNaul, J.P.; Stanford Research Institute, "Problems of Radome Use for Very Large Antennas."

H. Baum, Elmer, Clemens, Jules R.; Stanford Research Institute, "A Survey of Very High Power Microwave Transmitter."

I. Ray, R.D., Goodyear Aerospace Corporation; Stack, B.R., Stanford Research Institute; "Derivation of Expression for the System Gain of a Double-Hop Passive Satellite System."

J. McNaul, J.P.; Stanford Research Institute; "Potential Active Satellite Improvement Areas."

K. Stack, B.R.; Stanford Research Institute; "Criteria for Comparison of Performance of Active and Passive Communication Satellite Systems."

L. Stack, B.R.; Stanford Research Institute; "Space Segment Establishment and Maintenance Analysis."

M. Stack, B.R., Stanford Research Institute; "Determination of Channel Capacity of an Active Satellite."

N. Stack, B.R., Stanford Research Institute; "Approximate Cost of Large Ground Based Repeater Station."

APPENDIX A

SADDLE REFLECTOR DESIGN & PRELIMINARY STRUCTURAL ANALYSIS

SECTION I - INTRODUCTION

This appendix contains a design description of the saddle reflector, including possible packaging arrangements, deployment sequences and mechanisms and weight estimates. In addition, the results of a preliminary structural analysis are discussed and the surface deviations due to typical stimuli in orbit are considered.

The analyses reported herein were completed utilizing a reflector with an equivalent 400-foot diamter aperture, prior to the selection of the 325-foot reflector discussed in the body of this report.

It should be noted further, that the design analysis effects reported herein were not within the scope of the subject program, and were completed in connection with other efforts. However, the results pertaining to the saddle design are pertinent, warranting their inclusion in this report.

SECTION II - SADDLE DESIGN

A. SADDLE GEOMETRY

The saddle reflector planform shape can be seen in a photograph of the deployment model shown in Figure A-1. It is basically an octagon with the edges scalloped to represent the catenaries that carry the reflector membrane tension to the strong points at the tips of the structural members. Tips of the eight structural members are also visible in Figure A-1. For orientation purposes, the reflector surface shown in Figure A-1 will be termed the "reflector side" and the underside surface the "structure side."

With reference to the reflector side, the cross section of the concave and convex surfaces of the reflector are shown respectively in Figures A-2 and A-3. In Figure A-3, the reflector surface appears as the white object below the white backdrop. At the center of the reflector, the concave surface is evident from the black portion between the straight bottom of the backdrop and the reflector. The eight structural members extending from a hub can also be seen in the photograph along with the different heights at which the reflector is attached to the member tips to obtain the saddle contour. In Figure A-3, taken with the reflector rotated 90 degrees about the hub axis, the structure side of the reflector as the dark object against the white backdrop. The portion of the backdrop below the reflector, illustrates the convex surface cut (with respect to the reflector side) at the reflector centerline.

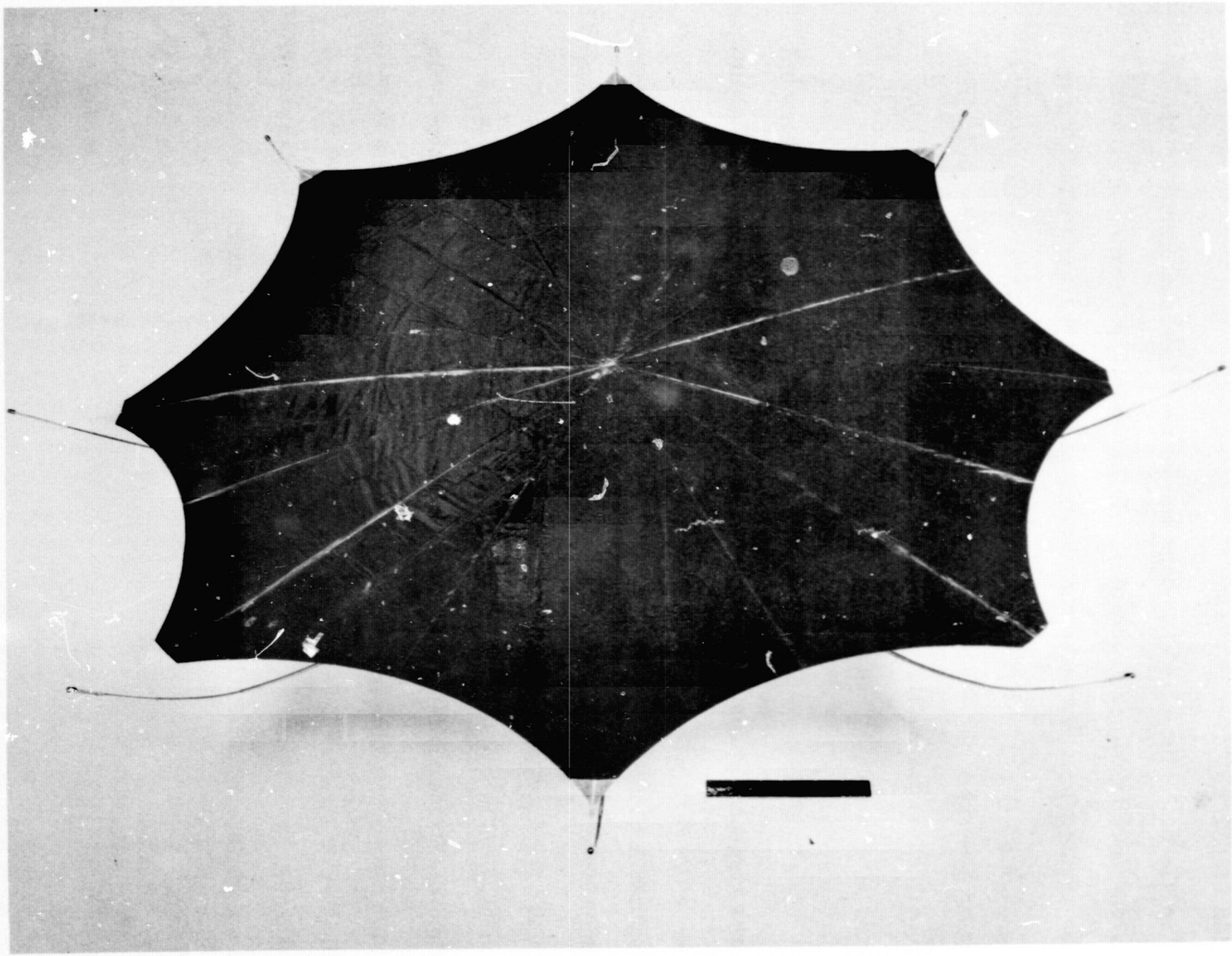


Figure A-1 - Saddle Geometry Model

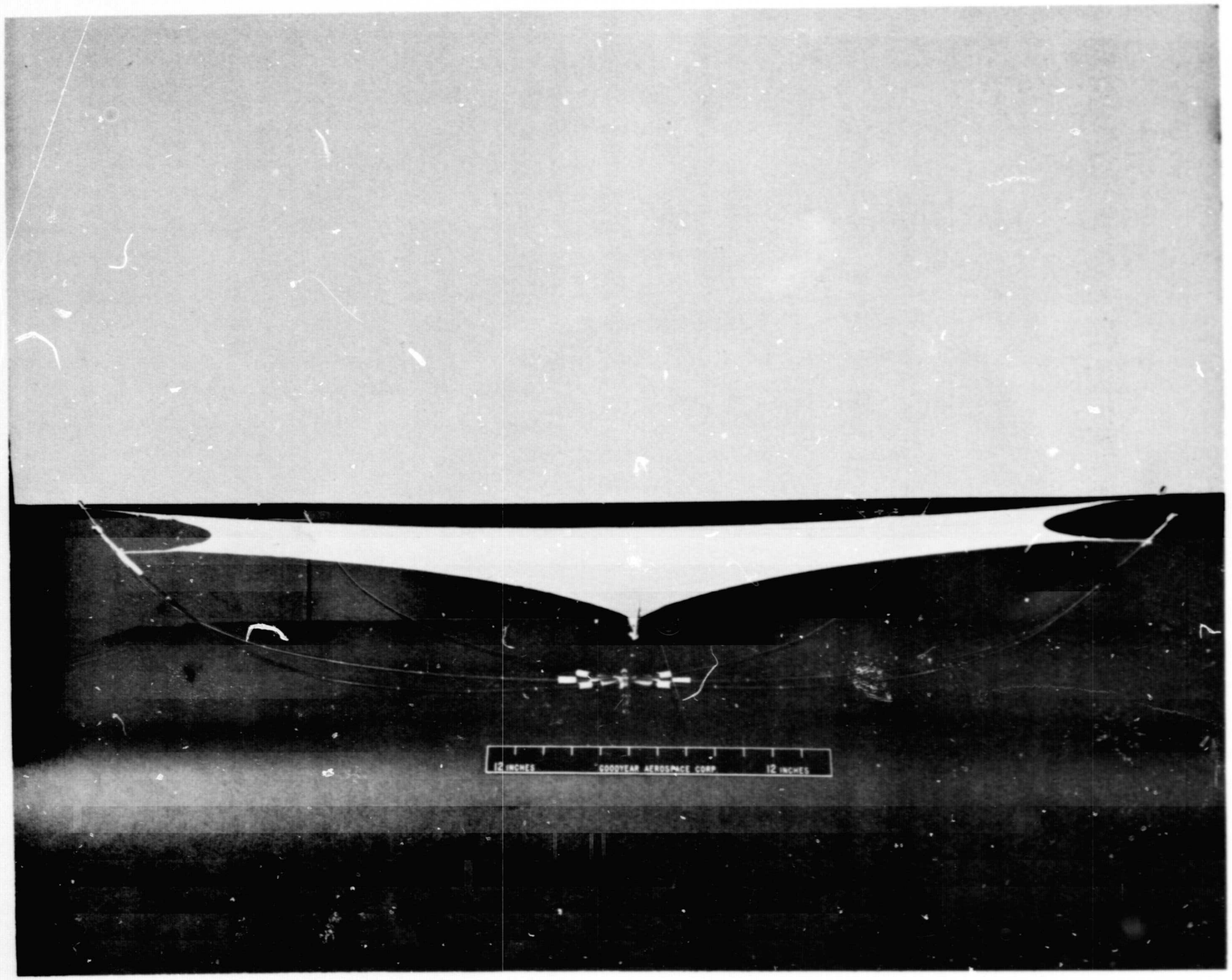


Figure A-2 - Saddle Convex Surface Cross-Section

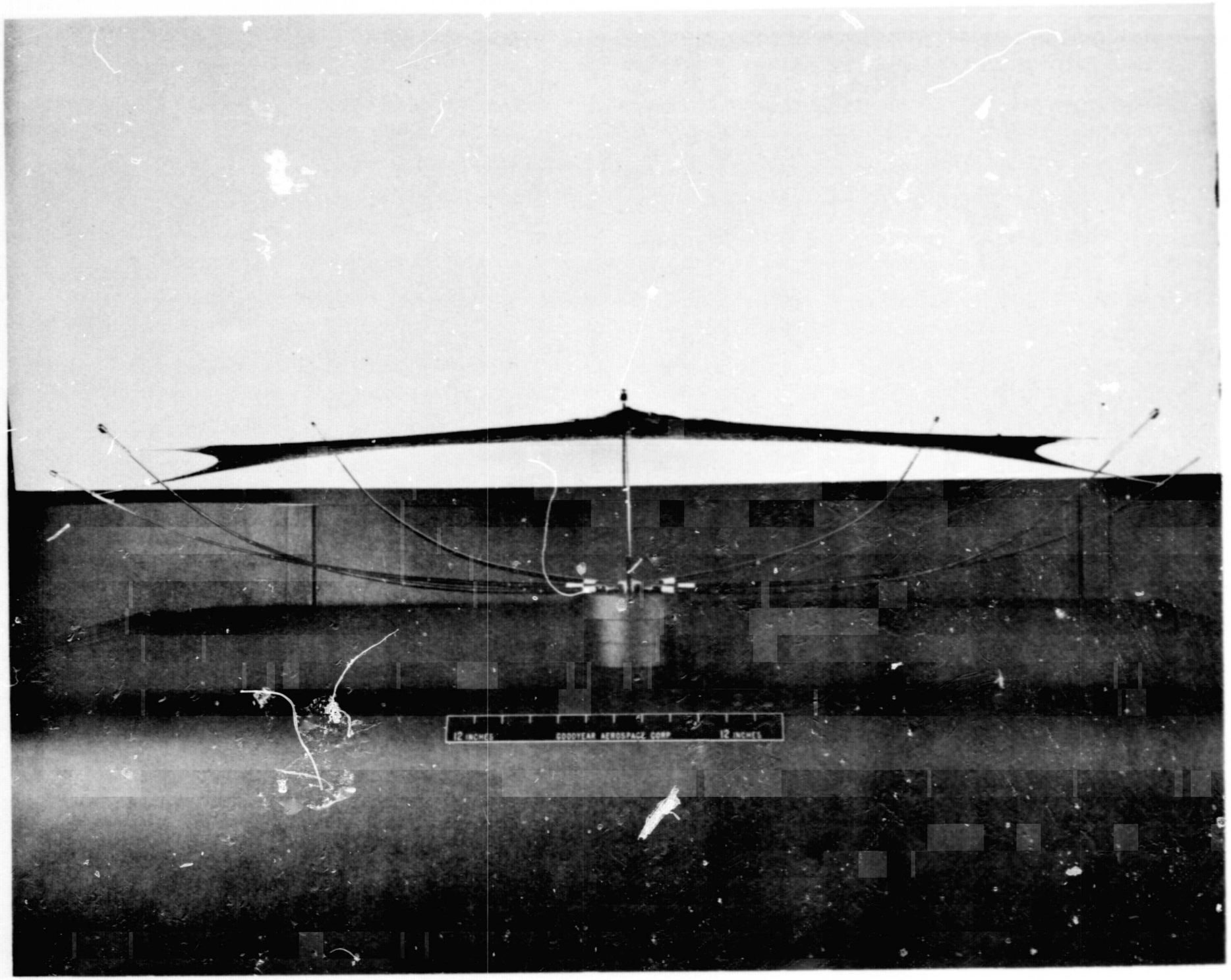


Figure A-3 - Saddle Concave Surface Cross-Section

For a baseline design, the geometry and dimensions shown in Figure A-4 were utilized. (The reflector surface area is equivalent to a 400 foot diameter disc.) As previously noted, the reflector has basically an octagonal planform with catenaries to distribute the load from the structural member attachment points. The reflector area lost from the catenary scallops and octagonal planform requires the maximum dimension across the reflector to be (464.8) (see Figure A-4). The reflector surface is tensioned by eight bowed structural members which are joined at a hub. While the tips of the structural members all have the same radial distance from the hub, the elevation of the member tips is controlled to produce the saddle shape of the reflector. As viewed from the bottom, the two member's tips lying in the plane, defined by the dotted-line octagon and the reflector center point, define the plane of the minimum concave radius of curvature, ρ, which was set at 6000 feet for the design. About an orthagonal axis, the tip members 9 feet above the dotted-line plane, along with the reflector center point, define the plane of the minimum convex radius of curvature. Forty-five degrees from the planes of minimum convex radius of curvature. Forty-five degrees from the planes of minimum convex and concave radii of curvature, the radii of curvature increases to infinity so that the remaining four tip members lie in the same horizontal plane as the reflector center point.

It should be noted that the radius of curvature may be increased without increasing structural loads or satellite weight.

A stress of 100 psi in a 1/2 mil aluminized Kapton reflector was used for the structural analysis. This corresponds to a tension load of 0.05 lbs/in. in the reflector. This tension load will reduce the height of cusps in the fold areas to less than 0.03 inches.

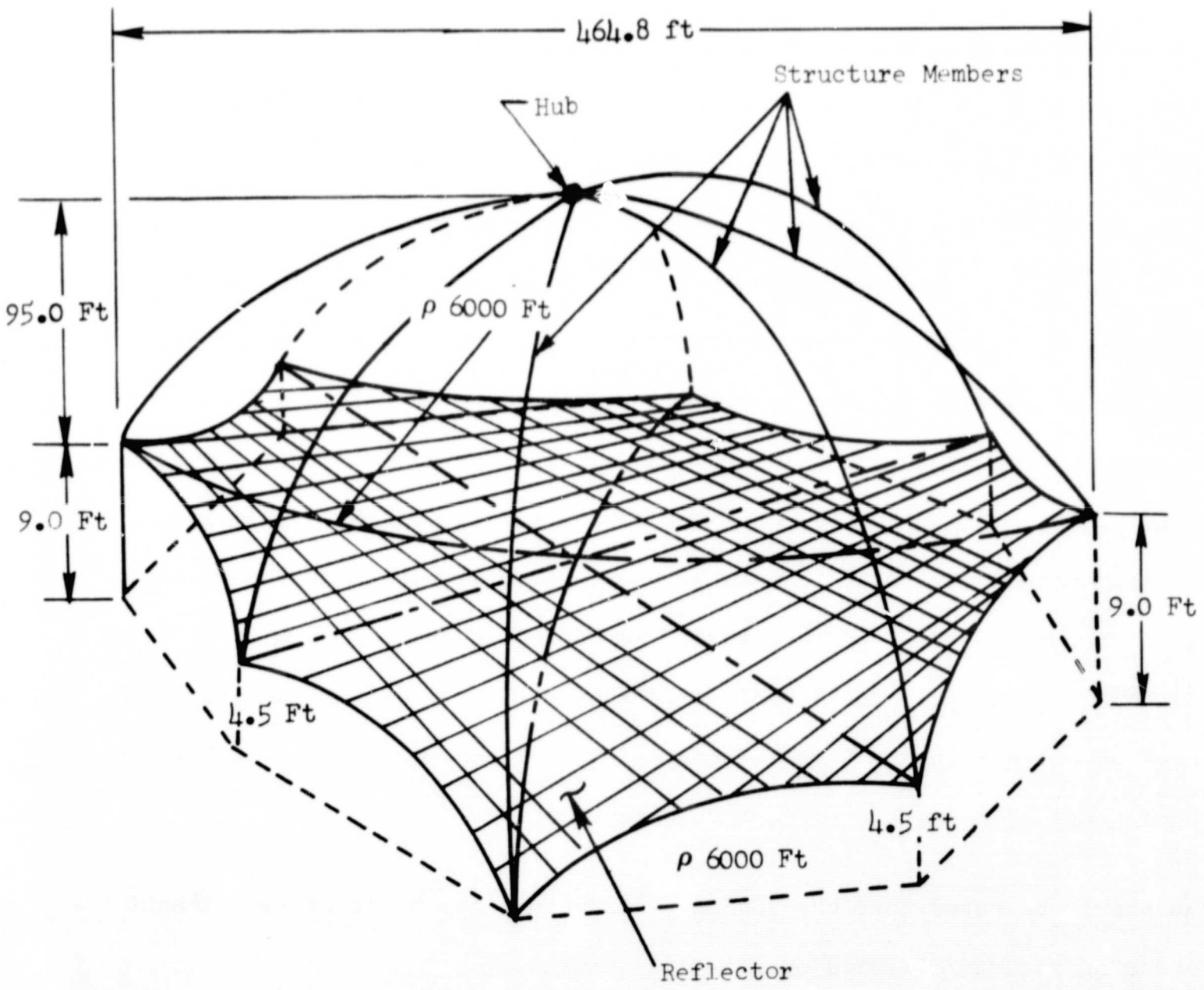
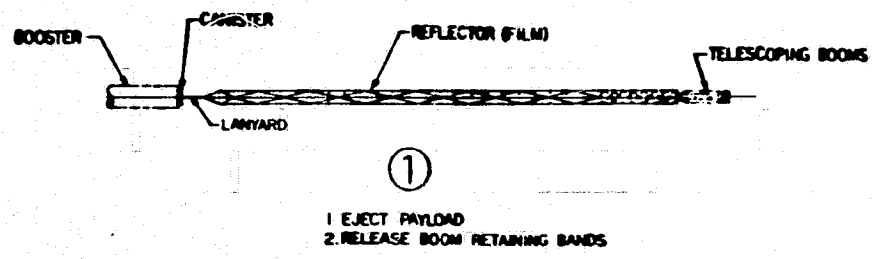


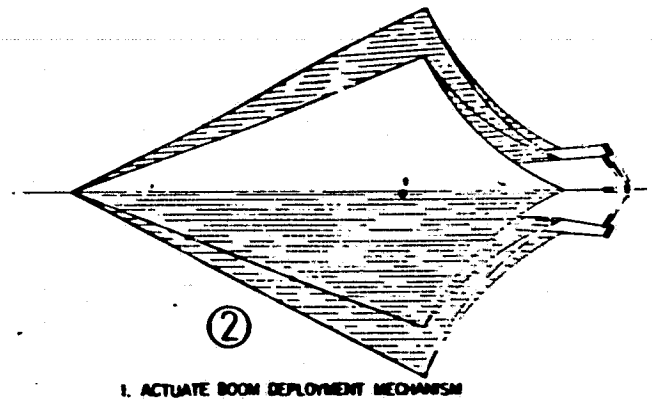
Figure A-4 - Saddle Reflector and Structure Geometry

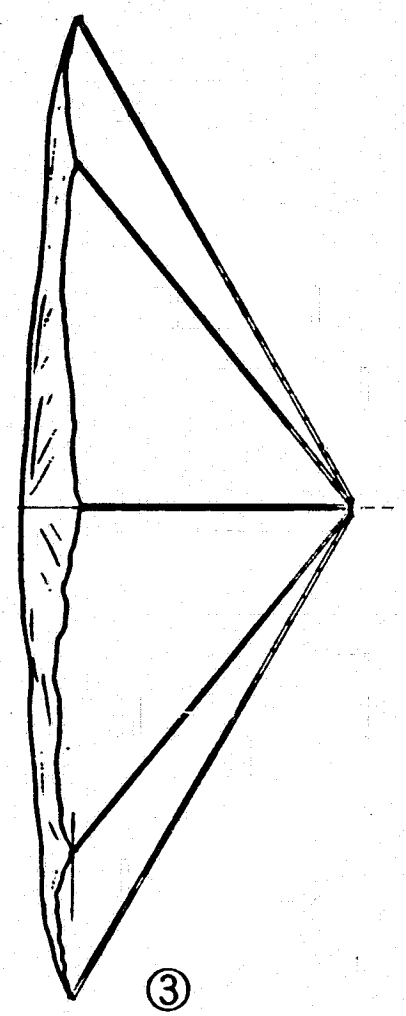
B. ARRANGEMENT AND DEPLOYMENT SEQUENCE

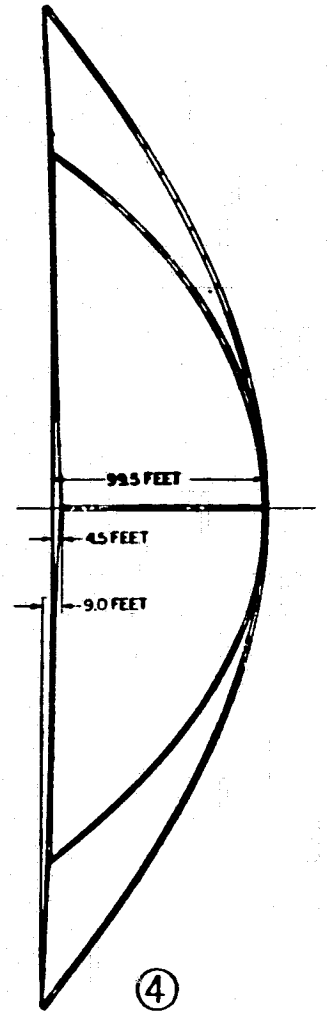
The deployed reflector side elevation and planform views are designated in Figure A-5. As can be seen in the side elevation view, the hub juncture of the structure is displaced 99.5 feet from the center of the reflector and the bowed structural members tension the reflective surface. The eight structural members, or booms, are made up of telescoping sections which are described later in Paragraph C. The reflector membrane consists of 1/2 mil Kapton film which is aluminized on both sides. Edge catenaries are used to carry the membrane tension load to the support points at the tips of the members. The catenary design has been optimized to provide minimum end load in the structural members. Attitude control thrusters and fuel supplies would be located at the tips of four of the structural members about orthogonal axes.

The deployment sequence of Figure A-5 can be more easily discussed by proceeding in reverse from the deployed to the packaged configuration. Starting with (4) the structural member deployment actuators (which are described in Paragraph C) are extended to rotate the bows to the position shown in (3), at which time the membrane is slack and the structural members are straight. The structural members are then telescoped to the position shown in (2) and the center of the membrane is at the apex point at the left in (2). The membrane is then accordion-folded along the phantom lines shown in (2). This results in a reflector semi-packaged shape,









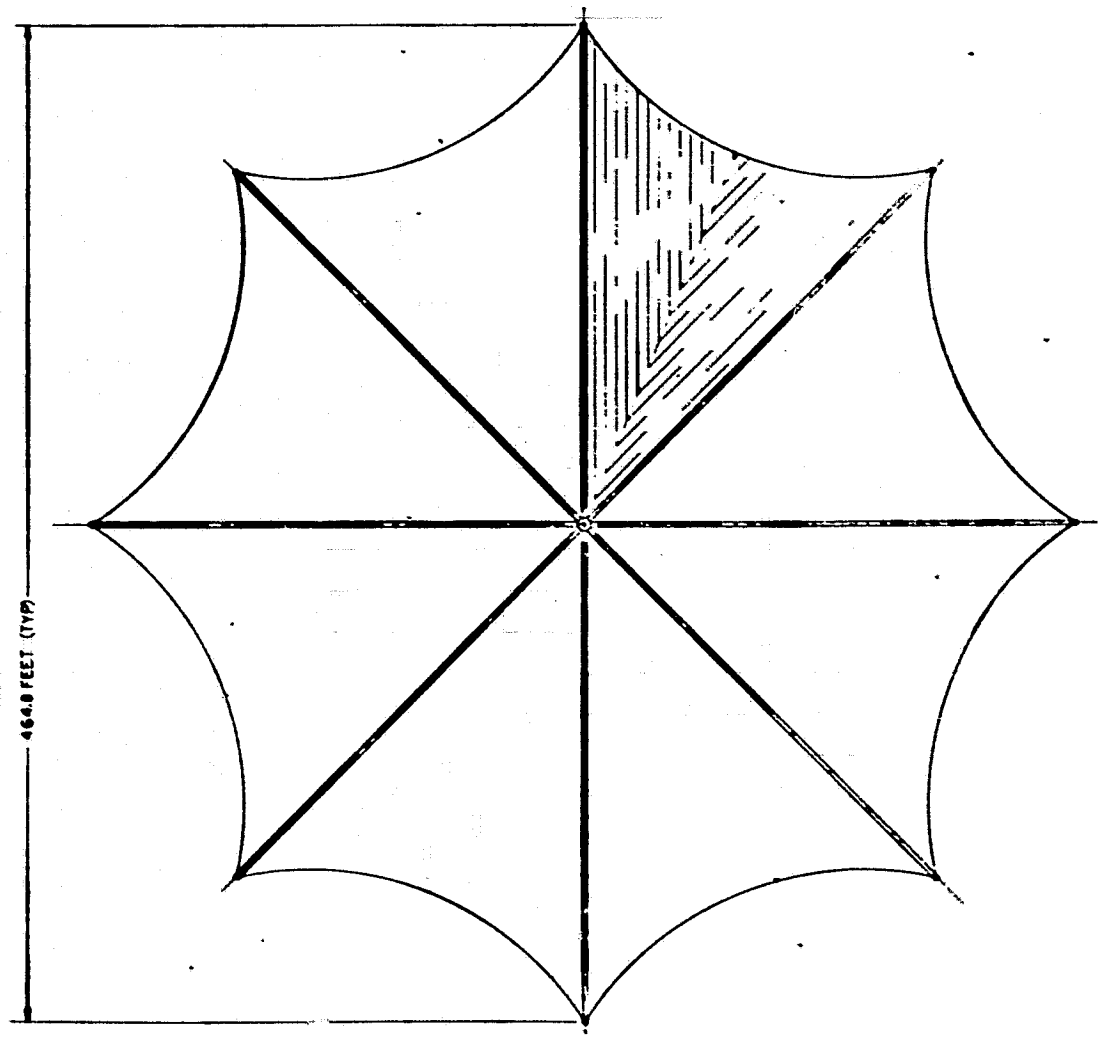


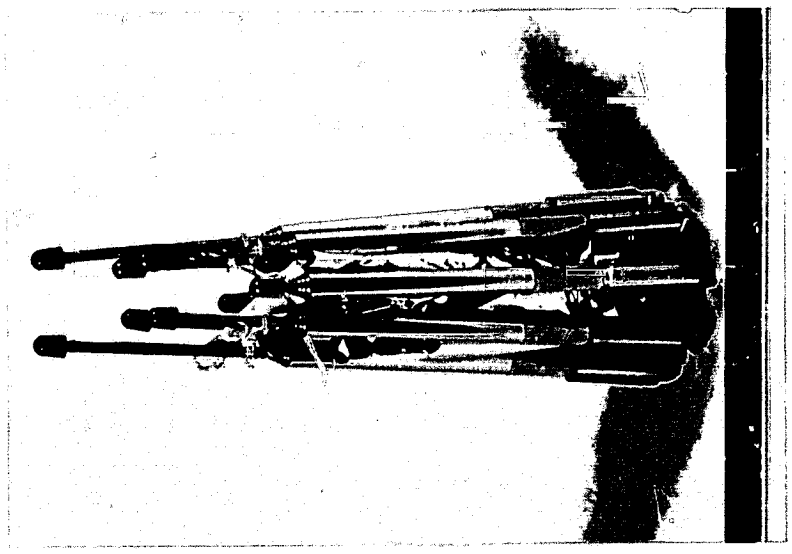
Figure A-5 - Saddle Reflector Arrangement and Deployment Sequence

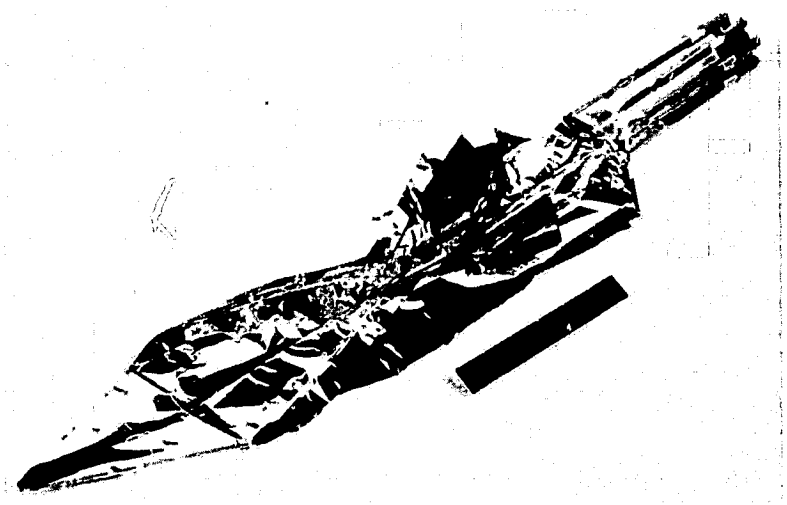
approximately 6-feet wide and half the reflector diameter in length shown in (1). The reflector is then accordion-folded at 6-foot intervals to provide the final package.

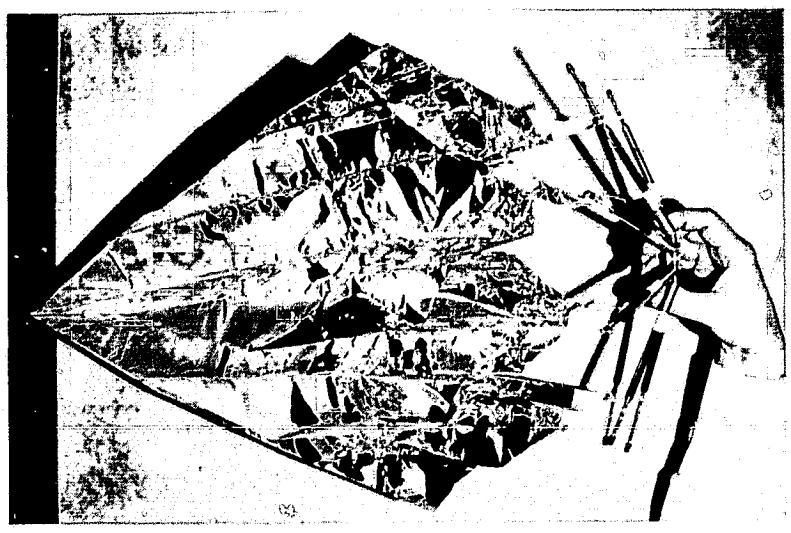
To more easily visualize the deployment sequence, a model was constructed which incorporated the mechanical aspects of the design. A series of photographs which depict the model in various stages of deployment are shown in Figure A-6. The final two photos in the sequence show the deployed reflector as viewed from the structure (back) side and from the reflector side.

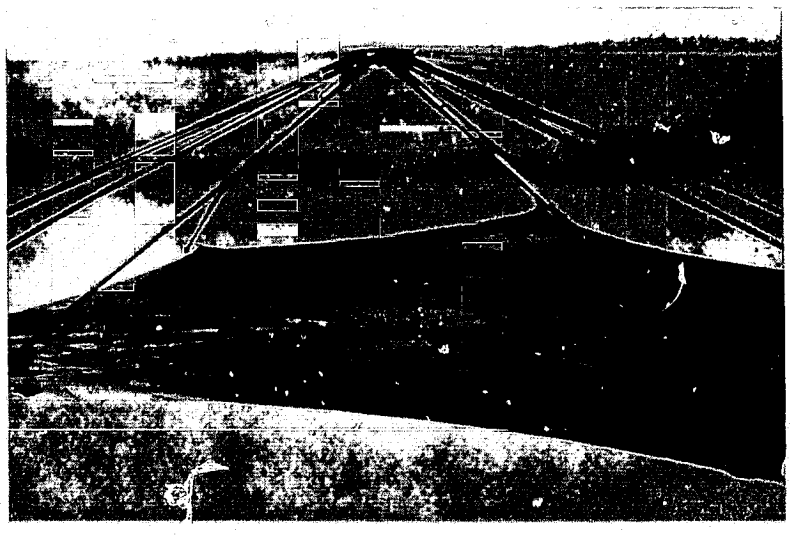
C. STRUCTURE DETAILS AND DEPLOYMENT MECHANISMS

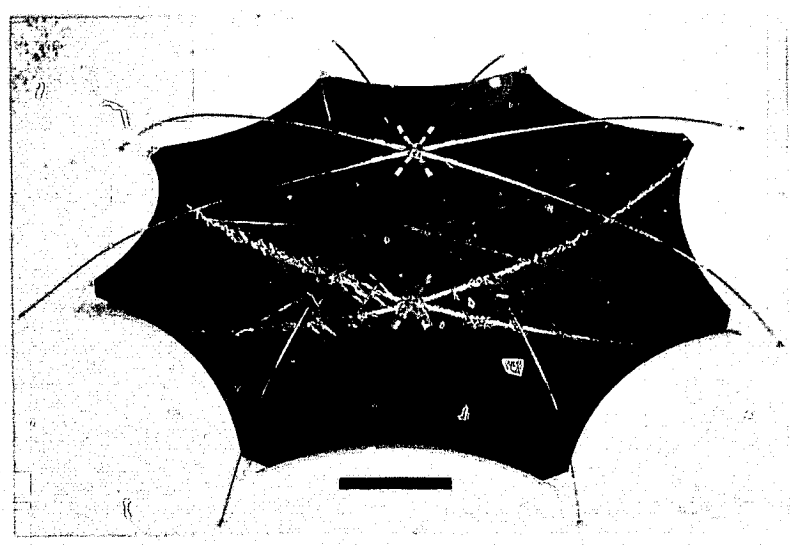
Two possible arrangements for the telescoping structural members are shown in the lower half of Figure A-7. The telescoping triangular truss results in a lighter weight structure with a total structure member weight of 2350 lbs. as compared to 3100 lbs. for the telescoping tube. Both structural member configurations have about 18 telescoping sections each 15-feet long. A unique feature of the telescoping truss is that a series of sliding trusses are incorporated to reduce the length of the individual truss bays from about 14 to 7 feet. This increases the column allowable of the four-inch diameter cap members and increases the effectiveness of the diagonal shear brace cables. Figure A-8 shows a model of the telescoping triangular truss in the retracted, partially deployed and deployed positions.











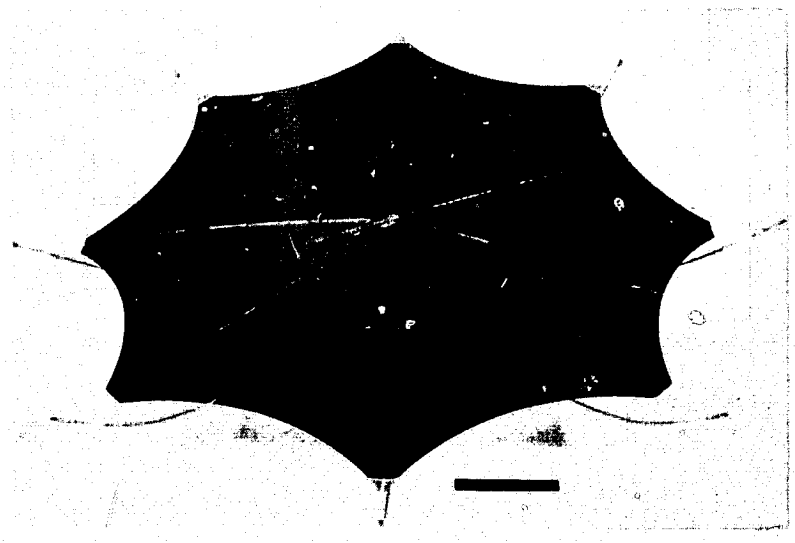
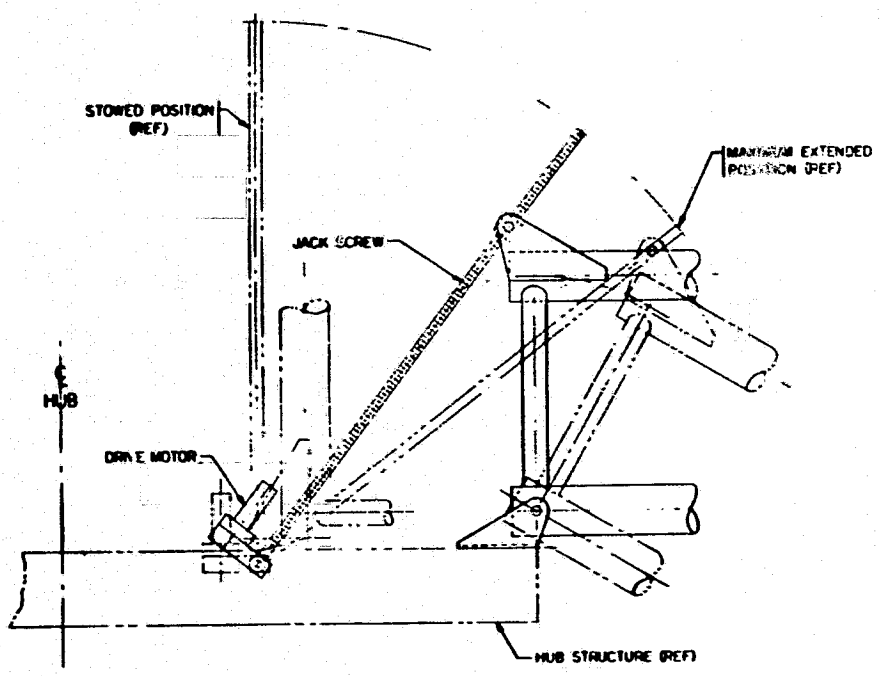
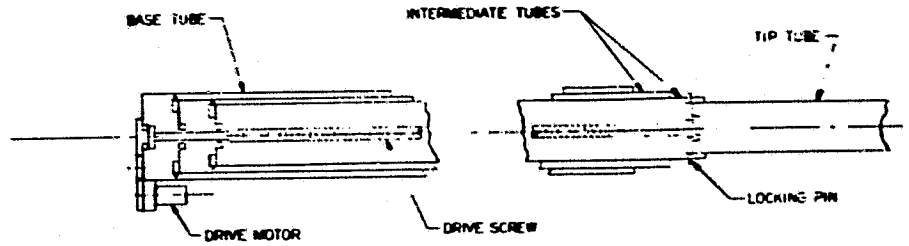


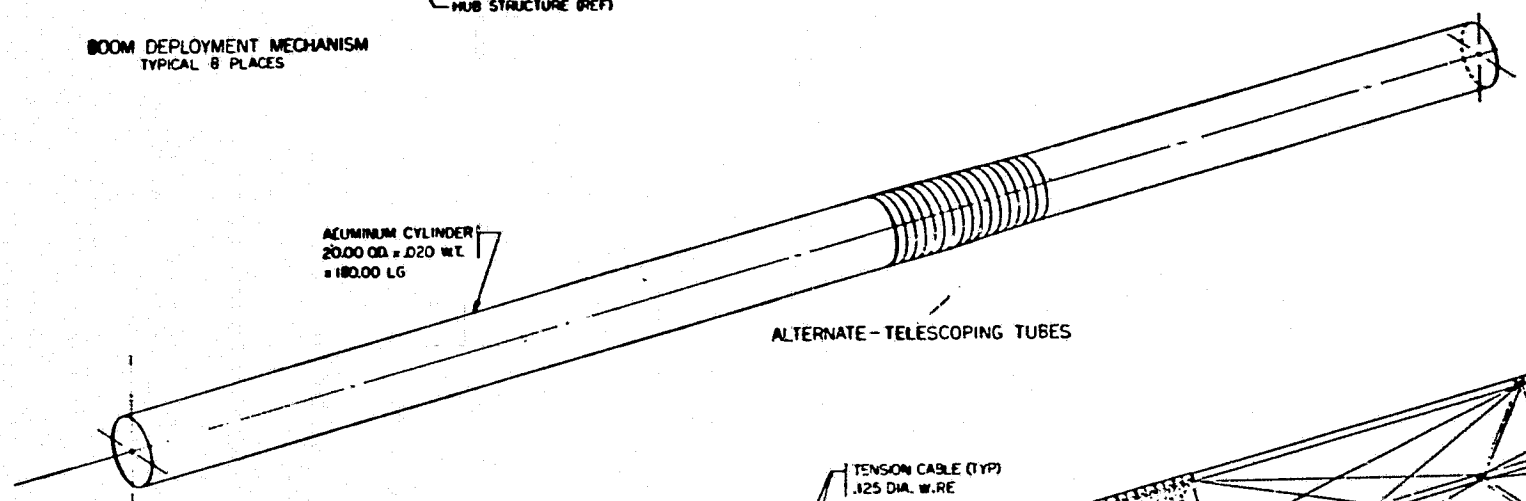
Figure A-6 - Model Deployment Sequence



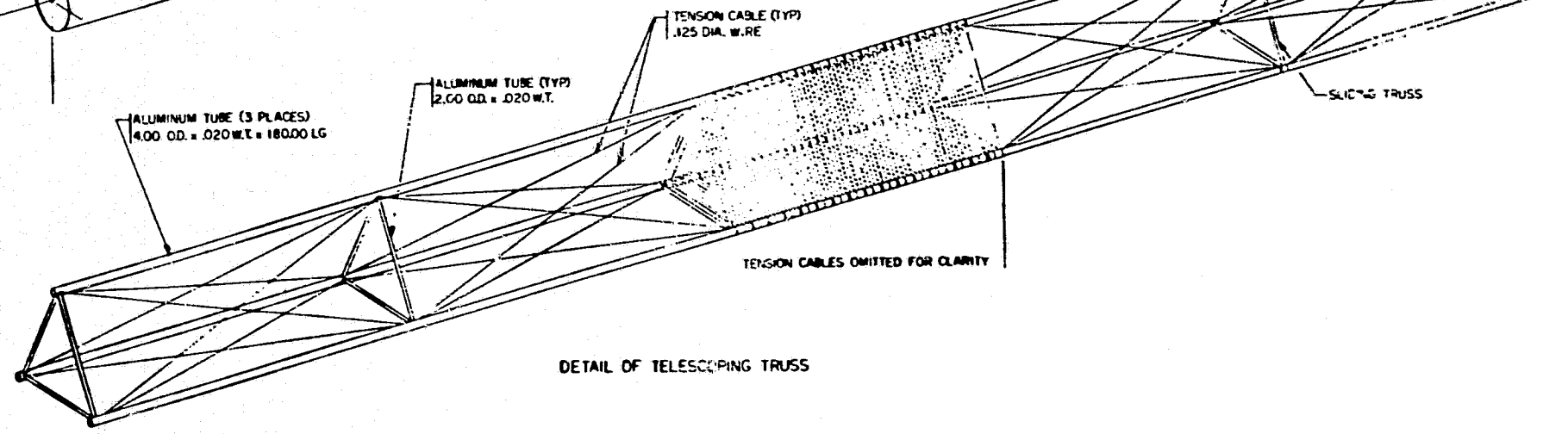
BOOM DEPLOYMENT MECHANISM
TYPICAL 8 PLACES



TELESCOPING MECHANISM - SCHEMATIC

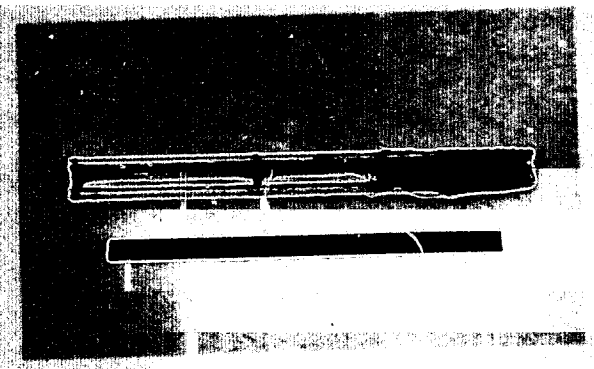


ALTERNATE - TELESCOPING TUBES

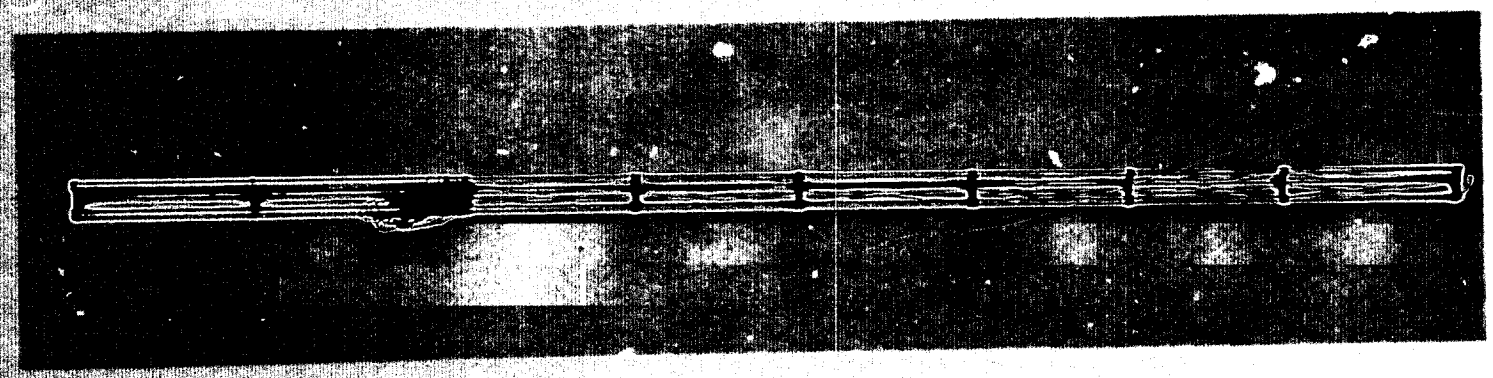


DETAIL OF TELESCOPING TRUSS

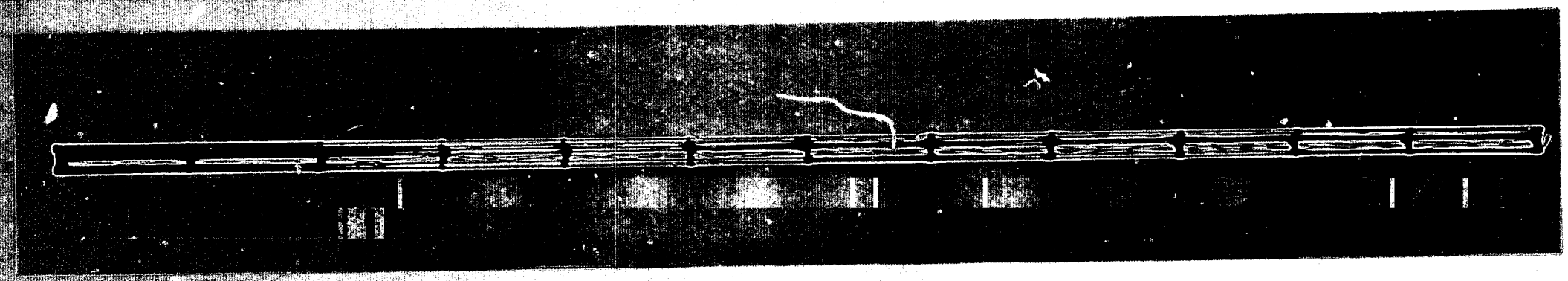
Figure A-7 - Structural Details and Deployment Mechanisms



Packaged



Partially Deployed



Deployed

Figure A-8. Telescoping Triangular Truss

A method of deploying the telescoping structural members is shown in the upper right-hand portion of Figure A-7. Each of the eight members would have a drive motor which rotates a 15-foot long drive screw. The sketch shows the top tube member deployed. In the retracted position, the tip tube ball-screw fitting would be at the left end of the drive screw. For deployment, the drive screw would extend the tip tube to the position shown, at which time the locking pins of the tip tube would engage the intermediate tube adjacent to the tip tube and start to move it outward. The ball screw fitting of this intermediate tube would then engage the threads at the left end of the drive screw and complete deployment of this intermediate tube. This process would continue until all the telescoping sections of the structural member were deployed.

The boom (structural member) deployment mechanism located in the hub is shown in the upper left-hand corner of Figure A-7. In the stowed position, the jack screw and structural member are both vertical. The jack screw is attached to a ball screw fitting on the top of the triangular truss and extending this fitting to a maximum position rotates the truss through 120 degrees which is the position at which the telescoping truss sections are extended with the reflector slack. The triangular truss member is then brought up to a horizontal position to bow the member and tension the reflector.

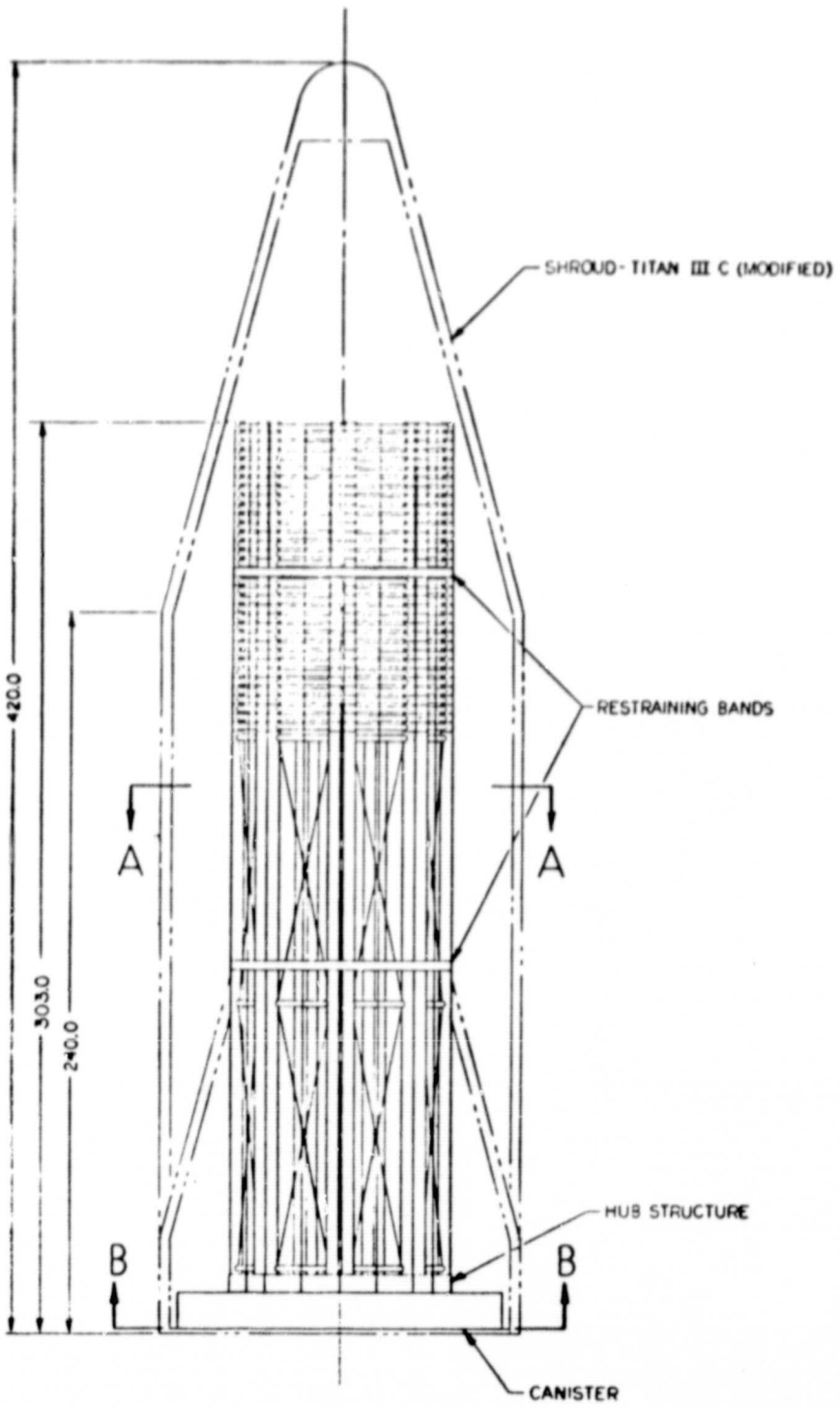
D. PACKAGED CONFIGURATION

The saddle reflector packaged configuration is shown on Figure A-9. The eight triangular truss members shown in Section AA are packaged within a 6-foot diameter. The complete satellite package height of approximately 25 feet will require a 17-foot extension to the Titan shroud. The reflector membrane would be packaged in a non-pressurized canister with the top of the canister serving as the bottom of the hub. Upon deployment the sides and bottom of the canister would remain attached to the launch vehicle.

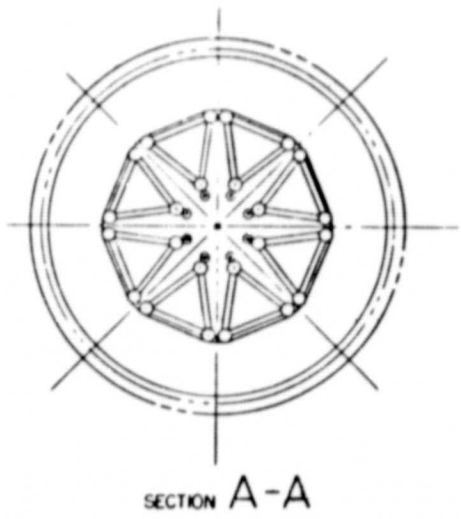
E. MEMBER GEOMETRY TRADE-OFFS FOR CONTOURING REFLECTOR

Three possible methods for providing different heights of the member tips thus generating the saddle shape are shown in Figure A-10. Designing the members with different length and with different inertias has initially been considered in the analysis.

A third method which appears capable of implementation is to change the tangency plane of the members at the hub. Inasmuch as linear actuators are already required to rotate the inboard end of the members as a part of the deployment sequence, this method offers promise of not only providing the required initial offsets of the member tips, but also supplying a vernier adjustment to compensate for manufacturing tolerances. It is conceivable that this method could also be utilized for providing a satellite with a variable reflector radii of curvature at different times to accomodate different test or operational requirements.



PACKAGED CONFIGURATION



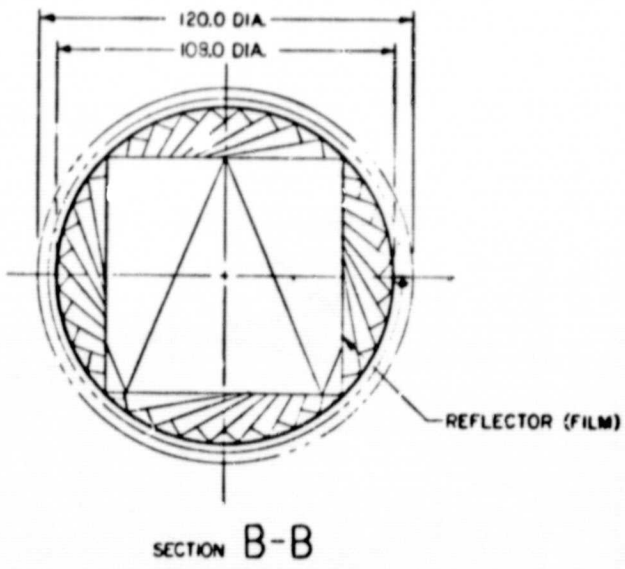
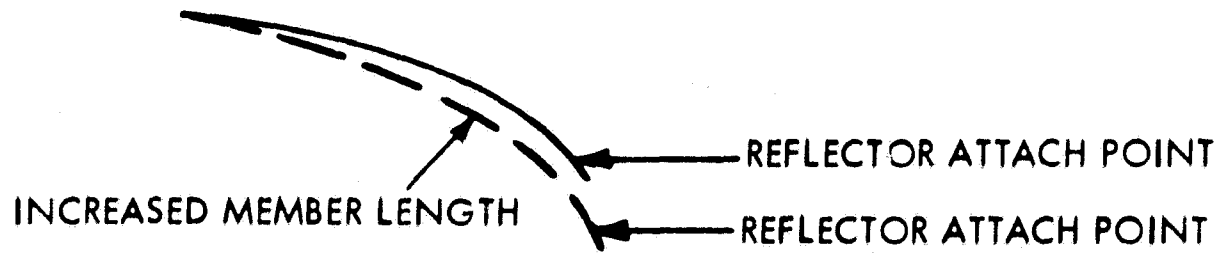
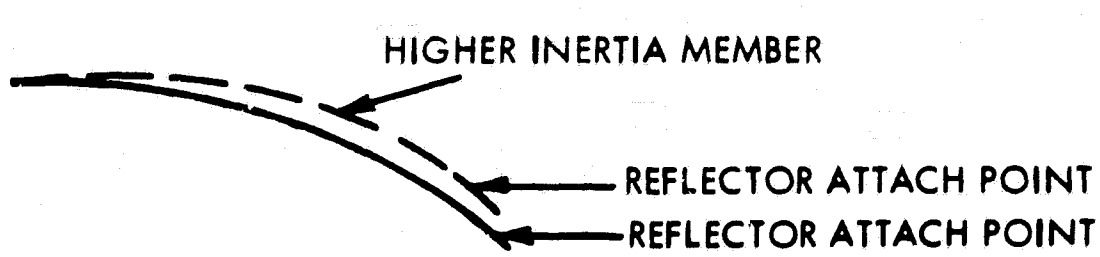


Figure A-9 - Packaged Configuration

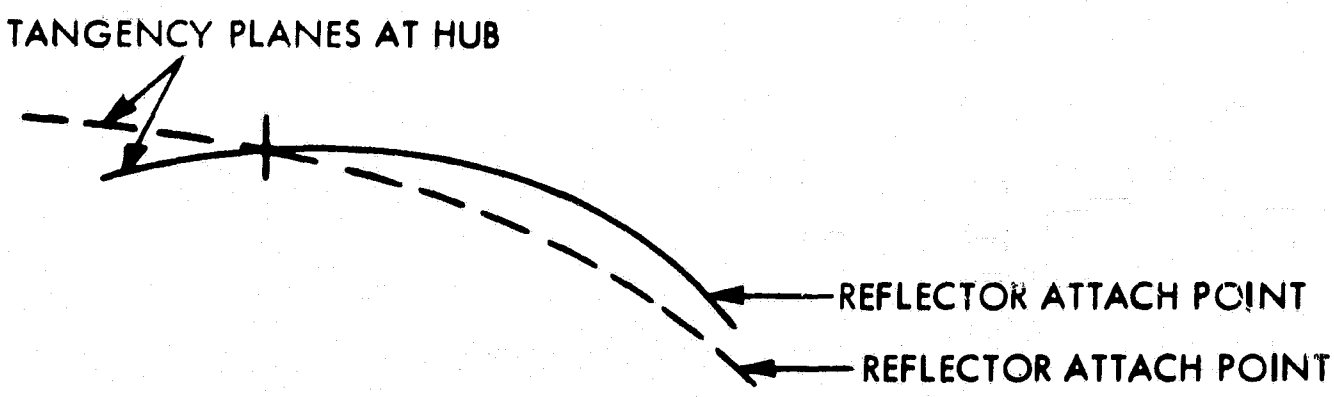
MEMBER LENGTH DIFFERENCES



MEMBER INERTIA DIFFERENCES



CHANGE OF MEMBER TANGENCY PLANE AT HUB



77.10 (5-63)
REF: ENGINEERING PROCEDURE S 017

Figure A-10 - Geometry Trade-offs to Provide Member End Point Off Sets For Contouring Reflector

Another trade-off area which merits further investigation is the separation distance between the hub and the reflector. This distance was set at 35 feet (40 percent of the radial distance from the hub to member tip) to make the structure geometry relatively insensitive to thermal deflections. However, later analysis has shown that this separation distance can be reduced possibly by 50 percent without greatly increasing the amount of thermal distortion in the reflector. The advantages of reducing this separation distance from the hub to the reflector are 1) the weight of the structure members can be reduced and 2) the center of mass of the structure is moved closer to the reflector, therefore, solar torques are lower and fuel requirements for attitude control thrusters can be reduced.

F. WEIGHT SUMMARY

Satellite weights have been estimated for the 400-foot equivalent diameter baseline configuration. Three different reflector constructions have been considered: 1/2 mil Kapton Aluminized one side, 1/2 mil Kapton aluminized both sides, and wire mesh consisting of 3 mil wires with a spacing of approximately 14 per inch. These weights are listed in Table I. The weight of the wire mesh reflector includes the weight of 1/2 mil photolyzable film for fabrication, handling and packaging of the wire mesh. This photolyzable film is removed by the solar radiation in space to reduce the area to mass ratio of the satellite and thus reduce orbital perturbations from solar pressure. The wire diameter and spacing is compatible with operation up to and including X-band. The aluminized Mylar constructions would not have

E-XD-15(7-64)(77-10)
REF. ENGINEERING PROCEDURE 1.017

TABLE I

400-Foot Diameter Saddle Reflector Weight Summary

	KAPTON REFLECTOR AL.1 SIDE WT: (LB)	KAPTON REFLECTOR AL.2 SIDES WT. (LB)	WIRE MESH REFLECTOR 3 MIL AL. WT. (LB)
REFLECTOR	500	550	750
STRUCTURE			
MEMBERS (TRIANGULAR TRUSS)	2350	2350	2350
DEPLOYMENT & HUB	200	200	200
TOTAL	3050	3100	3300

this frequency limitation.

A discussion of considerations and fuel requirements for station keeping and attitude control are contained in Appendix C.

Parametric weights were generated for the saddle satellite as a function of equivalent reflector diameter. Figure A-11 shows the results of this parametric analysis. Two assumptions were made concerning the packaging diameter available for the structural members.

The first was that the packaging diameter is a function of reflector equivalent diameter with packaging diameter assumed as follows:

Packaging diameter (Ft)	Reflector equivalent diameter (Ft)
3	100
6	400
12	1600

The weights for this analysis are shown by the upper curve of Figure A-4. The second assumption was that the packaging diameter was a constant 20 feet which would be compatible with the Saturn V launch vehicle. This program was run for diameters from 1000 to 1600 feet. This is shown by the lower curve on Figure A-11. This curve was then extrapolated to smaller diameters (reflector diameters) as shown by the dotted line.

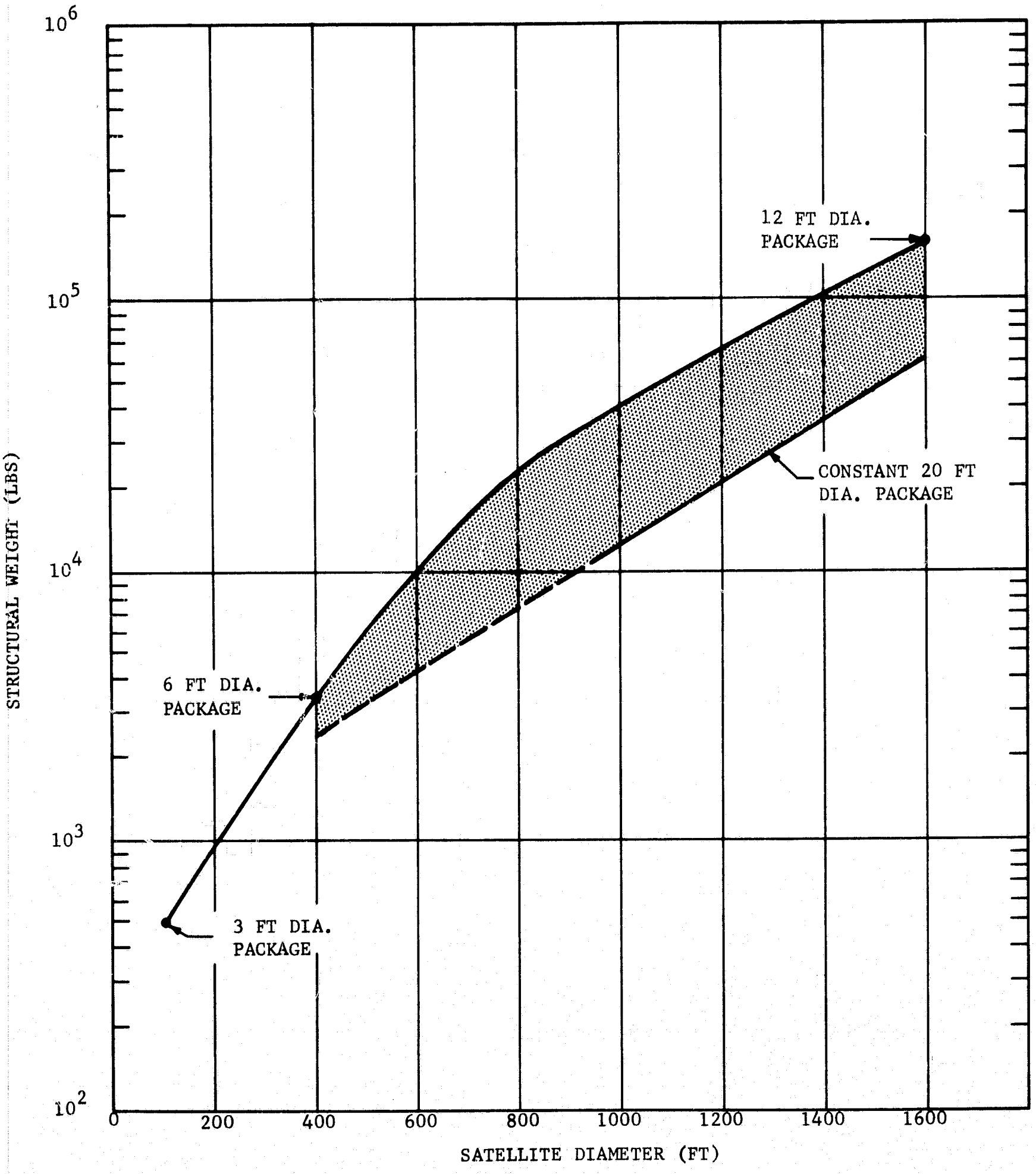


Figure A-11 - Reflector Parametric Weight

SECTION III - STRUCTURAL AND THERMAL ANALYSES

A. GENERAL

Structural and thermal analysis performed in support of the saddle reflector satellite design are summarized herein. The detailed structural analyses are contained in Reference 1. These analyses included determination of loads in structural members, effects of geometry changes on weight, deflections under the action thrust loads, structural weight variation with different initial reflector membrane tensions, and reflector geometry changes with temperatures in the space environment.

B. STRUCTURAL ANALYSES

1. Geometry and Loads

The geometry as shown in Figure A-5 of Section II was utilized for determining the loads. A reflector membrane tension of 0.05 lb/in (100 psi stress in the 1/2-mil Kapton aluminized film reflector) is considered sufficient to provide the required smoothness for the reflector. This tension will reduce the height of the cusps resulting from hard creases in the film as will occur during packaging to approximately 0.01 inches. The geometry of the catenary around the periphery of the membrane has been optimized to provide minimum tip load on the structural members. The values of catenary angles and tip loads are shown in Figure A-12 for the 400 feet equivalent diameter baseline design.

Reference 1: GER-13569 Structural Analysis of Saddle Shaped Reflector, Goodyear Aerospace Corporation, Akron, Ohio, December 1967.

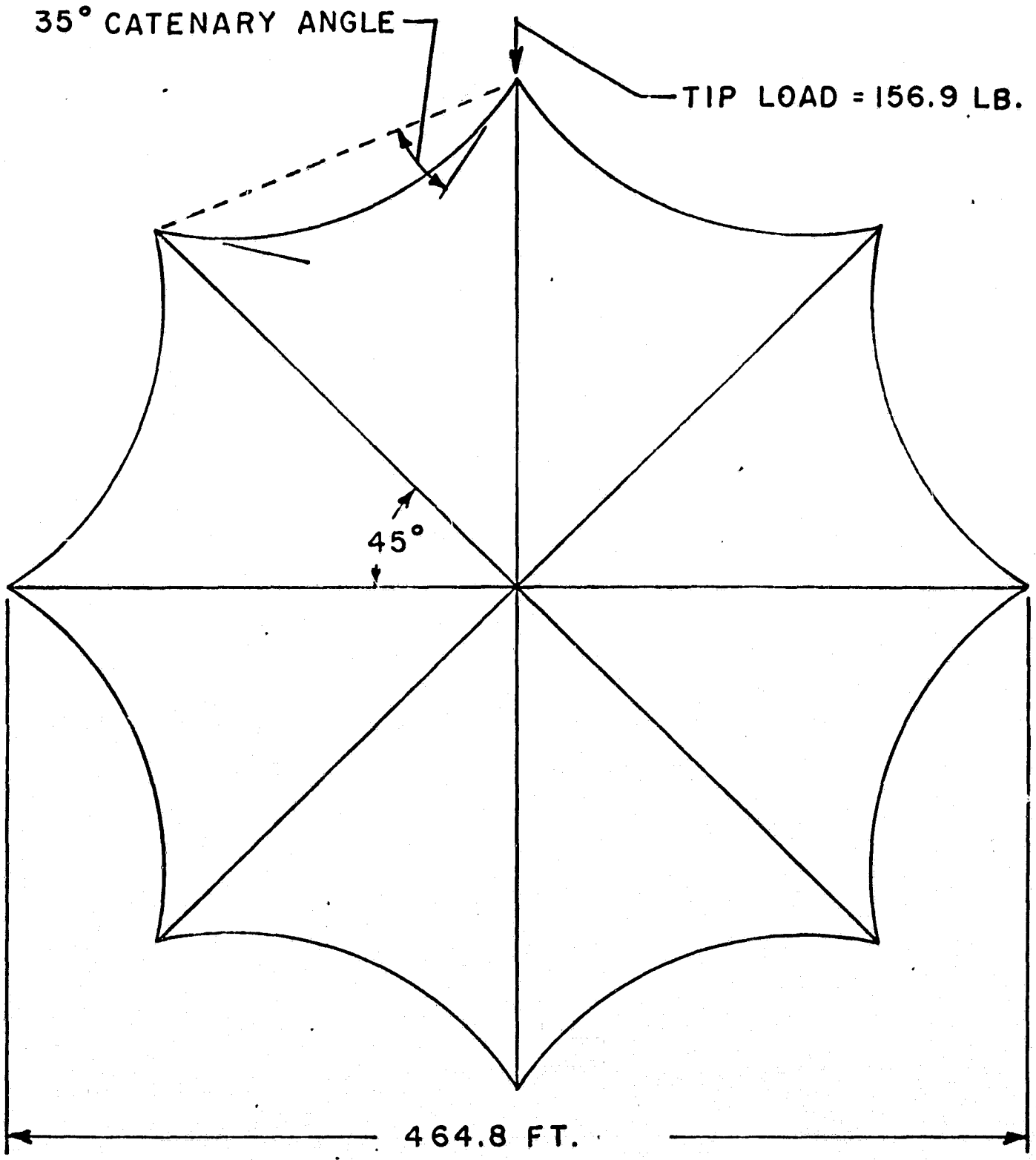


Figure A-12 - Reflector Planform Geometry and Tip Loads

2. Trade-Offs in Structural Members Geometry

The distance from the center of hub to the member tip is fixed by the reflector planform geometry. The length of the structural members and the required members section moment of inertia is a function of the separation distance between the reflector and the hub as shown by the "a" distance on Figure A-13. Figure A-13 shows the variation of bowed member length and inertia with separation distance or bow depth, "a". It was thought that a large tip angle, β, would be desirable for minimizing reflector thermal deflections since increases or decreases of membrane overall length would have less of a tendency to cause out of plane displacement of the member tip which in turn causes distortion of the reflector.

Therefore, a bow depth of 95 feet which provides a β angle of 35° was assumed for the baseline design.

It should be noted that the member tip load has been increased to 171 lbs. (over the 159.6 lbs. of Figure A-12) to account for the increased shear rigidity required for the bowed members.

Decreasing the bow depth decreases the member length and inertia. For example, if the bow depth is halved, the required member inertia is reduced by 10 percent and the member length is by about 6 percent. Since weight is generally proportional to these parameters, halving the bow depth would result in a savings of approximately 15 percent in the

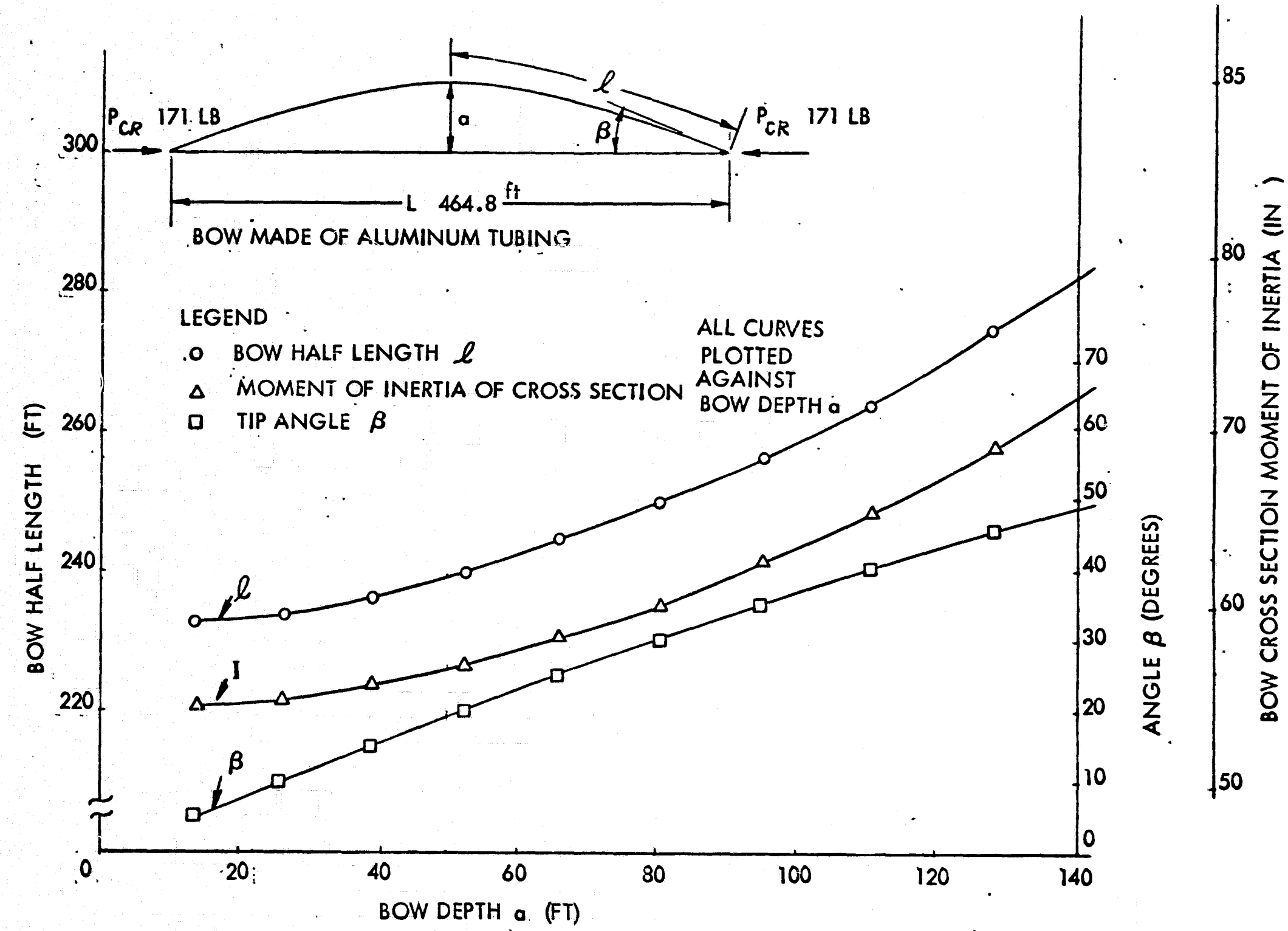


Figure A-13: BOW HALF LENGTH ℓ, CROSS SECTION MOMENT OF INERTIA AND TIP ANGLE β VERSUS DEPTH a

structural member weight. This example indicates that further optimization of the configuration is possible based on more detailed thermal deflection analysis. Reducing the bow depth moves the center of gravity of the configuration closer to the reflector surface upon which the majority of solar pressure force acts. Thus the solar torques and control fuel requirements associated with these solar torques can correspondingly be reduced.

Two cross-sections (see Figure A-14) were considered for the structural members which would be telescoped for packaging as shown on Figures A-7 and A-9. Both the triangular cross-section truss and 20-inch diameter tube have a 72-inch diameter package envelope. Since the cap material in the triangular truss can be located at a greater distance from the neutral axis, this provided the more efficient structural arrangement. As noted in the design section the weight of the telescoping triangular truss was 2350 lbs. as compared to 3300 lbs. for the telescoping tube.

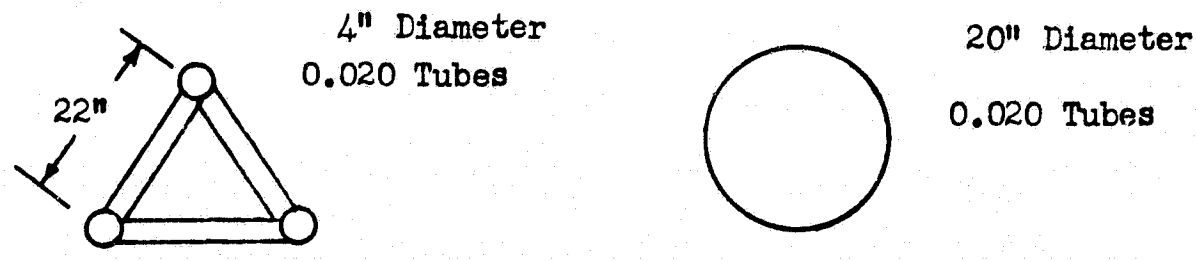


Figure A-14 - Structural Member Cross-Sections

3. Deflection Under Action of External Loads

In the analyses described in the previous paragraphs, the membrane tension has been considered to be the only load on the structural members. It can be shown that the solar pressure force of 1.3×10^{-9} psi will result in negligible change in reflector geometry. Consider the solar force, P, acting normal to the reflector on a 1-inch wide strip 465 feet long. The tension, T, is a membrane with a radius of curvature, ρ, of 6000 feet is given by the equation:

$$T = P\rho$$

$$= 1.3 \times 10^{-9} \times (6000 \times 12)$$

$$= 9.35 \times 10^{-5} \text{ lb/in}$$

This compares with a membrane tension of 0.05 lbs. per inch used for design of the structural members. The 100 psi stress level of the membrane would be increased to 100.19 psi or less than 0.2 percent.

To determine the deflection of the structure-reflector combination under the action of thrust loads applied at the tips of opposing structural members, analysis was made with the results shown in Figure A-15. The analysis shows that the configuration is stiffer with the tip loads applied in the direction of the hub. With tip loads applied away from the hub a two-pound load will result in 4-inch deflections of the tips. Inasmuch as the maximum continuous thrust of the attitude control jets is in the hundredths of a millipound range, it is concluded that the attitude control system will not significantly affect the satellite geometry.

A-ID-15(7-64)(77-10) REF: ENGINEERING PROCEDURE 5.017

V (lb)	Y (In.)
4.31	4.0
9.07	7.0
- 3.85	8.0
- 6.80	22.0

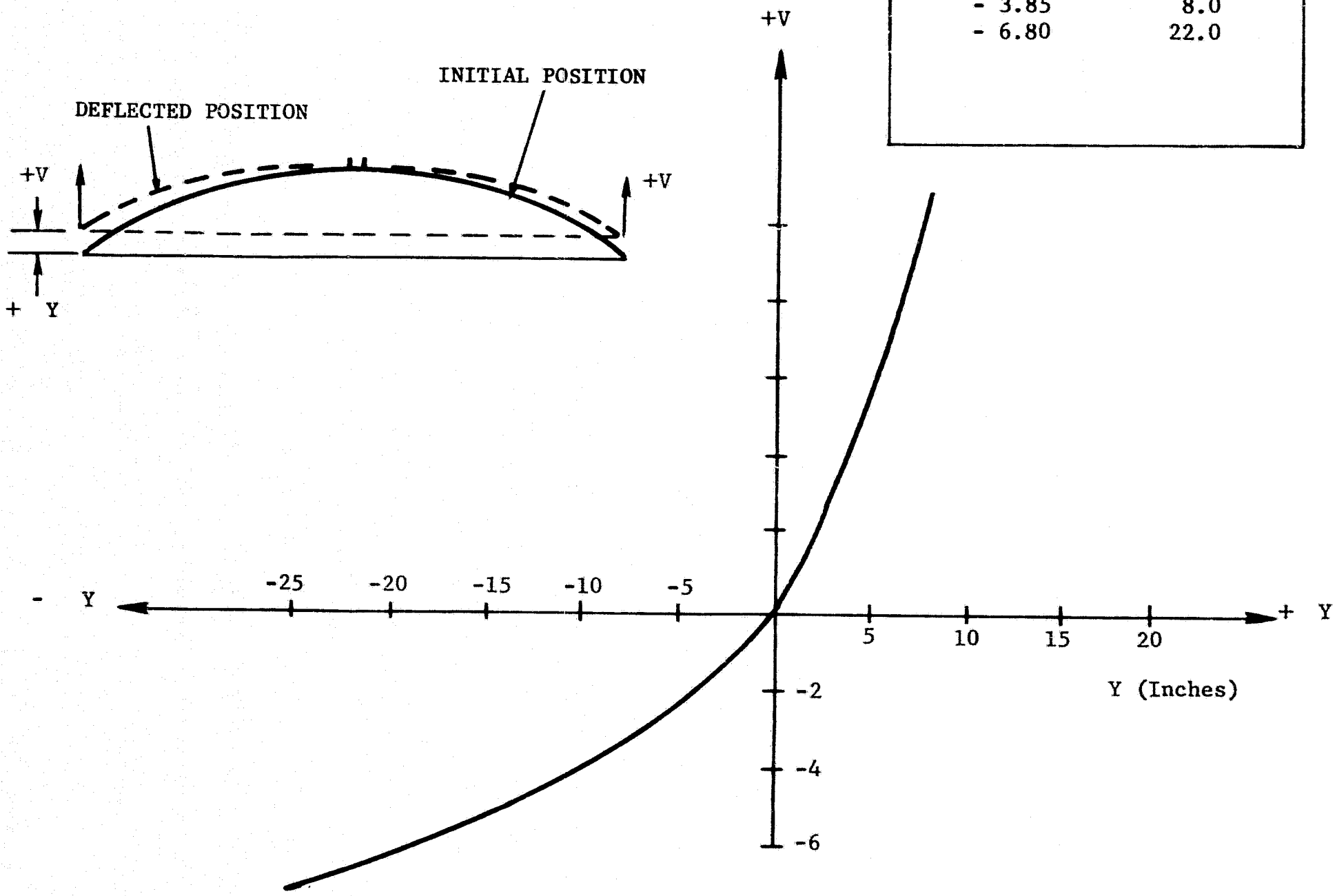


Figure A-15 - Deflections Under Equal Tip Loads

4. Structural Weight Variation with Different Initial Membrane Tensions

The weight of the structural members is significantly affected by the reflector membrane tension. The membrane stress of 100 psi will reduce the height of the creases incurred in folded areas during the packaging to approximately 0.01 inches which should provide a sufficiently smooth surface for operation at X-band. In addition to the effects of creases, the Kapton film as manufactured has a certain amount of waviness which decreases as the membrane stress is increased. Possibly a lower membrane stress would be adequate. If higher frequencies are considered, the 100 psi stress may not be sufficient. To indicate the structural weight variation, membrane stresses from 50 to 500 psi were considered and the resulting structural weights are presented in Table II for the 400-foot diameter reflector.

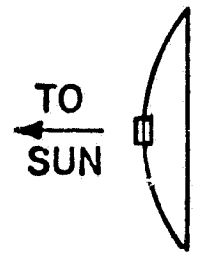
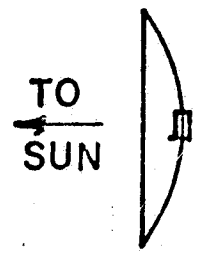
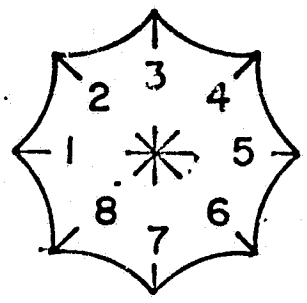
RF tests on previously packaged saddle reflector models would help to define the required membrane stress for the saddle reflector.

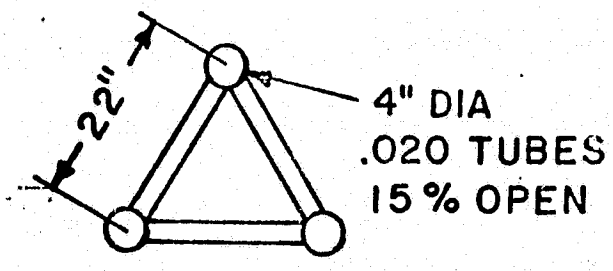
C. THERMAL ANALYSES

1. Reflector and Structural Member Temperatures

The reflector and structure temperatures for noon, midnight and twilight conditions are shown in Figure A-16. Aluminized Kapton film and aluminized wire mesh have been considered for the reflector. The final temperatures in the case of a Kapton film reflector aluminized on one side represent a condition after several years of radiation exposure which cause the

E-ID-15(7-50)(77-10) REF. ENGINEERING PROCEDURE S 017

CONDITION	REFLECTOR	REFLECTOR TEMP (°F)		STRUCTURE TEMP (°F)	
		INITIAL	FINAL	INITIAL	FINAL
NOON 	KAPTON: ALUMINUM ONE SIDE	90	240	230	215
	BOTH SIDES	330	330	235	235
	WIRE MESH ALUMINUM	235	75	165	135
MIDNIGHT 	KAPTON ALUMINUM ONE SIDE	0	0	−130	−130
	BOTH SIDES	330	330	−180	−180
	WIRE MESH ALUMINUM	235	75	40	115
TWILIGHT  	KAPTON: ALUMINUM ONE SIDE	−300	−300	INITIAL & FINAL MEMBERS NO. 1,5: 5	3,7: 130	2,4,6,8: 90
	BOTH SIDES	−300	−300	5	130	90
	WIRE MESH ALUMINUM	−300	−300	5	130	90



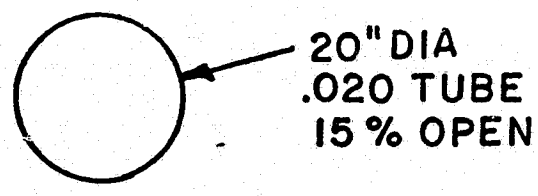


Figure A-16 - Temperature Summary

77-10 (5-63) REF: ENGINEERING PROCEDURE 5.017

film to darken and become opaque. For the Kapton film aluminized on both sides the initial and final temperatures are the same. The initial temperature of the aluminum wire mesh represents the temperature prior to photolyzation of the film. The photolyzable film is required for handling and packaging and is removed by solar radiation in space to reduce the area to mass ratio of the satellite and thus reduce orbital perturbations from solar pressure. The final temperature for the aluminum wire mesh is the temperature after film photolyzation which would be reached a few hours after deployment.

The noon and midnight conditions result in all the structure members having the same temperature. For the twilight condition the member viewing angles with respect to the sun are different and therefore the temperatures of the structural members are also different.

Figure A-16 also shows the two structural member cross-sections considered for the analysis. Through perforations of the structural member surface to provide 15 percent openness and coating the interior of the structural members black, the temperature differential across the tubes can be maintained to less than one degree F.

2. Thermal Deflections

The effects of temperature differences of the reflector and structure on the baseline design geometry are shown for the noon and midnight orbital positions in Figure A-17.

E-ID-15(7-64)(77-10)
REF. ENGINEERING PROCEDURE 5.017

TABLE II

EFFECT OF MEMBRANE TENSION ON STRUCTURAL WEIGHT OF THE 400 FT. NOMINAL DIAMETER ANTENNA

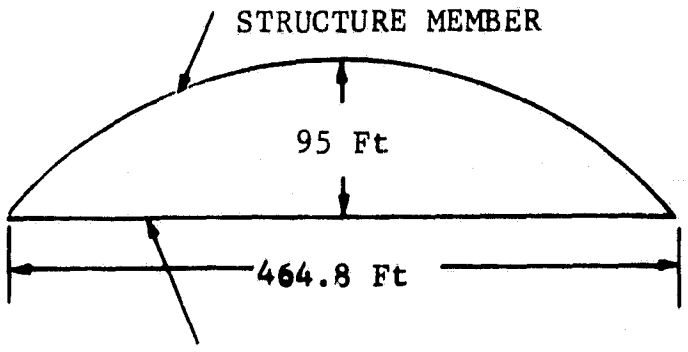
Membrane Thickness = 1/2 mil (KAPTON)

MEMBRANE TENSION	50 psi	100 =	300	500
Membrane Tension (Lb/In)	0.025	0.050	0.150	0.250
Compression Load Q=(Lb)	78.5	156.9	470.7	784.5
P_E = 1.09 Q	85.5	171.0	513.1	855.1
Angle β (Degrees)	35	35	35	35
ρ = sin (/2)	0.30071	0.30071	0.30071	0.30071
K (ρ)	1.6091			
E (ρ)	1.5340			
2E - K	1.4589			
1/k = 232.4/(2E - K)	159.298			
α = ZP (1/k)	95.0 Ft			
ℓ = (1/k) K	256.3 Ft			
$EI/10^7 = P_E (1/k)^2 x 10^{-6}$ (=I)	31.25	62.5	187.5	312.5
Tube Wall Thickness t	0.012	0.016	0.025	0.032
Space Truss Cross-Section Side, S	23.86	26.82	32.96	33.53
Tube Diameter D (in)	2.88	3.41	4.34	5.42
Bay Length b (inches)	50	56	65	80
Membrane Weight W_M	452.4	452.4	452.4	452.4 lb.
Tube Weight (Lb)	801.4	1265.2	2516.1	4022.1
Transverse Tubing	95.6	151.5	319.0	421.5
Cross Steel-Wire (1/8")	568	568.4	574.8	555.9
Sum of 4 Previous Items	1917.4	2437.5	3862.3	5451.9
Catenery, Seams Etc. (5% of Sum)	95.9	121.9	193.1	272.6
Total Structural Weight	2013.3	2559.4	4055.4	5724.5

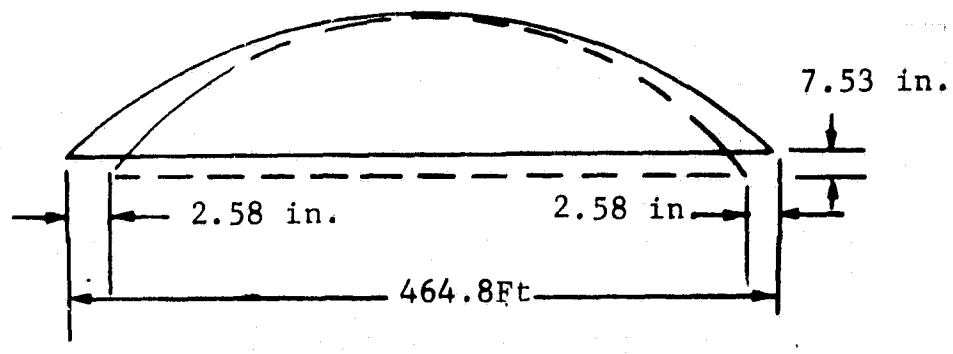
The structural weight of the 400 ft. nominal diameter antenna, W_S, in pounds may be represented in terms of the membrane tension, σ_M, (P s i) by equation,

$$W_S = 1600 + 8.25\,\sigma$$

E-ID-15(7-64)(77-10) REF: ENGINEERING PROCEDURE S.017



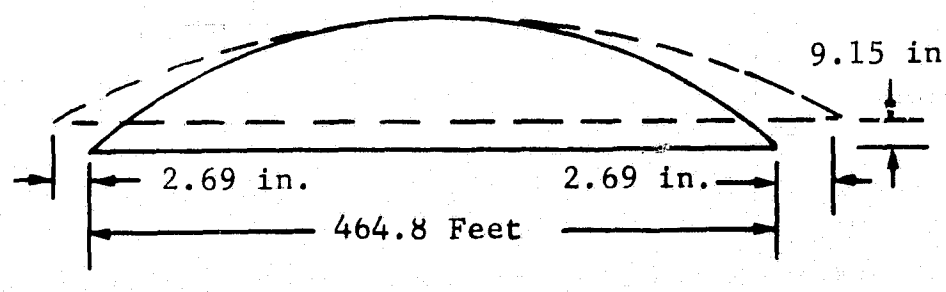
FABRICATION TEMPERATURE:
80°F



ORBITAL POSITION: NOON

——— Initial

– – – – Deflected



ORBITAL POSITION: MIDNIGHT

——— Initial

– – – – Deflected

Figure A-17 Thermal Deflection of Bows

The changes are referenced to the nominal geometry with structure and reflector fabricated at a temperature of 80 deg. F. For the noon positions the net effect on the reflector is to maintain the same relative position of the member tips in a vertical plane and slightly decrease the reflector diameter. This results in a radius of curvature change from 6000 to 5088 feet which can be considered negligible. A similar condition exists for the midnight condition where the radius of curvature changes from 6000 to 6012 feet. The membrane stress is also negligibly affected. The stress varies only a fraction of a psi from the nominal 100 psi.

The twilight heating condition was analyzed parametrically to determine the percentage of change in radius of curvature for various satellite diameters and normal radii of curvature (minimum convex and concave radius of curvature) of 6000, 12000 and 24000 feet. The temperature effect in all cases was to reduce the radius of curvature. The results are presented in Figure A-18.

The curves of Figure A-18 show that, for a specified radius of curvature, the larger the satellite diameter the less percentage change in radius of curvature will be. As an example, for the 400 feet equivalent diameter baseline saddle design with a minimum radius of curvature of 6000 feet for the twilight heating condition,this radius of curvature would be reduced by slightly less than 10 per cent or to about 5500 feet. The change in the radius of curvature (ρ) affects the radar cross-section

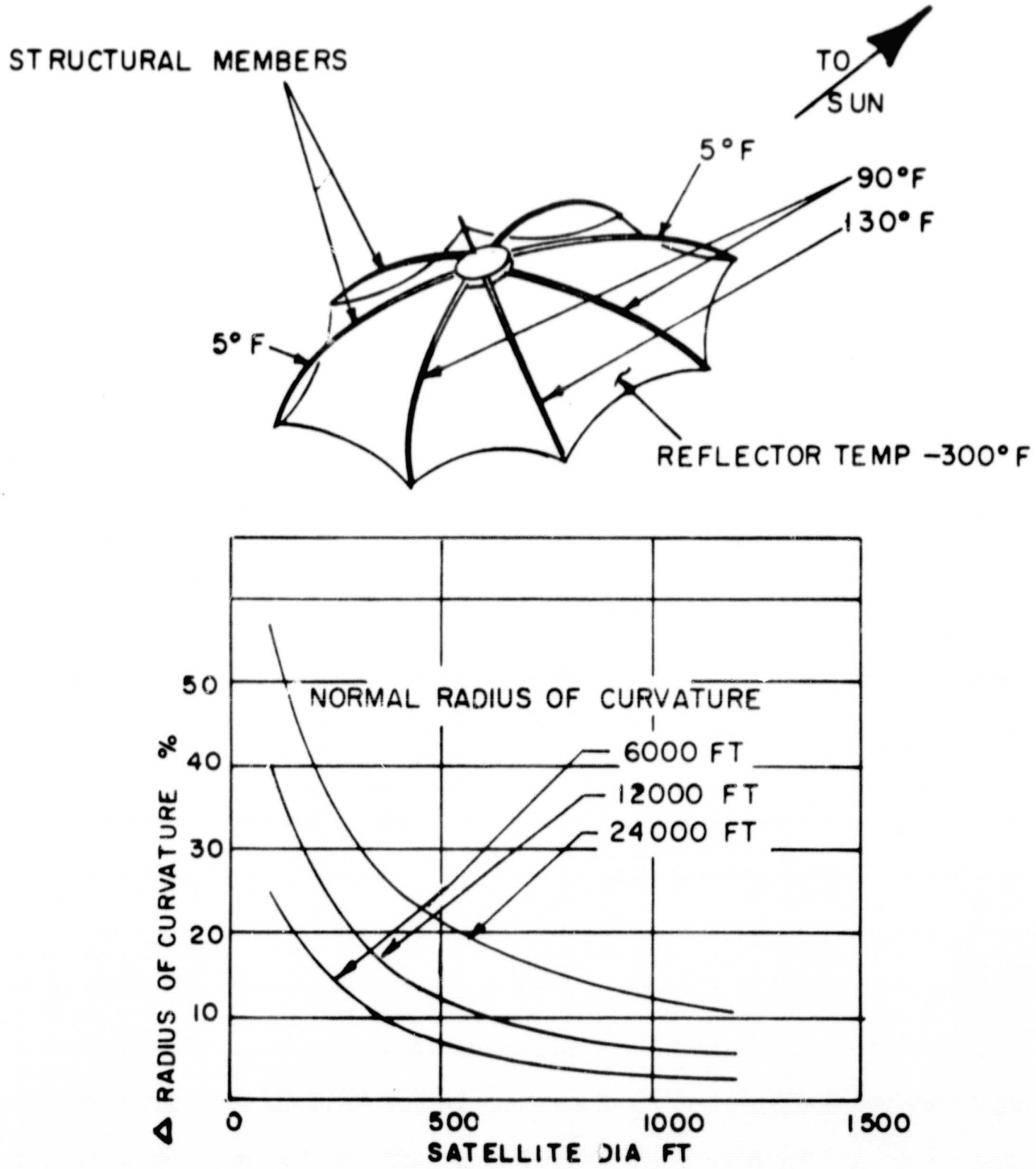


Figure A-18 - Radius of Curvature Change For Twilight Heating Condition

(σ) or gain (G) of the reflector in proportion to ρ^2 since

$$\sigma = \pi \rho^2$$

and

$$G = \frac{4\pi\sigma}{\lambda}$$

Therefore, the thermal deflections noted in figure A-18 correspond to a loss in gain which is scaled to the $\Delta\rho$ axis in the Figure. Then, for example, a reflector with a 12,000 foot radius of curvature and 300 foot diameter will experience a 2 db fade over the period of the thermal cycle.

APPENDIX B

SADDLE GAIN & REFLECTION CHARACTERISTICS

APPENDIX B

SADDLE GAIN & REFLECTION CHARACTERISTICS

A. INTRODUCTION

It is required to determine the rf cross-section and reflection pattern for the saddle satellite. RF cross-section estimation, using the methods of physical and classical geometrical optics in the high frequency spectrum are well known. The salient feature of geometrical optics is the assumption that the field quantities propagate along rays which are determined by the Fermat principle of least time, and that these rays obey the laws of reflection and refraction at the interface between two different media (Fresnel Law).

It should be noted that the geometrical optics method gives only the leading terms in the asymptotic high frequency solution of the scattering problem. However, when the scatterer is large, in terms of a wavelength, the scattering is essentially a local phenomenon; therefore, the method of geometrical optics (ray tracing) is an adequate approximate solution to the problem of determining the beam width of a Saddle reflector.

To determine the rf cross-section of a saddle reflector, the current distribution or physical optics method has been used. The essential feature of the physical optics method is that it approximates the current distribution over the illuminated area of a scatterer surface, using the geometrical optics

REF: ENGINEERING PROCEDURE S-057

concept. On the basis of geometrical optics, there is a sharply defined shadow region behind the scatterer in which the total field is zero and according to the boundary condition, the current distribution over the shadow area is also zero. The current distribution over the illuminated region is then obtained on the assumption that at every point, the incident field is scattered as though an infinite plane wave were incident on the infinite tangent plane at the point of an illuminated scatterer. This leads to a surface current of the value

$$J = 2 (\hat{n} \times H^i)$$

at each point of the illuminated region.

Where; $\hat{n}$ is the unit vector normal to the surface and H^i is the incident magnetic field.

In general, the dominant contribution to the rf cross-section of a Saddle reflector comes from the three distinct scattering centers:

(1) Specular Scattering

(2) Diffraction

(3) Surface Wave

The specular scattering gives a cross-section which is independent of frequency (geometrical optics) cross-section, namely

$$\sigma = \pi \rho_1 x \rho_2$$

Where

$\rho_1 x \rho_2$ are the principal radii of curvature in the two orthogonal planes. It must be noted that the equation $\sigma = \rho_1 x \rho_2$ is valid only for

the case where the depth (d) of the reflector is large in terms of a wavelength of the incident field,

$$d << \lambda ,$$

For this case only the first Fresnel zone contributes to the specular cross-section as given by the geometrical optics.

To estimate the complete diffraction patterns of a Saddle reflector as a function of the aspect angle, one has to consider the contribution to the rf cross-section by the first and the higher order diffraction processes.

In general, considering the geometrical shape of the reflector, the dominant contribution to the RCS is caused by the edge-discontinuity. Since the intensity and phase of the edge diffracted field are determined by the geometrical parameters of a reflector in terms of a wavelength of the incident field, the edge diffraction (first order diffraction) may significantly contribute to the RCS.

In general, the existence of the diffracted field causes a fluctuation in the nose-on-monostatic cross-section.

Existence of an interference pattern will be caused by phase difference between the specular and diffracted fields.

However, in the case of a saddle reflector due to the nature of geometrical factor the diffracted field reradiated by the convex-concave effective ring source is of the form $E_1 \exp(-\phi) + E_2 \exp(+\phi)$,

where

$\phi = 2\ kd$ = the phase factor of diffracted field

$K = \frac{2\pi}{\lambda}$

d = depth of reflector

$E_1 = E_2$

Therefore, due to the mutual cancellation of the phase factor it is not expected that there will be a signal fluctuation due to the first order diffraction even in the nose-on monostatic mode of operation.

The surface wave contribution to the RCS is expected to be effective at aspect angles near the edge which are beyond the bistatic angles of the communication mode of operation and therefore, the surface wave reradiation may be considered as irrelevant as far as the performance of a Saddle reflector is concerned.

Although the experimental evidence indicates that the seam effects indeed appear in the backscattering return as an amplitude oscillation, it is highly improbable that the seams will significantly contribute to the reflector cross-section.

B. BEAM WIDTH

The beam width of the Saddle reflector in the two orthogonal planes for the incidence on the optical axis (monostatic case) and off axis (bistatic) has been computed using the ray tracing method.

The general ray trace program Z07700 with the IBM 360 has been used to trace the reflected rays scattered by a Saddle reflector. The program initially purchased by GAC from the IBM Corporation has been modified and adapted to the GAC IBM 360. The program is capable of tracing either a single ray or a fan of rays emanating from a source at infinity. Information concerning the number, location and direction of the rays to be traced, constitute the ray input data. With this information in memory, the computer calculates the path of each ray reflected by a scattering surface.

The principal results obtained by ray-tracing for the Saddle reflector of a 460 by 460 foot square aperture and radius of curvature in the two orthogonal planes (concave and convex) of 6000 feet, indicate that the beam width (θ) of a Saddle reflector for both cases namely:

(a) Monostatic - incidence or optical axis

(b) Bistatic case - bistatic angle of 10 degrees is twice that of the aperture angle (ψ) of a Saddle reflector,

$$\theta = 2\psi$$

Because the scattered field is proportional to the area of the first Fresnel zone at the edge of optical coverage, the power level for a beamwidth defined by $\theta = 2\psi$ is six db down relative to the signal on optical axis. The 3 db down power level beamwidth of course, will be smaller than $\theta = 2\psi$ and wavelength dependent.

C. RF CROSS-SECTION

Knowing the current distribution over the illuminated area, it can be shown that the monostatic cross-section is given by the expression

$$\sigma = \frac{4\pi}{2} \quad |g|^2 ,$$

$$g = \int \ell \quad 2j \; K \; X \; \frac{d \; A(X)}{d \; X}$$

Where, X is the distance measured in the direction of incidence and dA(X) is the element area projected on the normal plane of constant X.

The expression for the factor g is valid under the following approximations:

(1) the amplitudes of the elemental spherical waves scattered by the elemental areas are essentially equal.

(2) The elemental spherical wave scattered by a two elemental area differs in phase only due to the difference in the perpendicular distances of the two areas from the normal plane.

In the case of a Saddle reflector the phase of scattered field by a concave elemental area is leading, that by convex is lagging.

$$\phi \text{ concave} = \frac{2K \; X}{\lambda} \qquad \phi \text{ concave} = \frac{-2K \; X}{\lambda}$$

Using a topographical map of the Saddle reflector, the elemental areas are found to be approximately of the form

$$A \; (X) \text{ concave} = \tfrac{1}{2} \; M \left[- X^2 + dX + \frac{d^2}{4} \right]$$

$$A \; (X) \text{ convex} = \tfrac{1}{2} \; M \left[X^2 + dX + \frac{d^3}{4} \right]$$

REF: ENGINEERING PROCEDURE S.017

where, for the test model

$$M = 134$$

$$d = 4.52 \text{ in.}$$

Using the above expressions for the elemental areas, the factor g is given by

$$g = \int_{-d/2}^{0} \ell^{2jK X} \frac{dA(X)}{dX} \text{ concave} + \int_{0}^{d/2} \ell^{-2jK X} \frac{dA(X)}{dX} \text{ convex}$$

By performing integrations, the factor g is found to be

$$g = j \frac{M}{2K} \left[d - \frac{1}{jK} \left(1 - \ell^{-jKd} \right) \right]$$

$$K = \frac{2\pi}{\lambda}$$

For large K,

$$g = \frac{Md}{2jK} \quad , \quad \text{and}$$

$$\sigma = \frac{4\pi}{\lambda^2} |g|^2 = \frac{M^2 d^2}{4\pi}$$

By inserting the parameters of the test model, the rf cross-section is found to be σ = 18.3 sq. m. = 12.63 db sm

Which is in close agreement with the rf cross-section obtained by experimental means.

D. RCS MEASUREMENTS

Measurement of a monostatic and bistatic rf cross-section were performed on the Saddle reflector with the principal radii of curvature

$\rho_1 = \rho_2 = 9$ ft and the diameter of aperture in the two orthogonal planes

REF: ENGINEERING PROCEDURE S-017

D = 44 inches (aperture subtended angle θ = 23.5°).

The rcs measurements consisted of:

(a) Monostatic and bistatic (20 degree bistatic angle) at 9.6 GHz.

(b) Bistatic, -10 and 20 degree bistatic angle at 16 GHz.

The results of measurements in the form of a 3-db and 6-db beamwidth contour are shown in Figures 1 through 4.

E. SATELLITE GAIN

The satellite gain of a passive reflector can be confusing since some rather high gain figures (compared to large antennas for example) can be obtained. This high gain is to be expected and can be explained by several approaches. The most accepted approach considers this high gain as being made up of an up-link (intercept) gain and a down-link (transmit) gain. That is

$$G_s = G_i \, G_t$$

where:

G = total gain of the passive reflector

G_i = intercept gain of the reflector

G_t = transmit gain of the reflector

The intercept gain is related to the effective area of the reflector by the following expression:

$$G_i = \frac{4 \pi A}{\lambda^2}$$

where:

A = effective area

λ = wavelength

The transmit gain or directivity for a 100 percent efficient antenna is given by this expression.

$$G_t = \frac{41,300}{\theta_E \theta_H}$$

where:

θ_E = E plane beamwidth in degrees

θ_H = H plane beamwidth in degrees

This considers a square beam pattern (θ_E x θ_H). For a circular beam pattern where $\theta_E = \theta_H$

$$G_t = \left(\frac{41,300}{0^2}\right) \left(\frac{4}{\pi}\right) = \frac{52,500}{\theta^2}$$

Therefore, the total gain is

$$G_s = G_i G_t = \left(\frac{4 \pi A}{\lambda^2}\right) \left(\frac{52,500}{\theta^2}\right)$$

The following expressions are true for the special case of the saddle or lenticular satellites:

$$A = \frac{\pi D^2}{4}$$

thus,

$$G_i = \left(\frac{\pi D}{\lambda}\right)^2$$

and

$$\theta = \frac{2D \times 57.3}{\rho} = \frac{114.6\ D}{\rho}$$

Therefore,

$$G_t = \frac{52{,}500}{\left(\frac{114.6\ D}{\rho}\right)^2}$$

$$G_t = \frac{4\ \rho^2}{D^2}$$

Therefore, the total gain is

$$G = \frac{\pi^2\ D^2}{\lambda^2} \times \frac{4\ \rho^2}{D^2}$$

$$G = \frac{4\pi}{\lambda^2} \times \pi\rho^2$$

where: $\pi\rho^2 = \sigma$ - the familiar radar cross section

F. CONCLUSIONS

The results of measurements have shown that the measured beamwidth (3 and 6-db down power level) of the Saddle reflector is in a close agreement with the beamwidth predicted by the geometrical optics or ray tracing method. It must be pointed out that the results of the ray tracing analysis have clarified the most significant point in regard to the performance of a Saddle reflector, namely the fact that the performance of the Saddle reflector very closely resembles the rf performance of a spherical cap reflector as far as the ground coverage is concerned. In fact the analysis has shown that the

theoretical ground coverage or beamwidth in terms of the aperture subtended angle (Ψ) is the same for both reflectors, namely:

$$\theta = 2\Psi$$

Because the scattered field is proportional to the area of the first Fresnel zone, the power level for a beamwidth defined by $\Psi = 2\theta$ is six db down relative to the on axis operation. The 3 db down beamwidth of course, will be smaller and frequencies dependent.

$$\Psi(-3 \text{ db}) < 2\theta$$

The computed value of rf cross-section for the test model is in close agreement with the measured rf cross-section. In fact, the computed rf cross-section is of the order of 18.3 sq. m. or 12.63 dbsm. The measurements yield a level of 13.8 to 14.8 dbsm with a 3 to 4 db ripple.

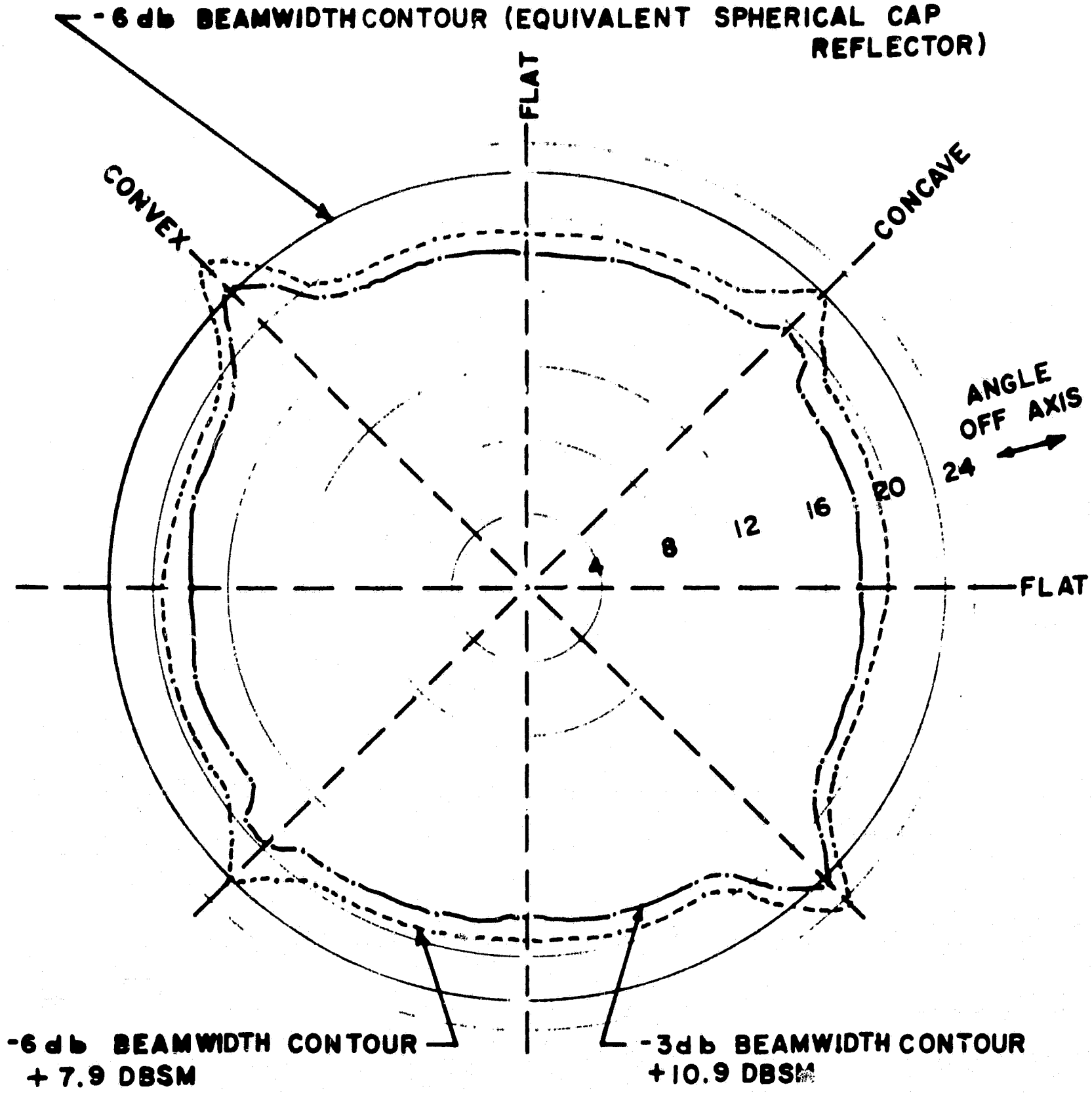


Figure 1. Beamwidth Contour Plot - Monostatic - 9.6 MHz

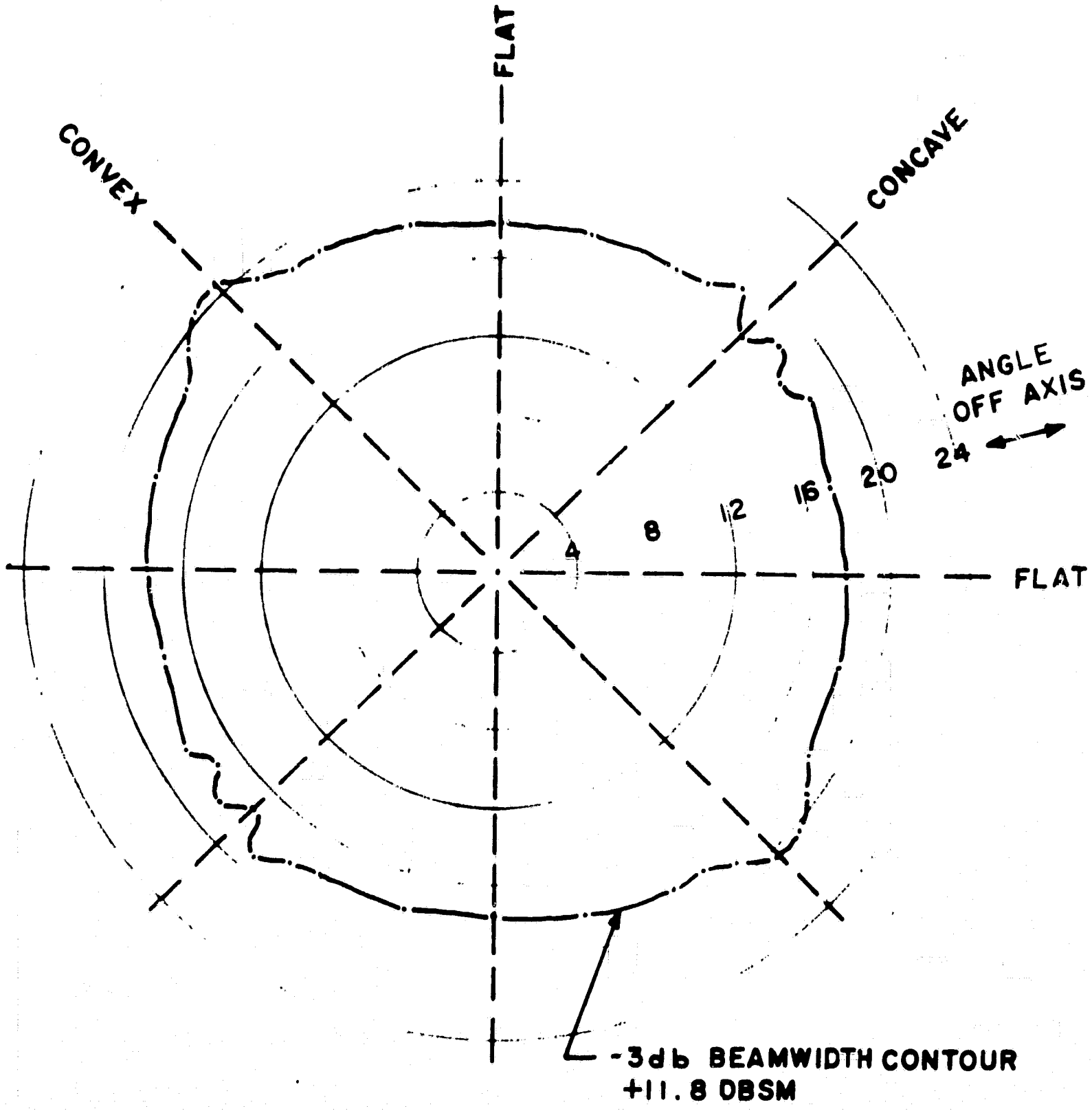


Figure 2. **Beamwidth Contour Plot - 20° Bistatic - 9.6 GHz.**

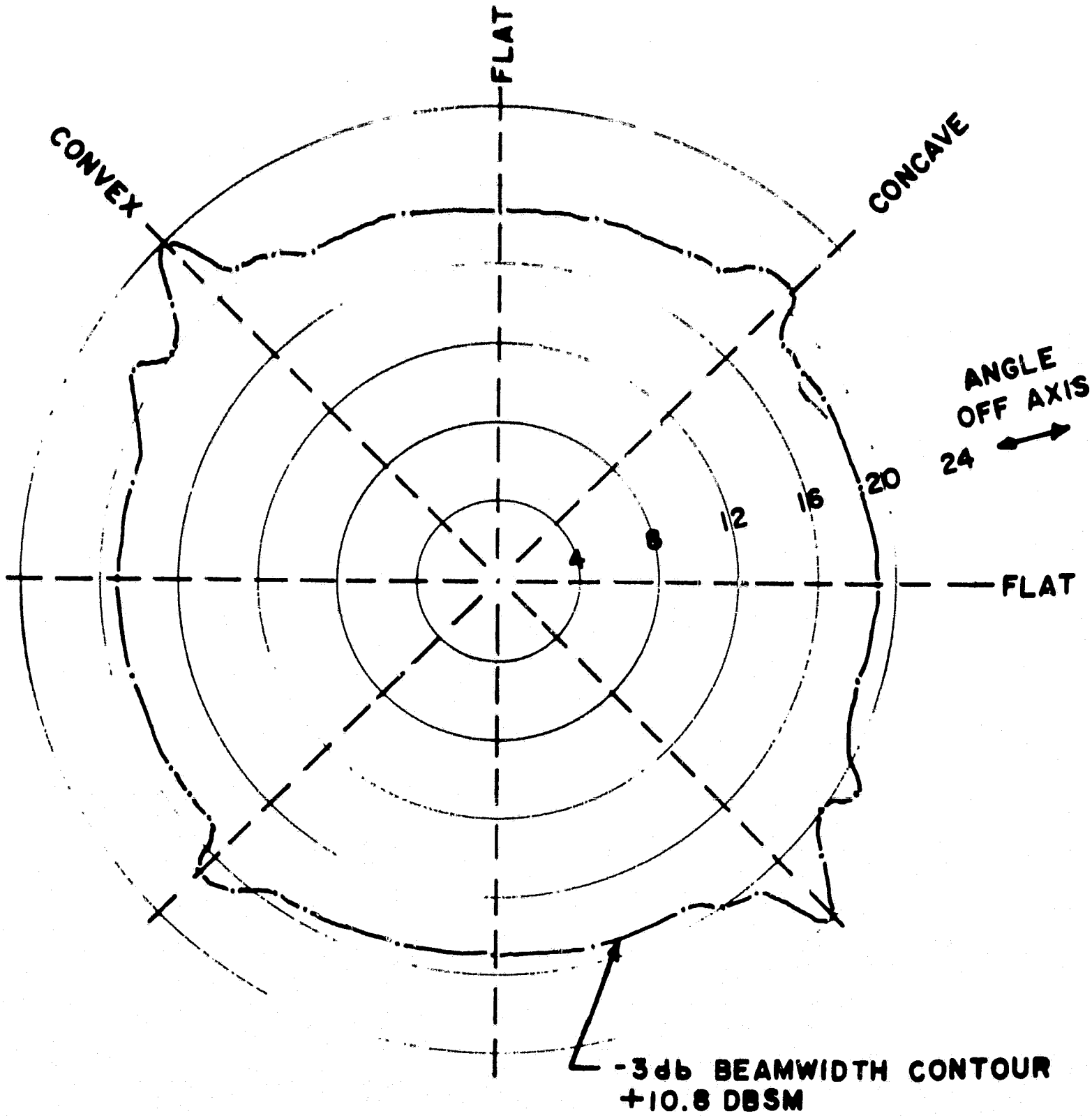


Figure 3. Beamwidth Contour Plot - 10° Bistatic - 16.0 GHz.

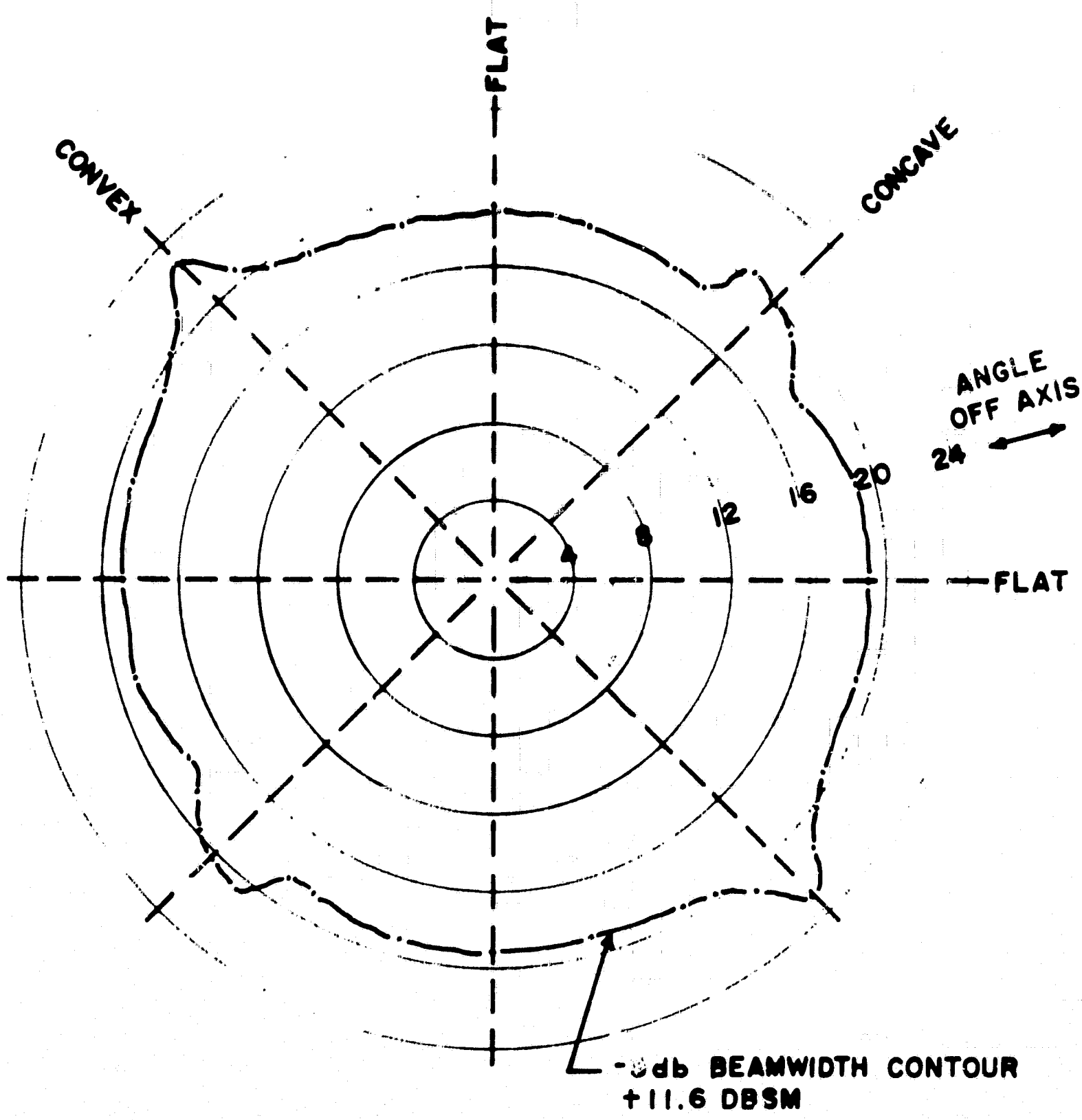


Figure 4. Beamwidth Contour Plot - 20° Bistatic - 16.0 GHz

APPENDIX C

POSITION KEEPING, ATTITUDE CONTROL, AND FUEL REQUIREMENTS FOR LARGE AREA-TO-MASS RATIO SATELLITES

I. INTRODUCTION

The appendix describes the analysis of orbital mechanics and attitude control for large flat satellites. Section II reviews the causes and effects of altitude and position errors and compares the station keeping fuel requirements for stationary and solar stable orbits. The results of Section II indicate that the stationary orbit results in excessive fuel requirements for station keeping. Consequently, Section III is concerned only with the solar stable orbit in estimating fuel requirements for attitude control. In Section IV, the stability of the orbital elements are examined in more detail considering the effects of solar radiation pressure and the gravitational perturbations due to the sun and the moon.

II. PRELIMINARY CONSIDERATIONS

A. INTRODUCTION

The major forces which produce attitude and position errors are reviewed and the penalties required to compensate for these forces are presented as a function of system weight. The need for attitude and position control and a position and attitude control system trade off study is also demonstrated.

Total position keeping fuel requirements are presented for a flat plate configuration with area-to-mass ratio of 23.6 ft^2/lb. Two orbits are considered, one stationary and the other a 24 hour solar stable. Thrusters are assumed for the position keeping system and the fuel weights presented are parametric on specific impulse. The specific impulse parameter covers the range from cold gas to ion engines.

Only total fuel requirements are presented herein. The total fuel needed for position keeping is derived from the sum of the individual Δ V requirements for each disturbance. These individual ΔV requirements are also presented.

B. EFFECT OF ERRORS

The effect of attitude and position errors on system performance can be demonstrated for the simple case of point-to-point communication via satellite. For simplicity a flat plate will be assumed in a stationary orbit midway between the transmitter and receiver. The incoming signal is reflected down to the receiver as shown in Figure 1. The geometry is assumed planer for convenience, and the distances approximate

B. EFFECT OF ERRORS (Continued)

a New York to Los Angeles system. The guidance system for this case must meet the requirement:

$$\hat{A} \times \hat{n} = \hat{n} \times \hat{B}$$

where $\hat{A}$ is the unit vector pointing toward the transmitter
$\hat{B}$ is the unit vector pointing toward the receiver
$\hat{n}$ is the surface normal unit vector

Figure 2 presents the effect of an attitude error on the reflected signal. The errors presented represent the distance along the ground that the reflected signal is removed from the receiver. This is illustrated on the diagram of Figure 2.

Figure 3 presents the effect of a position error on the reflected signal. The errors again represent the displacement of the reflected signal measured as a ground distance away from the receiver.

The data presented illustrates the effect of attitude and position errors. The data further demonstrates the need to eliminate position and attitude errors if point-to-point communication is to be achieved. Elimination of errors is dependent on the disturbing forces, and requires the incorporation of an attitude and position keeping system. The penalty in hardware, fuel, and complexity is in turn subject to trade-offs between position keeping, attitude, and beam-width (for other than point-to-point communication). The trade-offs will be discussed further in the next section on disturbing forces.

C. EFFECT OF DISTURBING FORCES

The effect of the major disturbing forces which tend to displace the satellite from its nominal synchronous position and attitude are presented. These forces are categorized as configuration dependent and non-configuration dependent.

C. EFFECT OF DISTURBING FORCES (Continued)

1. Position Keeping Disturbances (Non-configuration dependent)

Equatorial eccentricity - This force is due to the difference between the orbit radius vector and the local vertical. A velocity increment (Δ V) varying between 0 to 6 fps per year is required to compensate for this force. The magnitude of the Δ V is dependent on satellite position between the major and minor axes of the equatorial ellipse. The propellant required to maintain position is presented in Figure 4 for the worst case (ΔV = 6 fps per year).

Sun-Moon Gravity - The combined gravitational attraction of the sun and moon will force the inclination of an initially stationary orbit to undergo the sinuscidal variation (presented in Figure 5). The propellant required to compensate for this force is presented in Figure 6 as a function of satellite lifetime and thruster specific impulse. The abscissa indicates a permissible orbital inclination maximum from which corrective thrusts are applied which return the inclination to zero. The propellant required is therefore dependent on the tolerance permissible in orbital inclination. It is evident that any orbital inclination variation would require an attitude control system to meet a point-to-point communication mission. It is further evident that a trade-off exists between inclination and attitude control. This is one area suggested for further study.

2. Position Keeping Disturbances (Configuration dependent)

Solar Pressure - Solar force cause changes in the orbital eccentricity, period, inclination, and alignment of the line of apsides. To demonstrate the effect of solar pressure, a flat plate will again be used. Figure 7 shows the eccentricity buildup due to 100% specular solar force on a flat plate. The plate is initially in a stationary orbit with one face continually pointing down. Thickness is assumed negligible hence the total force acts along the radius vector. The propellant required to counteract this force is based

REF. ENGINEERING PROCEDURE S 017

on total torque impulse needed to eliminate the eccentricity buildup. Propellant requirements are presented in Figure 8 as a function of satellite lifetime and area to mass ratio for two I_{sp}. It is evident that propellant required to maintain stationary position is excessive even for the flat plate with zero thickness. Further study in this area is definitely required, particularly of more realistic configuration which include side forces (thickness).

A probable alternative to stationary orbit position keeping would be to determine a stable orbit and provide attitude control. This will be demonstrated for the flat plate under consideration. A stable orbit is one whose eccentricity and period remain constant while the line of apsides rotates with the earth-sun line. This orbit would theoretically require no position keeping propellant. However, the ground trace of the satellite would describe a line dependent on the orbital eccentricity. This produces an attitude steering requirement. Figure 9 presents the stable orbit eccentricities required for the flat plate with area-to-mass ratio dependency considered. The attitude steering requirement would be dependent on the ground trace drift. Figure 9 also presents the maximum longitude deviation off - nominal which is an indication of the steering required. The obvious trade-offs that need to be studied further include attitude propellant and logic for stable orbits for the more realistic configurations mentioned previously. It is expected that the attitude propellant requirements will be significantly lower than attempting to position keep against solar force.

A measure of the influence of side force was obtained by assuming a 6 degree offset in pointing. This corresponds to an equatorial orbit with the satellite reflecting toward the Northern hemisphere. A small component of the surface normal force due to solar pressure thus acts perpendicular to the orbital plane. Figure 10 presents the inclination time history from one orbit due to this small perpendicular component of solar force. The propellant required

to eliminate this inclination buildup is presented in Figure 11. Again it is evident that solar pressure produces severe propellant requirements. This again suggests that attitude steering be substituted for position keeping. This elementary side force evaluation reinforces the conclusion suggested previously. Namely, trade-offs between attitude and position keeping should be investigated further using more realistic configurations.

3. Attitude Disturbances (Configuration dependent)

The major forces which disturb the attitude of the satellite are due to solar pressure and gravity gradient torque. A cursory evaluation is made of the effect of these forces using a flat plate approximation for the saddle configuration. This configuration has the saddle reflector located below the total system CG. The configuration is disucssed in the COMSAT trade off analysis. The configuration is representative and amenable to a simple flat plate approximation. It therefore serves adequately to introduce and expose the effects and problems associated with attitude disturbances.

Solar Torque - As an approximation, the torque due to solar pressure is due to the CP-CG offset between the flat plate and the CG. To provide a side force the plate is assumed to be 10 percent diffuse. The torque histories over one orbital cycle were generated and a total torque impulse equated to the solar torques. This then permitted the evaluation of propellant requirements for varying CP-CG offset and plate size. Figure 12 presents the propellant required to overcome solar torque within the assumptions presented. The curves are for a 10 year lifetime. The shape of the curve (increasing then decreasing) is attributable to the solar torque increasing as the square of the diameter of the plate, while the gross weight is increasing by approximately the cube of the diameter. The previously suggested recommendation for further study with more realistic configurations applies here.

REF: ENGINEERING PROCEDURE 5 017

Gravity-Gradient Torque - The torque due to gravity gradient is dependent on the mass distribition of the satellite and the pointing angle offset from the local vertical. Figure 13 presents propellant required to continuously provide offset pointing for the parameters indicated on the graph. The data is based on the saddle configuration presented in the COMSAT study and is for a 10 year lifetime.

D. Δ V REQUIREMENTS

Total position keeping fuel requirements are obtained from the total ΔV requirement. Total ΔV is, in turn, obtained as the sum of the individual Δ V's required to overcome each disturbance. For the stationary orbit the disturbances include: earth triaxiality (E-W station keeping), sun-moon gravity (N-S station keeping), solar pressure, solar torque, and gravity-gradient torque. For the solar stable orbit, the disturbances are the same except for solar pressure which is eliminated. The individual ΔV requirements are now presented.

1. Triaxiality

The ΔV requirement is obtained from the total impulse required to overcome the gravitational component acting along the orbit tangent:

$$\Delta V = \frac{Ft}{m}$$

where, t = time

m = mass

$$F = \frac{1}{r}\frac{\partial V}{\partial \phi}$$

$$V = -m\frac{\mu}{r}\left[\frac{\epsilon R^2}{2r^2}\cos 2(\phi - \phi_o)\right] + \text{non } \phi \text{ terms}$$

ϵ = equatorial ellipticity $\cong 1.2 \times 10^{-5}$

ϕ_o = equatorial major axis $\cong$ 20 deg. W long

ϕ = satellite longitude over the equator

The satellite was assumed located at 95 deg. W long. (between New York and Los Angeles), and the Δ V requirement was found.

$$\Delta V \cong 2 \text{ fps/yr.}$$

2. Sun Moon Gravity

North-South station keeping requirements were obtained using Reference 1 and assuming a maximum permissible inclination of 1/4 degree. The Δ V values are presented below, and are independent of satellite mass or configuration.

Lifetime	Δ V
3 yrs	460 fps
5 yrs	796 fps
10 yrs	1630 fps

3. Solar Torque

Solar torque Δ V requirements were obtained using Figure 12. A 300 ft diameter satellite with 10% diameter CP-CG offset was assumed. The Δ V to overcome solar torque was determined to be:

$$\Delta V = 19.4 \text{ fps/yr}$$

4. Gravity-Gradient Torque

The Δ V requirement was obtained using Figure 13. A 300 ft diameter satellite with 6 degree offset pointing requirement was used. The Δ V was determined to be:

$$\Delta V = 3.6 \text{ fps/yr}$$

5. Solar Pressure

Solar pressure Δ V requirements are evaluated for the stationary orbit only. The solar stable orbit effectively eliminates these requirements. Solar pressure disturbs the orbit in two ways, in-plane and normal to the plane. These effects are evaluated independently.

a. <u>In-Plane</u>. The in-plane Δ V requirement is total impulse required to eliminate the eccentricity buildup due to solar pressure which is presented in Figure 7. Applying the technique of Reference 2 with tangential thrust, the Δ V requirements are determined as follows:

$$\Delta V = CV_c$$

where:

c = constant

V_c = circular velocity

and c is determined from:

$$\epsilon = 2C + C^2$$

where:

ϵ = eccentricity from Figure 7

Extrapolating the Δ V over one year provides the total ΔV requirements:

$$\Delta V = 858 \text{ fps/yr}$$

b. <u>Normal To Plane</u>. The 6 degree offset pointing requirement produces a solar force component normal to the orbital plane. This face component would produce the inclination buildup presented in Figure 10 of Reference 1. The Δ V required to offset this buildup is determined from the impulse required to eliminate the inclination. The impulse is applied at the line of nodes and evaluated from the following equation assuming Figure 10 is linear over a short initial orbit interval:

$$\Delta V^2 = 2V_c^2 (1-\cos i)$$

i = inclination

V = circular velocity

and for small i:

$$\Delta V = iV_c$$

Extrapolating Δ V over one year provides the total Δ V requirement:

$$\Delta V = 953 \text{ fps/yr}$$

E. RESULTS

Total Δ V requirements for the stationary orbit are obtained by summing the individual requirements presented herein. The requirements are presented in Table I. A tolerance of 1/4 degree in orbital inclination is assumed based on the sun-moon tolerance.

Total Δ V requirements for the solar-stable orbit are presented in Table II. A total latitude drift of 1.65 degrees occurs due to solar pressure (Figure 10) and the 1/4 degree sun-moon tolerance. A longitude drift of 3.6 degrees occurs due to the eccentricity of the stable orbit (ϵ = .031). The total Δ V required for the solar-stable orbit is the same as the stationary orbit except for the solar pressure requirements.

The data of Tables I and II were used to generate the fuel requirements for position keeping presented in Figures 14 and 15. The curves are self-explanatory. Fuel requirements are obtained from the Δ V requirements using the equation:

$$\Delta V = g_o I_{sp} \ln (m_i/m_f)$$

ΔV = velocity increment (fps)

g_o = 32.2 ft/sec^2

I_{sp} = specific impulse (sec)

m_i = initial weight (lb)

m_f = final weight (lb)

REF ENGINEERING PROCEDURE S 017

TABLE I

Stationary Orbit Total Δ V Requirements

Lifetime	Δ V
3 yrs	5968 fps
5 yrs	9976 fps
10 yrs	19990 fps

TABLE II

Solar Stable Orbit Total Δ V Requirements

Lifetime	Δ V
3 yrs	535 fps
5 yrs	922 fps
10 yrs	1880 fps

III. ATTITUDE CONTROL FUEL REQUIREMENTS

A. Introduction

GAC has shown in Section II that fuel needed to overcome solar force and maintain a stationary orbit, is excessive for a large satellite. A synchronous solar-stable orbit was shown to provide an alternative which eliminates the position keeping fuel needed to overcome solar force. Attitude steering is then required to compensate for the orbital position variations due to the eccentricity, and the small inclination of the synchronous solar-stable orbit.

Frick has shown in Reference (3) that the attitude steering fuel requirements are modest when a large satellite in synchronous orbit is required to track a point on the equator. This result was valid for small eccentricity and low inclination orbits.

The PasComSat mission requires the satellite to track any point on the earth's surface. This section shows that attitude steering fuel requirements are small for a large satellite in synchronous orbit, which is required to track any arbitrary point on the earth's surface. This essentially extends to the general case, the result of Reference (3). The steering fuel required due to the synchronous solar-stable orbit is therefore modest. The steering fuel requirements are therefore considerably less severe than position keeping fuel requirements for a large satellite required to point toward an arbitrary earth surface location. Further, steering fuel requirements will not prohibit the use of the solar-stable orbit.

Analysis

Frick has shown in Reference (3) that the attitude fuel required to steer a flat plate is as follows:

REF: ENGINEERING PROCEDURE S-017

In Pitch

For a once per orbit sinusoidal forcing function,

$$\frac{M_f}{M_o} = \frac{4\ r_o\ \omega_o}{g_o\ I_{sp}}\ \theta_o \quad \text{per orbit} \tag{1}$$

For a twice per orbit sinusoidal forcing function,

$$\frac{M_f}{M_o} = \frac{7\ r_o\ \omega_o}{g_o\ I_{sp}}\ \theta_o \quad \text{per orbit} \tag{2}$$

In Roll

For a once per orbit sinusoidal forcing function,

$$\frac{M_f}{M_o} = \frac{7\ r_o\ \omega_o}{g_o\ I_{sp}}\ \phi_o \text{ per orbit} \tag{3}$$

For a steady roll offset,

$$\frac{M_f}{M_o} = \frac{r_o\ \omega_o^{\,2}}{g_o\ I_{sp}}\ \phi_o\ t \tag{4}$$

where a uniform mass distribution was assumed for the flat plate. The symbols used are defined as follows:

M_f = mass of fuel required

M_o = mass of vehicle

r_o = radius of vehicle

ω_o = orbital angular rate

t = time

I_{sp} = specific impulse of fuel

g_o = gravitational acceleration

θ_o = amplitude of the pitch forcing function

ϕ_o = amplitude of the roll forcing function

The forcing functions which simulate the pitch and roll steering requirements for offset pointing are derived in Reference 8. The results are presented here for $\beta_o = 0$, where β_o is the initial longitude. This assumes the satellite to be at the same longitude as the tracking point initially.

Orbital Inclination

When the satellite is on a synchronous orbit inclined at an angle i to the equatorial plane, the ground trace is a figure eight pattern. The pitch and roll angles required to continuously track an arbitrary point on the earth are given for small i by the function:

$$\theta \cong \theta_{o_1} \cos \omega_o t - \theta_{o_2} \sin 2 \omega_o t \qquad (5)$$

$$\phi \cong \phi_{o_1} - \phi_{o_2} \sin \omega_o t \qquad (6)$$

where:

$$\left.\begin{aligned} \theta_{o_1} &\cong i\ e\ \sin\lambda \\ \theta_{o_2} &\cong \frac{i^2\ e}{4}\ \cos\lambda \end{aligned}\right\} \qquad (7)$$

$$\left.\begin{aligned} \phi_{o_1} &\cong e\ \sin\lambda \\ \phi_{o_2} &\cong e\ i\ \cos\lambda \end{aligned}\right\} \qquad (8)$$

i = orbital inclination

λ = latitude of earth point being tracked

e = R_o/r_s

R_o = earth radius

r_s = synchronous orbit radius

Equations (5) through (8) are obtained from Reference (5), with $\beta_o = 0$.

Eccentricity

For a synchronous equatorial orbit with small eccentricity (ϵ), the pitch and roll angles required to track an arbitrary point on the earth are given by the functions:

$$\left.\begin{aligned} \theta &\cong \theta_{o_3} \sin \omega_o t \\ \phi &\cong \phi_{o_3} \end{aligned}\right\} \qquad (9)$$

where

$$\left.\begin{aligned} \theta_{o_3} &\cong \frac{-2\, e\, \epsilon \cos\lambda}{1 - e \cos\lambda} \\ \phi_{o_3} &\cong e \sin\lambda \end{aligned}\right\} \qquad (10)$$

ϵ = orbital eccentricity

Equations (9) and (10) are obtained from Reference (5) with $\beta_o = 0$.

The fuel requirement for steering with offset pointing included is now obtained by substituting the forcing function amplitudes into the appropriate fuel equations (1) through (4). Note that the steady state deflection terms in roll are duplicated in the approximate forcing functions for inclination and eccentricity. These terms represent the steady gravity-gradient torque and should not be added to obtain a total fuel requirement. The fuel required will therefore be presented as that due to steady offset plus the oscillation about the steady offset.

Steady Deflection Fuel (For either inclination or eccentricity)

$$\frac{M_f}{M_o} \cong \frac{r_o \ \omega_o^2}{g_o \ I_{sp}} (e \sin \lambda \ ) \ t \qquad (11)$$

Fuel for Oscillation About Steady Offset Due to Orbital Inclination

Pitch

$$\frac{M_f}{M_o} \cong \frac{r_o \ \omega_o}{g_o \ I_{sp}} \quad i \ e \quad \left(4 \sin\lambda + \frac{7}{4} \ i \cos\lambda\right) \text{ per orbit} \qquad (12)$$

Roll-Yaw

$$\frac{M_f}{M_o} \cong \frac{7 \ r_o \ \omega_o}{g_o \ I_{sp}} \quad e \ i \cos\lambda \quad \text{per orbit} \qquad (13)$$

Fuel for Oscillation About Steady Offset Due to Orbital Eccentricity

Pitch

$$\frac{M_f}{M_o} \cong \left(\frac{8 \ r_o \ \omega_o}{g_o \ I_{sp}}\right)\left(\frac{e\epsilon \ \cos\lambda}{1 - e \cos\lambda}\right) \quad \text{per orbit} \qquad (14)$$

Roll-Yaw

$$\frac{M_f}{M_o} \cong 0 \qquad (15)$$

Results

The steering fuel required is now obtained for the satellite configuration of Section II. That configuration was approximately a flat plate with an area-to-weight ratio of 23.6 ft^2/pound. The following inputs will therefore be used for the synchronous orbit:

r_o = 150 feet

I_{sp} = 70 sec.

ω_o = $.728 \times 10^{-4}$ rad/sec

e = .151

g_o = 32.2 ft/sec^2

Steering fuel required for this configuration becomes:

Steady Deflection

$$\frac{M_f}{M_o} \cong .00117 \sin\lambda \qquad \text{per year}$$

Orbital Inclination

$$\frac{M_f}{M_o} \cong (2.68 \times 10^{-4})(i)\left[(4\sin\lambda + \frac{7}{4} i \cos\lambda) + (7 i \cos\lambda)\right] \quad \text{per year}$$

Eccentricity

$$\frac{M_f}{M_o} \cong (2.68 \times 10^{-4}) \frac{8 \epsilon \cos\lambda}{1 - (.151) \cos\lambda} \quad \text{per year}$$

Finally, if the point to be tracked is assumed located at 45 deg north latitude

($\lambda = 45°$)

and, if an inclination of 10 degrees is assumed, this being greater than that which would result from either the solar-stable orbit of Section II, or the sun-moon stable orbit of Reference (3), and, if an eccentricity (ϵ) of .031 is assumed, which is the solar-stable orbit of Section II, then the total fuel requirement becomes:

$$\frac{M_f}{M_o} \cong .0012 \quad \text{per year}$$

i.e., the total attitude steering fuel requirement for the PasComSat configuration of Section II will never be greater than approximately .12 percent M_o per year, if the solar-stable, or the sun-moon stable orbits are used.

IV. ORBITAL STABILITY OF PASSIVE COMMUNICATION SATELLITES

A. Introduction

This section describes the methods used and results of a study to determine the orbital stability of a large flat plate* passive communications satellite in a 24-hour orbit. Orbital stability as used here means the stability of orbital elements under the influence of solar radiation pressure and the perturbing effects of the gravity of the sun and the moon. Stability of elements for passive communication satellites is an important consideration for the following reasons:

(1) The passive nature of the satellite tends to result in large area-to-mass ratios and hence large fuel requirements to overcome solar radiation pressure forces.

(2) The maintenance of an orbital period of one day requires that the semi-major axis be held constant. It will be shown that this requirement implies that the eccentricity be held constant and that the major axis maintain a constant rate of angular rotation.

---

*The scope of this study was limited. Therefore, the saddle shape was approximated by a flat plate. In either cases the conclusions would be the same with slightly different numerical results.

(3) In many cases, there is a requirement to minimize the amount of steering required of a ground antenna. This requirement implies a small constant value of orbital inclination with respect to the earth's equator. It will be shown that this requirement necessitates that an angle of 90 degrees be maintained between the earth sun line and the line of nodes.

It will be shown that it is possible to achieve an orbit which is stable in eccentricity, major axis, inclination, and argument of perigee under the influence of solar pressure alone. It will also be shown that it is possible to minimize the inclination change due to sun-moon gravity effects. The cause and effect relationship between forces and orbit perturbations is understandable when either of these effects occurs by itself. However, the motion which results when both effects are present is more complicated due to their interrelationship.

Neither effect is predominant. Consequently, a study beyond the scope of this one would be needed to optimize the orbit under the influence of both solar radiation pressure

and semi-moon gravity.

B. Discussion

1. Stability of Major Axis

Reference (7) shows that in order for an orbit to be stable in major axis and consequently period, it must have a unique eccentricity which is also stable and which causes the perigee point to continuously align with the earth-sun line. For the case under consideration (A/M = 23.6 ft^2/lb, 24 hour orbit) the value of eccentricity was determined to be 0.031. Computer runs later led to the conclusion that $\epsilon = 0.028$ gave a more stable orbit. Figure 16 shows a comparison between stable and unstable eccentricities.

C. Stability of Inclination

It was also shown in Reference (7) that stability of inclination can be maintained under the influence of solar pressure alone if the ascending node is initially 90 degrees west of the earth-sun line and if the proper inclination is selected to maintain this relative orientation. For the satellite in question, this value of inclination was 0.206 degree.

REF: ENGINEERING PROCEDURE 3.01

Figure 17 shows the results of computer runs for three different cases. In the first case, the sun is initially 90 degrees ahead of the node and the inclination is 0.206 degrees. This is the stable case described above and it is also apparently stable in the three dimensional case where the angular relationship varies ± 10 degrees from the desired position. The other two cases represent departures from the stable case and the accompanying departures from stability are apparent.

The effect of sun-moon gravity on inclination is due to a coning of the normal to the orbital plane around an axis at an angle of 7° 20' to the north pole (Reference (4)).

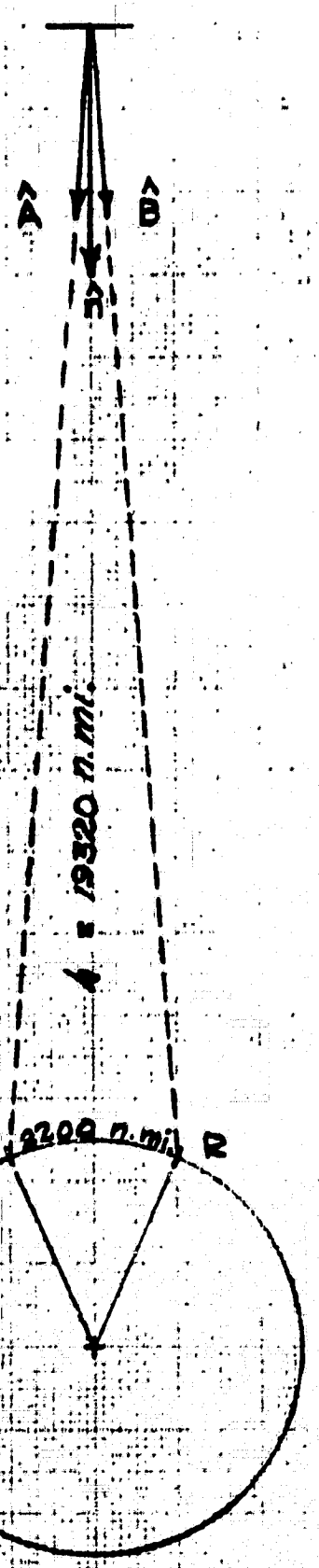
The effect of this coning on an initially zero inclination is shown in Figure 18. The inclination could be minimized for the greatest length of time by initially orienting the orbit such that inclination is decreasing (point A). The orbit would then decrease to zero and build up to the same value B over the life of the satellite.

However, this would never occur in practice since the solar radiation pressure would shift the orbit normal continuously

so that it would not remain in the same cone. Figure 19 shows a comparison between orbit histories for the solar radiation pressure stable orbit of Figure 17 and the same orbit with sun-moon gravitational effects included. Clearly, the inclination is no longer stable. Initially, the gravity effect decrease the inclination which in turn speed up the rate of rotation of the node position. With the node position gaining on the sun position, the solar pressure increases the inclination. Further attempts to gain a stable inclination under the influence of both types of perturbation should parametrically examine the variables of Figure 19 while varying the initial values of the node position and inclination.

FOR BETTER COPY CONTACT THE DOCUMENT ORIGINATOR.

IDEAL PASSIVE COMSAT GEOMETRY



Â - TRANSMITTER VECTOR

B̂ - RECEIVER VECTOR

n̂ - SURFACE NORMAL

T - TRANSMITTER

R - RECEIVER

FIG. 1

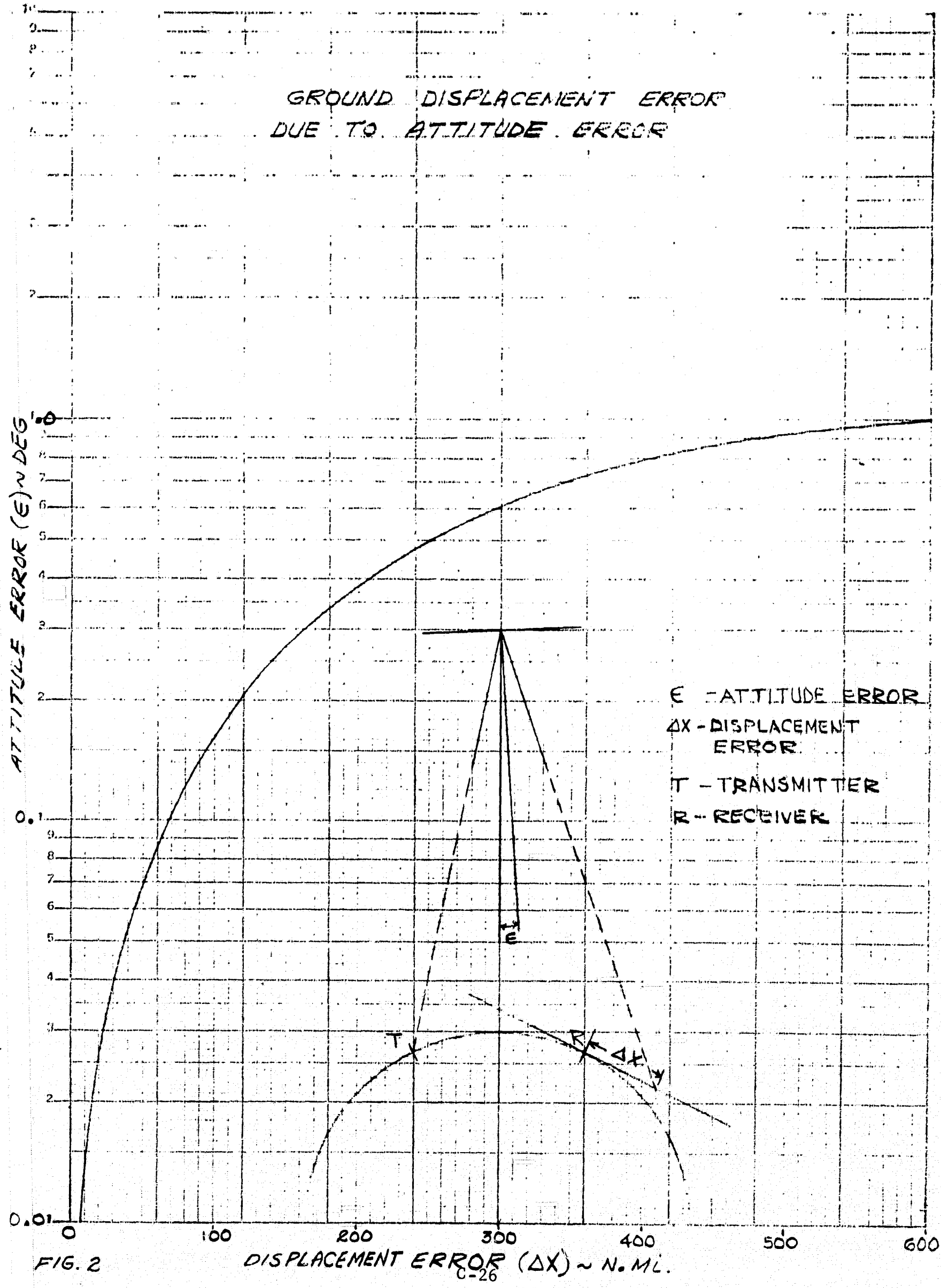


FIG. 2 DISPLACEMENT ERROR (ΔX) ~ N. MI.

GROUND DISPLACEMENT ERROR

DUE TO POSITION ERROR

T - TRANSMITTER
R - RECEIVER
Δx - DISPLACEMENT ERROR
δ - POSITION ERROR

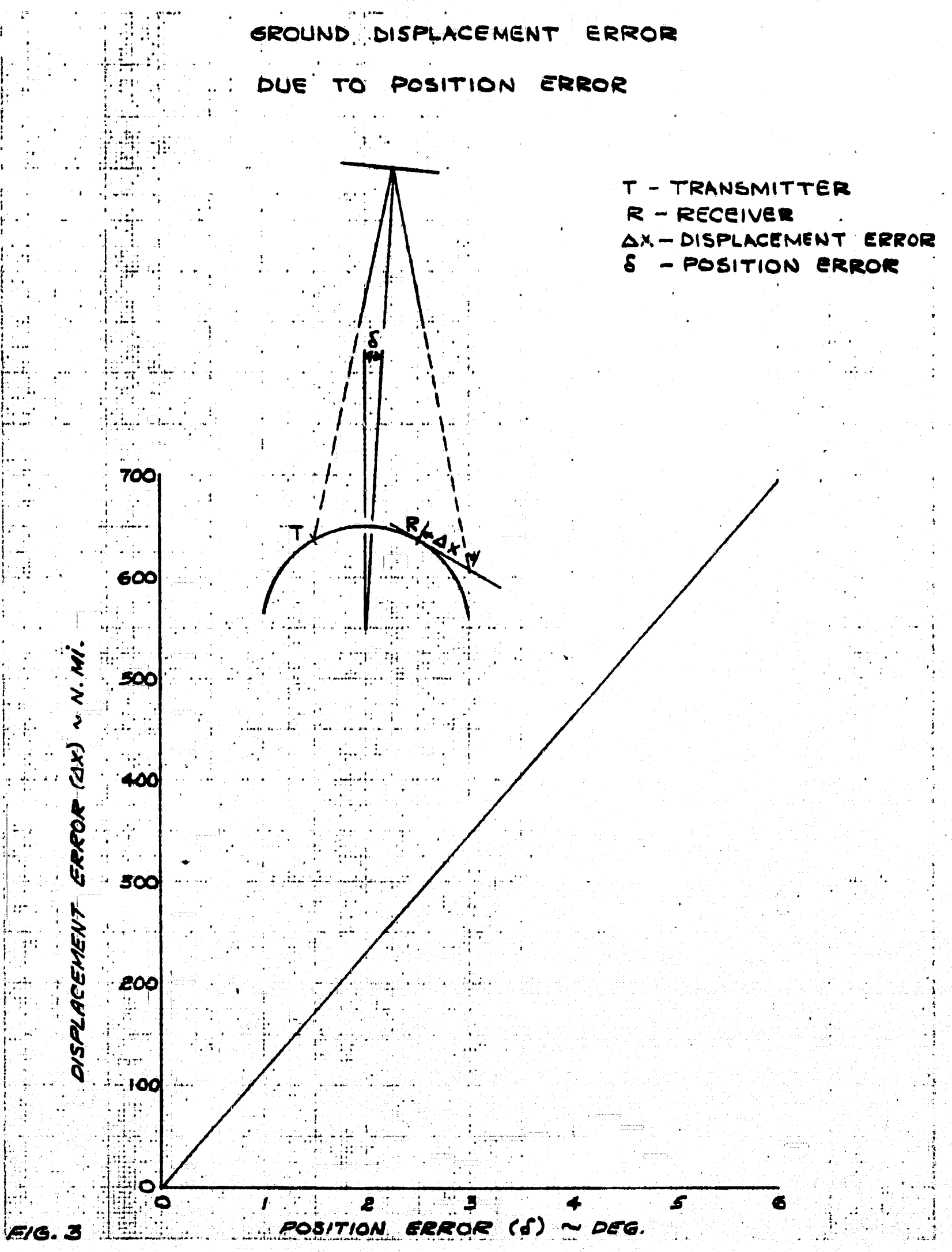


FIG. 3

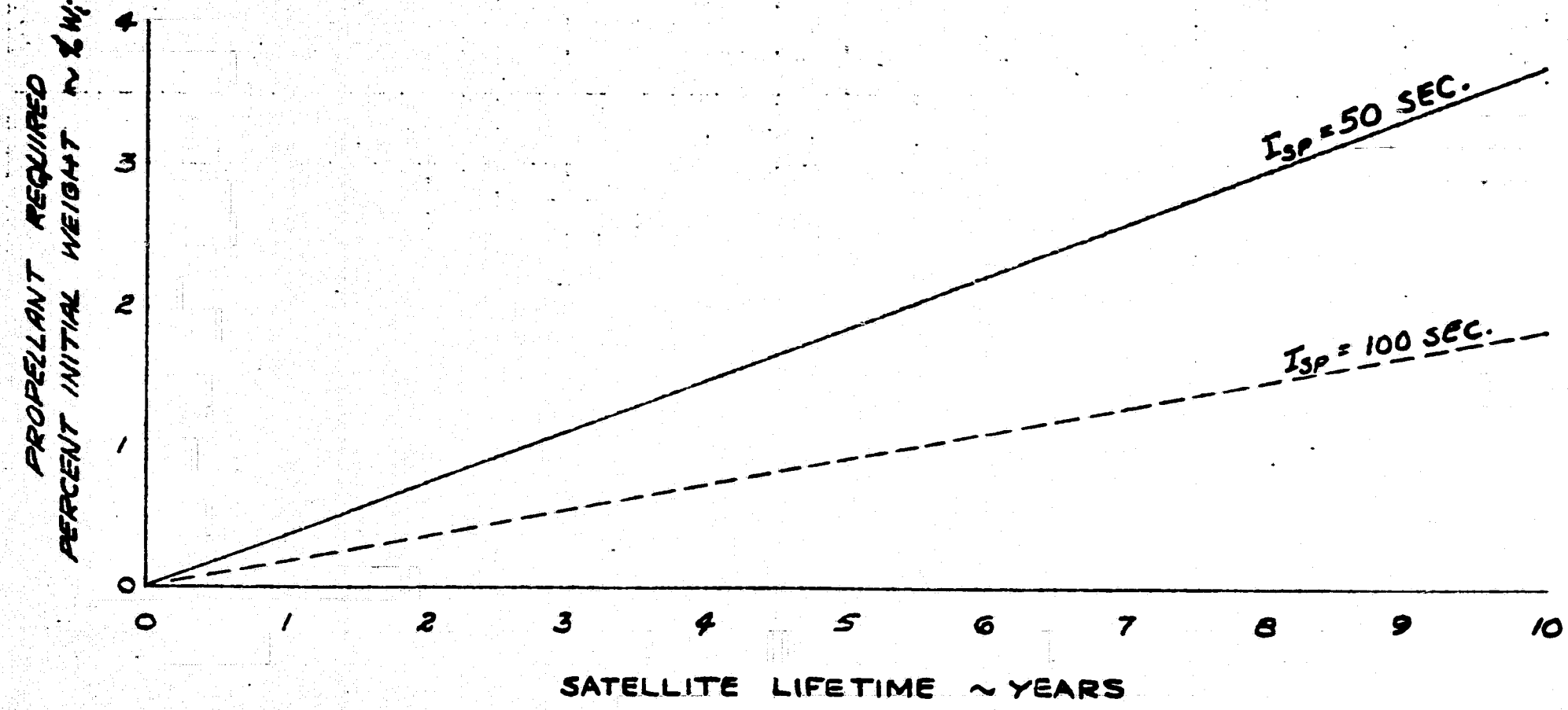
JR 220 (7-43)
REF: ENGRG PROCEDURE 3.017

FIG. 4

EAST - WEST STATIONKEEPING PROPELLANT
VS.
SATELLITE LIFETIME

(SYNCHRONOUS ORBIT)
(EQUATORIAL TRIAXIALITY - WORST CASE)

I_{SP} = SPECIFIC IMPULSE



INCLINATION BUILDUP

DUE TO

SUN - MOON GRAVITY

(FROM REF. 1)

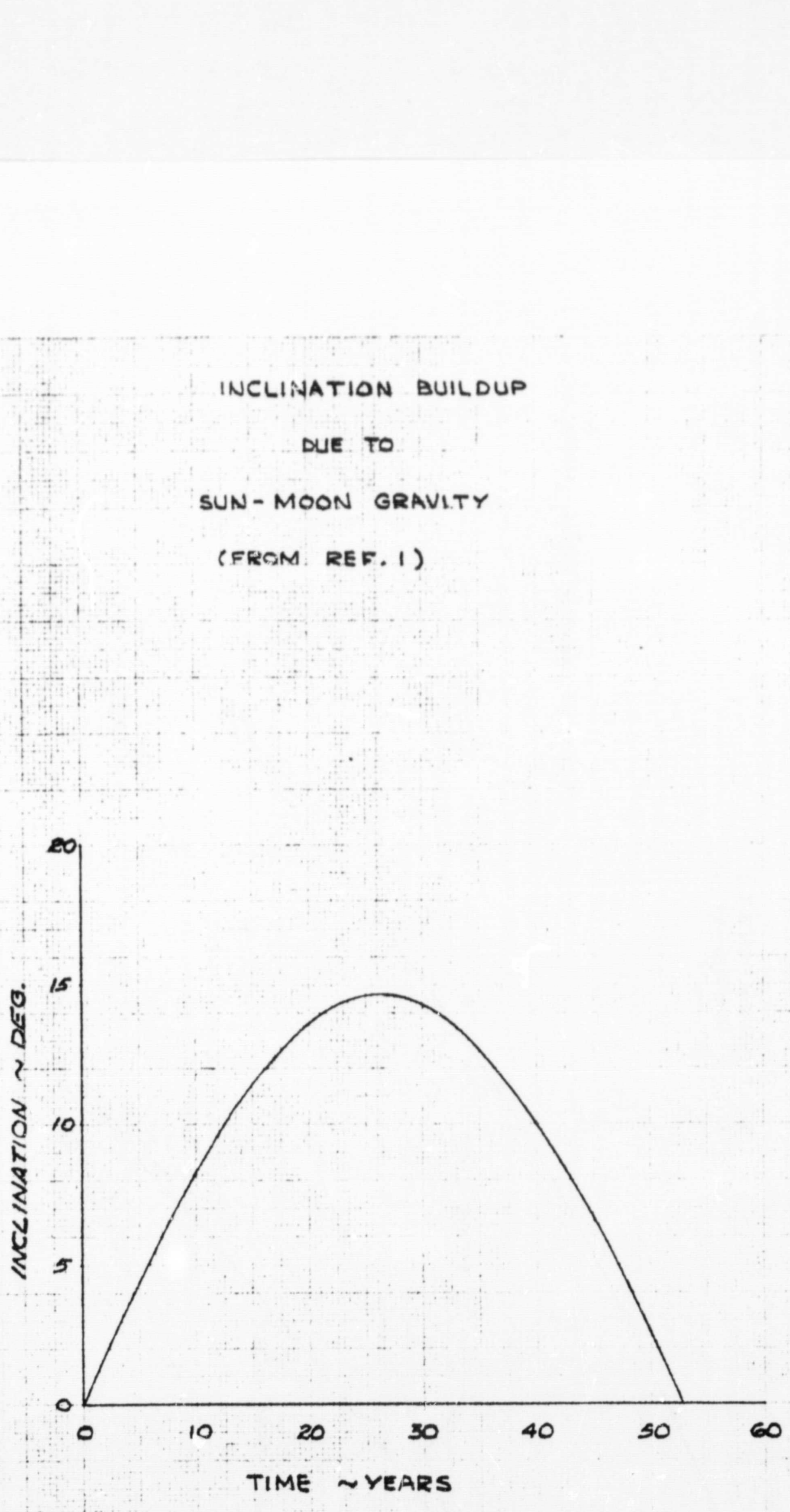


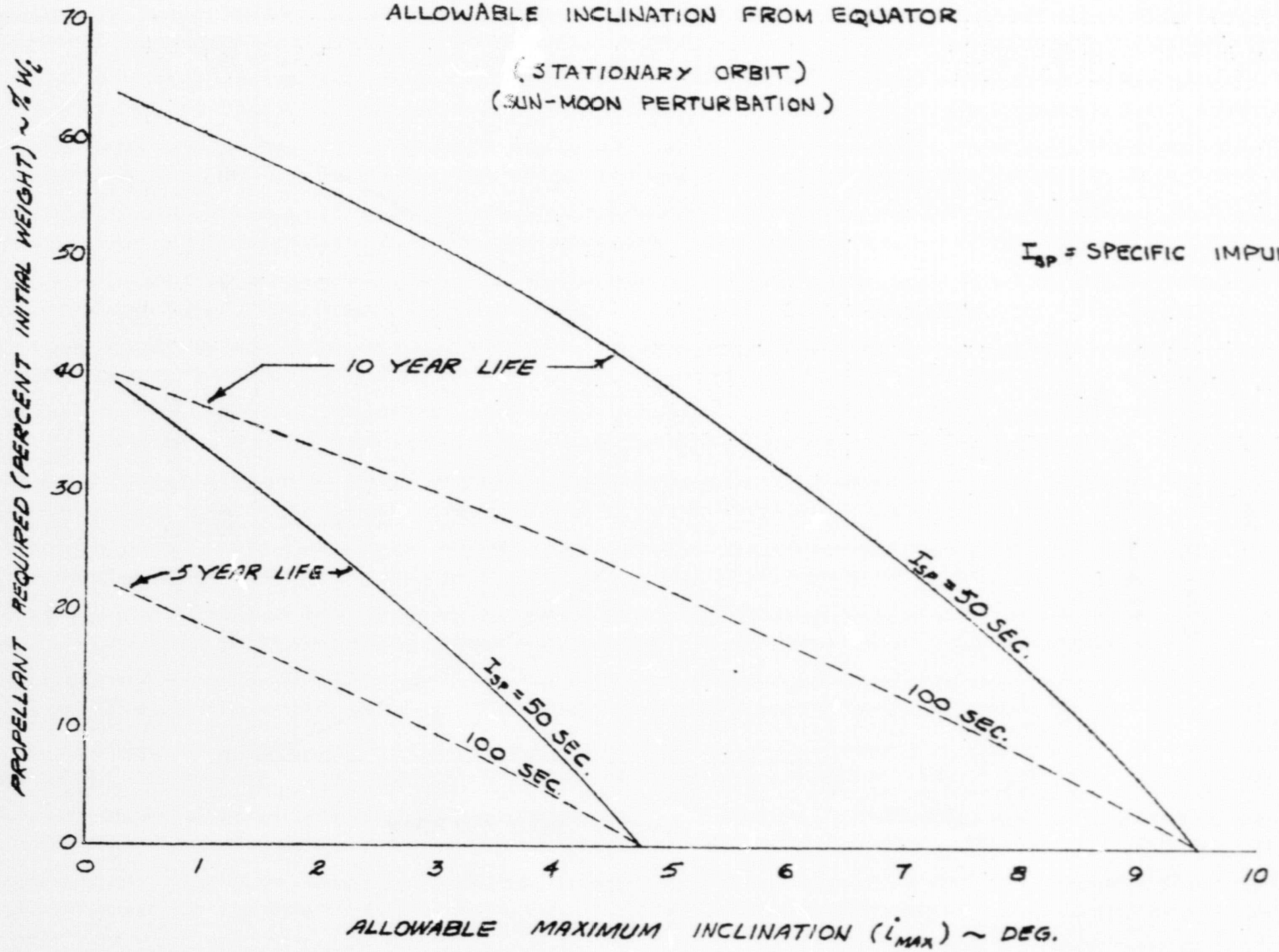
FIG. 5

JR 220 (7-63)
REF: ENGRG PROCEDURE S-017

FIG. 6

NORTH - SOUTH STATIONKEEPING PROPELLANT
VS.
ALLOWABLE INCLINATION FROM EQUATOR

(STATIONARY ORBIT)
(SUN-MOON PERTURBATION)



I_{SP} = SPECIFIC IMPULSE

"REPRODUCIBILITY OF THE ORIGINAL PAGE IS POOR;
FOR BETTER COPY CONTACT THE DOCUMENT ORIGINATOR."

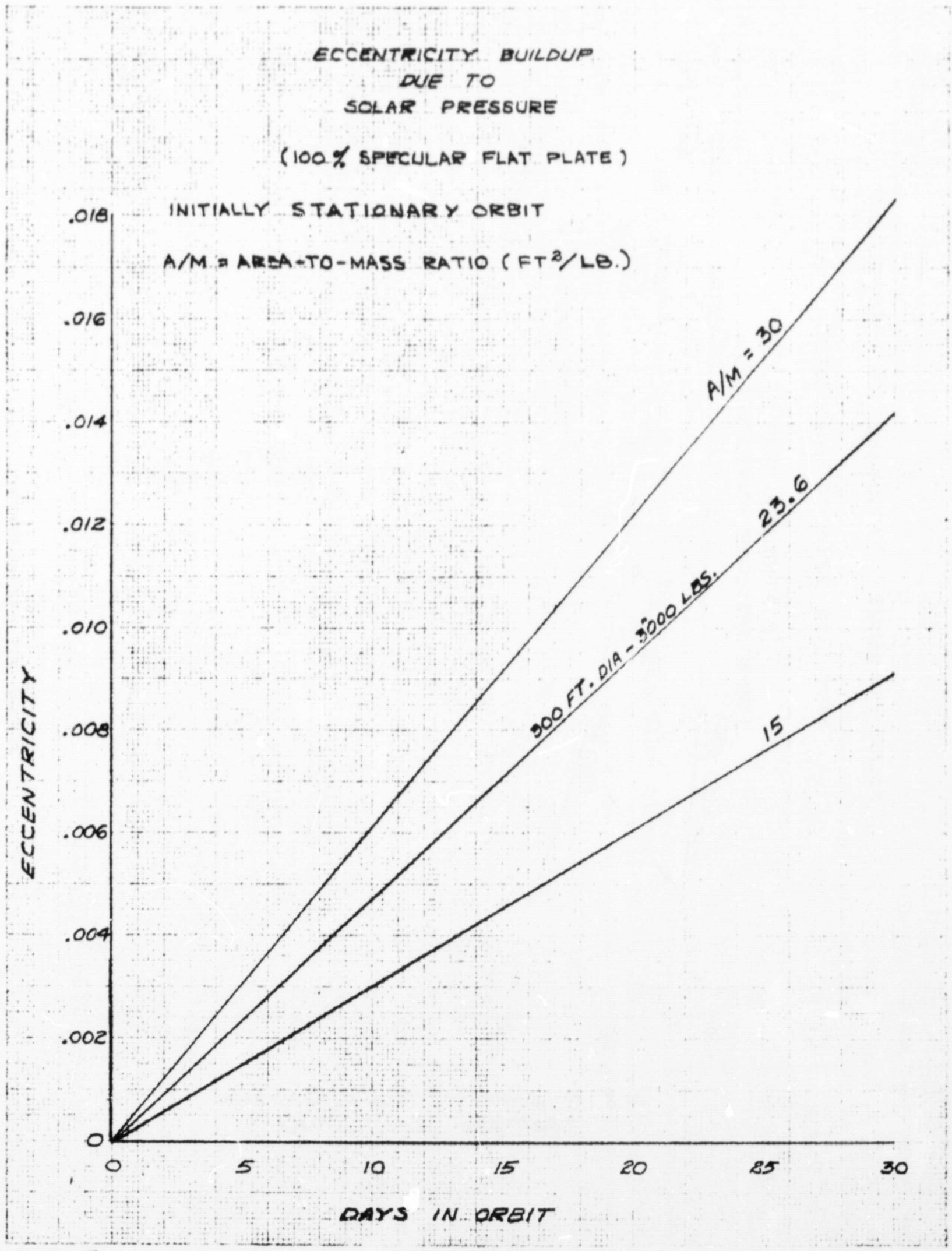


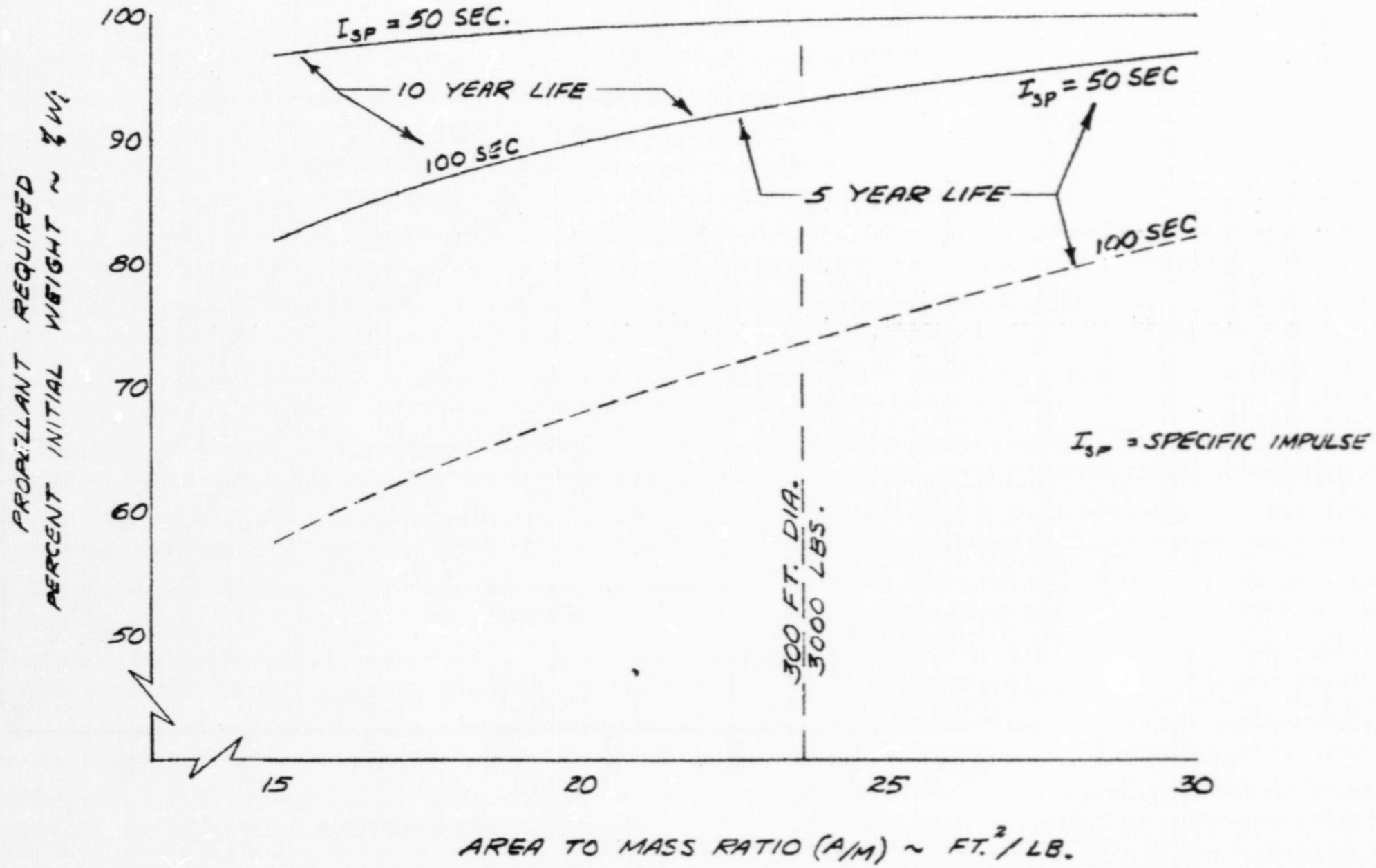
FIG. 7

JR 220 (7-63)
REF: ENGRG PROCEDURE S-017

FIG. 8

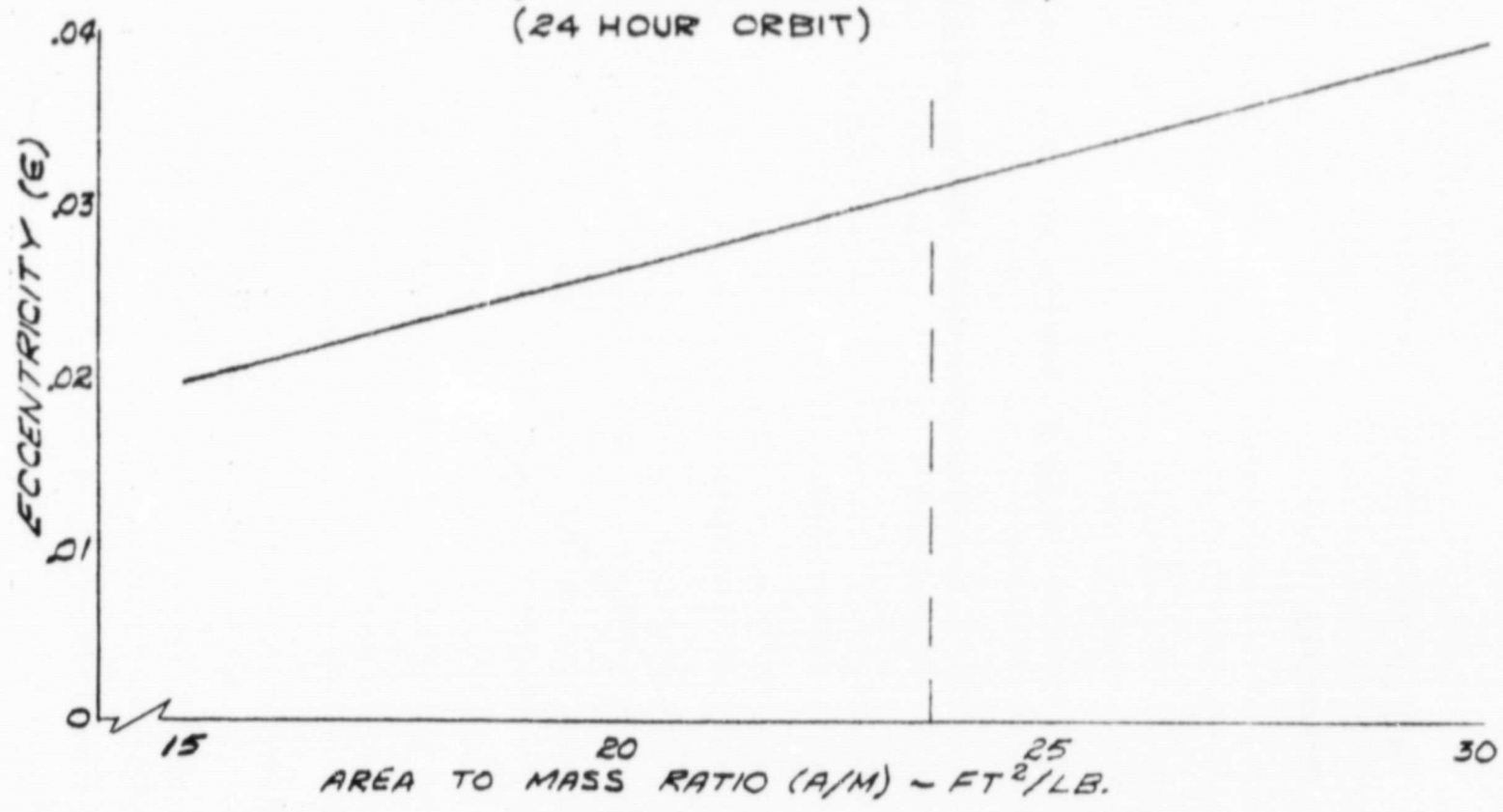
SOLAR PRESSURE STATIONKEEPING PROPELLANT
VS.
SATELLITE AREA TO MASS RATIO

(STATIONARY ORBIT)
(100 % SPECULAR FLAT PLATE)



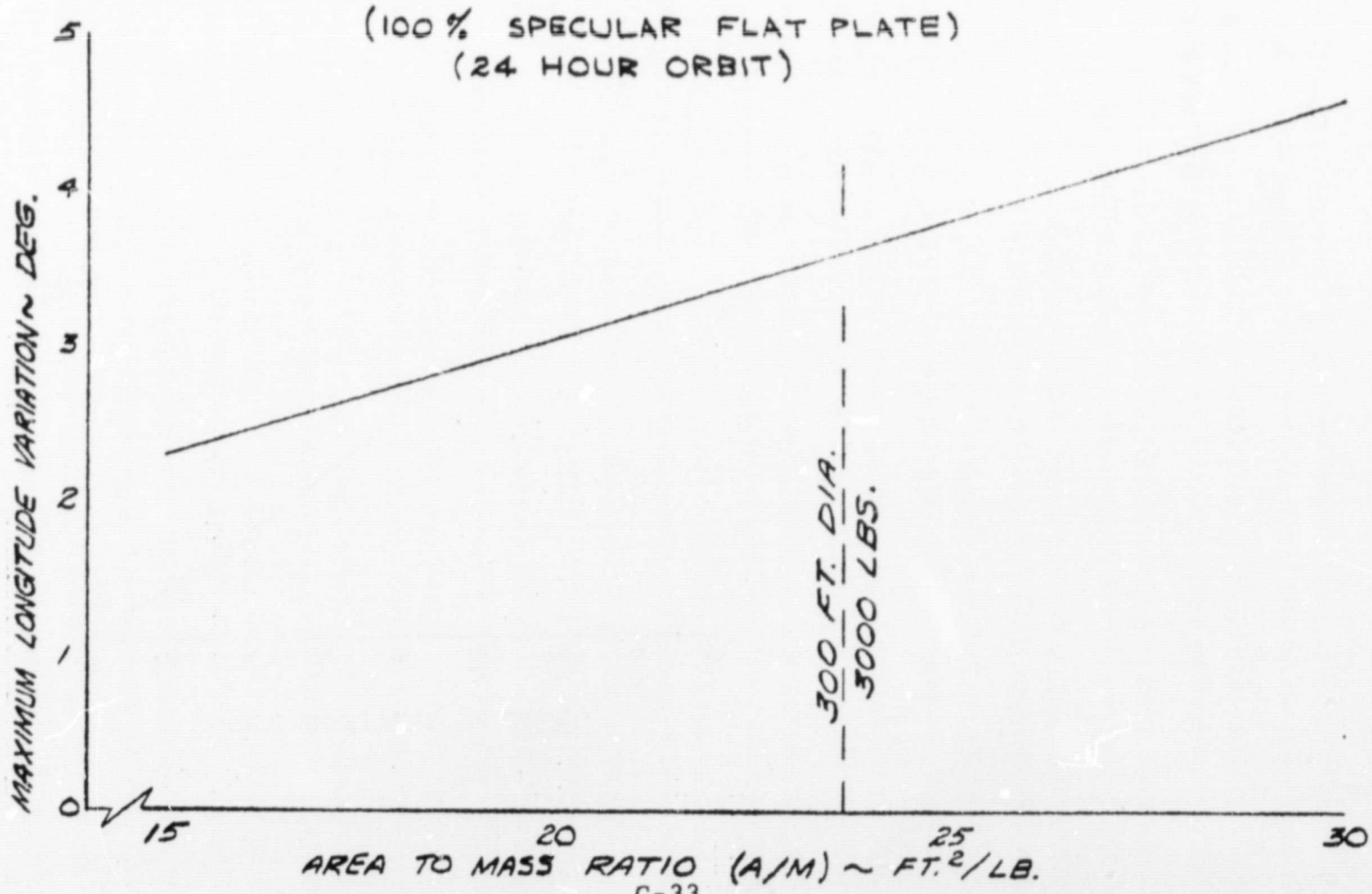
STABLE ORBIT ECCENTRICITY

(100 % SPECULAR FLAT PLATE)
(24 HOUR ORBIT)



STABLE ORBIT LONGITUDE VARIATION

(100 % SPECULAR FLAT PLATE)
(24 HOUR ORBIT)



JR 220 (7-63)
REF: ENGRG PROCEDURE S-017

FIG. 9

FIG. 10

ORBIT INCLINATION BUILDUP DUE TO 6 DEGREE OFFSET POINTING

100 % SPECULAR FLAT PLATE

AREA-TO-MASS RATIO = 23.6 FT^2/LB

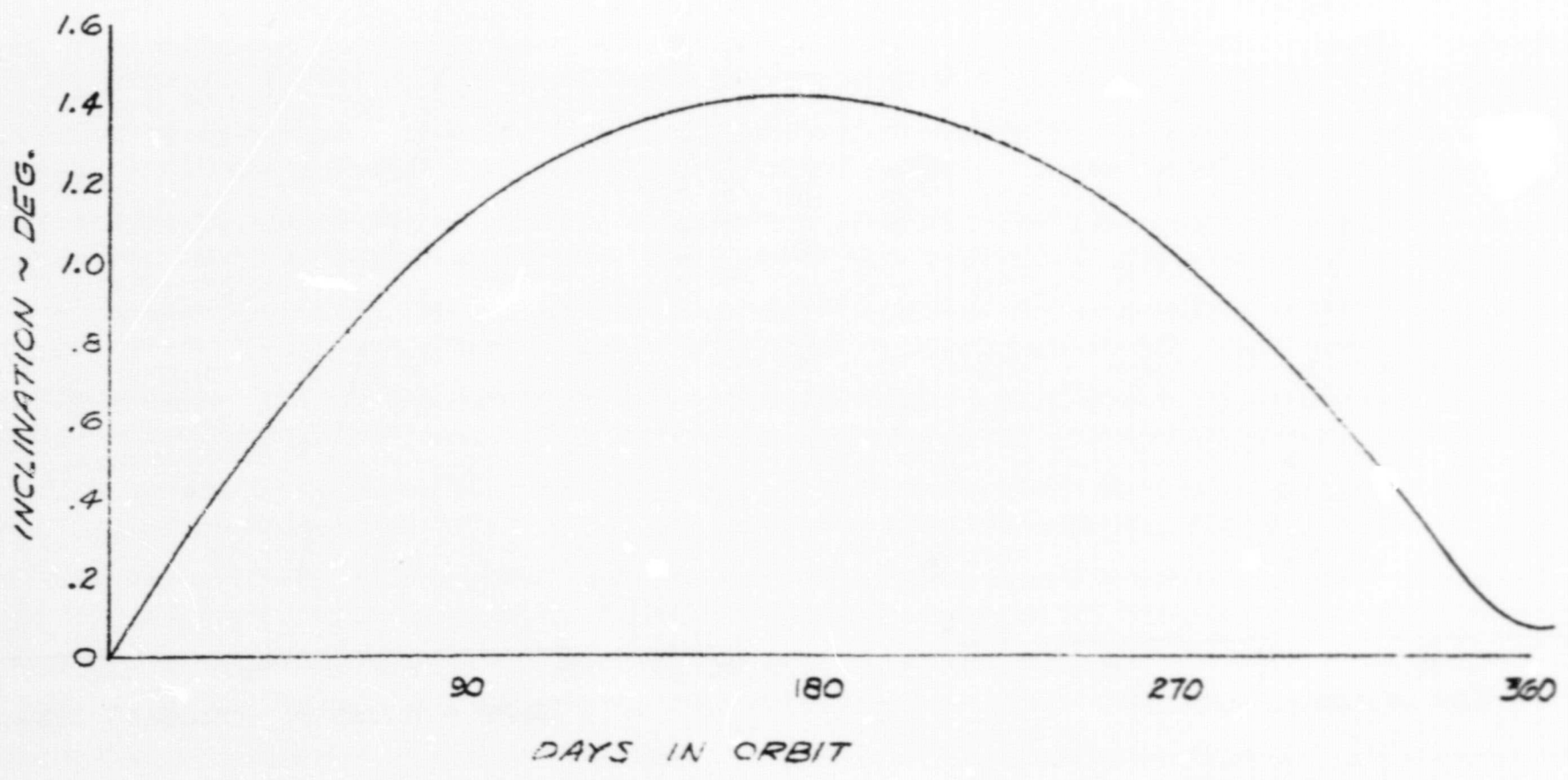


FIG. 11

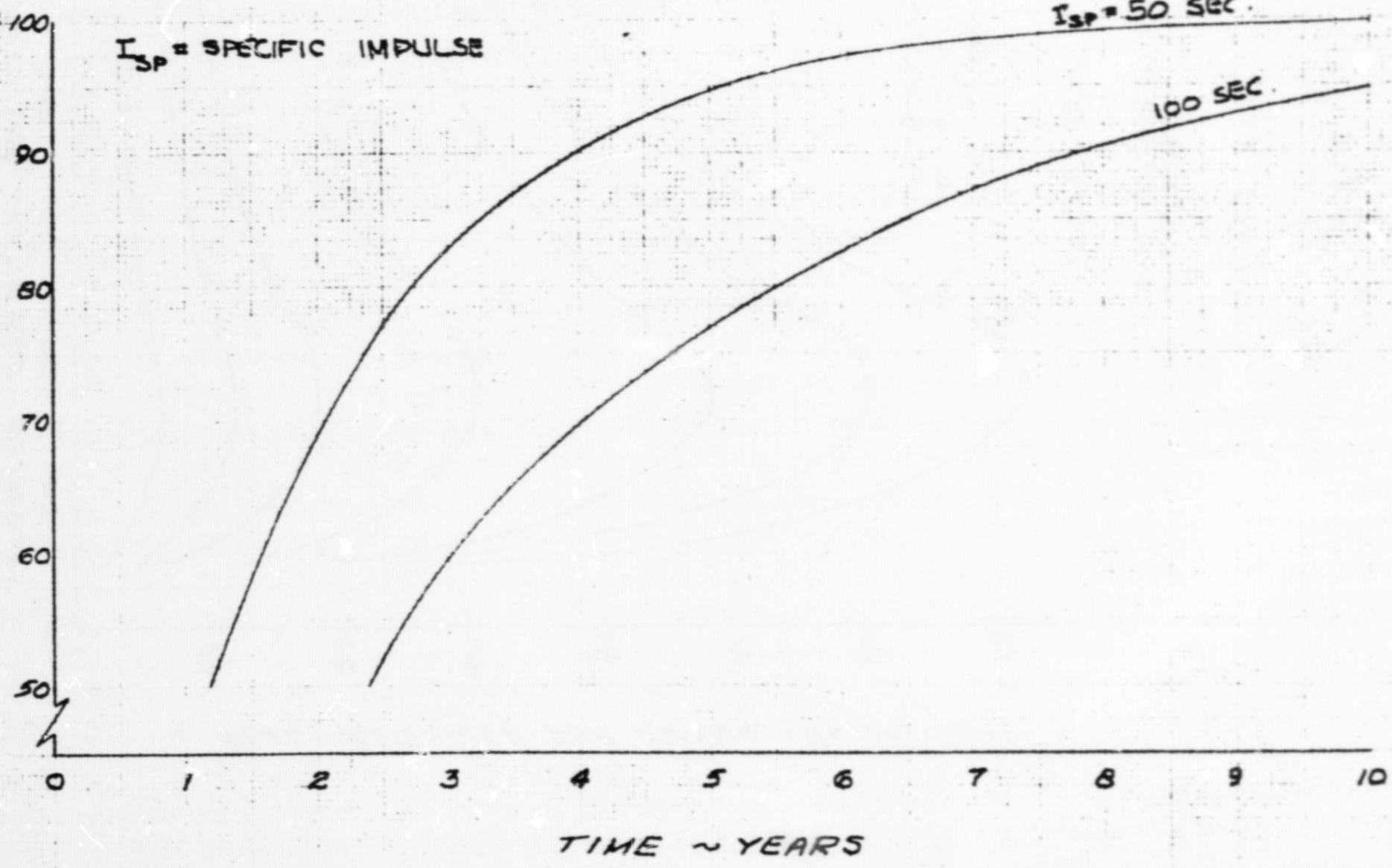
PROPELLANT REQUIRED TO ELIMINATE INCLINATION BUILDUP

6 DEGREE OFFSET POINTING

100 % SPECULAR FLAT PLATE

AREA TO MASS RATIO (A/M) = 23.6 % FT^2/LB.
(300 FT. DIA. - 3000 LBS.)

I_{SP} = SPECIFIC IMPULSE

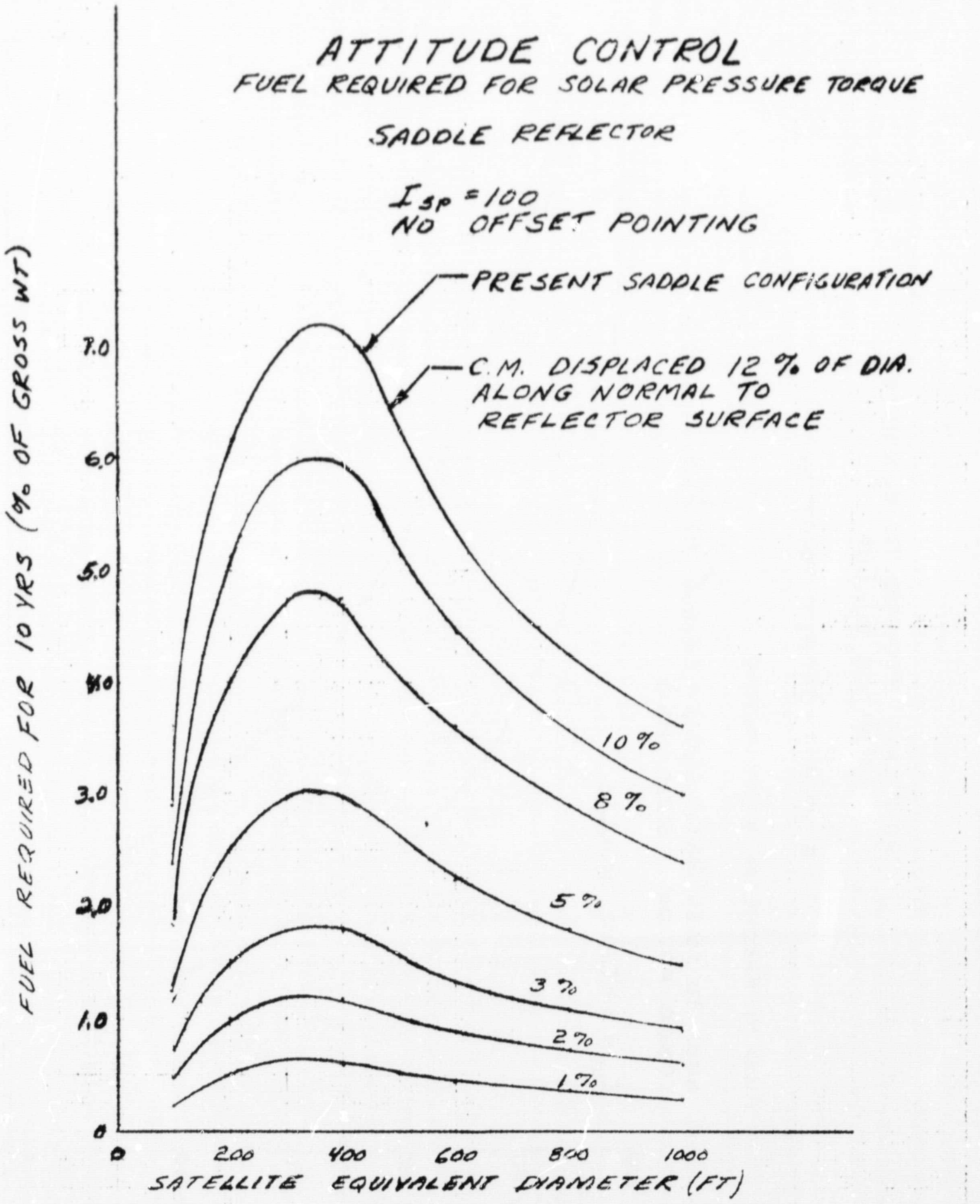


"REPRODUCIBILITY OF THE ORIGINAL PAGE IS POOR.
FOR BETTER COPY CONTACT THE DOCUMENT ORIGINATOR."

ATTITUDE CONTROL
FUEL REQUIRED FOR SOLAR PRESSURE TORQUE

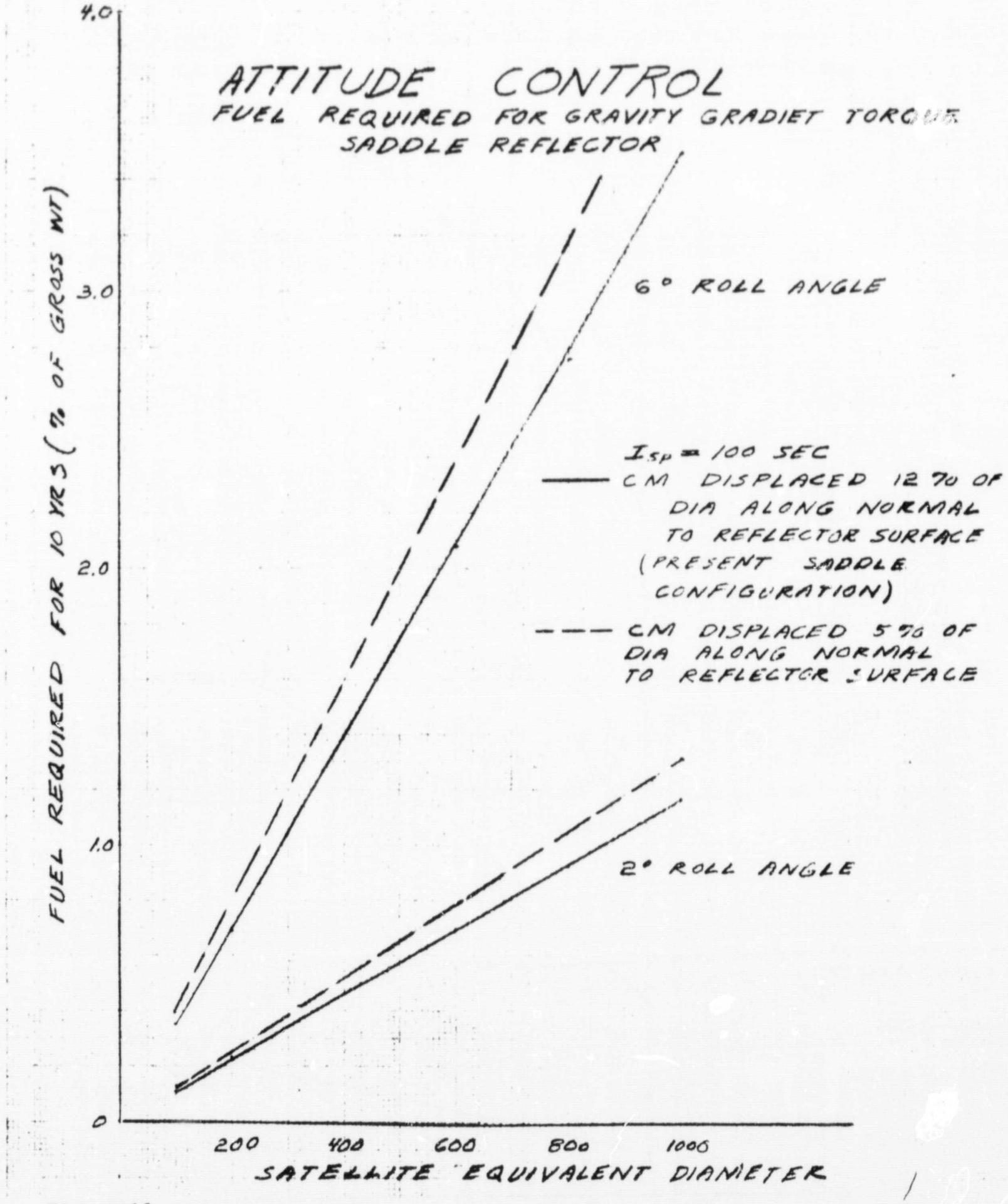
SADDLE REFLECTOR

$I_{sp} = 100$
NO OFFSET POINTING



REF: ENGRG PROCEDURE S-017

FIG. 12



JR 220 (7-63)
REF: ENCAG PROCEDURE S-017

Figure 13.

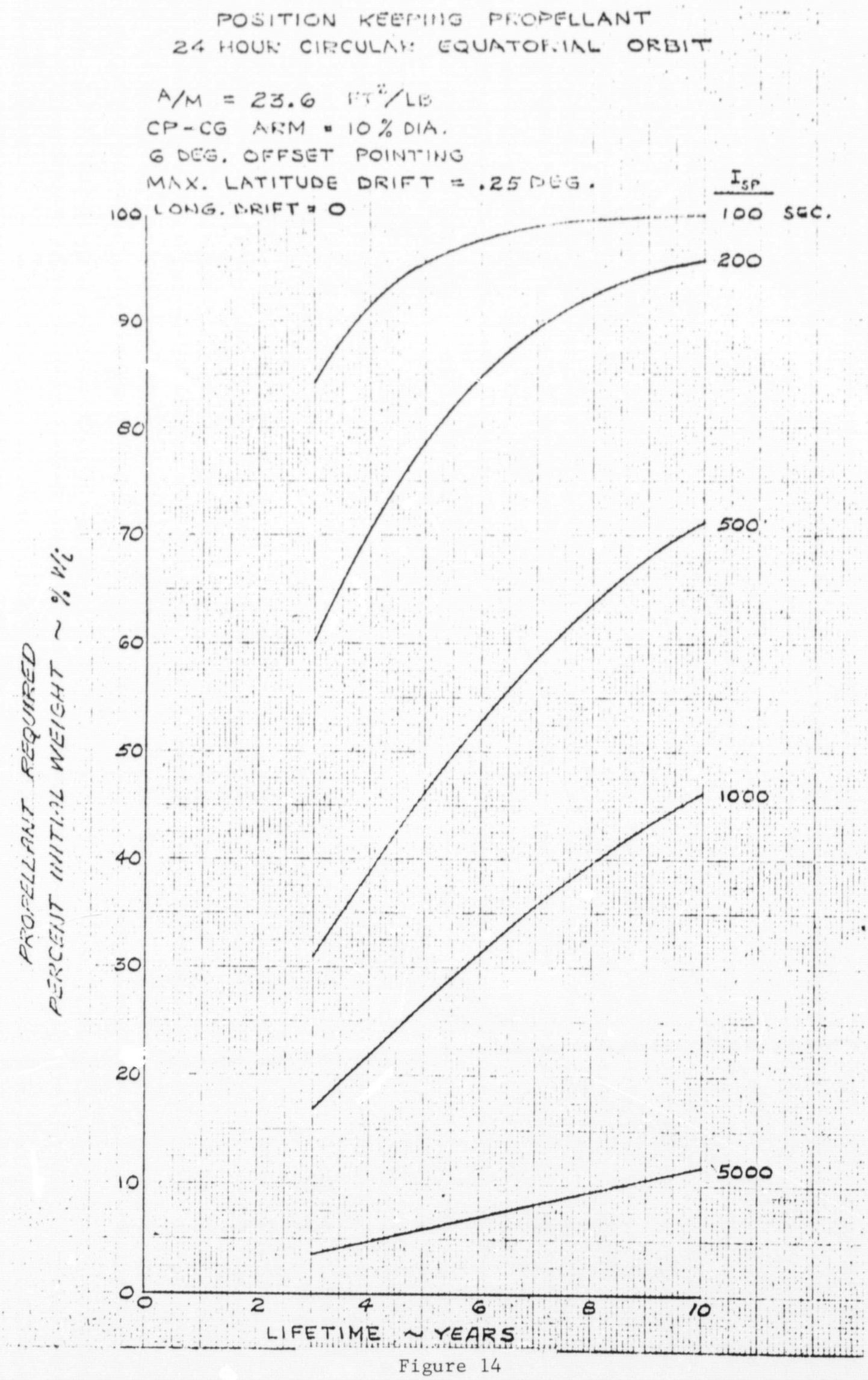

POSITION KEEPING PROPELLANT
24 HOUR CIRCULAR EQUATORIAL ORBIT
A/M = 23.6 FT²/LB
CP-CG ARM = 10 % DIA.
6 DEG. OFFSET POINTING
MAX. LATITUDE DRIFT = .25 DEG.
LONG. DRIFT = 0
I_{SP}
100 SEC.
200
500
1000
5000
PROPELLANT REQUIRED
PERCENT INITIAL WEIGHT ~ %
100
90
80
70
60
50
40
30
20
10
0
0
2
4
6
8
10
LIFETIME ~ YEARS

Figure 14

POSITION KEEPING PROPELLANT
24 HOUR SOLAR-STABLE EQUATORIAL ORBIT

A/M = 23.6 FT²/LB.
CP-CG ARM = 10 % DIA.
6 DEG. OFFSET POINTING
MAX. LATITUDE DRIFT = 1.65 DEG.
MAX. LONG. DRIFT = 5.6 DEG.
ECCENTRICITY = .031

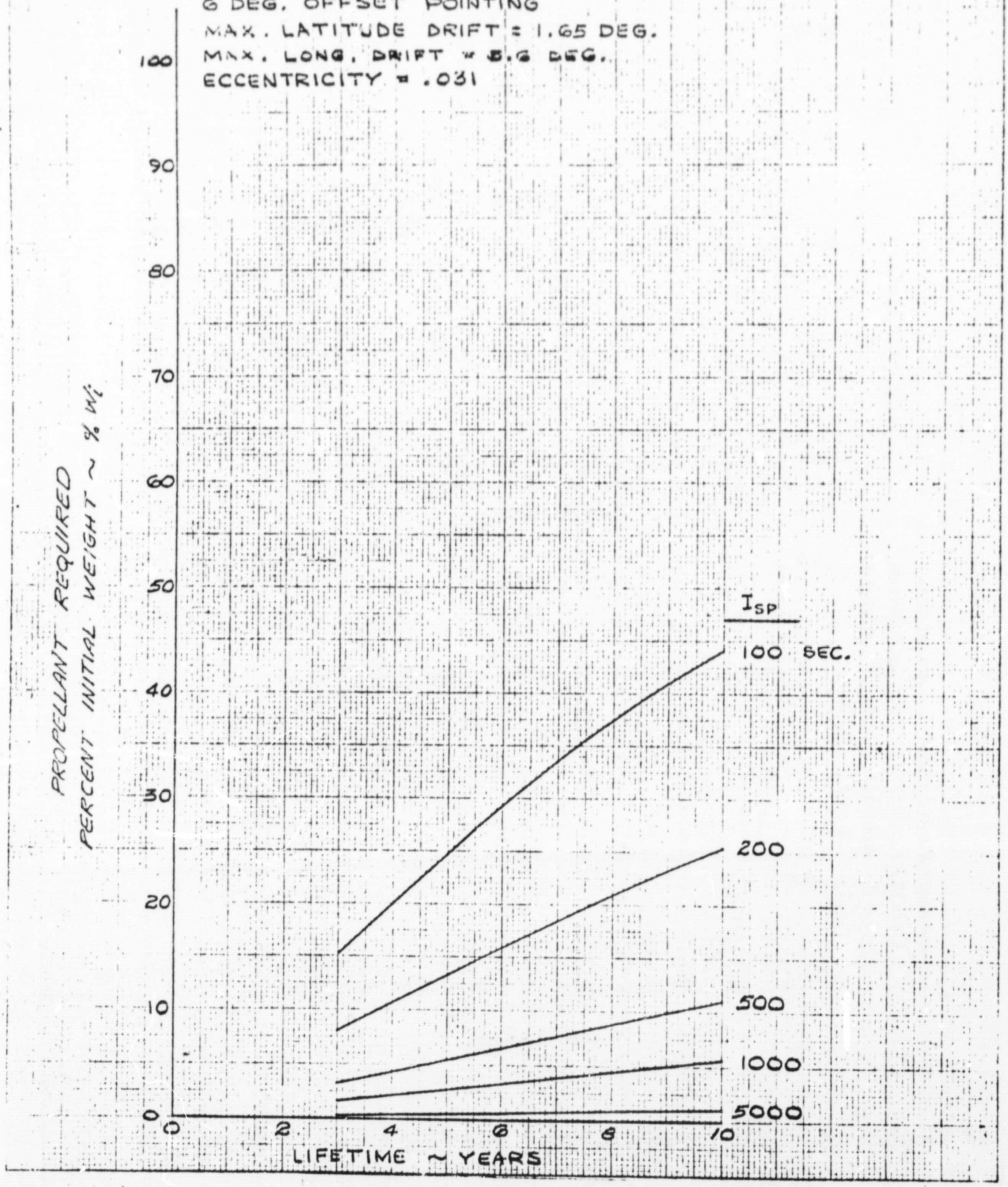


Figure 15

"REPRODUCIBILITY OF THE ORIGINAL PAGE IS POOR;
FOR BETTER COPY CONTACT THE DOCUMENT ORIGINATOR."

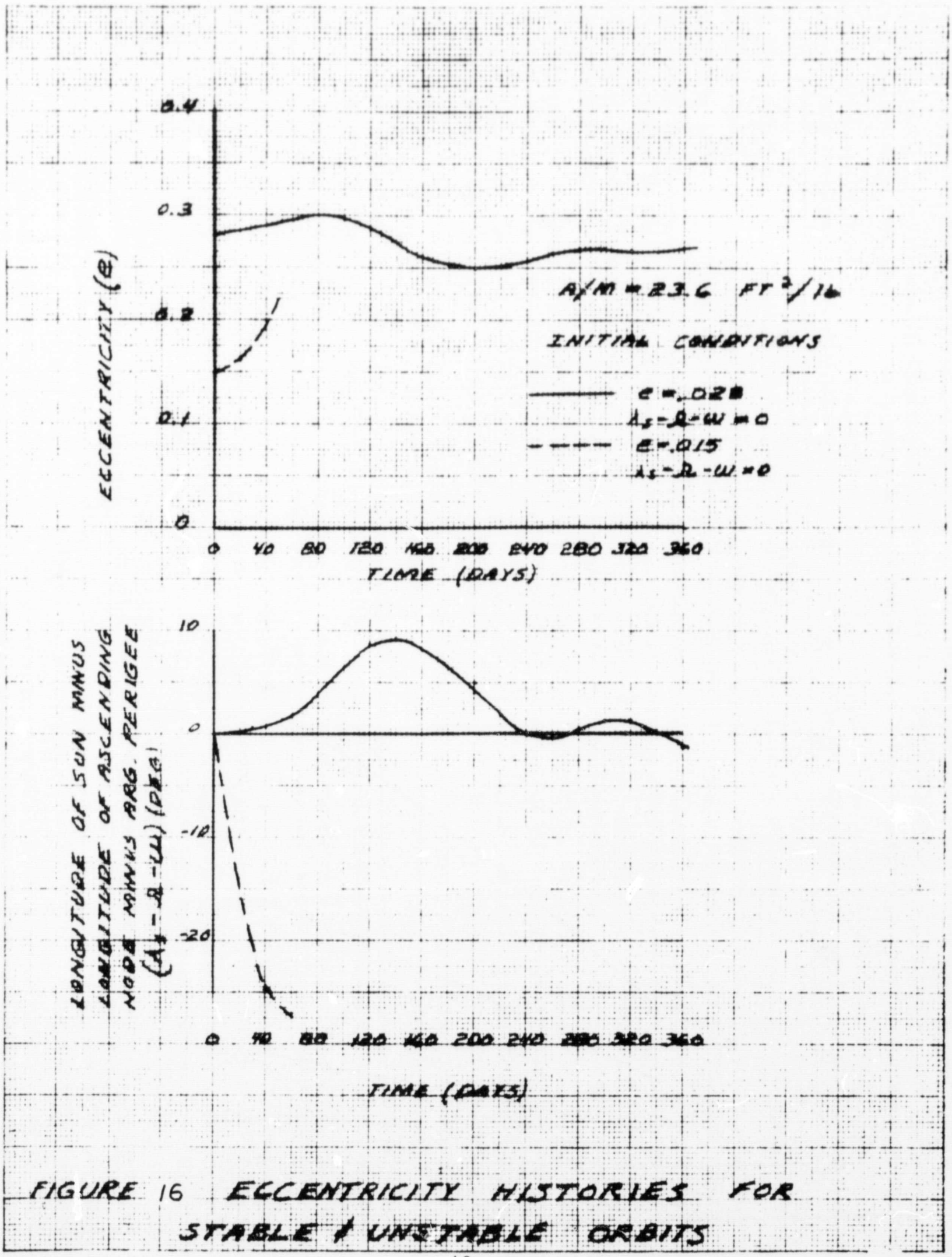


FIGURE 16 ECCENTRICITY HISTORIES FOR STABLE & UNSTABLE ORBITS

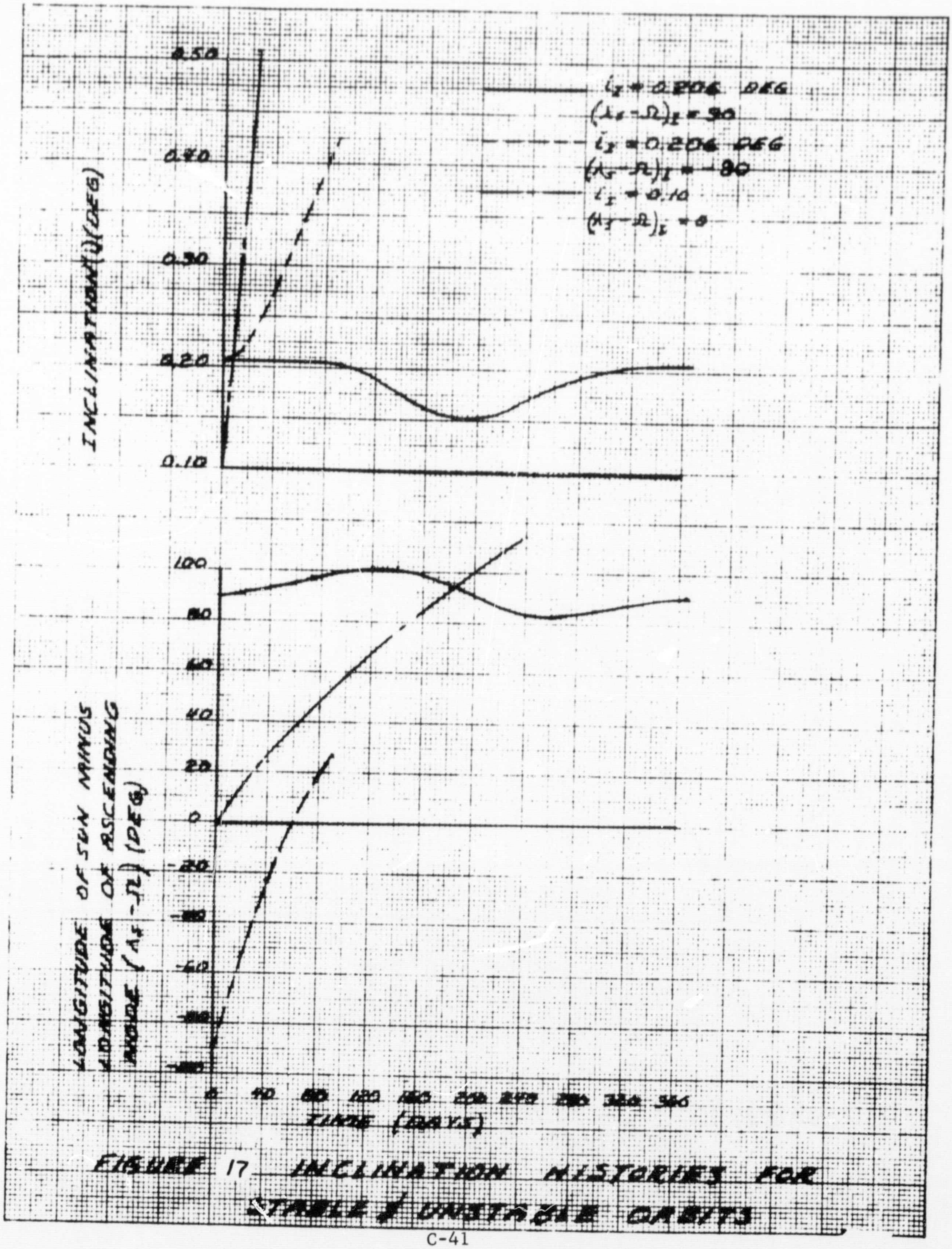


FIGURE 17 INCLINATION HISTORIES FOR STABLE & UNSTABLE ORBITS

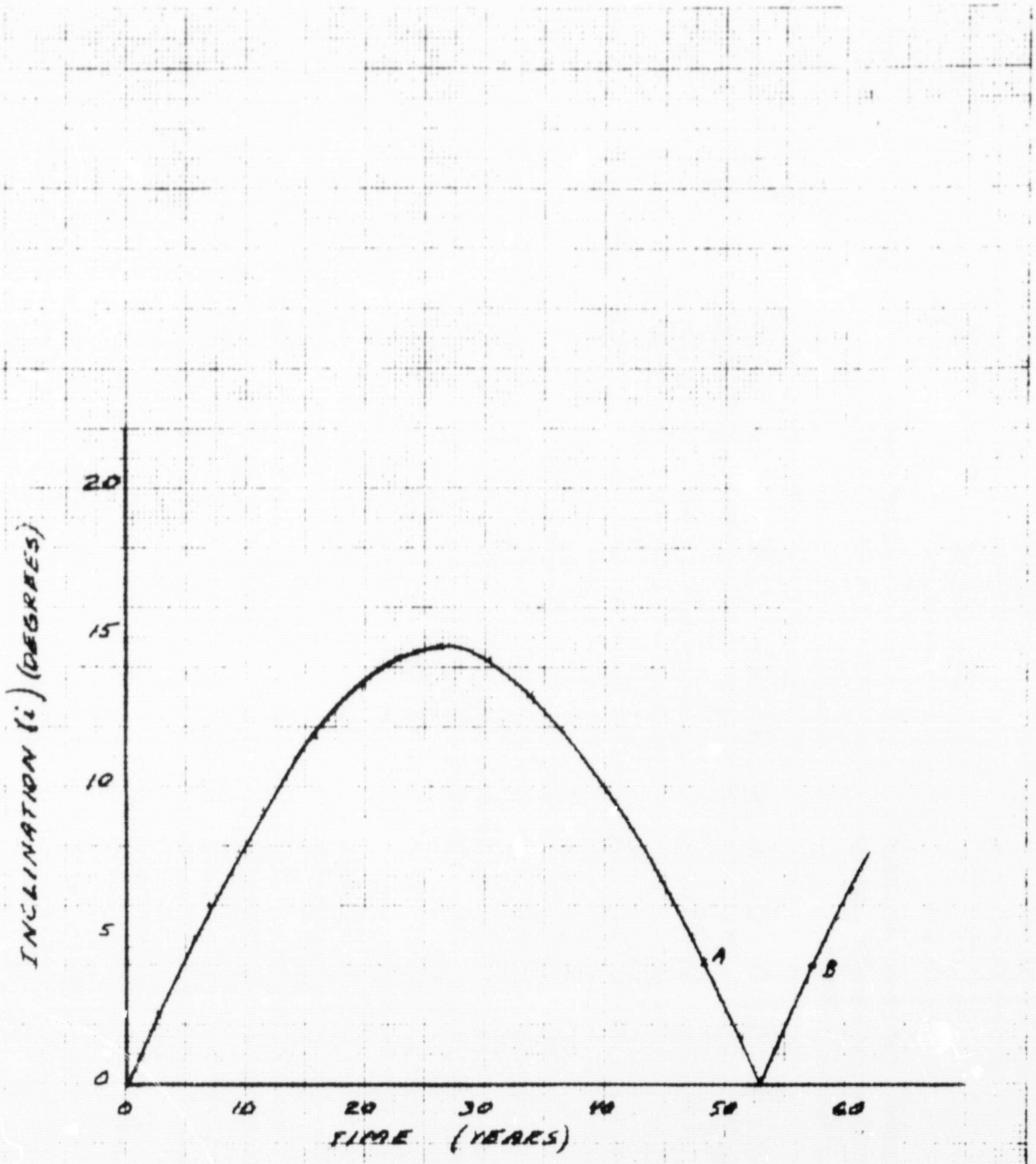


FIGURE 18 INCLINATION HISTORY OF AN INITIALLY EQUATORIAL 24 HR ORBIT INFLUENCED BY SUN-MOON GRAVITATIONAL PERTURBATIONS ONLY

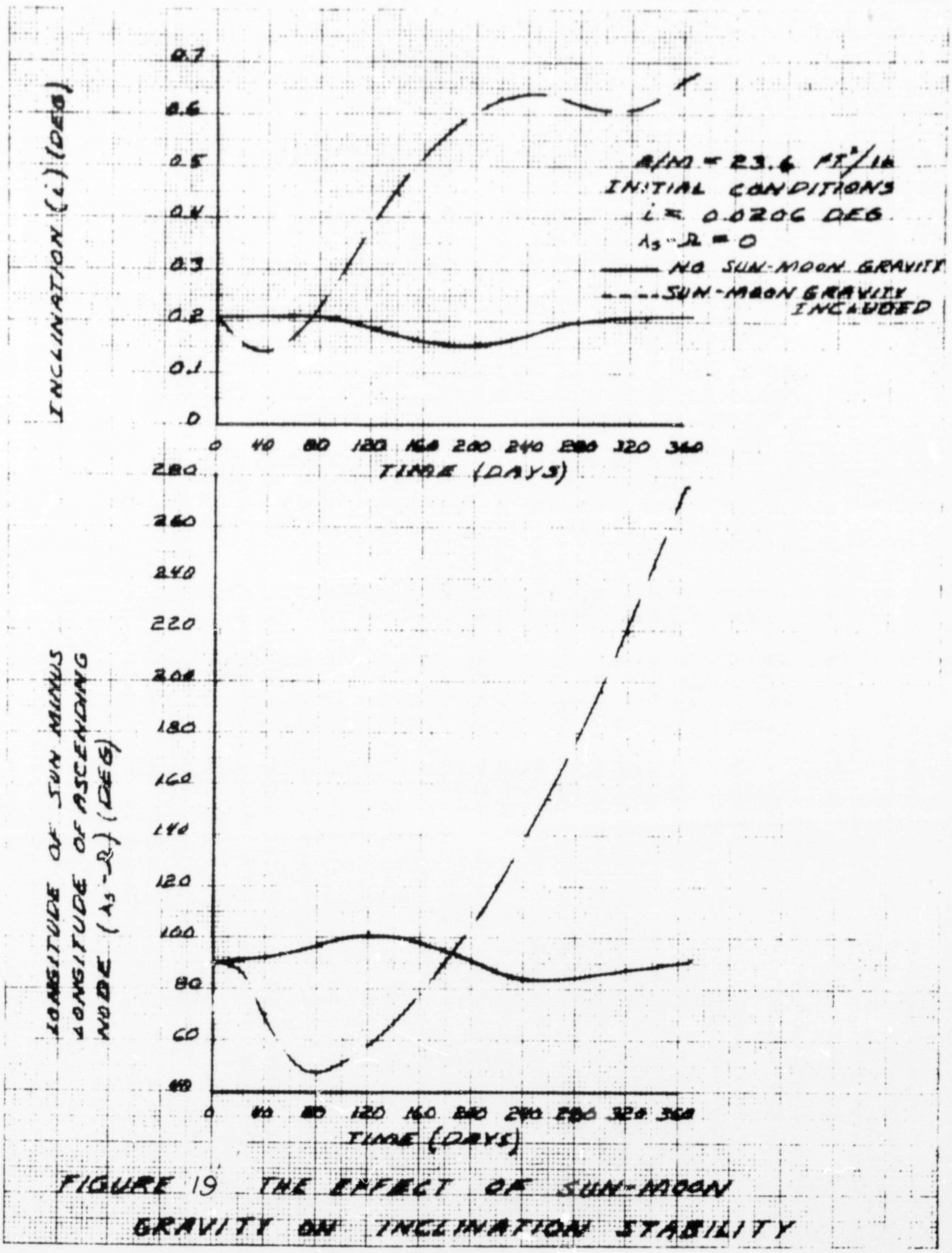


FIGURE 19 THE EFFECT OF SUN-MOON GRAVITY ON INCLINATION STABILITY

REFERENCES

1. Billik, B. H., Cross-Track Sustaining Requirements for a 24-Hr. Satellite, J. Spacecraft, Vol. 4, No. 3, March 1967.

2. Nedelk, J., Feasibility of Changing Position Along a Circular Orbit by Thrusting Along the Radius Vector, SP-5461, Goodyear Aerospace Corporation, Akron, Ohio, 4 April 1967.

3. Frick, R. H., Fuel Requirements for Attitude Control of Large Orbiting Apertures, Memorandum RM-4610-NASA, June 1965.

4. Frick, R. H., Orbital Regression of Synchronous Satellites Due to the Combined Gravitational Effects of the Sun, the Moon and the Oblate Earth, R-454-NASA, August 1967.

5. Nedelk, J., PasComSat Steering Fuel Requirements with Offset Pointing Included, GAC Memorandum SP-6290, April 1968. (Appendix D of GER-12993 S/15, Progress Report for April 1968, Advanced Passive Communication Satellite System Comparison Studies).

6. Perrine, Scott, Solar Pressure Perturbations on the Orbit of a Flat Reflector, Aero-Astrodynamics Laboratories, NASA MSFC.

7. Schneider, L. J., Orbital Stability of Passive Communication Satellites, GAC Memorandum FD-1035, May 1960, (Appendix H of GER-12993 S/16, Progress Report for May 1968, Advanced Passive Communication Satellite System Comparison Studies).

8. Nedelk, J., PasComSat Steering Fuel Requirements with Offset Pointing Included, GAC Memorandum SP-6290, 8 April 1968.

APPENDIX D

STUDY OF THE CAPABILITIES OF PARABOLIC ANTENNA SYSTEMS WITH LARGE EQUIVALENT APERTURE

STUDY OF THE CAPABILITIES OF PARABOLIC ANTENNA SYSTEMS WITH LARGE EQUIVALENT APERTURES

1.0 INTRODUCTION

This appendix is devoted to the evaluation of the capabilities of antenna systems with large equivalent apertures. The physical limitations, state of the art, and potential improvements are discussed. The objective of the study is to estimate the maximum gain that can be obtained with a single parabolic dish ground antenna. Multiplate antennas and arrays are considered in other appendixes.

1.1 BACKGROUND

Recent progress in microwave technology and digital information processing has already resulted in noticeable advances in the state of the art of large size antenna systems and has laid foundations for further improvements in the operating performance of such antennas.

Of particular usefulness was the application of computer aided analytical techniques to the design of large antenna structures. Fully steerable high precision antennas require an extremely high degree of dimensional stability under all operating conditions. This factor dominates the design of all major components of the system. A typical antenna is composed of a number of redundant, three dimensional configurations of structural elements and the overall behavior of the structure is dependent on the interaction of each member with the others. Until relatively recently idealized two dimensional models were used to analyze such three dimensional structures. While this technique was satisfactory for low tolerance applications, it is inadequate for the large size high precision structures. Application of statistical design methods has received some recent consideration[1] particularly in attempts to express wind loading in a statistical manner.

All references are listed on the last page of this Appendix .

The application of computer aided analysis techniques permitted a better understanding of the various limitations and constraints in the design of large dishes. The impetus behind the development of new techniques was in a large measure provided by the work in the field of radio astronomy antennas and in particular by the studies of the CAMROC antenna sponsored by the NSF and undertaken by the MIT Lincoln Laboratories. Little practical experience is available in the area of large size communication antennas (above 100 feet in diameter) and because of the improvements in the efficiency of active satellites, the design trend appears to be toward reducing the size of such antenna systems rather than towards increasing them. Accordingly, reliable data on the cost and operating designs of large communication antennas are rather scarce.

Caution is necessary before the experience acquired with radio astronomy antennas is directly applied to the design of large antennas serving communication applications. Radio astronomy operations are characterized by the following major factors which directly influence the design of antennas for that purpose, and which are not compatible with communication usage.

a. Astronomical observations are not normally made during periods of heavy rain or other adverse climatic conditions. Accordingly, high performance under such conditions is not required. This fact has an important effect on the consideration of the use of radomes.

b. Radio-astronomy antennas are normally required to cover a wide range of frequencies rather than to operate in a restricted band of frequencies which is the case in communications applications. Accordingly, it is not desirable to optimize the system for operation at one frequency and broad band designs are favored. In addition the effort associated with the change of the feed and electronics when the operating frequency is changed makes the use of antenna arrays for radio astronomy less desirable.

c. For astronomy work losses in gain can be partially compensated by increased time of integration, since "real time" operation is not required. This is opposite to communication requirements where real time operation is a primary requirement.

d. In some cases, fluctuations in gain due to tropospheric turbulence,[2] while inconsequential in astronomy applications may cause an occasional total loss of communications if the information rate is high.

It is apparent therefore that the design of large antennas for communication applications is based on different sets of basic operational criteria then that for astronomy applications. One must be careful therefore in indiscriminently comparing the design and operational performance data and in drawing conclusions from such data.

2.0 LIMITS ON THE GAIN OF ANTENNA

The gain of an ideal parabolic reflector with reflecting area A_o and operating at a frequency corresponding to the wavelength λ is given by

$$G = \frac{4\pi A_o}{\lambda^2} \qquad \ldots\ldots\ldots\ldots \quad (1)$$

The gain of the parabolic reflector, with an effective area A_{eff} can be expressed by the following relation

$$G = \frac{4\pi A_{eff}}{\lambda^2} \qquad \ldots\ldots\ldots\ldots \quad (2)$$

The ratio of the effective area A_{eff} to the area of the circle bounded by the edge of a dish of diameter D_o is known as the overall antenna aperture efficiency η_T

$$\eta_T = \frac{A_{eff}}{A_o} \qquad \ldots\ldots\ldots\ldots \quad (3)$$

Thus $$A_{eff} = \eta_T A_o = \eta_T \frac{\pi D_o^2}{4}$$

Substituting in (2)

$$G = \eta_T \pi^2 \left[\frac{D_o}{\lambda}\right]^2 \qquad \ldots\ldots\ldots\ldots \quad (4)$$

Equation (4) represents the maximum possible gain of an antenna having a diameter D/λ (λ = operating wavelength). This relationship is plotted in Fig. 1 for $\eta_T = 1.0$ (perfect antenna). The values of gain shown in Fig. 1 represent the limit which can never be achieved in practice. These limiting values of gain have been calculated for antennas with diameters of 85, 100, 210, and 400 feet operating at 2, 4, 6, 8 GHz and are shown in Table 1 below.

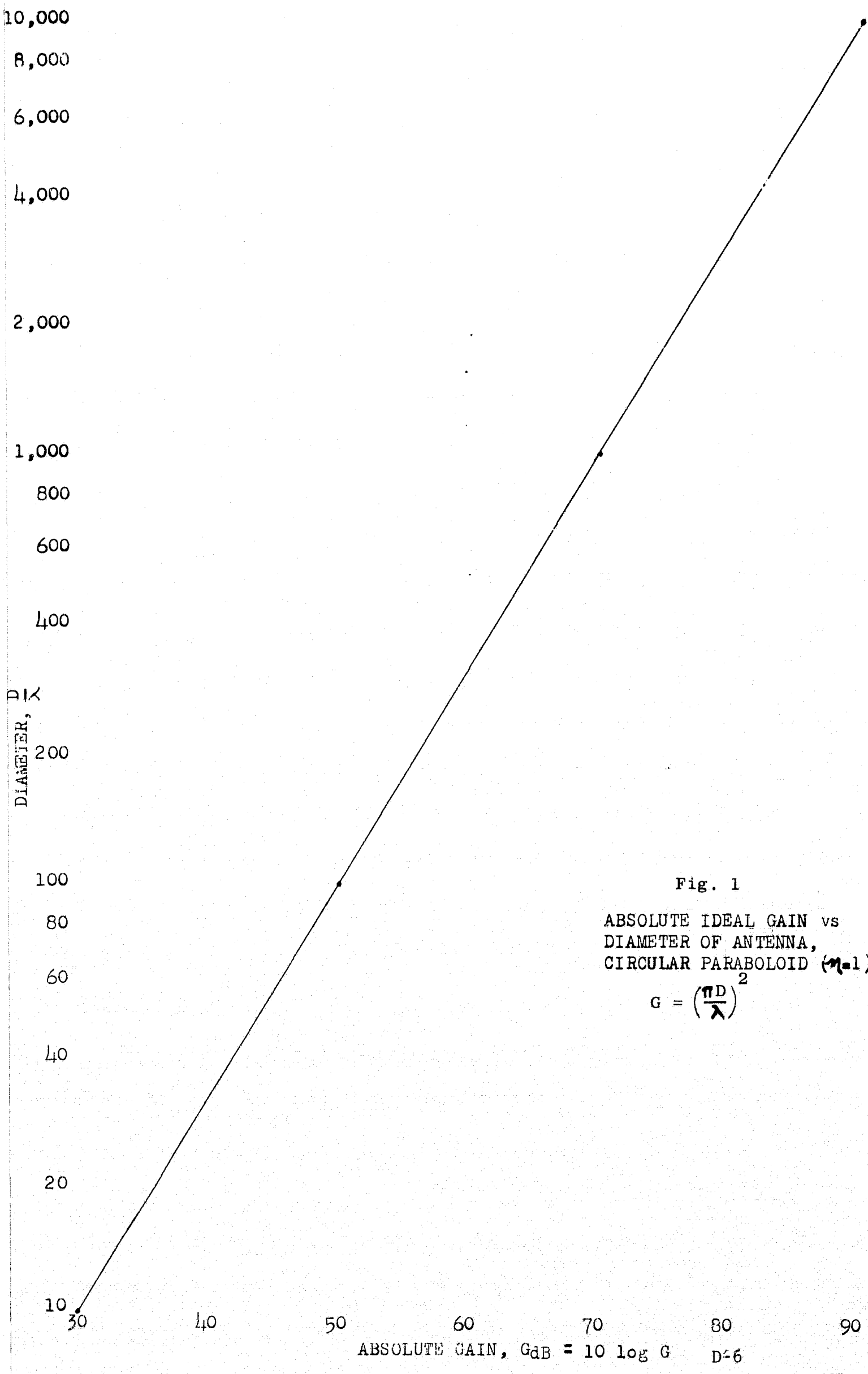


Fig. 1

ABSOLUTE IDEAL GAIN vs
DIAMETER OF ANTENNA,
CIRCULAR PARABOLOID (η=1)

$$G = \left(\frac{\pi D}{\lambda}\right)^2$$

Table 1
Idealized Maximum Gain dB
($\eta = 1$)

Antenna Diameter	Operating Frequency GHz			
	2	4	6	8
85	54.7	60.7	64.2	66.7
100	56.1	62.1	65.6	68.1
210	62.5	68.6	72.1	74.6
400	68.1	74.2	77.7	80.2

In practice these idealized gains are reduced by a factor η_T which represents the overall aperture efficiency of the antenna, which is a composite of several factors and could therefore be written as

$$\eta_T = \eta_1 \eta_2 \eta_3 \eta_4 \eta_5 \quad \ldots\ldots\ldots\ldots \quad (5)$$

η_1 = degradation due to random phase errors in the phase front of the aperture produced by deviations from the ideal reflector surface due to manufacturing tolerances, gravitional forces, wind, thermal effects, etc.

η_2 = illumination efficiency. The illumination efficiency denotes the ability of the source of energy to produce uniform illumination of the entire reflector surface. When the incident energy density on the reflector is a constant over the entire surface, the illumination efficiency is 100%.

This factor also encompasses the effects of shadowing of the primary and secondary illuminating fields. It includes blockage effects due to secondary reflector support legs, subreflector itself, and in prime focus feed systems, the feed support legs.

η_3 = spillover efficiency. The spillover efficiency denotes the ability of the energy source to illuminate only the reflector while minimizing the energy radiated elsewhere.

η_3 = (1-S) where S is the fraction of the total power in spillover

η_4 = (1-R) where R = power reflection coefficient

η_5 = (1-a) where a = fractional power absorption due to resistive losses.

For purposes of analysis which follows, the composite value of $\eta_2 \cdot \eta_3 \cdot \eta_4 \cdot \eta_5$ will be called η_x.

Thus $\eta_T = \eta_1 \cdot \eta_x$ ..... (6)

The value of η_1 depends on antenna diameter and operating frequency (as shown later in the text, it may vary from approximately 0.95 for 100-foot antennas operating at 6 Gc to 0.55 for 200-foot antennas at 4 Gc for example).

To obtain an indication of the relative importance of the other factors, the typical values are shown below:

$\eta_2 \cdot \eta_3$	$\approx .6$
η_4	$\approx .99$
η_5	$\approx .95$
η_x	$\approx .56$

In the following paragraphs, the first three factors are discussed (η_1, η_2 and η_3). The last two, η_4 and η_5, are relatively unimportant and will not be considered in this report.

3.0 LOSS IN GAIN DUE TO SURFACE IRREGULARITIES

The effect of such irregularities has been analyzed by Ruze[3] utilizing statistical methods.

Ruze has shown that the relationship between the loss of gain and the surface deviation can be expressed by the following formula:

$$\frac{G}{G_o} = \exp\left[-\left(\overline{\delta^2}\right)\right] + \frac{1}{\eta}\left(\frac{2c}{D}\right)^2 \exp\left[-\left(\overline{\delta^2}\right)\right] \cdot \sum_{\eta=1}^{\infty} \frac{\overline{\delta^{2\eta}}}{\eta \cdot \eta!} \quad \ldots\ldots \quad (7)$$

where

G/G_o = reduction in axial gain relative to no-error gain

D = antenna diameter

c = radius of area where phase values are completely correlated

$\overline{\delta^2}$ = phase front variance produced by r.m.s. surface error (d) on a shallow reflector (large f/D).

For reasonable tolerance losses and for correlation regions (c) small compared to the antenna diameter the second term of equation (7) can be neglected yielding

$$G = G_o \exp -\left[\delta^2\right] \quad \ldots\ldots\ldots\ldots \quad (8)$$

or

$$\frac{G}{G_o} = \exp -\left[\frac{4\pi d}{\lambda}\right]^2 \quad \ldots\ldots\ldots\ldots \quad (9)$$

or

$$G = \eta_x \left[\frac{\pi D}{\lambda}\right]^2 \exp -\left[\frac{4\pi d}{\lambda}\right]^2 \quad \ldots\ldots\ldots\ldots \quad (10)$$

where

η_x = antenna aperture efficiency

λ = wavelength at operating frequency

d = effective reflector tolerance (reflector r.m.s. deviation from best fit paraboloid) expressed in the same units as λ.

It is apparent that the exponential term in equation (10) will reduce the value of G as $\frac{d}{\lambda}$ increases.

A few words are necessary concerning the validity of assumptions on which the derivation of formula 10 is based. These assumptions were as follows:

1. The deviations from best fit paraboloid are random with gaussian distribution

2. The errors are uniformly distributed over the antenna aperture

3. Region over which the errors are substantially constant is large compared to a wavelength (reflector is smooth in wavelength measure) and the number of such uncorrelated regions across the aperture is large.

From practical experience with large antennas, the following comments can be made[4] concerning these assumptions:

1. Photogrammetric measurements of actual antennas indicate that the reflector deviations although not strictly random and guassian are distributed in a bell shaped curve.[5,6]

2. Similarly, photogrammetric measurements and deformation calculations after structural compensation indicate that the assumption of uniform distribution of errors over the aperture is not grossly violated.

   It should be noted that uniform distribution of mechanical deviations will cause an approximately uniform distribution of phase errors if the reflector is shallow (large f/D). For deep reflectors, the effective tolerance d is not equal to the surface tolerance. Further, reflector deformations can be measured either in axial direction (z) or normal to

the surface (n). The relations between these quantities are:

$$d = \frac{\Delta n}{\sqrt{1 + (r/2f)^2}}$$

$$d = \frac{\Delta z}{1 + (r/2f)^2}$$

f = focal length of the paraboloid

r = distance from center of aperture

As a result, loss in gain computed from reflector axial or normal mean square error is too high by a factor A which is plotted in Fig. 2. For shallow reflectors, this factor approaches unity.

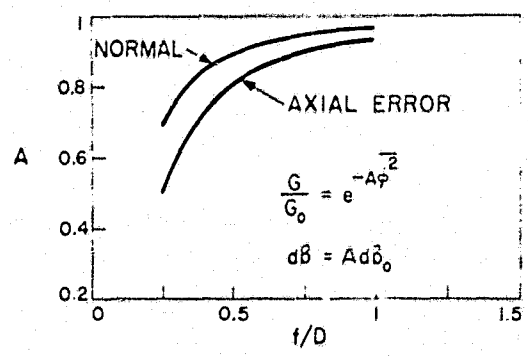


Figure 2. Correction factor due to reflector curvature.

3. The theory requires that the number of uncorrelated regions in the aperture be large ($D \gg 2c$). It has been found that this number depends on the reflector panel sizes or spacing of target points. It should also be mentioned that fixed circular correlation regions have been assumed in the development of equation (8) whereas certain structural factors would yield elliptical correlated regions of various sizes.

Experimental measurements with Haystack Radio Telescope have yielded the value of correlation radius C = 4.4 ft resulting in D/2c = 120/2x4.4 = 13.6 and the rms surface error d = .053 inch.[7]

It is evident from equation (10) that the value of gain will increase as the square of frequency until errors due to surface deviations take over. After then an abrupt reduction in gain will result. Equation (10), therefore, represents the upper bound on the obtainable gain of a practical antenna system. Maximizing equation (10) with respect to frequency, we find that the maximum gain occurs at the wavelength of

$$\lambda_{max} = 4\pi d \qquad \ldots\ldots\ldots\ldots \qquad (11)$$

at which point the loss in gain relative to an ideally smooth surface (d=0) is 4.3 dB. Substituting (11) into (10), we obtain the value of maximum gain

$$G_{max} = \frac{\eta}{16e}\left(\frac{D}{d}\right)^2 \qquad \ldots\ldots\ldots\ldots \qquad (12)$$

The parameter $\frac{D}{d}$ represents a measure of manufacturing accuracy and effectively limits the maximum obtainable gain.

The deviation d is expressed in equations (10), (11), and (12), as an rms value. The relationship between the peak deviation and the rms deviation has not been conclusively established. References in the literature[8] indicate that measurements on existing reflectors show that peak deviation is approximately equal to three times the rms value. This is partially a result of a "truncation" process in manufacturing whereby large errors are corrected but not the small ones. However, this assumption was challenged by many and no general agreement on this point exists.

3.1 DISCUSSION

The implications of equations (9), (10), (11), and (12) are presented graphically in Figs. 3 through 8.

Fig. 3 shows a plot of equation (9) and indicates the fractional loss in gain produced by an r.m.s. surface error d expressed in wavelength measure. From this figure, the data in Table 2 have been computed.

Table 2
Losses in Gain Due to Imperfect Dish Surface

R.M.S. Error	Loss in Gain $\frac{G}{G_o}$ dB	%	Corresponding RMS Surface Tolerance in Inches at Specified Frequency, which will result in the loss of gain shown in Column 2							Efficiency η_1
			1 Gc	2	3	4	6	8	10	
0.012λ	0.1	2.3	.142	.071	.047	.036	.024	.018	.014	.977
0.017λ	0.2	4.5	.201	.1005	.067	.05	.0335	.025	.02	.955
0.027λ	0.5	10.9	.320	.160	.107	.08	.0535	.04	.032	.891
0.038λ	1.0	20.6	.450	.225	.148	.113	.074	.057	.045	.794
0.054λ	2.0	36.9	.64	.32	.213	.16	.107	.08	.064	.631
0.066λ	3.0	50.0	.78	.39	.26	.195	.13	.0975	.078	.500
0.080λ	4.3	62.9	.945	.4725	.315	.2362	.158	.1181	.095	.371
0.094λ	6.0	75.0	1.11	.555	.37	.2775	.185	.13875	.111	.250

Table 2 shows the results of r.m.s. surface roughness on the gain of the antenna. Column 1 indicates the r.m.s. error in wavelength measure, Column 2 the corresponding dB loss in gain (relative to an antenna with no surface error), and Column 3 represents this same loss expressed in percent of power that could be radiated with a smooth surface.

Thus if we wish to limit the loss in gain to 20% of the gain available with a perfectly smooth dish, a surface rms accuracy of approximately 0.038 λ is required. Similarly for a 10% loss, the tolerance of 0.027λ would be needed. (λ = operating wavelength in feet = $\frac{.984}{f_{Gc}}$)

Column 1 expresses the surface tolerance in wavelengths, and is therefore independent of frequency of operation. For operation at a specified frequency, the values of rms surface tolerance (in inches) which will result in the loss in gain shown in Column 2 have been calculated and are shown in Columns 4

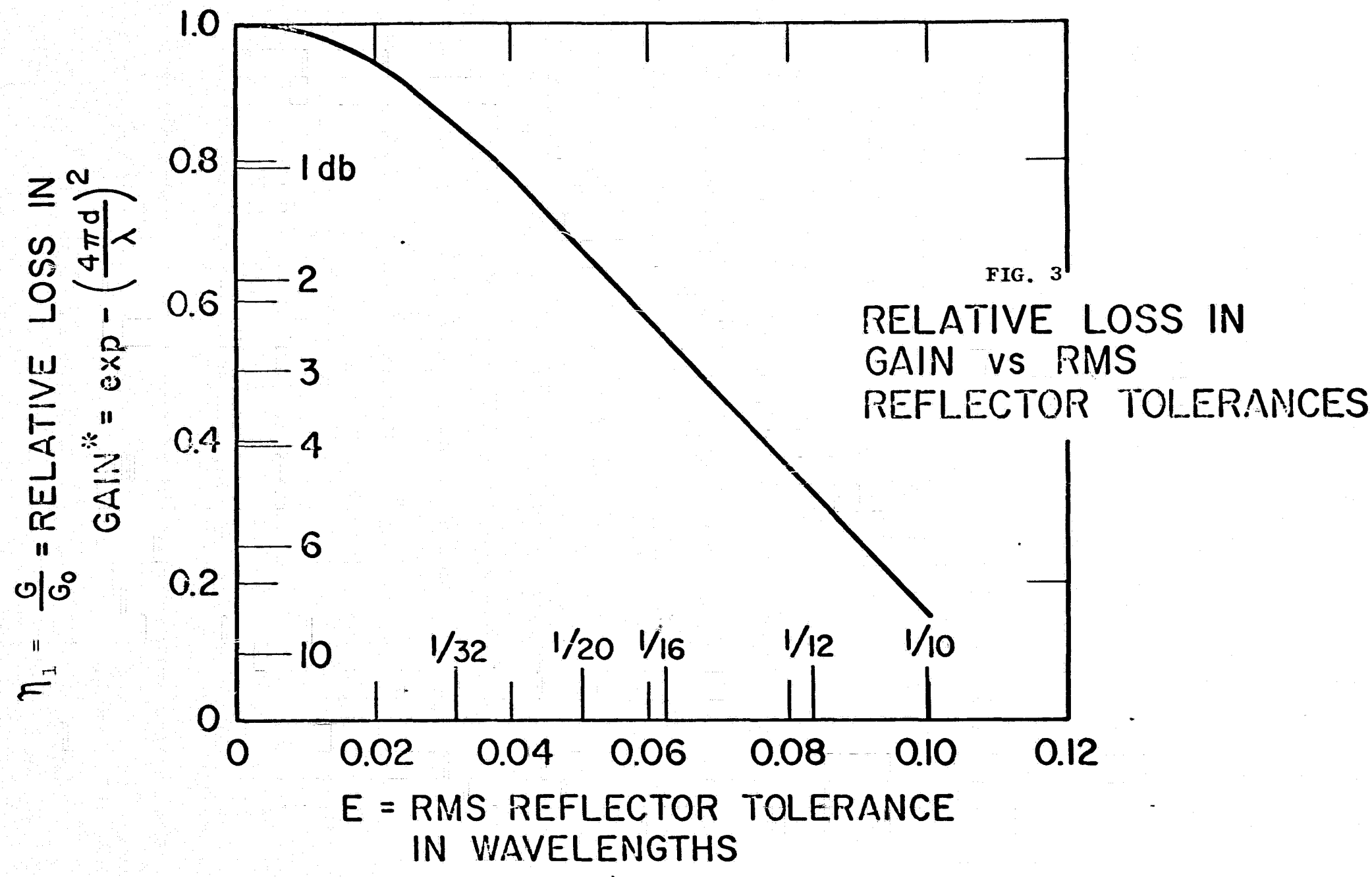


FIG. 3

RELATIVE LOSS IN GAIN vs RMS REFLECTOR TOLERANCES

*G = GAIN WITH SURFACE ERRORS

G_o = GAIN WITHOUT SURFACE ERRORS

through 10. The resulting efficiency η_1 is shown in the last column. Thus an antenna operating at 8 GHz with a surface tolerance of 0.04 inches rms will have $\eta_1 = 0.891$ regardless of diameter.

These results are also plotted in Figs. 4 and 5 which indicate the efficiency (or loss in gain) at a given frequency for a specified surface tolerance (Fig. 4) or the rms error required to achieve a given efficiency at a specified frequency (Fig. 5).

When the loss of gain resulting from surface roughness, shown in Fig. 3, is subtracted from the ideal gain obtainable with perfect surface (shown in Fig. 1), we obtain the maximum gain curve shown in Fig. 6. Point B represents the maximum gain obtainable with rms surface tolerance d_o. The value of this gain is given by equation (12) and the frequency at which it occurs by equation (11). Note that the maximum gain point B is 4.3 dB below the ideal gain (point A) obtainable with smooth reflector surface. It is apparent that as surface tolerance is decreased ($d_o \rightarrow 0$), point B will move up and to the right yielding higher gain and higher frequency of operation. These relationships are plotted in Fig. 7 which show the locus of maximum gain point B for selected antenna diameters, the frequencies at which the maximum gains occur and the corresponding rms deviations. Fig. 7 is plotted for three values of efficiency $\eta_x = 1, 0.7, 0.5$. The top lines corresponding to $\eta_x = 1$ for each diameter show only the effects of surface roughness as expressed by the value of η_1. In plotting it, it was assumed that antennas are otherwise perfect, i.e., η_x in equation (10) = 1.

The representative gain-frequency characteristics of antennas having diameters of 210 and 400 feet are plotted in Figs. 8 and 9, respectively, showing their performance for selected surface tolerances. These curves are plotted assuming an efficiency of 0.6 and clearly show the effects of surface roughness on antenna gain.

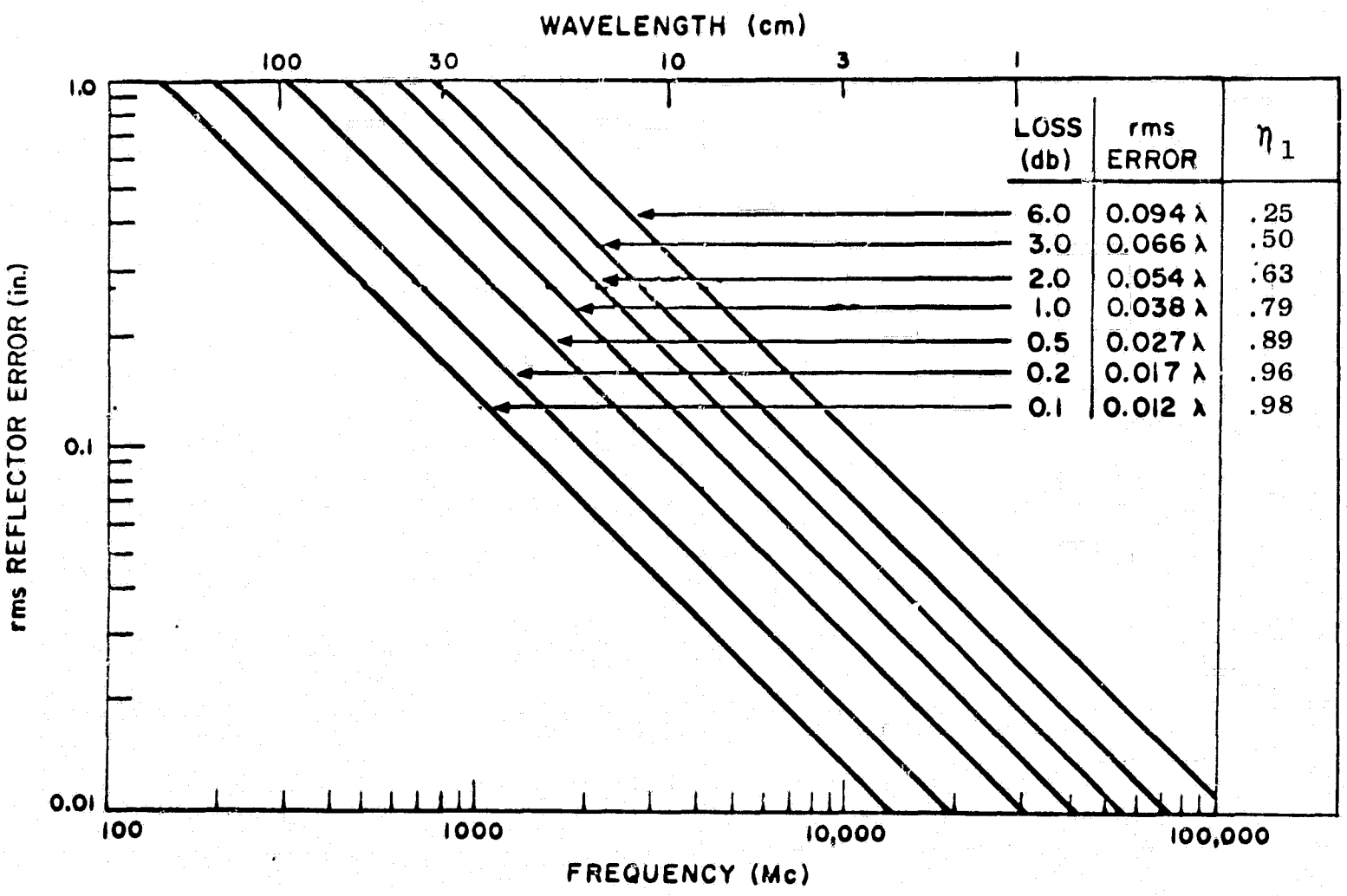


Figure 4. Loss due to reflector tolerance.

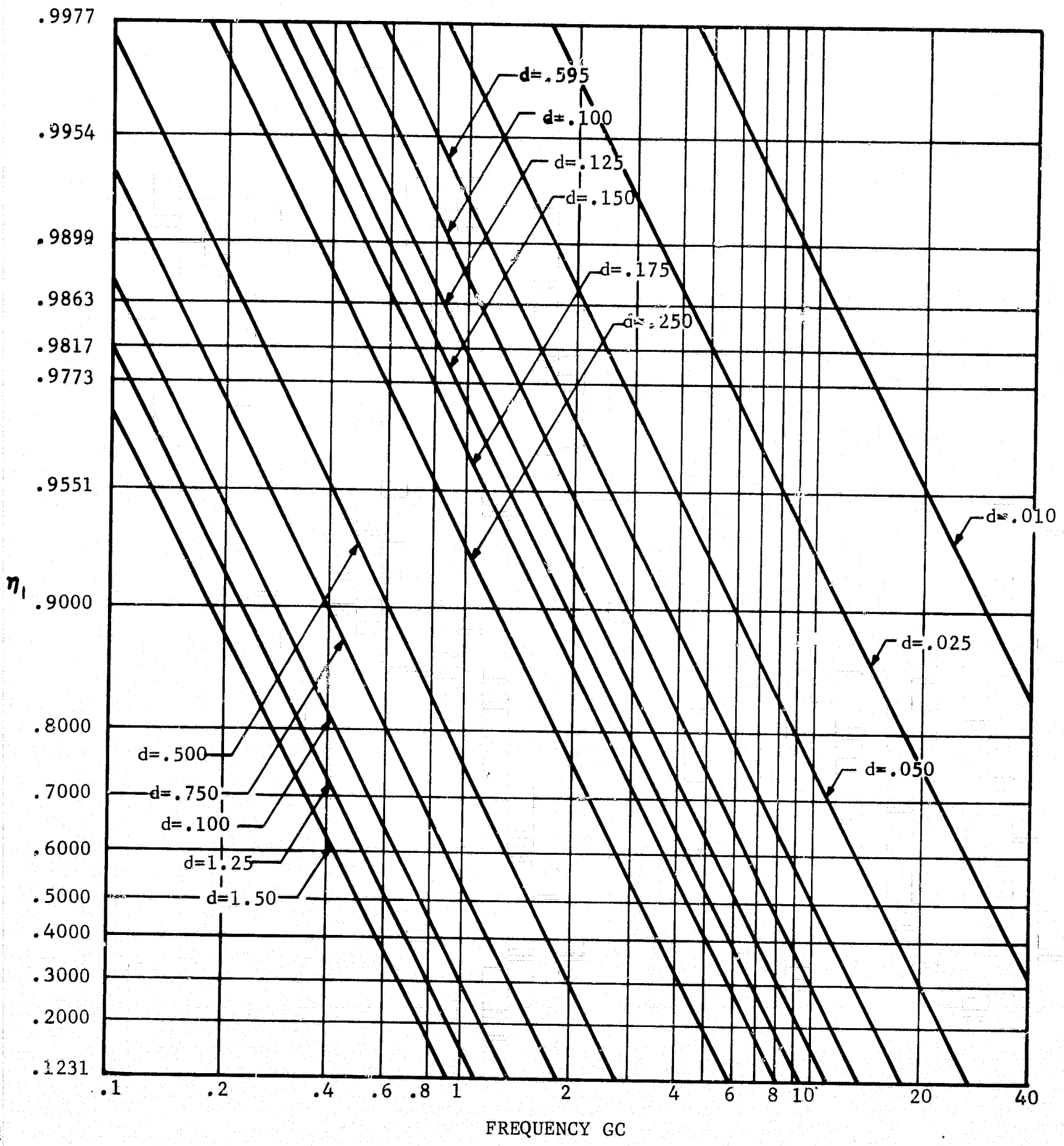


Figure 5 RMS Surface Error (Inches) Which Will Yield A Given Efficiency At Specified Frequency.

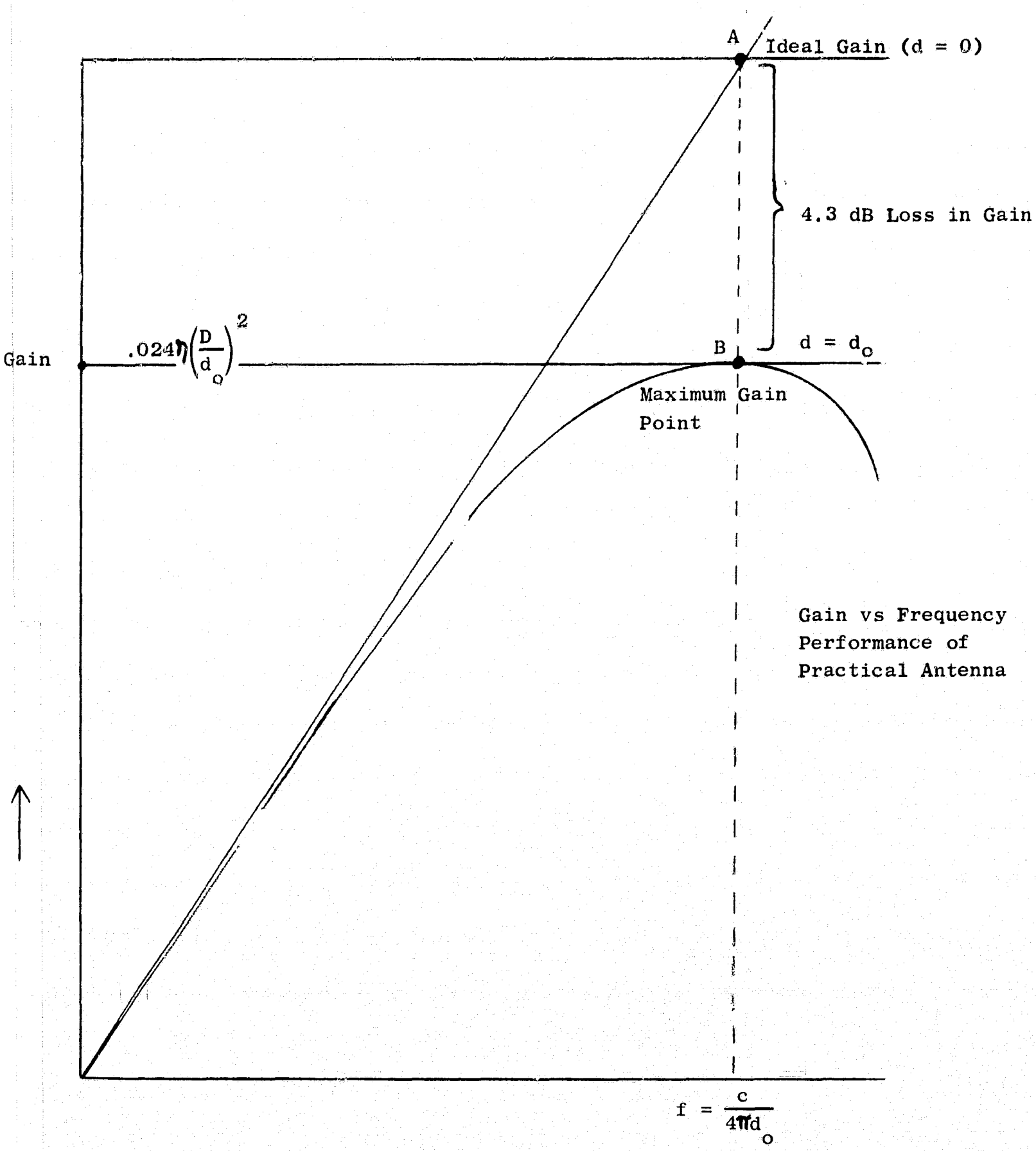


Fig. 6
Effect of Reflector Surface Roughness on Antenna Gain

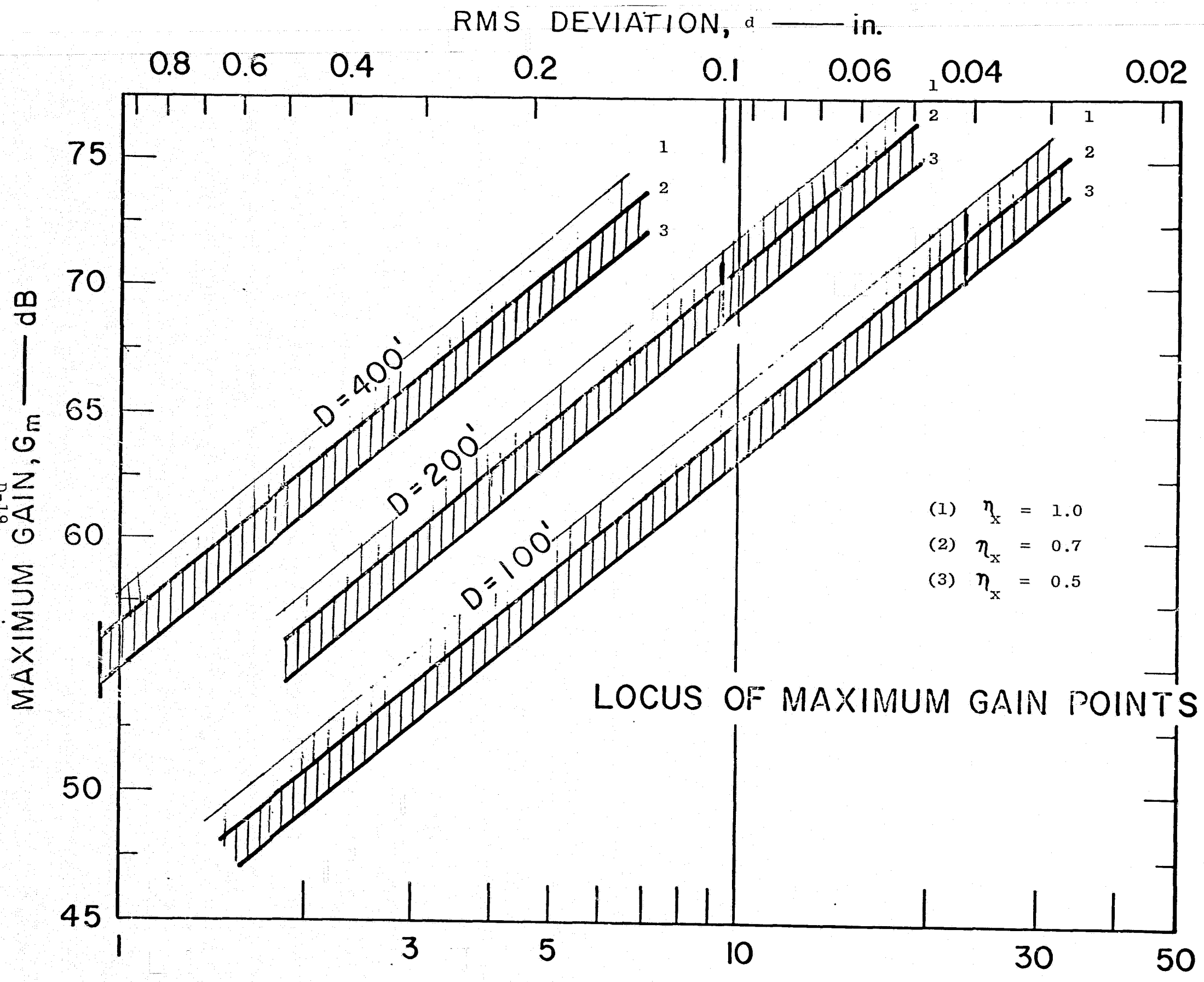


Fig. 7. FREQUENCY OF MAXIMUM GAIN, f_m — GHz

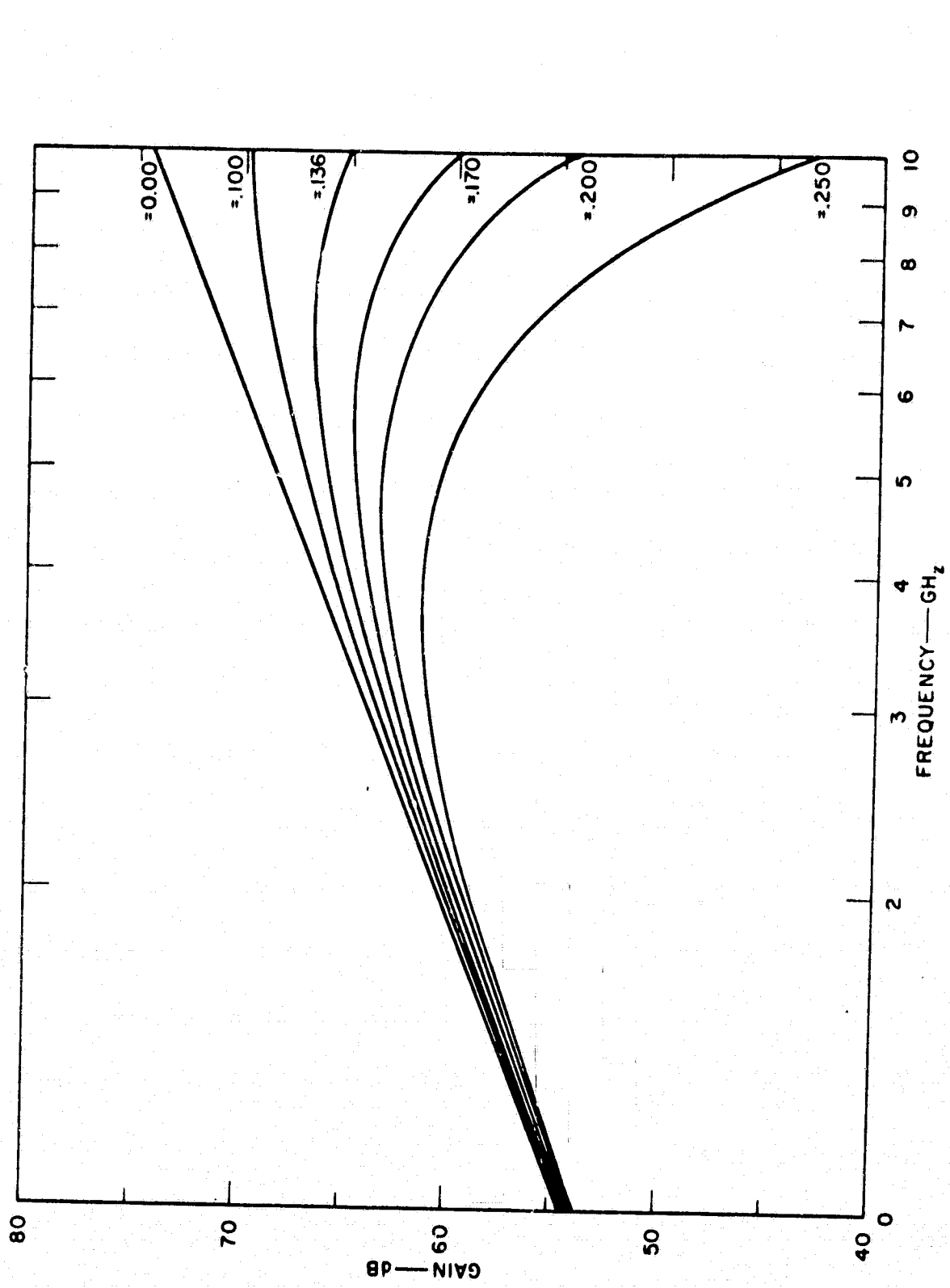


FIG. 8 GAIN vs FREQUENCY PERFORMANCE OF, 210 ft. ANTENNA

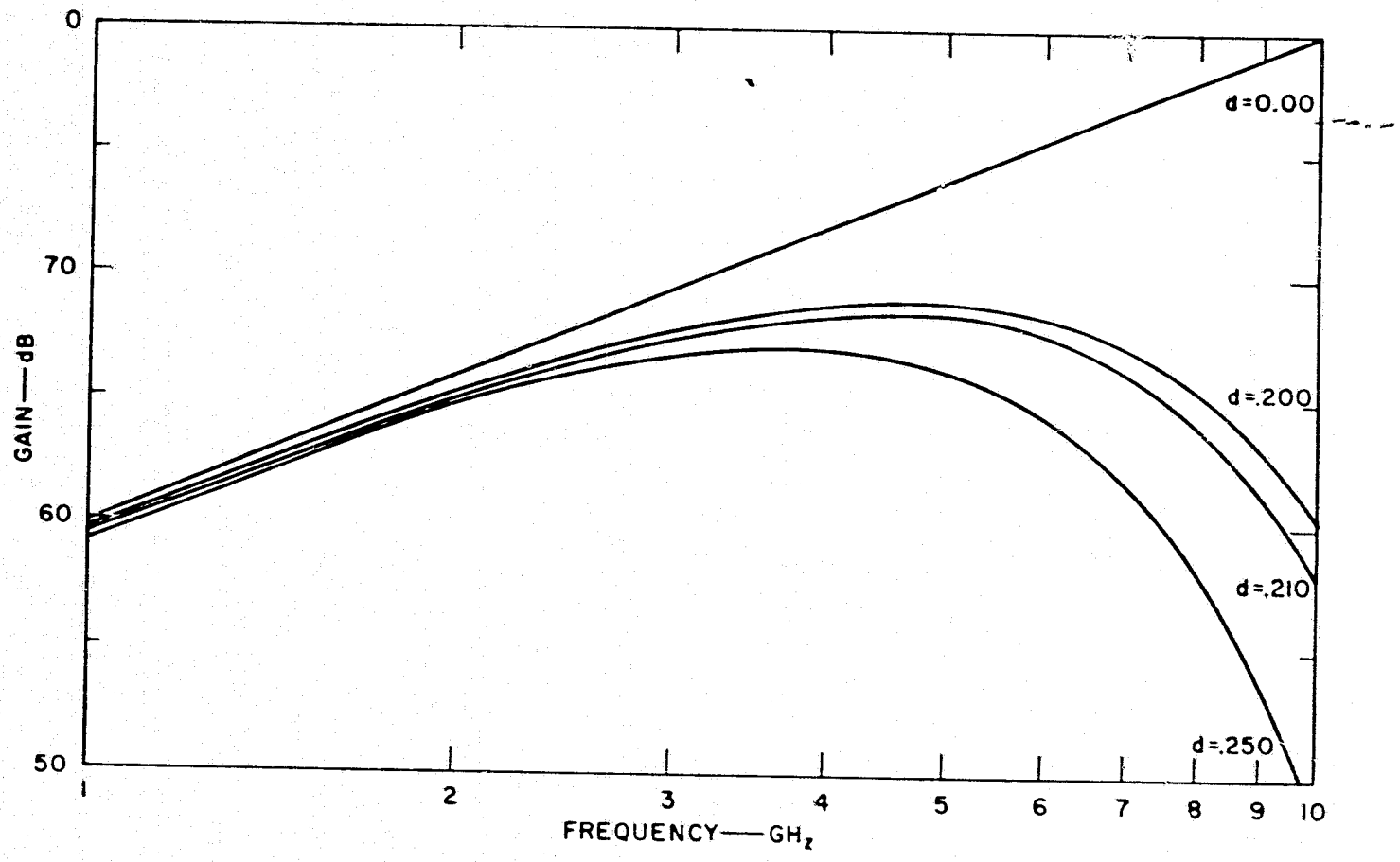


FIG. 9 GAIN vs FREQUENCY PERFORMANCE OF 400 ft. ANTENNA

4.0 ILLUMINATION EFFICIENCY

In conventional design utilizing parabolic-hyperbolic Cassagrainian geometry, the antenna aperture distribution is almost a direct image of the illumination of the subreflector. Consequently an illumination taper across the subreflector will result in higher concentration of energy near the center of the main aperture causing an apparent loss of on-axis gain in the far field. Table 3 shows the reduction in gain and the improvement in side lobe levels for a circular parabolic aperture distribution represented by a power low equation.[9]

$$\text{Distribution} = \left[1 - \left(\frac{2r}{D}\right)^2\right]^p \qquad \text{..... (13)}$$

where D is the diameter of the aperture.

Table 3

Secondary Pattern Characteristics Produced by a Distribution $(1 - \alpha^{2p})$ over a Circular Aperture

p	Loss in Gain		First Side Lobe Level dB Below Peak Gain	(λD) Half Power Beamwidth	
	Numeric	dB		Radians	Degrees
0	1.0	0	17.6	1.02	58.45
1	0.75	1.25	24.6	1.27	72.7
2	0.56	2.5	30.6	1.47	84.3
3	0.44	3.56		1.65	94.5
4	0.36	4.44		1.81	103.9

If one assumes a parabolic distribution (p=1) with an edge taper q (defined as ratio of the field at the edge to that at the center of the aperture), the loss in gain or illumination efficiency η_2 may be defined as follows:

$$\eta_2 = \frac{1}{1 + \frac{1}{3}\left(\frac{1-q}{1+q}\right)^2} \qquad \text{.....} \qquad (14)$$

4.1 APERTURE BLOCKAGE

When the feed and its supporting structure physically obstruct the aperture a loss of antenna gain results which is proportional to the edge taper and the fraction of area which is obstructed. For an antenna having a parabolic distribution, the loss in gain is given by the formula:

$$x = \text{loss in gain} = 20 \log (1 - \alpha)\left(1 - \alpha\frac{1-q}{1+q}\right) \qquad \text{.....} \qquad (15)$$

where q is the edge taper

α is the fraction of the aperture area which is blocked

$(1 - \alpha)$ is then the fraction of total area which is not blocked by the obstruction.

The loss in gain for a parabolic distribution is shown in columns 5 and 6 of Table 4 as a function of edge taper q for an assumed blockage of 7% of the total area. The total efficiency and corresponding loss in gain are shown in the last two columns of Table 4. Horn parabolas and horn-lens antennas do not suffer from blockage effects.

Table 4

Total Efficiency as a Function of Illumination, Edge Taper and Aperture Blockage for Parabolic Distribution

Edge Taper dB (20 log q)	Fractional Edge Taper (q)	Illumination Efficiency η_2	Corresponding Loss in Gain dB	α Blockage Efficiency (7% Blockage)	Corresponding Loss in Gain dB	$\eta_2 \cdot \alpha = \eta_2^*$	Corresponding Loss in Gain dB (to η_2^*)
0	1.000	1.000	0.0	.865	.630	.865	.630
1	0.892	0.998	0.01	.858	.665	.856	.675
2	0.795	0.995	0.02	.851	.700	.847	.720
3	0.707	0.991	0.04	.844	.735	.837	.775
4	0.631	0.984	0.07	.838	.769	.824	.839
5	0.563	0.975	0.11	.831	.802	.811	.912
6	0.510	0.965	0.15	.826	.830	.797	.980
7	0.446	0.954	0.20	.819	.866	.781	1.066
8	0.398	0.940	0.27	.814	.897	.765	1.167
9	0.355	0.930	0.31	.808	.925	.752	1.235
10	0.316	0.918	0.37	.803	.952	.737	1.322
12	0.251	0.894	0.49	.794	1.002	.710	1.492
15	0.178	0.860	0.65	.782	1.065	.673	1.715
20	0.100	0.817	0.88	.769	1.143	.628	2.023
25	0.006	0.751	1.24	.749	1.253	.563	2.493
∞	0.0	0.750	1.25	.748	1.261	.561	2.511

4.2 RECENT IMPROVEMENTS

Recently, promising improvements in Cassegrainian antenna performance were reported[10]. These improvements have been obtained by shaping both of the reflector surfaces to achieve an almost uniform amplitude and phase illumination in the aperture of a Cassegrainian antenna.

Used by the WDL Division of Philco Corporation in the design of the 90' reflector for the Italian comsat station, the technique consists in reflecting the feed energy first from an energy dispersing subreflector and then from the phase correcting main reflector. The shape of the subreflector differs slightly from the hyperbola. This redistributes the energy radiated by the feed to provide uniform amplitude illumination of the main reflector. The phase front of the scattered field is distorted from the nearly spherical front scattered by a hyperbola and is corrected by the main reflector whose shape deviates from a best-fit paraboloid as required to effect this correction. This particular design was evaluated by JPL and it was found that the shaped reflector system yields an antenna efficiency of 94% at maximum gain based on the assumption that the phase error is zero. (It is believed that this can be well approximated in practice if the surface of the main reflector is defined by the experimentally determined phase pattern of the fields scattered by the subreflector.) This efficiency figure includes blockage loss computed on the basis of 7 degree vertex blockage but does not include quadripod blockage or manufacturing and erection tolerances for the reflecting surface.

The performance of the shaped antenna as compared with a very well designed conventional Cassegrain antenna indicates an increase in performance of 0.68 dB at maximum gain and 0.91 dB at maximum figure of merit (defined as the ratio of antenna gain to antenna system temperature). System temperature equals antenna noise temperature plus 25°K.)

The shaped reflector technique appears to be an extremely promising method of achieving the maximum potential of a reflector type antenna. However, the final aperture distribution is perfectly uniform only for the one pattern distribution that was used to generate the specially shaped surfaces.

5.0 SPILLOVER EFFICIENCY η_3

In both the prime focus feed systems and in Cassegrainian systems (hyperbola/parabola), these efficiencies are optimized by suitable design of the antenna feed. It is quite evident, however, that one cannot design a feed, the radiation pattern of which would be uniform within the angle subtended by the reflector to be illuminated and would be zero for all angles outside this region. In practice, a gradual taper from the central maximum to a null must be accepted.

The result is that even if all the radiated energy is intercepted by the reflector, the illumination will not be uniform with the resulting loss in efficiency. Thus a compromise between these two uncompatible effects must be made and it has been customary in standard Cassegrainian and prime focus systems to allow approximately a 10 dB taper of the illumination at the edge of the parabolic reflector. This results in a combined spillover-illumination efficiency between 70-80%. There is no spillover in horn-parabolas or horn lens antennas.

The spillover efficiency η_3 and the corresponding loss in gain resulting from the edge taper q are shown in Table 5. The last column of this table shows the product of the spillover and illumination efficiencies (from Table 4) and the corresponding overall loss in antenna gain.

Table 5

Loss in Antenna Gain as a Function of Spillover and Illumination Efficiencies (7% Blockage of Aperture)

				7% Blockage		No Blockage	
Fractional Edge Taper (q)	Edge Taper dB (20 log q)	Spillover Efficiency η_3	Corresponding Loss in Gain dB	Combined Spillover and Illum.Efficiency $\eta^*_2 \cdot \eta_3$	Corresponding Loss in Gain dB	$\eta_2 \cdot \eta_3$	Corresponding Loss in Gain dB
0.398	8	0.71	1.49	.545	2.66	.668	1.76
0.316	10	0.75	1.25	.552	2.57	.689	1.62
0.251	12	0.79	1.02	.561	2.51	.706	1.51
0.178	15	0.81	0.91	.545	2.63	.696	1.56
0.100	20	0.83	0.81	.522	3.03	.678	1.69
0.006	25	0.84	0.75	.473	3.25	.631	1.99
0.0	∞	0.85	0.71	.477	3.21	.636	1.96

5.1 IMPROVED FEED DESIGNS

Low feed efficiences are sometimes tolerated for the sake of low side lobes, but when maximum energy collection is required, the lag in feed design is apparent.

What is needed is a synthesis technique for designing an appropriate compromise for specific tasks. Control of feed patterns would allow the designer to balance efficiency, side lobes and the noise temp of antenna, and to produce symmetrical beams with low cross polarization.

Research in developing a method of feed pattern synthesis related to the technique utilizing multimodes in circular pipes developed at JPL[11] but of a more general nature has recently been reported[12]. The work is based on a concept of a feed capable of absorbing nearly all of the focal plane energy produced when a linearily polarized uniform plane wave is incident normally on the di:h aperture. By reciprocity the feed would approach perfect radiation efficiency (no spillover) and produce fields across dish aperture which are uniform in amplitude, phase and polarization.

With circular polarization, an increase in spillover efficiency can be obtained if the feed has nearly equal beamwidth in all planes at all levels down to the illumination at the edge of the reflector. This would also permit circular symmetry for the main and subreflectors around the boresight axis which is desirable from construction standpoint.

A conical feed horn having these properties has been developed at JPL[13]. Tests of such a horn yielded 98.7% of total energy being contained in a symmetrical main beam with 0.6% lost in sidelobes and 0.7% in cross polarization.[14] This represents an improvement over conventional conical horns which on the average contain about 2.7% energy in the sidelobes and another 2.7% in cross polarization components resulting in a loss of at least 5.4% of radiated energy.

"Dielguide" Techniques

Recently[15] a new development in the area of improvement of spillover efficiency has been described by Radiation, Inc. The technique employs dielectric guiding structures (DIELGUIDE) which are placed between the primary feed and reflector or subreflector. The reduction of spillover is accomplished through the phenomenon of total internal reflection. The operation is indicated in Fig. 10.

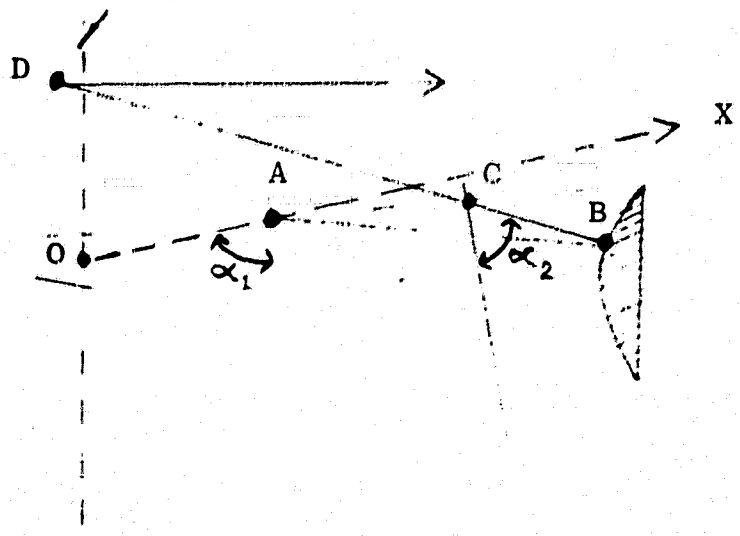


Fig. 10
Principle of Dielguide Technique

With a Cassegranian system radiated electromagnetic ray OX intersects the boundary of the dielectric at point A. If the angle α is greater than the critical, this ray which would normally miss the subreflector (path OAX) is now redirected towards point B where it is reflected and intersects the dielectric boundary at point C. This time, however, the angle of α_2 is less than critical and the ray passes across the boundary

to the main reflector where it is reflected at point D. With properly chosen parameters, the energy redirected by the dielectric boundary can be "folded" into the angular region subtended by the reflector in a manner which results in a more uniform illumination thereby improving illumination efficiency. Since the relationship for the critical angle does not contain frequency, the bandwidth of these systems depends on that of the primary feed and the requirement for sufficient electrical boundary length to effect total internal reflection.

In both Cassegranian and prime focus systems, the feeds can be made self supporting, thus requiring no spars with their attendant aperture blockage. Also, subreflectors can be made much smaller than with conventional feeds further reducing the blockage.

As a result of engineering tests, the following efficiencies have been calculated from scatter pattern data obtained from a Cassegrain Dielguide feed ultimately used with small reflectors.

Table 6
EFFICIENCY OF DIELGUIDE TECHNIQUES

Frequency	Spillover Efficiency η_2 Percent	Illumination Efficiency η_3 Percent	$\eta_2 x \eta_3$ Percent
7.2 GHz	91.0	96.0	87.3
7.8 GHz	94.5	93.5	88.2
8.4 GHz	95.3	94.2	89.7

The application of the above techniques to large size high power antenna systems has not as yet been fully investigated. Although there appears to be no reason why they should not work, Dielguides have been tested at peak powers of 3.0 megawatts and average 4 kw at 5.6 GHz, showing no breakdown or detectable heating. Whether the feeds could be made self supporting depends on the mechanical design and environmental operating conditions.

In summary, the Dielguide technique appears to provide a way to substantially improve the efficiency of antennas.

6.0 LOSS IN GAIN DUE TO ANTENNA POINTING ACCURACY

For large parabolic reflectors with uniform illumination, the beam angle B in degrees between half-power points can be calculated from

$$B = 58.45 \frac{\lambda}{D} \text{ degrees}$$

However, since in actual antennas illumination intensity across the aperture often is not uniform, but tapers off towards the edges with a corresponding reduction in gain, increase in beamwidth and reduction in sidelobes, a more realistic expression* is:

$$B \approx 70 \frac{\lambda}{D} \text{ degrees} \approx \frac{70}{fD} \text{ degrees} \quad \ldots\ldots\ldots\ldots\ldots \quad (16)$$

Substituting (1) into (16), we obtain an approximate equation relating gain and beamwidth

$$G \approx \frac{43400\eta_T}{B^2} \quad ** \quad \ldots\ldots\ldots\ldots\ldots \quad (16a)$$

where f = frequency in gigahertz

D = aperture diameter in feet

The loss in antenna gain due to pointing accuracy of the antenna can be determined as a function of the pointing angle α (measured from the antenna boresight) relative to the 3 dB beamwidth B. This is shown in Fig. 11 where the loss in gain is plotted against the normalized pointing error angle $\frac{2\alpha}{B}$.

The pointing accuracy in parabolic antennas is partially dependent on the ratio of the focal length to aperture diameter. If f/D is small (deep dish) strong supports can be provided for feed or subreflector thereby improving stability. Practical values of f/D are between 0.25 and 0.5.

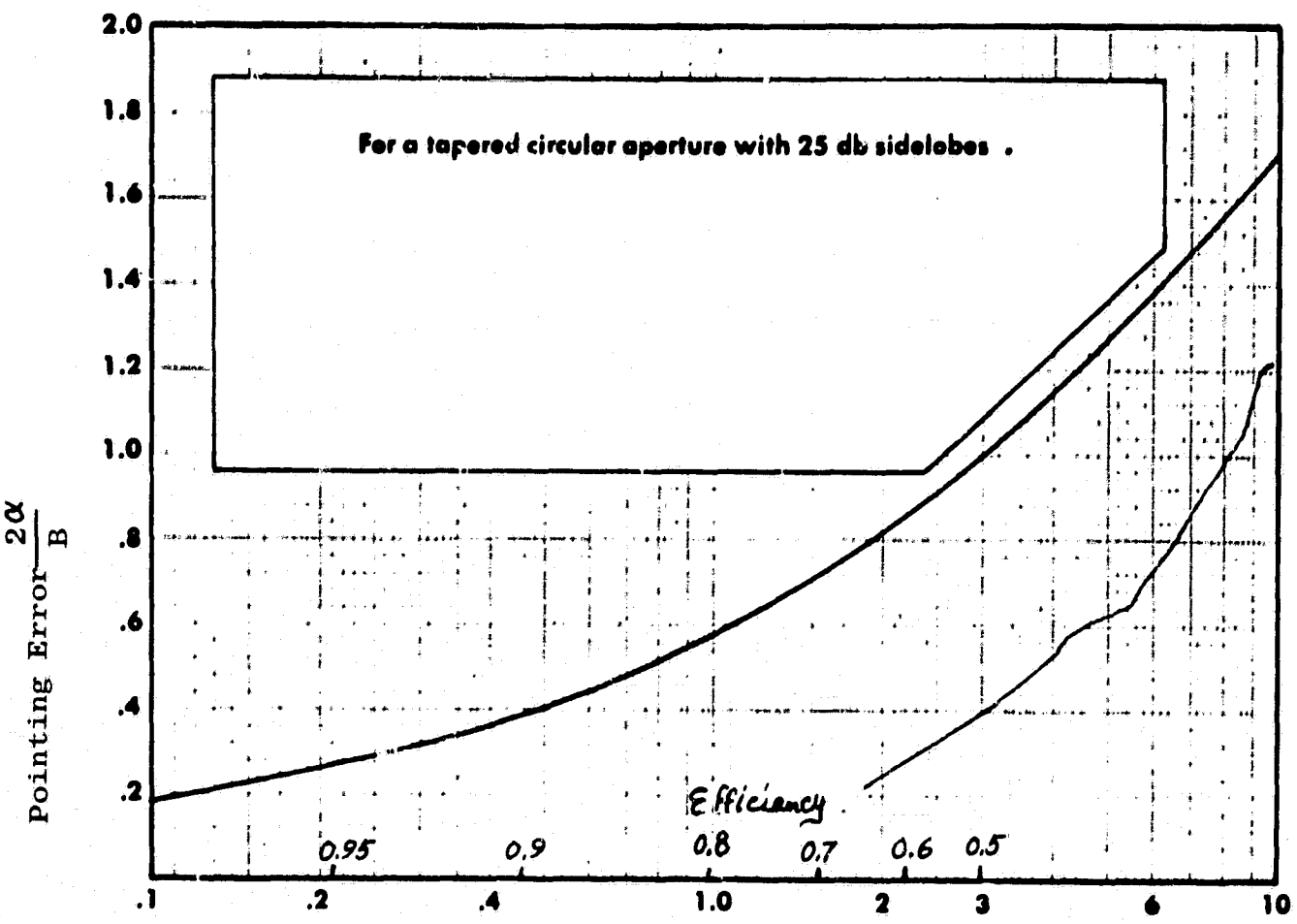
---

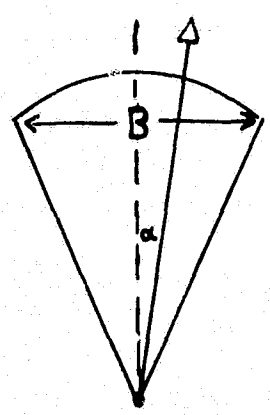
* Expression (16) corresponds approximately to a parabolic illumination distribution $\left[1 - \left(\frac{2r}{D}\right)^2\right]$, see Equation (13).

** A useful expression relating gain to beamwidth in two principal planes is $G \approx \frac{27000}{\theta_H \theta_E}$ which reduces to (16a) fr $\eta \approx 0.56$ and $B = \sqrt{\theta_H \theta_E}$

Fig. 11*

LOSS IN ANTENNA GAIN DUE TO POINTING ERROR





3 dB beamwidth

---

* From: The Microwave Engineers' Handbook, 1965 Edition.

7.0 SUMMARY

To summarize our results, we note that the contributions to the antenna loss in gain are due primarily to the surface rms tolerance if frequencies of operation are high and diameters large. From other effects the most serious source of loss in gain is the combined illumination, blockage, spillover efficiency which from Table 5 for parabolic distribution and a taper of 10 dB is approximately 0.55. If blockage is disregarded, the value is 0.69.

Other effects not discussed in this report such as power reflection (η_4) and ohmic losses (η_5) plus pointing inaccuracies and polarization losses may well produce a combined efficiency in the range of 0.9. Thus the value of η_x, the total efficiency of a parabolic antenna (not including the effects of surface roughness), is approximately -

$0.55 \times .9 \approx 0.50$ with 7% aperture blockage

$0.69 \times .9 \approx 0.62$ with no blockage.

Recent improvements in antenna designs described in this section indicate potential increases in the efficiency factor. Accordingly, a figure of 0.6 for overall efficiency including approximately 5% aperture blockage will be used as a state-of-the-art figure in this study.

8.0 EXISTING STATE OF THE ART

In the preceding sections we have discussed the various factors which result in the loss of antenna gain and have derived formulae permitting the calculation of these losses. We now wish to examine the characteristics of the antennas that have actually been constructed and are operational.

An extensive survey of published data was conducted. The results are shown in Table 7 in which the beamwidth B was computed from the approximate formula (16), i.e., $B \approx \frac{70}{fD}$ degrees.

A gain-frequency plot of various large size antennas presently in operation which appeared in technical press is reproduced in Fig. 12.

Table 7

Typical Antennas

	DIAMETER (D) (FEET)	TOLERANCE (IN RMS) (INCHES)	PRECISION (D/E)	FREQUENCY (GHz) (1)		BEAMWIDTH (MIN) (2)
Radio Astronomy Antennas						
1. Jodrell Bank	250	1.2	2,500	0.65		26
2. Greenbank	300	0.47	7,600	1.66		8.5
3. Stanford	150	0.55	3,270	1.42		20
4. Parkes-CSIRO	210	0.14	18,000	5.60		3.5
5. Michigan	85	0.043	23,600	18.00		2.75
6. Lebedev	72	0.025	34,500	31.00		1.9
7. Haystack	120	0.04	36,000	20.00		1.8
8. Haystack	120	0.025(3)(4)	58,000(3)	32.40(3)		1.1(3)
9. CAMROC	400	0.13(4)	37,000	6.00		1.71
Communication Antennas				Operating Freq. +	(1)	
10. GPO - Goonhilly	85	0.1	10,200	4.17	7.4	11.9
11. JPL - Goldstone	85	0.1	10,200	2.4	7.4	20.6
12. JPL - Goldstone	210	0.17	14,800	2.4	4.2	
13. JPL - Goldstone	210	0.125(4)	20,150			
14. KDD - Japan	66	0.12	6,600	4.17	6.5	15.3
15. Radio Research Lab - Japan	108	0.2	6,480	4.17	3.7	9.33
16. Deutche Bundespost - Raisting	92	0.04	27,600	4.16		
17. Philco, Italy	90	0.04	27,000			

(1) Frequency at which loss due to reflector surface tolerance is 3 dB.

(2) Half-power beamwidth at indicated frequency (or at operating frequency) $B \approx \frac{70}{fD} \times 60$.

(3) Expected after rerigging.

(4) In radome.

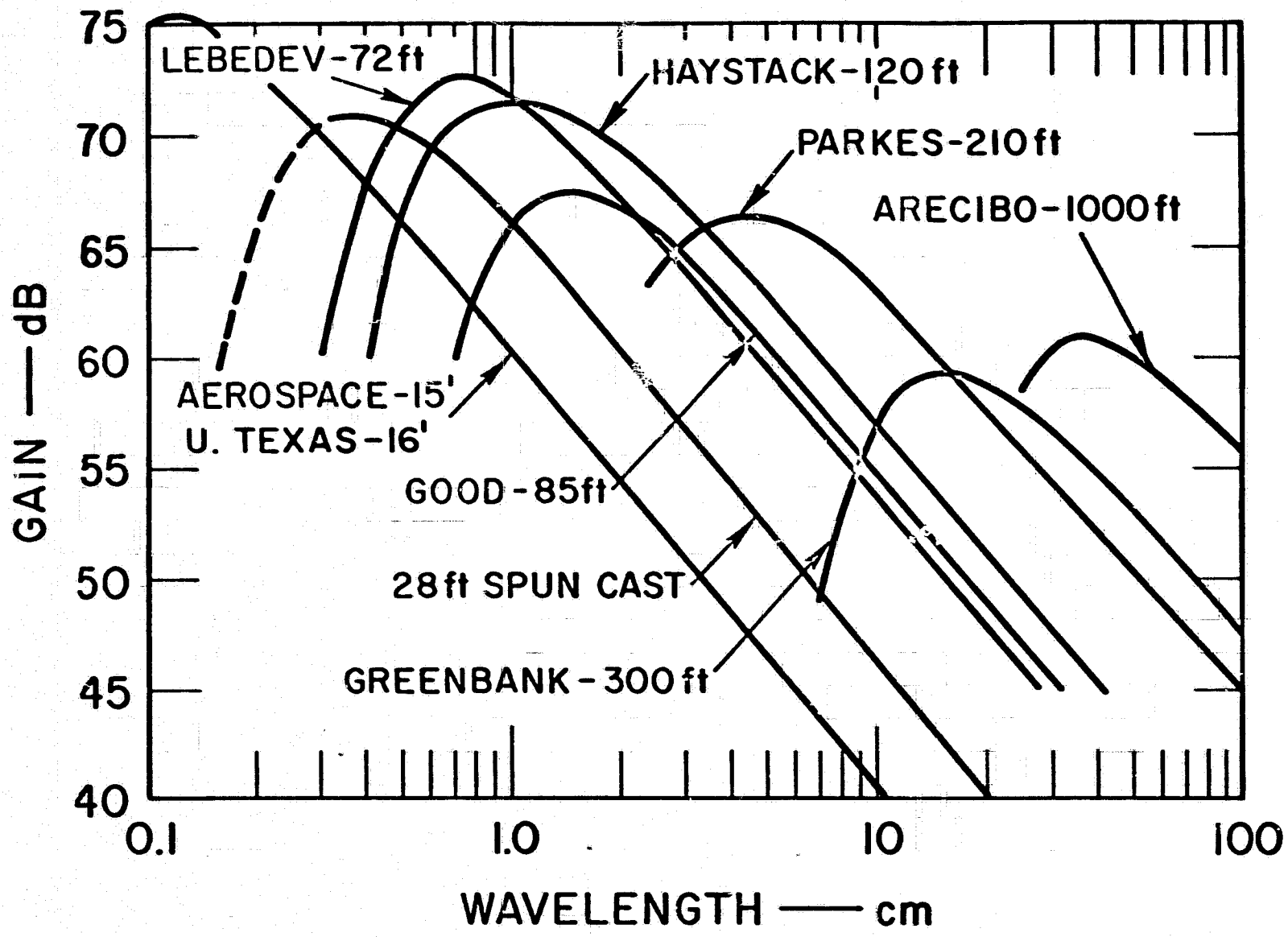


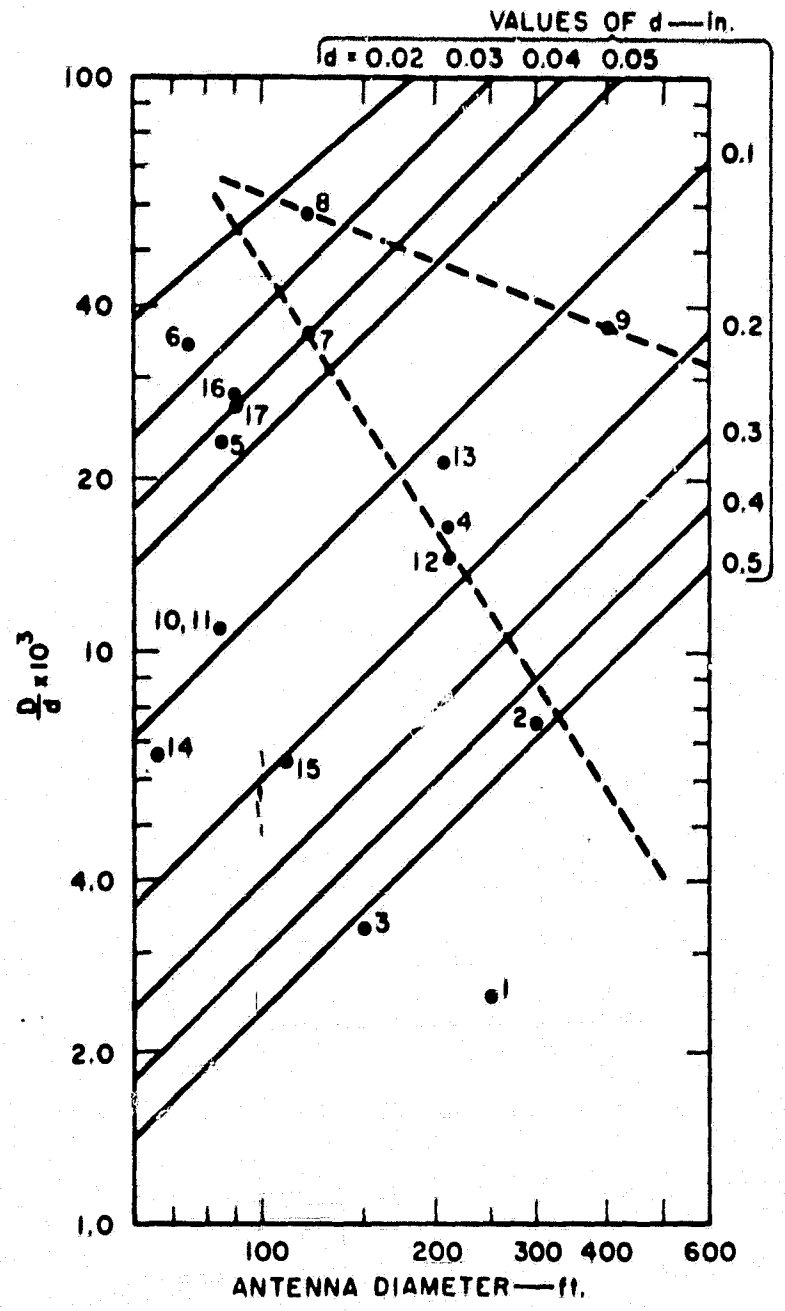
FIG. 12 GAIN OF LARGE PARABOLOIDS

In order to estimate the practical limits on surface tolerances, the values of "manufacturing precision" parameter D/d for existing antennas listed in Table 7 and are plotted in Fig. 13. This curve shows a rather wide variation of values. The lower dashed line represents the average upper limit of manufacturing precision on dishes presently in existence. The dashed top line represents design objectives for two radome enclosed reflectors. Corresponding values of d are also indicated. Note that a value of $\frac{D}{d}$ (which is a measure of maximum gain) of about 36000 is the highest that has been attained in practice at this time. This corresponds to a tolerance of approximately 0.033 inches rms for a 100-foot antenna and represents the approximate limit that can be met with present day manufacturing techniques without incurring substantially higher costs.

The survey of all large antenna manufacturers in the U.S. produced a general consensus that a "shop practice" rms surface tolerance for antennas in the range of diameters from 85-100 feet is approximately 0.04 inches. No such agreement exists for larger antenna sizes. In general the accuracy obtained in the JPL 210-foot Goldstone antenna (0.17 inches) was accepted as representing the state of the art.

Using these figures, we can now derive an approximate expression for the limits on the gain of practical antennas. Since in actual practice the size of the antenna obviously affects the total manufacturing precision, let us include this effect in our calculation by deriving a quantity q called "manufacturing precision per foot of antenna diameter."

$$q = \frac{d}{D} \cdot \frac{1}{D} = \frac{d}{D^2} \qquad \ldots\ldots\ldots\ldots \qquad (17)$$



RADIO ASTRONOMY ANTENNAS
1. JODRELL BANK
2. GREENBANK
3. STANFORD
4. PARKES - CSIRO
5. MICHIGAN
6. LEBEDEV
7. HAYSTACK
8. HAYSTACK (In radome)
9. CAMROC (In radome)

COMMUNICATION ANTENNAS
10. GPO, GOONHILLY
11. JPL, GOLDSTONE (85 ft)
12. JPL, GOLDSTONE (210 ft.)
13. JPL, GOLDSTONE (210 in radome proposed)
14. KDD, JAPAN
15. RADIO RESEARCH LAB, JAPAN
16. DEUTCHE BUNDESPOST, RAISTING
17. PHILCO, ITALY

FIG. 13 MANUFACTURING PRECISION OF EXISTING AND PROPOSED ANTENNAS.

Computing this quantity for the case of a 100-foot antenna with a 0.04 inch rms surface tolerance, we obtain

$$q = \frac{.04}{12x100} \times \frac{1}{100} = \frac{1}{3x10^6} = 3.33 \times 10^{-7}$$

Similarly for a 210-foot antenna with an rms tolerance of 0.17 inches, we obtain

$$q = \frac{.17}{12x210} \times \frac{1}{210} = \frac{1}{3.1x10^6} = 3.23 \times 10^{-7}$$

These two results are remarkably similar and suggest that as a first approximation the relationship between the rms surface tolerance and antenna diameter could be expressed by the following equation:

$$\frac{d}{12D^2} \approx 3.3 \times 10^{-7}$$

where d is the rms surface tolerance in inches;
D is the antenna diameter in feet.

$$\therefore \quad d \approx 12 \times 3.3 \times 10^{-7} \times D^2$$

$$\approx 4D^2 \times 10^{-6} \text{ inches} \qquad \ldots\ldots\ldots\ldots\ldots \quad (18)$$

$$\text{or} \quad d \approx \frac{4D^2}{12} 10^{-6} \text{ feet} \qquad \ldots\ldots\ldots\ldots\ldots \quad (19)$$

If this relationship is adopted, we obtain the following rms surface tolerances for various antenna diameters.

Table 8
Relationship Between Antenna Diameter
and RMS Surface Tolerance

D_{ft}	d_{inch}
100 ft	0.04
200 ft	0.16
300 ft	0.36
400 ft	0.64

Discussion with manufacturers and the analysis of antenna design possibilities for a 400-foot antenna included in the CAMRC[3] report[16] indicate that these values are reasonable for exposed antennas. We can therefore substitute (19) into the equation for antenna gain:

$$G = \eta\left(\frac{\pi D}{\lambda}\right)^2 \exp - \left(\frac{4\pi d}{\lambda}\right)^2 \qquad \text{.....} \qquad (20)$$

with the following result -

$$G = \eta\left(\frac{\pi D}{\lambda}\right)^2 \exp - \left(\frac{4\pi}{\lambda} \cdot \frac{4D^2}{10^6} \cdot \frac{1}{12}\right)^2 \qquad \text{.....} \qquad (21)$$

The solution of this equation is given in Table 9 which indicates the gain with ideally smooth surface and $\eta = 0.6$ in column 1, the loss in gain due to surface roughness (column 2) and the net total gain G (column 3).

The total gain G is plotted in Fig. 14 for frequencies from 1 to 10 Gc as a function of antenna diameters 100-400 feet. This curve shows the maximum gains that can be obtained from an antenna in which the rms surface tolerance varies as $4D^2 \times 10^{-6}$ and the aperture efficiency is 0.6. It can be seen that the highest obtainable gain under these conditions is 67.8 dB which occurs at 10 Gc with an antenna diameter of approximately 130 feet.

It should be remembered that Fig. 14 represents the gains of "shop practice" antennas, i.e., those that can be constructed with standard procedures without incurring special costs. If more gain is required, it can be obtained by improving the surface tolerance over and above those shown in Table 8.

Table 9
Gain of Various Size Antennas
$\eta = 0.6$

Frequency Gc	Gain With Smooth Reflector (d=0) dB	Loss in Gain Due to Surface Roughness $d=4D^2 \times 10^{-6}$ dB	Net Gain of Antenna dB
Diameter = 100			
10	67.8825	-.790088	67.0924
9	66.9673	-.639971	66.3273
8	65.9442	-.505656	65.4386
7	64.7844	-.387143	64.3972
6	63.4454	-.284432	63.161
5	61.8618	-.197522	61.6643
4	59.9236	-.126414	59.7971
3	57.4247	-7.11079 E-2	57.3536
2	53.9029	-3.16035 E-2	53.8713
1	47.8822	-7.90089 E-3	47.8743
Diameter = 125			
10	69.8207	-1.92893	67.8918
9	68.9055	-1.56243	67.3431
8	67.8825	-1.23451	66.6479
7	66.7226	-.945173	65.7774
6	65.3836	-.694413	64.6892
5	63.8	-.432231	63.3178
4	61.8618	-.308628	61.5532
3	59.363	-.173603	59.1894
2	55.8411	-.077157	55.7639
1	49.8204	-1.92893 E-2	49.8011
Diameter = 150			
10	71.4043	-3.99982	67.4045
9	70.4892	-3.23985	67.2493
8	69.4661	-2.55988	66.9062
7	68.3062	-1.95991	66.3463
6	66.9673	-1.43994	65.5274
5	65.3836	-.999955	64.3837
4	63.4454	-.639971	62.8055
3	60.9466	-.359984	60.5866
2	57.4247	-.159993	57.2648
1	51.4041	-3.99982 E-2	51.3641
Diameter = 175			
10	72.7433	-7.41016	65.3331
9	71.8281	-6.00223	65.8259
8	70.8051	-4.7425	66.0626
7	69.6452	-3.63098	66.0142
6	68.3062	-2.66766	65.6386
5	66.7226	-1.85254	64.8701
4	64.7844	-1.18563	63.5988
3	62.2856	-.666914	61.6187
2	58.7637	-.296406	58.4673
1	52.743	-7.41016 E-2	52.6689

η = 0.6

Frequency Gc	Gain With Smooth Reflector (d=0) dB	Loss in Gain Due to Surface Roughness $d=4D^2 \times 10^{-6}$ dB	Net Gain of Antenna dB
Diameter = 200			
10	73.9031	-12.6414	61.2617
9	72.988	-10.2395	62.7484
8	71.9649	-8.0905	63.8744
7	70.8051	-6.19429	64.6108
6	69.4661	-4.55091	64.9152
5	67.8825	-3.16035	64.7221
4	65.9442	-2.02262	63.9216
3	63.4454	-1.13773	62.3077
2	59.9236	-.505656	59.4179
1	53.9029	-.126414	53.7765
Diameter = 225			
10	74.9262	-20.2491	54.6771
9	74.011	-16.4018	57.6093
8	72.988	-12.9594	60.0286
7	71.8281	-9.92205	61.9061
6	70.4892	-7.28967	63.1995
5	68.9055	-5.06227	63.8432
4	66.9673	-3.23985	63.7274
3	64.4685	-1.82242	62.6461
2	60.9466	-.809963	60.1367
1	54.9259	-.202491	54.7235
Diameter = 250			
10	75.8414	-30.8628	44.9786
9	74.9262	-24.9989	49.9273
8	73.9031	-19.7522	54.1509
7	72.7433	-15.1228	57.6205
6	71.4043	-11.1106	60.2937
5	69.8207	-7.7157	62.105
4	67.8825	-4.93805	62.9444
3	65.3836	-2.77765	62.606
2	61.8618	-1.23451	60.6273
1	55.8411	-.308628	55.5325
Diameter = 275			
10	76.6692	-45.1862	31.483
9	75.7541	-36.6008	39.1532
8	74.731	-28.9192	45.8118
7	73.5711	-22.1413	51.4299
6	72.2322	-16.267	55.9651
5	70.6485	-11.2966	59.352
4	68.7103	-7.2298	61.4805
3	66.2115	-4.06676	62.1448
2	62.6896	-1.80745	60.8822
1	56.669	-.451862	56.2171

η = 0.6

Frequency Gc	Gain With Smooth Reflector (d=0) dB	Loss in Gain Due to Surface Roughness $d=1D^{-2}x10^{-6}$ dB	Net Gain of Antenna dB
Diameter = 300			
10	77.425	-63.9971	13.4279
9	76.5098	-51.8377	24.6722
8	75.4868	-40.9582	34.5286
7	74.3269	-31.3586	42.9683
6	72.988	-23.039	49.949
5	71.4043	-15.9993	55.405
4	69.4661	-10.2395	59.2266
3	66.9673	-5.75974	61.2076
2	63.4454	-2.55988	60.8855
1	57.4247	-.639971	56.7848
Diameter = 325			
10	78.1203	-88.1473	-10.027
9	77.2051	-71.3993	5.80582
8	76.182	-56.4142	19.7678
7	75.0222	-43.1922	31.83
6	73.6832	-31.733	41.9502
5	72.0996	-22.0368	50.0628
4	70.1614	-14.1036	56.0578
3	67.6625	-7.93325	59.7293
2	64.1407	-3.52589	60.6148
1	58.12	-.881473	57.2385
Diameter = 350			
10	78.764	-118.563	-39.7986
9	77.8488	-96.0357	-18.1869
8	76.8257	-75.88	.945699
7	75.6659	-58.0956	17.5702
6	74.3269	-42.6825	31.6444
5	72.7433	-29.6406	43.1026
4	70.8051	-18.97	51.835
3	68.3062	-10.6706	57.6356
2	64.7844	-4.7425	60.0419
1	58.7637	-1.18563	57.5781
Diameter = 375			
10	79.3632	-156.243	-76.8797
9	78.4481	-126.557	-48.1087
8	77.425	-99.9955	-22.5705
7	76.2651	-76.559	-.293895
6	74.9262	-56.2475	18.6787
5	73.3426	-39.0607	34.2818
4	71.4043	-24.9989	46.4055
3	68.9055	-14.0619	54.8437
2	65.3836	-6.24972	59.1339
1	59.363	-1.56243	57.8005

η = 0.6

Frequency Gc	Gain With Smooth Reflector (d=0) dB	Loss in Gain Due to Surface Roughness $d=4D^2 \times 10^{-6}$ dB	Net Gain of Antenna dB
Diameter = 400			
10	79.9238	-202.262	-122.339
9	79.0086	-163.833	-84.824
8	77.9856	-129.448	-51.4624
7	76.8257	-99.1086	-22.2829
6	75.4868	-72.8145	2.67229
5	73.9031	-50.5656	23.3375
4	71.9649	-32.362	39.6029
3	69.4661	-18.2036	51.2625
2	65.9442	-8.0905	57.8537
1	59.9236	-2.02262	57.9009

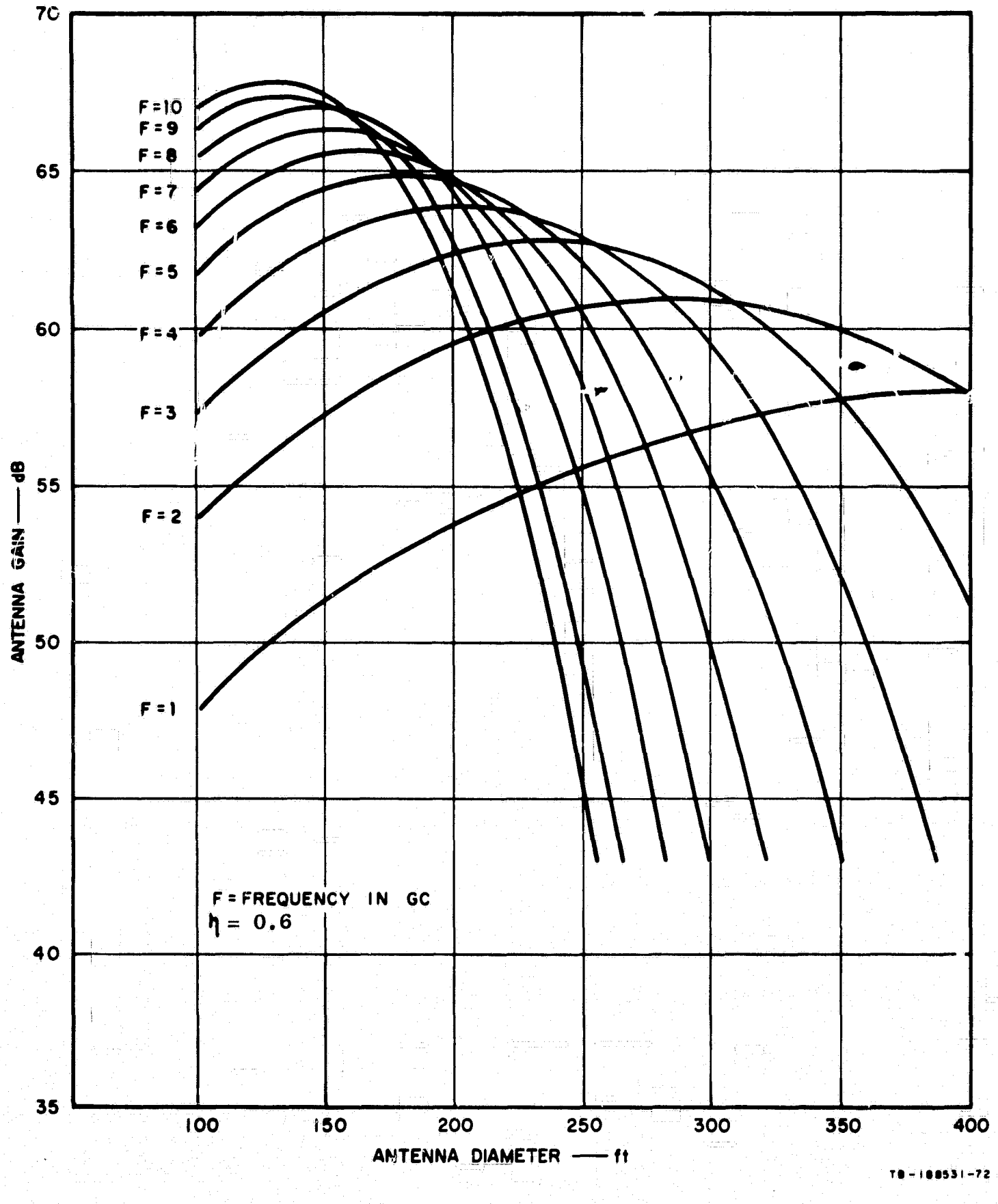


FIG. 14 ANTENNA GAIN vs. DIAMETER
(rms surface deviation = $4D^2/10^6$)

9.0 CONCLUSIONS

The general conclusion, reached as a result of this study, is that the increase in antenna diameter past approximately 150 feet does not result in increases in gain at frequencies above 6 Gc unless premium cost is paid for custom made reflector surfaces.

Under our assumption of the relationship between antenna diameter and its tolerance, and a 60% aperture efficiency (η_x), the optimum performance for various frequencies are as follows.

Table 10
Optimum Antenna Performance
Under Practical Conditions

Frequency Gc	Approximate Maximum Gain dB Obtainable in Practice with Surface Toler.$=4D^2 10^{-6}$	Approximate Antenna Diameter D ft
1	58	400
2	60.9	288
3	62.6	238
4	63.9	200
5	64.8	180
6	65.6	163
7	66.3	150
8	66.9	144
9	67.3	136
10	67.8	130

If aperture efficiency increases to 100% (ideal), 2.2 dB additional gain would result.

References

1 Design & Construction of Large Steerable Aerials, IEE Conference Publication No. 21, p. 274.

2 Final Report "Feasibility Analysis of a Deep-Space Receiving Terminal Array of Large Equivalent Aperture," Contract NAS 1-3075, Stanford Research Institute, May 1964, p. 38.

3 "Antenna Tolerance Theory - A Review," J. Ruze, Proceedings IEEE, Vol. 54, No. 4, April 1966.

4 Ibid, p. 637.

5 J. W. Findlay, "Operating experience at the National Radio Astronomy Observatory," Ann. N.Y. Acad. Sci., vol. 116, pp. 25-40, June 1964.

6 P. G. Mezger, "An experimental check of antenna tolerance theory using the NRAO 85-foot and 300-foot telescopes," 1964 Internat'l Symp. on Antennas and Propagation, pp. 181-185.

7 Design & Construction of Large Steerable Aerials, IEE Conference Publication No. 21, p. 838.

8 "Antenna Tolerance Theory - A Review," J. Ruze, Proceedings IEEE, Vol. 54, No. 4, April 1966.

9 S. Silver, "Microwave Antenna Theory and Design," McGraw Hill, 1949.

10 JPL Space Program Summary 37-35, p. 266.

11 "Beam Shaping by the Use of Higher Order Modes in Conical Horns," P. D. Potter, et al, 1963 NEREM Record.

12 Design & Construction of Large Steerable Aerials, IEE Conference Publication No. 21, p. 262.

13 P. D. Potter, "A New Horn Antenna with Suppressed Sidelobes and Equal Beamwidth," The Microwave Journal, June 1963, p. 71.

14 W. F. Williams, "High Efficiency Antenna Reflector," Microwave Journal, July 1965, p. 81.

15 H. E. Bartlett and R. E. Mosely, "Dielguides - Highly Efficient Low Noise Antenna Feeds," The Microwave Journal, Dec 1966.

16 "A large Radio-Radar Telescope, CAMROC Design Concepts," The Cambridge Radio Observatory Committee, 15 January 1967.

APPENDIX E

ALTERNATE ANTENNA DESIGNS

ALTERNATIVE ANTENNA DESIGNS

I INTRODUCTION

A. General

When considering the building of an array of large aperture, several approaches come to mind as being feasible and providing the necessary technical capability. The technique most frequently used at the present time, at least for equivalent sizes of 100-200 feet in diameter, is that of a fully steerable paraboloid. Design techniques for maximizing efficiency, minimizing noise and achieving usable tracking rates have been thoroughly studied and applied in practice. However, since the cost of a steerable paraboloid rises exponentially with diameter, this technique may not be most appropriate in terms of cost for very large areas, particularly if some reduced performance characteristics can be tolerated. Investigations tend to show also that cost is not greatly reduced if allowable steering excursions are reduced.[1]

Thus it becomes important to look at alternative methods of obtaining high gain. Three approaches are examined in this paper. These are parabolic antenna arrays of large equivalent aperture, a fixed spherical reflector with a movable feed, and multiple plate antennas. Technical design considerations are first examined and then cost comparisons are made. Finally, some conclusions are drawn.

One point must be clearly kept in mind when considering alternate antenna concepts. This is that most such concepts trade off a reduction

---

1 D. H. Shinn, "Requirements for Aerial Mounts for Following Satellites," in Design & Construction of Large Steerable Aerials, IEE Conference Publication Number 21 (London: Institution of Electrical Engineers, 1965) p. 4.

in performance for cost and that this reduction in performance is often in reduced steerability or reduced bandwidth. Thus the question immediately arises as to the feasibility of station location and satellite placement such that such limited steerability is acceptable over the economic life of the system. If the satellite station keeping system should fail and the satellite start to drift, it could probably still be used if the earth antenna had sufficient steerability. If the system use is going to be continuous, or at least equal to the life of the ground station, this does not present a problem, but if some special purpose system use is contemplated, where the requirement may terminate after a few years, or require the movement of the satellite to a new physical location, the cost of the ground station may have to be written off during this short time period, thus raising its yearly operating cost prohibitively. For the purpose of this paper, it will be assumed that the system use will extend at least as long as the useful physical life of the earth station, which may be optimally located and that satellite position may be maintained over the life of the satellite. Deviations from these assumptions will have to be factored into technical and cost comparisons.

It is very hard to develop firm conclusions from the available information on the alternative antenna designs considered for two reasons. First of all, the costs and design techniques used are highly dependent on the system parameters under consideration. Secondly, most studies of these techniques in the past have evolved around their use as radio telescopes or deep-space receiving systems. There has not been any detailed consideration of their use for active satellite communication systems because the need did not exist. However, a passive system, such as that under consideration in this study, does require very high ERP and received signal gain. Thus questions of bandwidth and transmitter power become important. Because of time and effort limitations on the present study, it was not possible to do a complete engineering design study based on a specific system concept.

The following study has primarily attempted to review the technical and cost literature in view of the general passive satellite system requirements and to draw general conclusions as to the applicability of the various techniques.

B. Advantages of a Radome

Before examining the alternative techniques mentioned above, some consideration should be given to the possibility of reducing the structural costs of large antennas by the use of a radome. A recent study by the Cambridge Radio Observatory Committee on a fully steerable radio telescope has shown the potential savings of this technique.[2]

The CAMROC study has indicated that an increase in antenna size of approximately 10% will fully compensate for any radome losses.[3] However, the reduction in the structure cost made possible by the reduced environmental loading will more than pay for the increased antenna size.[4] While very great cost savings were projected, there was a considerable range for the estimates of a 400-foot diameter environmental antenna, despite the detailed study that went into it by a variety of firms.[5]

It is entirely possible that the use of a radome could reduce the costs of some of the designs to be discussed, particularly the fixed spherical reflector. However because of the lack of detailed design data, these potential savings are not reflected in the study.

---

2 A Large Radio-Radar Telescope: CAMROC Design Concepts, 2 Volumes, (Cambridge, Mass.: Cambridge Radio Observatory Committee, 15 January 1967).

3 Ibid, p. 2-9.

4 Ibid, p. 2-8.

5 Ibid, p. 6-6.

II TECHNICAL CONSIDERATIONS

A. Parabolic Antenna Arrays of Large Equivalent Aperture[6]

One way of obtaining high gain without the use of excessively large and costly parabolic reflectors is the use of multiple parabolic antenna arrays phased so as to give an equivalent aperture larger than any single antenna. If it can be assumed that the cost of large antennas is not a linear function with size, but that it increases at some exponential rate, then there is conceivably some point at which equal performance for a lower cost can be obtained using phased arrays rather than a single large antenna. At the present time at least one major experimental installation of this type exists where four 30-foot antennas have been arrayed to make an equivalent 60-foot aperture.[7] This array has been used in several space communication experiments.

The adaptive phased array is intended to exploit the full capabilities of the concept by the implementation of continuous self-adjustment of the phases of the array elements, to optimize the coherent summing of antenna outputs for enhancing the signal-to-noise ratio (SNR) in the receiving mode, or for enhancing the power density in the desired direction in the transmitting mode. The degree of enhancement by the array over a single one of its elements may be as high as the number of array elements and, conceptually, there is no limit to the enhancement that can be achieved by adding more elements with automatic phase control. Assuming that the noise in the

---

6 This section draws heavily on the work done by SRI on Contract NAS1-3075, for the NASA Langley Research Center. See Feasibility Analysis of a Deep-Space Receiving Terminal Array of Large Equivalent Aperture, R. B. Battle (Ed.) (Menlo Park, Calif.: Stanford Research Institute, May 1964).

7 J. W. Eberle, "An Adaptively Phased, Four-Element Array of Thirty-Foot Parabolic Reflectors for Passive (Echo) Communication Systems," IEEE Transactions on Antennas and Propagation, Vol. AP-12, pp. 169-176, March 1964.

various channels is not coherent and that the signals in the various channels may be summed coherently, a SNR equal to the summation of the input SNRs may be obtained.[8] Practically, however, there are economic and technical limitations to the number of elements that can be operated efficiently.

Assuming that equivalent aperture efficiencies could be obtained for both the larger and smaller antennas, then the minimum number of smaller antennas, N min, required to achieve an aperture equivalent to that of the larger antenna is related to the antenna diameters by the equation

$$N \text{ min} = \left(\frac{D_1}{D_2}\right)^2 \qquad (1)$$

Where D_1 is the large antenna diameter in feet and D_2 is the array antenna diameter in feet. Additional antennas in the array might be necessary to compensate for anticipated antenna and receiver breakdowns to maintain a given SNR or to compensate for reduced aperture efficiency due to wind loading or other structural effects.

Besides having the potential of cost savings, a phased array has the additional advantage of relative immunity to system failure. While the added complexity of the phased array increases the probability of failure of a subsystem, the inherent redundancy of a number of units operating in parallel greatly reduces the chance of total system failure and tends to reduce the system degradation caused by individual subsystem failures. The antenna array system includes the summation of the various signals on a weighted basis, where the weighting is proportional to the SNR in a given channel. This results in high reliability since a noisy or inoperative channel will automatically reduce its own weighting and the remaining

---

8 J. H. Schrader, "Receiving System Design for the Arraying of Independently Steerable Antennas," IRE Transactions on Space Electronics and Telemetry, Vol. SET-8 (June 1962), p. 149.

channels will be fully operative and contribute to the combined SNR. A maser preamplifier failure on a single 500-foot dish would result in the loss of all communication until it was repaired; whereas, the failure of a preamplifier on a single dish of a 25 element array would result in only a fraction of a dB reduction in SNR. In an operational communication system, this becomes an important factor in the measurement of system performance.

1. General Design - The number of individual antennas required is a function of the equivalent size desired and the individual array size (see Equation 1). Table I shows the number required for both a 400- and 500-foot equivalent size. The number of antennas required is indicated for the precise size shown to synthesize a given aperture. However, the deviations are a small percentage of the total antenna diameter in each case, and may be neglected as far as cost considerations are concerned for a general analysis. Thus, the number of antennas and the standard diameter will be used in the remainder of the analysis.

In the general design, individual antennas are arranged in a pattern suitable for the elevation angles and azimuth coverage desired. For example, for arrays traversing a generally east-west direction with look angles down to 4 degrees of the horizon, a north-south, three-column configuration of 35 antennas, gives an extreme dimension of a little over 3000 feet.[9] While the array geometry is primarily determined by the scan requirements, it is important that the extreme dimension of the array should be as small as possible in order to minimize the amount of variable time delay that must be built into the receiving network (see below). About one microsecond of variable delay is required for each 1000 feet of array dimension.

---

[9] Battle, Op Cit, p. 23. For a more detailed discussion of array geometry, see pages 121-139.

Table I

Number of Required Antennas

Standard Diameter (feet)	400 FT			500 FT		
	Number of Antennas	Diameter to Synthesize 400 ft Aperture (feet)	Variance from Standard Diameter (feet)*	Number of Antennas	Diameter to Synthesize 500 ft Aperture (feet)	Variance from Standard Diameter (feet)*
60	44	60.2	+ 0.2	69	60.2	+ 0.2
85	22	85.1	+ 0.1	35	84.5	- 0.5
120	11	120.5	+ 0.5	17	121.3	+ 1.3
150	7	151.0	+ 1.0	11	150.8	+ 0.8
210	4	200.0	-10.0	6	204.1	- 5.9

* Because the variance from standard diameter is small in all cases, they would not have a significant effect on antenna costs, and they thus have been ignored in the remainder of the report.

The signals received by the elements of the array of parabolic antennas must be processed to obtain a single signal as nearly as possible equivalent to the signal that would have been received by a single antenna having an aperture equal to the total aperture of the array. At the array center (a convenient reference point rather than a specific physical location), the received carrier frequency will be different from the transmitted frequency because of Doppler effects and propagation delays which will cause variations in the signals received by the various elements of the array. Those phase and frequency variations which are common must be removed from all signals and the additional individual phase and frequency variations must be removed from each signal. A functional block diagram of a receiver designed for this purpose is shown in Fig. 1.[10]

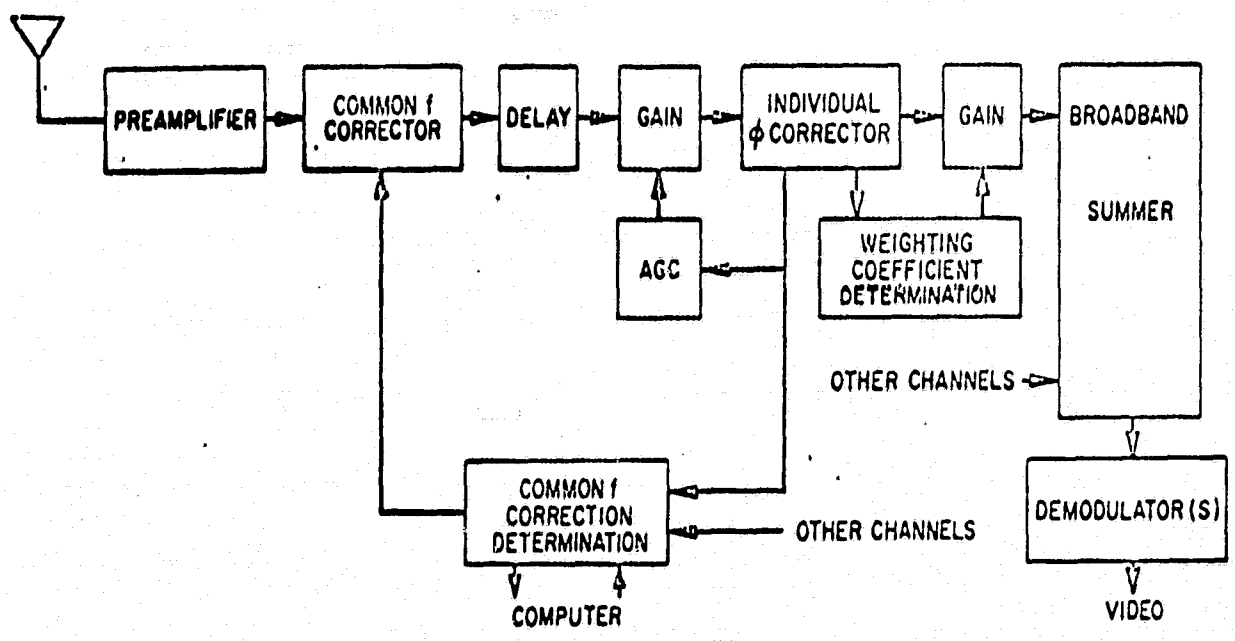


FIG. 1 RECEIVER FUNCTIONAL DIAGRAM.

SOURCE: Feasibility Analysis of a Deep-Space Receiving Terminal Array of Large Equivalent Aperture (Menlo Park: SRI, 1964), p. 68.

---

10 Ibid, p. 68.

To date most discussions have been limited to systems with a small number of antennas having minimal end to end separations and operating over relatively limited bandwidths, where all phase corrections can be made in the phase-lock receiver. The existing four-element array at Ohio State University is of this design.[11] However, for larger arrays and wider bandwidths, in order to ease the requirements on the signal processor during and after signal acquisition, all possible use should be made of available information. For the most part, the various delay corrections can be calculated from the array geometry and the array look angle. The various time delays associated with each antenna element must be inserted with an accuracy of ± 0.01 microsecond for a video bandwidth of 10 MHz, and the relative locations of the phase centers of each antenna element must be known to ± 3 feet while the time delays inherent in the cables and electronic systems of each separate antenna element must be known to within ± 0.003 microseconds for the same bandwidth.[12]

The time delays inserted in the transmission lines leading from the various antennas must be varied with the elevation and azimuth pointing angles, and the devices producing them must have sufficient bandwidth and linearity so as to not cause undue distortion in the communication signal. These variable time delays may be obtained by either electrical or mechanical means; however, previous studies have indicated, for a somewhat similar application, that:

> "The most useful delay for the phased array is the ultrasonic line employing a crystal for the sound-carrying medium and variable path length between transducers to obtain delay variation." 13

---

11 Eberle, Op Cit, p. 174.

12 J. H. Schrader, "A Phase-Lock Receiver for the Arraying of Independently Directed Antennas," IEEE Transactions on Antenna and Propagation, Vol. AP-12, March 1964, p. 156.

13 Battle, Op Cit, p. 81.

Thus the combination of programmable variable time delays between each antenna and the receiver and multi-loop phase-lock receivers will permit the phasing of a large number of individual antenna elements to equal in SNR performance to a large equivalent antenna.

Similar techniques must be used to permit the enhancing of the power density when transmitting. To date the bulk of the work in this area has evolved around phased arrays designed to achieve beam movement without physical movement of the antenna. In addition, self-phasing arrays have received considerable attention.[14] However, most antenna arrays considered to date have involved relatively small radiating elements with relatively low power RF devices, distributed over a relatively small area when compared to the requirement for megawatts of generated power coupled into an effective antenna gain of 70 dB or more, as may be required for passive communication satellite systems. Even where arrays of large aperture antennas have been considered for various deep-space applications, it has generally been assumed that sufficient ERP could be generated by a single large antenna and high power transmitter and that the arrays would only be used for reception.[15]

The use of an array of antenna elements for transmission requires the insertion of variable time delays between the single, coherent exciter and the various transmitters at the antenna elements. These time delays would have to be set using the same information derived for setting the time delays in the receiving paths. Since the power amplifiers would be located at each antenna, the delay elements would only have to operate at low power, and noise would not be as severe a problem as in the receiving paths. Fixed time delays in the transmission paths would have to be known precisely. Despite the general agreement that enhancement of ERP is

---

14 M. I. Skolnik and D. D. King, "Self-Phasing Array Antenna," IEEE Transactions on Antennas and Propagation, Vol. AP-12, March 1964, pp. 142-149.

15 P. Gene Smith, "Systems Capabilities of Arrays of Large-Aperture Antennas, IEEE Transactions on Aerospace and Electronic Systems, Vol. AES-2, May 1966, pp. 240-251.

feasible using this technique, the problem appears to be considerably more severe than designing a receive-only phased array and much less study and experimentation has been devoted to it. Thus, it must remain a serious question.

2. Design Problems - At the present time, no arrays of large aperture antennas are known to exist above an equivalent aperture of 60 feet in the 6-10 Gc range. Thus, the design of such a system is subject to some uncertainty. Phase-lock receivers of the general capabilities required have been built and general system designs worked out on paper. However, detailed system designs and equipment specifications have not been completed.

Particular emphasis must be placed on the specification and development of the special purpose electronic equipment which would be required for such an array. This would include:[16]

a. Servo control equipment

b. Antenna position readout equipment

c. Phase-lock receivers with computer controlled bandwidth, gain, and frequency

d. Variable, wideband delay lines

e. Communication summing and processing equipment

f. Computation and control facilities and procedures

g. Calibration, alignment, and monitoring instrumentation

h. Meteorological measurement and monitoring equipment.

In addition, reliable information is still lacking on turbulence effects on propagation through the ionosphere and the troposphere. This data will effect the maximum array size, maximum usable frequency, and the maximum desirable antenna size for the array. All these factors of course affect the total system cost.

---

16 Battle, Op Cit, p. 27.

3. Conclusions - The use of phased arrays of large equivalent aperture appears to be a lower cost approach to obtaining very high gain at X-band frequencies where full antenna performance (steerability) is required. However because of the nature of the electronics involved, it may be difficult to obtain very wide coherent bandwidths (750 MHz). Also considerably more detailed attention should be given to the problems involved in generating a very high ERP by the use of individual transmitters at each antenna element.

With existing state of the art, the implementation of transmitting and receiving arrays for satellite communications would require substantial R&D effort.

B. Multiple Plate Antenna Systems

In 1961, Dr. L. J. Chu proposed a new concept for a large, scanning antenna to the National Science Foundation Advisory Panel on Radio Telescopes.[17] This design was analyzed by A. C. Schell and has been called the multiple plate antenna, or multiplate antenna.[18] This has subsequently been described after the completion of further design analysis.[19] The design essentially divides the aperture area into a large number of flat reflectors each of which can be adjusted in orientation and height. The aperture tolerances are held small by mounting each unit on a rigid support near the earth, rather than on a large raised structural support. The plates are arranged in a desired pattern around a feed tower on fairly flat ground. The use of a flat base for the plates compels narrow band operation

---

17 Report of the Advisory Panel on Radio Telescopes," Astrophysics Journal, 134 (November, 1961), pp. 927-939.

18 A. C. Schell, The Multiple Plate Antenna, Unpublished Doctoral Thesis, Massachusetts Institute of Technology, August 21, 1961.

19 A. C. Schell, "The Multiplate Antenna," IEEE Transactions on Antennas and Propagation, AP-14 (September 1966), pp. 550-560.

for fixed settings, but the adjustability of the plates permits operation over a wide frequency range and permits relatively rapid beam-steering.

1. Design Considerations - A representative design for such an antenna consists of approximately 500(tes, 20 feet by 20 feet, arranged in four elliptical areas around a central tower. Each ellipse has a major axis of 1200 feet lying along a radial from the base of the tower and has a minor axis of 600 feet. The operating frequency of the antenna system ranges from 400 to 3000 mc, assuming an open loop control system for positioning the plates. The feed tower would be 1000 feet high, and would be a more rigid version of existing TV towers. Because of the natural movement at the feed location of such a tower under environmental conditions of wind and temperature, the feed position must be servo controlled using a laser beam as the position sensing device. Studies have shown that the position can be sensed to within 1/4 inch at 1000 feet and can be servo controlled to within 1 inch of a reference line for winds of 30 knots or less.[20]

One installation of this general type has been in existence in the USSR for a number of years.[21] In this case, however, the feed is located on the ground with the plates adjusted from the vertical to 45° (resulting in beam steering from horizon to zenith). Because of the feed location on the ground, this installation had relatively low efficiency when installed.[22] Horizontal beam steering is accomplished by rotating the feed so that it points at a different section of the reflecting plates.

---

20 Ibid, p. 558.

21 S. E. Khaikin and N. L. Kaidanovskii, "A New Radio Telescope of High Resolving Power," in Paris Symposium on Radio Astronomy, R. N. Bracewell (Ed.), (Stanford, Calif: Stanford University Press, 1959), pp. 166-170.

22 Private communication between A. C. Schell, AF Cambridge Research Laboratories and B. R. Stack, Stanford Research Institute, December 27, 1966.

Another experimental multiplate antenna has been built and tested by the Air Force.[23] This installation was not built as an operational antenna system but was primarily designed "to measure the gain, beamwidth, sidelobes, phase errors, and the relative change of gain and apparent temperature vs. beam angle of a representative test section."[24] Because of the experimental nature, only limited azimuth steering was provided (only one plate area was provided, rather than the four surrounding the feed tower needed for full 360° azimuth steering). In this experimental set-up, manual positioning of the plates was provided, which while reducing costs, greatly increased the time necessary to make beam position and operating frequency changes. Conclusions of the test program indicated:

> Good agreement with the calculated pattern was obtained .....Measurements of the relative change in gain and apparent temperature with beam angle indicate that the calculated curves for these quantities do provide accurate measures of antenna behavior.[25]

2. Design Problems - Considering the use of a multiplate antenna raises several problems inherent in its design which affect performance and a number of uncertainties in its implementation which affect the total system cost.

One of the first design problems is that of the change in antenna efficiency, and noise temperature with beam angle to the vertical. This reduction occurs because of physical effects of the individual reflecting plates. As the angle of the plates is changed to keep the beam directed at the feed for various beam angles, the apparent area of the plates in a

---

23 A. C. Schell, P. R. Franchi, W. B. Goggins, Jr., and G. R. Forbes, "An Experimental Evaluation of Multiplate Antenna Properties," IEEE Transactions on Antennas and Propagation, AP-14 (September 1966), pp. 543-550.

24 Ibid, p. 543.

25 Ibid, p. 549.

plane normal to the beam direction varies. In addition, as plates are tilted, the ground underneath them is uncovered to the feed resulting in energy hitting the ground directly (gap loss) or indirectly via double reflection from the underside of the adjacent plates (shadowing loss). There are also diffraction effects due to the plate edges which causes a further reduction in efficiency. This loss can be reduced by increasing the size of the plates, but this increases the cost of the antenna system. However, this effect is rather small compared to the other losses mentioned. The reduction in efficiency of a typical multiplate antenna for various beam angles is given by:

$$\eta \approx 0.97 - 2 \times 10^{-4}\ \theta^2 \qquad (2)$$

where θ is the beam angle in degrees from the horizontal.[26] The addition to the apparent antenna noise temperature due to the gaps is roughly proportional to the degree of efficiency reduction.[27] The loss in antenna efficiency is shown in Table II for angles up to 60°.

Table II
Relative Antenna Efficiencies Versus Beam Angle

Beam Angle ($^{\circ}$ From Zenith)	0	10	20	30	40	50	60
Relative Antenna Efficiency*	.97	.95	.89	.79	.65	.47	.25

* Does not include feed efficiencies.

In addition to efficiency reductions the bandwidth of the antenna varies with beam angle since path lengths from a point-source feed to a

---

26 Allan C. Schell, "Ground-Based Antennas for Satellite Communications," Communication Satellite Systems Technology, Richard B. Marsten (Ed.), Progress in Astronautics and Aeronautics, Vol. 19 (New York: Academic Press, 1966) p. 471.

27 Ibid.

reference-wavefront plane are not equal. These path length differentials will limit the effective bandwidth for a given plate setting to a few percent at best.[28] The problem also increases with antenna size so that bandwidths would probably be limited to under 10 Mc for point feeds. Techniques have been suggested which would ease this bandwidth limitation. These techniques include line feeds, multipoint feeds, and variable phase center feeds.[29]

The proper position for each individual plate is calculated based on desired beam angle and operating frequency and the necessary information is sent to the plate actuators, which may be either hydraulic or mechanical.[30,31,32] Each time the beam is moved or the operating frequency changed, new plate positions must be calculated and the necessary information sent to each plate. Since the plate position is not controlled on a closed loop basis, i.e., corrections are not made for slight plate movements caused by environmental effects such as wind or snow, the upper frequency of operation is probably on the order of 2000-3000 MHz. To close the positioning loop would require a real time sensor at each plate to determine its position and provide a correction signal to reposition the plate. If this were done, it has been speculated that the maximum operating frequency of the antenna could be

---

28 Ibid, p. 472.

29 Schell, "Multiplate," Op Cit, pp. 556-558.

30 Study of a Multiplate Antenna Control System, Final Report, Contract No. AF 19(628)-2948 (Los Angeles: ITT Gilfillan, Inc., May 1964).

31 Preliminary Design Study of a Flat Plate Reflector and Support Unit, Scientific Report No. 1, Contract No. AF 19(628)-2995, (Framingdale, N.Y.: Republic Aviation Corporation, April 1964).

32 Preliminary Design Study of a Flat Plate Reflector and Support Unit, Final Report FR-64-14-69, Contract No. AF 19(628)-2994 (Fullerton, Calif.: Hughes Aircraft Co., 8 May 1964).

raised to X-band.[33] This would add considerable complexity to the control and reflector plate positioning systems, however.

Another potential problem area involves the tower supporting the feed and the feed positioning device. Because of the size of the reflecting area (a maximum horizontal distance of 2500 feet on the ground has been suggested) the feed must be relatively high in the air, about 1000 feet. Any structure this high has a natural tendency to sway with wind pressures and temperature differentials. Studies of existing TV towers and design studies of an appropriate servo controlled feed platform on the tower indicate that excursions can be kept reasonably low.[34,35] The system suggested would include a verticle laser beam generated on the ground with sensors located on the feed platform. A two-axis servo system could keep the feed platform positioned to within 1/4". Movements of the tower due to thermal differentials in the guy wires and tower structure are sufficiently slow and predictable that pre-calculated correction signals can be supplied to the feed platform servo system.

Finally there is the basic question of interference potential--both to the receiving system of the multiple antenna and from the transmitting section to other receiving systems. With the feed elevated to 1000 feet, the system appears to be extremely susceptible to interference and may have to be limited in its geographical location to areas relatively void of other systems in its operating or adjacent frequency bands.

---

33 Private communication between A. C. Schell, AF Cambridge Research Laboratories, and B. R. Stack, SRI, December 27, 1966.

34 John K. Groseclose, Tower for Multiplate Antenna, Engineering Report No. 1, Contract No. AF 19(628)-2977 (Columbus, Ohio: Dresser-Ideco Company, October 1964).

35 John K. Groseclose, Tower for Multiplate Antenna, Final Engineering Report, Contract No. AF 19(628)-2977 (Columbus, Ohio: Dresser, Ideco Company, April 1965).

3. Conclusions - Where very large effective areas are required, operating frequencies are below 3000 MHz, and steering requirements are limited, the multiplate antenna looks like an attractive alternative to a single steerable environmental parabolic antenna. However, frequencies above 3000 MHz, very wide operating bandwidths and wide steering requirements may limit the usefulness of the technique, and certainly raise questions of limitations in the design techniques. Any use such as this would require further detailed engineering study.

C. Spherical Reflectors

To achieve beam movement, the steerable parabolic reflector assumes that the reflector and feed will be moved as a unit, and the multiplate antenna assumes that the feed will remain stationary while the antenna surface is repositioned. A third approach to beam steering is that of using a fixed spherical reflector with a feed assembly which moves to illuminate different portions of the reflector. The reflecting surface looks the same to a feed which is moved in a circular arc concentric with the spherical surface. Because of inherent spherical aberration, spherical reflectors are not perfect reflecting devices. Several techniques in feed design have been suggested to correct these aberrations.

Since parallel rays which strike a concave spherical reflector cross the axis after reflection, a line source coincident with the sphere's axis can be phased so as to correct for the spherical aberrations. Several types of feeds for this purpose have been suggested and experimental results obtained using small spherical reflectors.[36] Since the pattern of a line source is frequency dependent, bandwidths of antenna systems using this

---

36 Roy C. Spencer, Carlyle J. Sletten, and John E. Walsh, "Correction of Spherical Aberration by a Phased Line Source," Proceedings of the National Electronics Conference, Vol. 5, (1950) pp. 320-333.

technique are relatively narrow. This feed technique has been used in the 1000-foot spherical reflector constructed at Arecibo, Puerto Rico.[37]

Another approach to using a spherical reflector is to use a movable Gregorian subreflector and feed. The Gregorian subreflector provides identical paths from a point source feed to a plane wavefront. Beam steering is accomplished by moving the subreflector and feed as a single unit. This technique has been tried on a spherical reflector having a 10-foot aperture, and showed good results at both X- and K-band frequencies as compared to theory.[38] Sidelobe levels are relatively high and hard to suppress because of the nature of the reflector geometry.[39] However, the operating bandwidth can be as wide as a paraboloid with a subreflector, since the Gregorian system is independent of frequency up to the limits of surface tolerance.

By choosing the feed system to illuminate less than the overall reflecting surface, the antenna beam may be steered over a relatively wide angle without appreciable loss of gain. The ratio of effective diameter, D_e, to total reflector diameter, D, is given by the relationship:

$$\frac{D_e}{D} = \sin \frac{180 - \theta}{2} \qquad (3)$$

where θ is the beam scan angle. Alternatively, the ratio of the effective area, A_e, to the total reflector area, A, for various beam scan angles is given by:

---

37 Thomas C. Kavanagh and David H. H. Tung, "Arecibo Radar--Radio Telescope--Design and Construction," Journal of the Construction Division, Proceedings of the American Society of Civil Engineers, Vol. 91, No. CO1 (May 1965), p. 73.

38 F. S. Holt and E. L. Bouche, "A Gregorian Corrector for Spherical Reflectors," IEEE Transactions on Antennas and Propagation, AP-12, No. 1 (January 1964), pp. 44-47.

39 Ibid, p. 47.

$$\frac{A_e}{A} = 1/2 \left[1 - \cos (180 - \theta)\right] \qquad (4)$$

This ratio is plotted for beam scan half angles up to 60° (total beam scan of 120°) in Table III.

Table III
Relative Antenna Efficiencies Versus Beam Angle
Spherical Antenna

Beam Angle $\frac{\theta}{2}$							
^{o}From Zenith (Beam Scan half-angle)	0	20	20	30	40	50	60
Relative Antenna Efficiency * Effective Area	1	.97	.89	.75	.67	.41	.25
Total Area							

* Does not include feed efficiencies.

As may be seen, the relative efficiencies are very close to those shown for the multiplate antenna, Table II, p. 15. Thus in both cases, although for somewhat different reasons, antenna efficiency falls off as the beam scan angle is increased. However, in the case of the multiplate antenna, the efficiency falls off only if the beam is moved to the off zenith positions; whereas in the case of the spherical antenna, as long as the reflector illumination is set by the feed design to permit the scan angle desired, the relative efficiency shown is obtained. This effect primarily manifests itself in total cost, since, in the case of a 120° scan angle, a total antenna area four times the effective area must be built to hold the gain constant.

Two installations of spherical antennas of any great size are known to exist. One is a privately sponsored 90-foot spherical antenna designed and built by Lockheed, Sunnyvale, Calif., and the other is the 1000-foot

radio telescope built near Arecibo, Puerto Rico. Thus experience using this technique is relatively limited. Some of the problems involved in the Arecibo construction are representative of what could be expected in the design of a 400-foot (effective diameter) antenna having a reasonable amount of beam steering. Thus to achieve a 60° beam scan angle and a 400-foot equivalent aperture would require a total diameter of approximately 460 feet while a 500-foot effective area would require a total diameter of approximately 580 feet. To achieve 120° of beam steering would require total diameters of 800 and 1000 feet respectively.

The Arecibo antenna is a segment of a sphere having a radius of 870 feet, an aperture of 1000 feet, and a depth of 158 feet. The reflector itself is built by stabilizing a grid of pretensioned cables with additional tie-down cables. The grid of cables was then covered with a wire mesh ($\frac{1}{2}$" x $\frac{1}{2}$" openings). This results in an rms surface tolerance of one inch for an initial operating frequency of 430 MHz although it is intended to operate as high as 900 MHz. Obviously, this surface tolerance would not be acceptable at frequencies usually associated with satellite communications (4-9 GHz). It is very doubtful that the basic construction technique, prestressed wire cables, could be used to obtain tolerances usually associated with antennas operating at these higher frequencies (rms values $<$ .20 inches). These higher tolerances will undoubtedly require rigid structures with their attendent higher cost. Of course, diameters smaller than 1000 feet would simplify the problem, but the largest known antenna with a rigid structure and a tight surface tolerance has a diameter of only 90 feet. Because of the lack of reflector movement, it is undoubtedly easier to obtain tighter tolerances than in the case of fully steerable paraboloid, but even in the case of a spherical antenna the cost of maintaining a given surface tolerance goes up with size, and for a given diameter there is undoubtedly a given limit which can be achieved with present techniques. Because of the limited experience to date, these limits are hard to define. It may be possible that the use of a radome would make the tolerances easier to achieve.

For large spherical antennas the ease of construction and cost is highly dependent on the amount of site preparation which is required. For example, the Arecibo site was a large natural depression. Despite this advantage, nearly 300,000 cu yards of material had to be excavated and 250,000 cu yards of compacted fill had to be put in position.[40]

In conclusion, the spherical antenna does appear to be a useful approach where beam steering can be limited, although experience with very large reflectors to date has been limited to surface tolerances below those required for satellite communications. However, this approach does appear to warrant further design studies if the use of such a large reflector is considered.

III COST ESTIMATES

It is very difficult to develop cost estimates to compare alternative antenna techniques without considering comparative specifications and doing considerable detailed design and costing. Within the scope and effort available for this program, this does not appear possible. Thus the best approach appears to be to use data developed by other studies to present a general comparison of the three techniques.

A. Parabolic Antenna Arrays

SRI in a previous study has estimated the cost of a 500-foot equivalent aperture at $35 million without a transmit capability.[41] It is estimated that the cost of adding a transmit capability to the antennas would be from 5-10%, depending on the design difficulty which is encountered, or a total estimated cost of $36.7 - $38.5 million. This does not include the

---

40 Kavanagh and Tung, Op Cit, p. 80.

41 Battle, Op Cit, p. 179.

costs which might accrue from the reduced cost of building 39 identical 85-foot antennas and may include design factors not needed in a communication satellite antenna. The design was intended to duplicate a 500-foot fully steerable receiving antenna for deep space applications.

B. Multiple Plate Antennas

Schell has estimated the cost of a multiplate antenna equivalent to a 1550-foot parabolic dish as follows:[42]

Plates	$12.0 M
Closed loop position control (X-band operation)	6.0 M
Antenna platform and feed	1.0 M
Feed and waveguide	2.0 M
Site preparation and building	.6 M
	$21.6 M

Electronics would probably add about another $1 M to the cost. In addition, Schell has estimated that a production run of 100 multiplate antennas of an equivalent diameter of 60 feet would result in a unit cost of approximately $90,300 each.[43] He goes on to point out that in quantities of 300 the cost would be reduced 40% to $64,500. These two figures would indicate a cost curve rising exponentially with size, but the general costs shown would indicate great savings over conventional steerable parabolic antennas. It must be remembered, however, that performance, particularly gain falls off with beam movement from vertical and this must be taken into account when comparing costs.

These costs must also be regarded as approximate since no major installation of this type has been built. Of particular uncertainty is the cost of increasing the plate position accuracy to permit operation at X-band.

---

42 Private conversation, Op Cit.

43 Schell, "Ground Based Antennas," Op Cit, p. 473.

PRECEDING PAGE BLANK NOT FILMED.

C. Spherical Reflectors

Very little cost information exists on spherical reflectors of any size. Schell has estimated that the cost of the 1000-foot Arecibo antenna is $7,376,000 and the 90-foot Lockheed antenna is $60,000.[44] The cost per square foot of aperture is thus approximately $9.30 and $9.40 respectively. Accepting the limitations inherent in extrapolating these two figures to antenna sizes inbetween, Schell feels "it is not unreasonable to assume that the cost of a spherical reflector antenna varies approximately linearly with area."[45] Even if one accepts a cost of approximately $9.00 per square foot for a medium to large sized spherical reflector, the effects of providing for beam scanning on the relative antenna efficiency must be taken into account, as shown in Table III. Also the cost of maintaining high surface tolerance for larger size reflectors must be factored in. Thus in the extreme case of providing 120° of beam scanning, an effective area 4 times that required for no beam scanning must be provided at a net cost of $36.00 per square foot of effective area, neglecting the cost of very tight surface tolerance. However, it should be remembered that in some cases, particularly with larger reflectors, multiple feeds can probably be used, thus permitting several simultaneous beams within the beam scan coverage.[46]

IV GENERAL CONCLUSIONS

Three alternative approaches to obtaining large equivalent apertures at X-band frequencies have been examined. These are parabolic antenna arrays of large equivalent aperture, a fixed spherical reflector with a movable

---

44 A. C. Schell and P. Blacksmith, "A Comparison of Three Antenna Techniques in Terms of Cost Versus Performance," in Design & Construction, Op Cit, p. 137.

45 Ibid.

46 Schell, "Ground Based Antennas," Op Cit, p. 471.

feed, and antennas with multiple, adjustable plates and a fixed feed. There has been a limited amount of experience with large sizes of all three types, which severely restrict the amount of generalization possible, and limits the degree of accuracy in cost projections. Despite these limitations some general conclusions can be drawn. These are as follows:

1. Where full performance at X-band frequencies or above is required (i.e., horizon to horizon beam scanning and gains over 75 dB at X-band), the technique of using multiple phased, fully steerable arrays of large equivalent aperture may be the only feasible approach. Using this technique, the tight surface tolerances needed for high gain at X-band frequencies can be obtained for the equivalent of a very large aperture. In effect the technique transforms the mechanical complexity of obtaining high surface tolerance in large antenna structures to electrical complexity in the interconnection and signal summing equipment. However, operating bandwidths may be limited.

2. Both the multiplate antenna and the fixed spherical reflector offer the potential of having reduced costs for a given reflector size over that of a single large fully steerable antenna or a phased array of smaller antennas. Because of the relatively small size of the individual reflectors in the multiplate antenna, high equivalent surface tolerance may be easier to obtain if the problems of reflector plate positioning and feed platform positioning can be solved.

3. For systems where limited beam steering is appropriate (over the life of the antenna system), the fixed spherical reflector appears to be an attractive approach in terms of cost. Even assuming a cost of $36 per square foot of effective area, the total cost of a 500-foot system is only slightly over $7M. A major uncertainty here is the cost of maintaining a tight surface tolerance to permit the use of such an antenna at 10 GHz. Only a detailed engineering design study could adequately determine the

required additional cost. Here again the use of a radome to reduce environmental loading of the antenna may substantially reduce obtaining the required surface tolerance.

APPENDIX F

AN APPROXIMATE EXPRESSION FOR THE COST-GAIN RELATIONSHIP IN LARGE PARABOLIC ANTENNAS

ABSTRACT

An approximate formula is developed for application to large parabolic antennas that permits the determination of cost as a function of required gain at a specified frequency.

I INTRODUCTION

The objective of this report is to develop an approximate formula for the cost of large parabolic antennas that produce a required gain at a specified operating frequency.

The cost of such antennas has normally been expressed in terms of the antenna diameter according to the formula

$$\text{Cost} = nD^p \tag{1}$$

where D is the antenna diameter in feet and n and p are constants. The weakness of this formula is quite apparent. Antennas are designed to produce gain that is a function of the diameter (D), frequency (F), deviation from ideal reflector profile (d), and overall antenna electronic properties (η). The following formula relating these parameters was developed by Ruze[1*] and will be used in our study.

$$G = \eta\left(\frac{\pi DF}{c}\right)^2 \exp -\left(\frac{4\pi F}{c}\, d\right)^2 \tag{2}$$

where

η = Efficiency

D = Diameter

c = Speed of light

F = Operating frequency

d = rms deviation of reflector surface from best-fit paraboloid.

The use of Eq. (1), although it yields the cost, does not impart any knowledge as to the exact gain of the antenna. Without such knowledge, Eq. (1) conveys little information except in an "intuitive sense," which is often misleading.

As a result, we have attempted to develop an expression for the cost of large parabolic antennas that would answer the following question:

*References are listed at the end of the report

"What is the minimum cost of G dB of gain at an operating frequency of F GHZ, and what is the best antenna diameter and the required rms reflector surface tolerance under these conditions?"

To answer this question the following approach has been developed.

Since the gain of an antenna depends on its diameter (D) and on the rms surface tolerance (d), as shown in Eq. (2), the cost of this gain is a function of the cost of D and the cost of d. The least total cost will be obtained for a specific set of values of D and d which must be determined by minimization of the cost equation. In order to accomplish such minimization, d must be expressed in terms of D (or vice-versa). Thus the following steps are necessary.

Step 1: Express the rms surface tolerance as a function of the antenna diameter:

$$d = f(D). \tag{3}$$

This is a subjective decision based on available data and knowledge of manufacturing techniques. The value of the rms surface tolerance obtained in this manner is called "basic tolerance corresponding to the diameter D." Any other tolerance d_1 will then be expressed as a fraction (a) of d -- i.e.,

$$a = \frac{d_1}{d} \tag{4}$$

or

$$d_1 = ad$$

and substituting in Eq. (3), we obtain

$$d_1 = af(D). \tag{5}$$

Step 2: Express gain in terms of D and d_1.

Using equation (2) for antenna gain G, we obtain

$$G = X(D)\ y(d_1). \tag{6}$$

Substituting Eq. (5) into Eq. (6), we obtain

$$G = X(D)\ y(af(D)) \tag{7}$$

Step 3: Determine fractional increase in antenna cost "b" associated with fractional change of basic tolerance d (represented by a):

$$b = k(a) \tag{8}$$

or

$$a = k_1(b) \tag{9}$$

This cost relationship can be determined from available data and constitutes a subjective input. Substituting Eq. (9) into Eq. (7), we obtain

$$G = X(D)y\left[k_1(b), f(D)\right]. \tag{10}$$

Equation (10) can now be solved for b, yielding

$$b = N(D,G). \tag{11}$$

Thus the fractional increase in antenna cost (b) associated with a change in the basic rms surface tolerance of the antenna can be expressed as a function of antenna diameter and the gain that will be produced.

Step 4: Determine the cost of the basic antenna with diameter D and associated tolerance d defined by Eq. (3):

$$C_B = M(D) \tag{12}$$

This cost equation is the one that is normally quoted as "the cost of an antenna with diameter D" and is sometimes represented by Eq. (1).

Step 5: Obtain the formula for the cost of an antenna with any diameter D and any tolerance d_1. This relation can be obtained by combining Eqs. (11) and (12):

$$C_T = M(D) \times b \tag{13}$$

$$= M(D)\ N(D,G). \tag{14}$$

Step 6: Minimize the total cost. Equation (13) represents the total cost of an antenna with arbitrary rms surface tolerance and

diameter. It is of interest to minimize this cost for any required gain G. This can be accomplished by setting G at the required value, differentiating Eq. (14) with respect to D, and equating the result to zero. This will yield the value of D_{opt} that satisfies the minimum cost condition:

$$\frac{dC_T}{dD} = 0 = \frac{d(M(D))}{dD} N(D,G) + M(D) \frac{d\ N(D,G)}{dG} . \qquad (15)$$

Since G is a constant we can solve Eq. (15) for D, obtaining D_{opt} as a function of given gain G. We can now use this value of D_{opt} in Eq. (11) to find the corresponding value b_{opt} of b. The total minimum cost of the antenna is found from Eq. (13) using values of D_{opt} and b_{opt}.

Step 7: Determine the value of rms surface tolerance d_1 required to produce gain G with antenna diameter D_{opt} for minimum cost condition. Substituting the value of b_{opt} found above into Eq. (9), we find "a", which is then used together with D_{opt} in Eq. (5) to find the rms tolerance d_{opt}.

The procedure of the last two steps can be summarized as follows:

(A) $\frac{dC_T}{dD} = 0$ yields the value of D for minimum cost $D = D_{opt}$.

(B) Using D_{opt}, compute:

b_{opt} from Eq. (11) for given G

C_{MIN} from Eq. (13), using D_{opt} and b_{opt}

d_{opt} from Eqs. (8) and (5).

For a required value of gain G, we thus obtain the minimum cost C_{MIN} and the corresponding values of antenna diameter D and rms surface tolerance d_1.

The development of the Eqs. (1) through (14) is described in this report. The assumptions on which they are based are discussed in some detail in order that the reader may get a clear conception of all the

factors affecting the accuracy of the final result.

The discussion is divided into four sections, as follows:

(1) Determination of the relationship between the rms reflector surface tolerance and the antenna diameter.

(2) Determination of the variations of antenna cost with changes in diameter.

(3) Determination of the variations of antenna cost with changes in the rms surface tolerance of the reflector.

(4) Calculation of minimum cost for a given gain at specified frequencies.

As will become apparent from the discussion that follows, the accuracy of data upon which the various relationships are based was in many instances rather poor. Accordingly, the final formula for the cost of gain can be considered only as an approximation. It is believed, however, that it represents a new and useful tool since it yields an indication of the least amount of money that must be paid to achieve the required antenna gain at a specified frequency.

Since the form of Eqs. (1) through (14) can be selected according to one's judgment, many alternative forms can be used. The values for cost will be affected by the form of the equations; the procedure, however, remains the same in all cases.

II DEVELOPMENT OF THE FORMULA

A. The Relationship Between the RMS Reflector Surface Deviation from Best-Fit Paraboloid and the Antenna Diameter

1. Sources of Error

Ruze[1] and others have shown that the departure of the reflector surface from true paraboloidal form results in small phase errors in the wave front across the antenna aperture, which in turn causes a reduction in the gain of the antenna. The relationship between antenna gain and such rms surface deviation is shown in Eq. (2), where the exponential term represents the loss in gain due to imperfect reflector surface.

Total mechanical deviation from best-fit parabolid is a function of several factors. Some of these factors, such as distortions produced by the effect of gravity in various positions of the reflector, are entirely predictable and could be corrected. Other effects, such as those due to wind gusts, are entirely unpredictable and must be treated in a statistical sense. In this report, it is assumed that the value of d in Eq. (2) represents the maximum mechanical rms surface deviation from true parabolic crossection of the installed antenna reflector due to all effects under average operating conditions.

Since most of our information is based on the data pertinent to Comsat antennas and the 210-foot JPL Goldstone antenna, it is assumed that antenna construction will be such as to meet all environmental specifications applicable to those antennas. Roughly, it implies full steering capability, and operation in wind gusts up to 30 mph and over a range of atmospheric conditions normally specified for exposed antennas.

2. Development of Formula for the RMS Surface Tolerance (d)

The survey of all large antenna manufacturers in the U.S. produced a general consensus that a "shop practice" rms surface tolerance for antennas in the range of diameters from 85 to 100 feet is approximately 0.04 inch. No such agreement exists for larger antenna sizes. In general the claimed accuracy obtained in the JPL 210-foot Goldstone antenna (0.17 inch) was accepted as representing the state-of-the-art.

We will now attempt to derive a relationship between the antenna diameter D and the state-of-the-art surface tolerance d. It should be kept in mind that the values of d which we are interested in are not these found in the field installations but those which represent the best that can be accomplished with today's state-of-the-art within limits of practicality. Accordingly, since some of the existing antennas have been deliberately made "cheap and dirty" the rms surface tolerances encountered in the field cannot be used in our work.

The derivation of the relationship between the "best" antenna tolerance and the diameter will be based on the two values of tolerance which represent the state-of-the-art (i.e., 0.04 inches per 100 ft antenna and 0.17 inches per 210 ft antenna).

Using these figures we can now derive an approximate expression for the limits on the gain of practical antennas. Since in actual practice the size of the antenna obviously affects the total manufacturing precision, let us include this effect in our calculation by defining a quantity q called "manufacturing precision per foot of antenna diameter:"

$$q = \frac{d}{D} \times \frac{1}{D} = \frac{d}{D^2} \ . \qquad (16)$$

Computing this quantity for the case of a 100-foot antenna with a 0.04-inch rms surface tolerance, we obtain

$$q = \frac{0.04}{12 \times 100} \times \frac{1}{100} = \frac{1}{3 \times 10^6} = 3.33 \times 10^{-7} \ .$$

Similarly, for a 210-foot antenna with an rms tolerance of 0.17 inch, we obtain

$$q = \frac{0.17}{12 \times 210} \times \frac{1}{210} = \frac{1}{3.1 \times 10^6} = 3.23 \times 10^{-7}.$$

These two results are similar and suggest that as a first approximation the relationship between the rms surface tolerance and antenna diameter could be expressed by the following equation:

$$\frac{d}{12D^2} \approx 3.3 \times 10^{-7}$$

where d is the rms surface tolerance in inches, and D is the antenna diameter in feet. Thus,

$$d \approx 12 \times 3.3 \times 10^{-7} \times D^2$$

$$\approx 4D^2 \times 10^{-6} \text{ inches} \qquad (17)$$

or

$$d \approx \frac{4D^2}{12} 10^{-6} \text{ feet.} \qquad (18)$$

If this relationship is adopted, we obtain the rms surface tolerances for various antenna diameters as shown in Table I.

Table I
RELATIONSHIP BETWEEN D AND d

Diameter, D (feet)	RMS Surface Tolerance, d (inches)
100	0.04
210	0.176
300	0.360
400	0.640

While it is recognized that Eq. (17) is only an approximation, it is felt that it yields results that are in reasonably good agreement with what is considered today's state-of-the-art. In view of nonavailability of better data it is satisfactory for the purposes of our study. The rms surface tolerance is defined by Eq. (18) as a function of any diameter D of the antenna and will be referred to as "basic surface deviation." The reader is again reminded that it represents the theoretical best that can be obtained and is not intended to represent the average of the tolerances of existing field antennas.

We can now substitute Eq. (18) into Eq. (2) with the following results:

$$G = \eta\left(\frac{\pi DF}{c}\right)^2 \exp -\left(\frac{4\pi F}{12c} \times \frac{4D^2}{10^6}\right)^2 . \qquad (19)$$

(The factor 12 in the denominator of the exponential term is required since D is expressed in feet while d is in inches.)

The plot of this equation for various values of operating frequency F is shown in Fig. 1. Figure 1 shows clearly that the increase in gain resulting from larger antenna diameters is more than offset by the loss of gain resulting from larger rms surface deviations associated with larger diameters [as expressed by Eq. (17)].

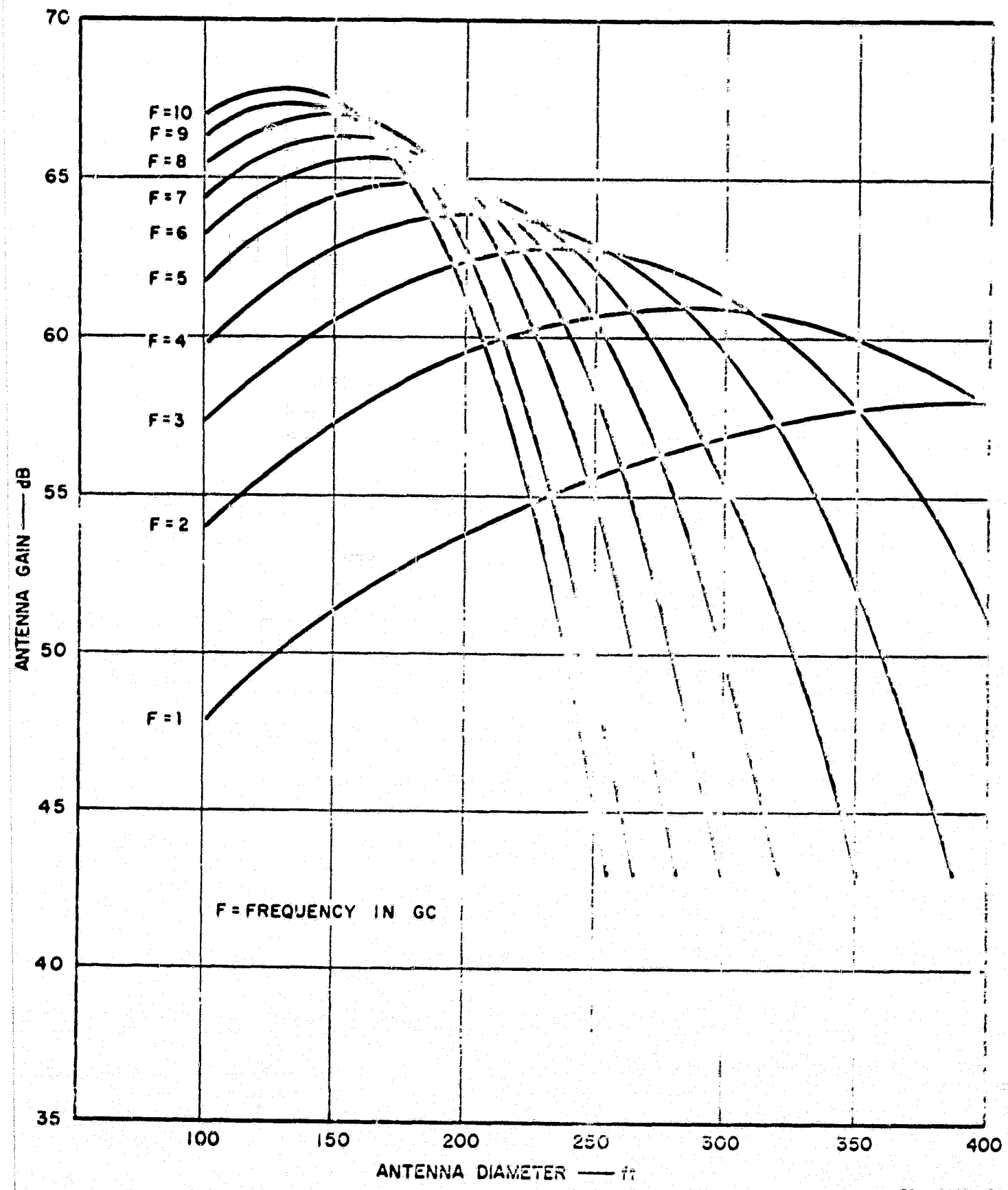


FIG. 1 ANTENNA GAIN vs. DIAMETER
(rms surface deviation = $4D^2/10^6$)

Accordingly, at each frequency a certain maximum gain can be obtained as diameter is varied. If the required gain is less than this maximum, it can be obtained by selecting an appropriate antenna diameter (with its corresponding "basic surface deviation"). However, if the required gain is greater than the maximum indicated in Fig. 1, the only way to obtain this gain is to select the best diameter and to improve the associated rms surface deviation over that indicated by Eq. (17).

The determination of the optimum diameter and of the necessary improvements in rms surface deviation constitutes a trade-off based on cost and is considered later in this paper.

B. Variations of Antenna Costs with the Improvement in the RMS Surface Tolerance

When the relationship between the rms surface tolerance and the antenna diameter was selected [Eq. (17)], it was based on the assumption that the manufacturing precision of the total structure decreases linearly with diameter of the antenna. This result agrees with the available data on operating antennas. Thus, to the first approximation, one is inclined to assume that when the original precision is high it will be more difficult to improve it, and accordingly the cost of such improvement would be greater than in cases of lower precision.

This argument, however, is slightly misleading since we should not look at the manufacturing precision d/D but at the "manufacturing precision per foot of diameter" (d/D^2), as expressed by Eq. (17), since this expression takes into account the overall size of the structure.

On this basis, the "precision per foot of diameter" remains roughly constant, and when the overall structure is considered, it is as difficult to improve the overall precision of a 400-foot dish as it is to do it for a 100-foot dish. Accordingly, the cost of improvement should be similar in both cases.

This argument is restricted to cases where rms surface tolerance improvement can be obtained without major redesign of back-up structure of the reflector. Since, as noted previously, the total tolerance is a function of the individual panel tolerance, the panel alignment and the design of the back-up structure, the true variations in cost associated with the improvement of tolerance would have to be estimated on the basis of an analysis of the cost of these various factors. Since such an analysis was not possible and since very little information is available on the subject, a much more generalized result had to be accepted.

In order to arrive at a plausible conclusion, the argument presented above and other pertinent factors were discussed with several individuals considered experts in the field.

The Camroc"[2] studies were reviewed and other pertinent data taken into consideration. On the basis of all these inputs, it was concluded that over a restricted range of variation an inverse relationship between the fractional improvement in rms tolerance and the fractional increase in the cost of the antenna (at a given diameter) would represent the best possible compromise. Accordingly, the following formula was adopted:

$$b = \frac{1}{a} \tag{20}$$

where b represents the factor by which the cost of an antenna must be multiplied when the original rms surface tolerance d is multiplied by a factor "a" (an improvement in tolerance requires that "a"<1). Hence,

$$d_1 = da = d/b \ . \tag{21}$$

Thus if the rms surface tolerance is reduced by a factor of two ($a=\frac{1}{2}$), the cost of the antenna will increase by the factor two ($b=2$).

Although the limitations of this approach are recognized, it is felt that for a limited range of variation of rms surface deviation

this approximation is as good as can be obtained without a major research effort.

The exact range of variation of rms surface tolerance that can be obtained in practice is difficult to estimate, and we have not pursued it further. Final results are presented in a form where the value of b and the corresponding rms tolerance are clearly shown, and the reader can use his own judgment as to where the limits of physical realizability lie.

C. Variations of Antenna Cost with Changes in Diameter

There exists very little reliable information concerning the cost of communication antennas larger than 100 feet in diameter. Since such costs are to a large extent dependent on the antenna specifications and on other factors of a nontechnical nature, it is difficult to predict them with any great accuracy. An extensive survey of all manufacturers and designers has not yielded the required information. Accordingly, in order to proceed with our program, we have decided to assume two cost figures as "bench marks"--one for Comsat type antennas in the range of 85 to 100 feet, and the other for the Goldstone 210-foot antenna. This choice was dictated primarily by the fact that we are interested in steerable communication antennas that are well represented by the two examples mentioned above and also by the fact that reliable information on similar antennas in other sizes was almost nonexistent.

For antennas in the range of 85 to 100 feet, we have obtained actual costs for existing installations, which include the manufacture, installation, construction, integration, and testing of the entire antenna subsystem but do not include electronics (power transmitter, receiver, etc.) or communications equipment. The cost of spares, boresight facility, and necessary documentation is included.

Because of proprietary nature of the information, individual figures cannot be given. The median cost for these antennas (appropriately adjusted for variations in specifications) is approximately $2 million for an equivalent diameter of 100 feet.

The figure for Goldstone's 210-foot antenna presented more difficulty.

At the suggestion of NASA, we have accepted the figure of $12 million[3] as the cost of the antenna subsystem covering the same items previously listed. This figure is slightly below the actual costs, but it was accepted on the assumption that since the basic engineering has been accomplished, succeeding antennas in this range of diameter will cost less than the original one. We were unable to obtain any other reliable information on the cost of 200-foot antennas.

Since the scope of our program would not permit the evaluation of all the factors that affect the final cost of an antenna installation, we have accepted without further investigation the assumption that the relationship between antenna costs and antenna diameter is of the form:

$$C = nD^p \tag{22}$$

where n and p are constants and D is the diameter of the antenna. The relationship of this form has been used in the literature[3] for some time and could probably be justified by the analysis of the costs of presently existing antennas. In order to calculate the constants n and p, we have substituted into Eq. (22) the values of cost and diameter discussed above with the following results:

(a) $2 \times 10^6 = n \times 100^p$

(b) $12 \times 10^6 = n \times 210^p$

and therefore

$$\frac{(b)}{(a)} = 6 = \left[\frac{210}{100}\right]^p$$

$$\log 6 = p \log 2.1$$

or

$$\left.\begin{aligned} p &= \frac{\log 6}{\log 2.1} = \frac{.778}{.322} = 2.42 \\ \text{and therefore} \\ n &= \frac{2\text{x}10^6}{100^{2.42}} = 28.8 \end{aligned}\right\} \qquad (23)$$

Thus,

$$C = 28.8\ D^{2.42}. \qquad (24)$$

The reader is cautioned that the accuracy of this formula is dependent on the design specifications of the antenna and it should therefore be used as an indication of costs rather than to calculate their exact magnitudes. The important assumption underlying this relationship is that it represents the cost of any antenna of diameter D with its associated tolerance given by Eq. (17).

D. Calculation of the Cost of Antenna Gain

The three major assumptions on which the development of the formula for the cost of gain of an antenna is based and which were discussed in detail in the preceding sections are summarized below.

(1) $d = \frac{4D^2}{10^6}$ (17)

(2) $C = 28.8\ D^{2.42}$ (24)

(3) $b = \frac{1}{a}$ (20)

(4) $d_1 = da = \frac{d}{b}$. (21)

Thus the cost of an antenna with diameter D and rms surface tolerance ($d_1 = d/b$) is as follows:

$$\text{Cost} = 28.8\ D^{2.42} \times b \qquad (25)$$

or in general terms,

$$\text{Cost} \propto nD^p \times b \ . \tag{26}$$

It now remains to determine the relationship between the values of the antenna diameter D and the improvement in surface tolerance (1/b) that will minimize the cost of the antenna for a specified gain.

Using Eqs. (2), (17), and (20), we can express the gain of any antenna as follows:

$$G = \eta\left(\frac{\pi DF}{c}\right)^2 \exp -\left[\frac{1}{b} \times \frac{4\pi F}{12c} \times \frac{4D^2}{10^6}\right]^2 . \tag{27}$$

Rearranging,

$$\ln G = 2 \ln\left[\sqrt{\eta}\ \frac{\pi DF}{c}\right] - \left[\frac{1}{b} \times \frac{16\pi FD^2}{12c \times 10^6}\right]^2$$

or

$$\ln G = 2 \ln\left[k_2 D\right] - \left[\frac{k_1}{b} D^2\right]^2 \tag{28}$$

where

$$\frac{16\pi F \times 10^9}{12c \times 10^6} = k_1 = k_1^* F_{GC} \tag{29}$$

and

$$\frac{\sqrt{\eta}\pi F \times 10^9}{c} = k_2 = k_2^* F_{GC} \tag{30}$$

where F is in Gc.

Solving for b,

$$b = \frac{k_1 D^2}{(2 \ln\left[k_2 D\right] - \ln G)^{\frac{1}{2}}}$$

or

$$b = \frac{k_1 D^2}{\sqrt{2 \ln\left(\frac{k_2 D}{\sqrt{G}}\right)}} \ . \tag{31}$$

Equation (31) is valid for $(k_2 D)^2 > G$. Note that since $(k_2 D)^2$ represents the antenna gain with a perfectly smooth reflector, and G is the required gain, this restriction means that one cannot ask for more gain than that obtainable with an ideal reflector, other factors being equal.

We can now substitute the value of b from Eq. (31) into the cost equation (26):

$$\text{Cost} = nD^p \times \frac{k_1 D^2}{\sqrt{2 \ln \frac{k_2 D}{\sqrt{G}}}} \quad , \tag{32}$$

To find the value of D that will result in minimum cost for any given value of G, Eq. (26) can now be differentiated with respect to D and equated to 0. Note that constants k_1 and k_2 are both functions of frequency F. Accordingly, the frequency of operation must also be specified.

Differentiating Eq. (32) with respect to D, we have

$$\frac{dC}{dD} = npD^{p-1} \times b + nD^p \frac{d}{dD} (b).$$

Differentiating Eq. (26) and substituting for $\frac{d}{dD}$ (b), we get

$$\frac{dC}{dD} = npD^{p-1} \times b + nD^p \left[\frac{2k_1 D}{\left(2 \ln \frac{k_2 D}{\sqrt{G}}\right)^{\frac{1}{2}}} - \frac{k_1 D}{\left(2 \ln \frac{k_2 D}{\sqrt{G}}\right)^{3/2}} \right]$$

$$= \left(npD^{p-1} \times b\right) + \left(nD^p \times \frac{2b}{D} \left[1 - \frac{1}{4 \ln \frac{k_2 D}{\sqrt{G}}}\right]\right)$$

$$= nbD^{p-1} \left[p + 2\left(1 - \frac{1}{4 \ln \frac{k_2 D}{\sqrt{G}}}\right)\right] . \tag{33}$$

Equating Eq. (33) to zero to find the minimum and neglecting the trivial solutions D=0 and b=0, we have:

$$p + 2 = \frac{1}{2 \ln \frac{k_2 D}{\sqrt{G}}} \quad . \tag{34}$$

Therefore

$$2 \ln \left(\frac{k_2 D}{\sqrt{G}}\right) = \frac{1}{p+2}$$

or

$$\ln G = 2 \ln (k_2 D) - \frac{1}{p+2} \quad . \tag{35}$$

Equation (35) yields the best value of diameter D for a required gain G when the cost is minimum.

We had from Eq. (31),

$$2 \ln \left(\frac{k_2 D}{\sqrt{G}}\right) = \left(\frac{k_1 D^2}{b}\right)^2 .$$

Substituting into Eq. (34), we get

$$\sqrt{p+2} = \frac{b}{k_1 D^2}$$

or

$$b = k_1 D^2 \sqrt{p+2} \quad . \tag{36}$$

Since b represents both the cost multiplying factor [Eq. (26)] and the rms surface tolerance multiplying factor [Eq. (21)], it is the basic parameter in our analysis. The value of b at the point of minimum cost is given by Eq. (36). Note that this value of b is a function of D and gain G, which are uniquely related at the minimum cost point by Eq. (35).

Equation (35) determines the relationship between the required gain and the diameter of the antenna that results in minimum antenna cost. (The corresponding value of required surface tolerance d_1 can be obtained by substituting Eq. (36) into Eq. (21):

$$d_1 = \frac{d}{b} = \frac{4D^2}{10^6 b} = \frac{4D^2}{10^6 k_1 D^2 \sqrt{p+2}} = \frac{4 \times 10^{-6}}{k_1 \sqrt{p+2}} \times \frac{1}{F} \quad . \tag{37}$$

Equation (37) shows that in order to obtain the minimum cost for any specified gain G, the surface tolerance at any given frequency F should be kept constant at a value given by Eq. (37). The corresponding value of the diameter D varies with G as shown in Eq. (35). The reason why tolerance d_1 remains constant can easily be seen from the fact that since d varies as D^2 [Eq. (17)], and b also varies as D^2 [Eq. (36)], the ratio $d/b = d_1$ remains independent of D. Note that this means that as we increase the diameter we keep the rms tolerance constant. From our previous discussion it is apparent that sooner or later a limit will be reached where it will not be possible, with existing manufacturing techniques, to continue this process. The reader should remember that when b=1 the rms surface tolerance corresponds exactly to the "basic tolerance" defined by Eq. (17). Since we have assumed that the "basic tolerance" represents the best that can be done with the existing state of the art (for "basic" cost), assuming values of b>1 means that we are pushing beyond the state of the art as far as the ratio d/D is concerned. The relation between antenna diameter and gain when the rms surface tolerance is given by Eq. (37) is plotted in Fig. 2.

The next step is to calculate the absolute minimum cost of an antenna that yields a prescribed gain. The total minimum cost is given by Eq. (26) as a function of diameter D and factor (b). The value of (b) for minimum cost condition has been found in Eq. (36). Substituting Eq. (36) into Eq. (25), we obtain the general expression for minimum cost:

$$C_{MIN} = nD^p \, k_1 D^2 \sqrt{p+2}$$

$$= nk_1 \sqrt{p+2} \; D^{(p+2)} \; . \qquad (38)$$

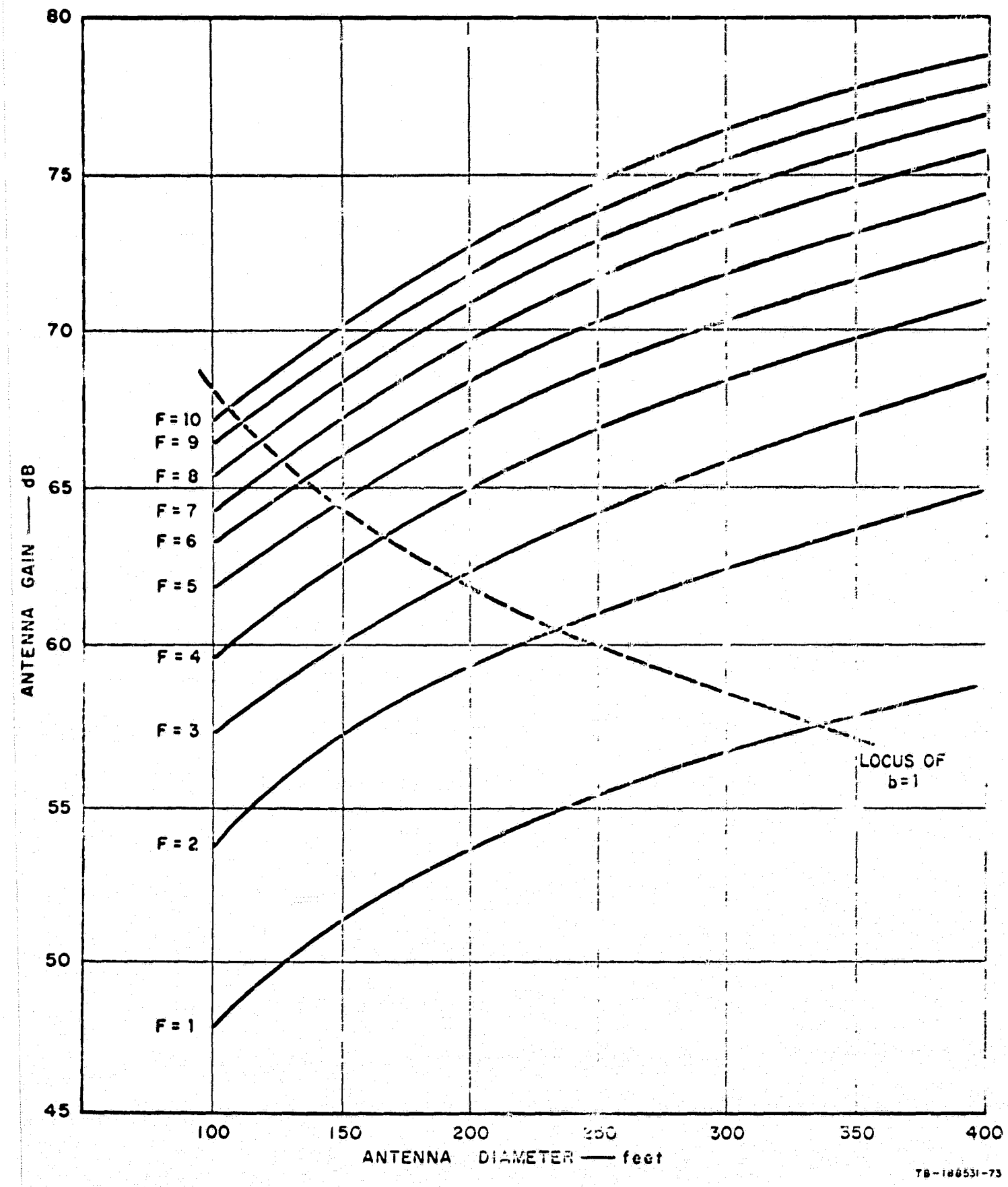


FIG. 2 MINIMUM COST RELATIONSHIP BETWEEN ANTENNA GAIN AND DIAMETER
(rms surface deviation = $4D^2/bx10^6$ = constant)

Expressing in dB,

$$10 \log (C_{MIN}) = 10 \log (nk_1\sqrt{p+2}) + (p+2)\ 10 \log D \quad . \qquad (39)$$

Using constants from Eqs. (23), (29), and (30) we obtain

$$C_{MIN} = 2.647 \times 10^{-5}\ D^{4.42}\ F_{GC} \qquad (39A)$$

or in dB,

$$\left(C_{MIN}\right)dB = -45.772 + 4.42(10 \log D) + 10 \log F_{GC} \qquad (39B)$$

When cost is minimum, the relationship between gain and diameter is given by Eq. (35) as

$$\ln G = 2 \ln (k_2 D) - \frac{1}{p+2}$$

or

$$G_{dB} = 2(10 \log (k_2 D)) - \frac{4.34}{(p+2)} \qquad (40)$$

where dB indicates the decibel ratio (10 log G)

and therefore

$$10 \log D = \frac{G_{dB}}{2} + \frac{4.34}{2(p+2)} - 10 \log k_2 \quad . \qquad (41)$$

Substituting Eq. (41) into Eq. (39), we obtain

$$10 \log C_{MIN} = 10 \log (nk_1\sqrt{p+2}) + \frac{4.34}{2} + \frac{(p+2)}{2} G_{dB} - (p+2)\ 10 \log k_2$$

$$\left(C_{MIN}\right)_{dB} = \left(\frac{p+2}{2}\ G\right)_{dB} + \left[10 \log \left(\frac{nk_1\sqrt{p+2}}{k_2^{(p+2)}}\right)\right] + \frac{4.34}{2} \quad . \qquad (42)$$

Thus, 10 log $\left(C_{MIN}\right)$ vs. 10 log G is a straight line with slope $\frac{p+2}{2}$ at any given frequency. Substituting the values of constants from Eqs. (29) and (30),

$$k_1 = \frac{4\pi F \times 10^9}{3c \times 10^6}$$

$$k_2 = \frac{\sqrt{\eta}\pi F \times 10^9}{c}$$

We note that the factor $\frac{k_1}{k_2^{(p+2)}}$ can be expressed as

$$\left[\frac{4c^{(p+1)}\ 10^{-6}}{3(\eta)^{\left(\frac{p+2}{2}\right)}\ (\pi\ 10^9)^{(p+1)}}\right]\frac{1}{F^{(p+1)}} \quad .$$

Let the square bracket be represented by k_3

$$k_3 = \frac{4}{3}\left(\frac{c}{\pi \cdot 10^9}\right)^{p+1} \eta^{-\left(\frac{p+2}{2}\right)} 10^{-6} \qquad (43)$$

Therefore

$$\frac{k_1}{k_2^{(p+2)}} = k_3 \times \frac{1}{F^{(p+1)}} \quad . \qquad (44)$$

Substituting Eq. (44) into Eq. (42),

$$10 \log C_{MIN} = \left(\frac{p+2}{2}\right) G_{dB} - (p+1)\ 10 \log F + 10 \log (n\sqrt{p+2}\ k_3) + 2.17 \quad . (45)$$

Thus, the relationship between cost and gain at any frequency F is

$$\left.\begin{aligned} C &= G^{\frac{P+2}{2}} \times \frac{Z}{F^{(p+1)}} \\ \text{where} \\ Z &= n\sqrt{p+2} \times \frac{4}{3}\ (0.312)^{p+1} \times 10^{-5.783} \times \eta^{-\frac{p+2}{2}} \end{aligned}\right\} \qquad (46)$$

Substituting into Eq. (45)

$$10 \log C_{MIN} = \frac{p+2}{2} G_{dB} - (p+1)\ 10 \log F - 51.8 \qquad (47)$$

Note that the values obtainable from Eq. (46) represent conditions when no restriction exists on "b". This is equivalent to assuming that when "b" becomes less than one (or a>1) the tolerance is <u>increased</u> over its

basic value with corresponding reduction in cost. These reduced costs can be computed for the following values of constants pertinent to our case:

$$p = 2.42$$
$$n = 28.8 \qquad (48)$$
$$\eta = 0.6$$

and are shown in Table III, at the end of the text. It can be seen from Eq. (47) that for each dB change in antenna gain the cost changes 2.21 dB.

This discussion can be summarized in the sketch below.

Values of b	Cost of Antenna	RMS Surface Deviation
b>1	$c>28.8D^{2.42}$	$d<4D^2x10^{6}$
b = 1	$c=28.8D^{2.42}$	$d=4D^2x10^{6}$
b<1	$c<28.8D^{2.42}$	$d>4D^2x10^{6}$

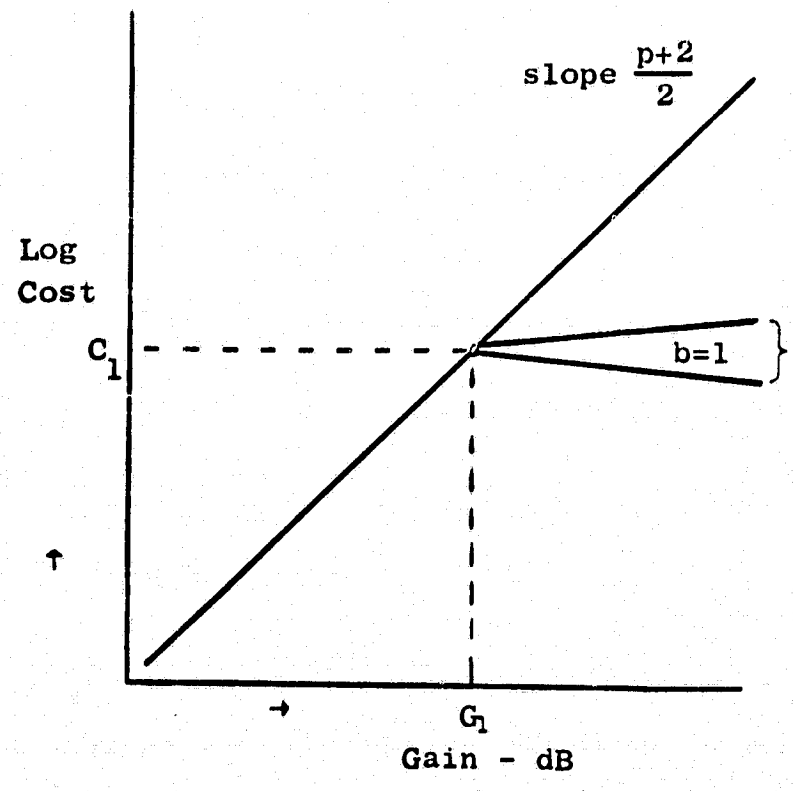


FIG. 2A

The value of gain G_1 corresponding to the point at which b reaches unity on the graph of log G vs. log C represents the maximum gain that can be obtained with the "basic rms surface tolerance" of $4D^2x10^{-6}$

inches. For higher gains the tolerance must be reduced, and the cost is given by Eq. (46). If the same formula is used for lower gains, it would correspond to the case of the rms tolerance increasing with the corresponding reduction in costs as shown in Table III.

Let us calculate the values of G_1 and C_1 in Fig. 2A corresponding to b=1 for various frequencies. This will indicate when rms surface tolerances are equal to their state-of-the-art values.

From Eq. (36) we know that at b=1 (for least cost),

$$D = \sqrt{\frac{1}{k_1\sqrt{p+2}}} \quad . \tag{49}$$

Substituting Eq. (49) into the cost equation (26) we can calculate the cost of gain at point b=1, as follows:

$$C = nD^p$$

$$= n\left(\frac{1}{k_1\sqrt{p+2}}\right)^{\frac{p}{2}} \tag{50}$$

but $k_1 = k_1^* F$ from Eq. (29), where

$$k_1^* = \frac{4\pi}{3c}\, 10^3 \quad .$$

Thus,

$$C = \frac{n}{\left(k_1^* \sqrt{p+2}\right)^{p/2}} \times \frac{1}{F^{p/2}} \quad . \tag{51}$$

From Eq. (51) we can calculate the costs of gain at any frequency when b=1. The changes in these costs relative to the cost at F=1 GC are:

$$\Delta C = \left(\frac{1}{F}\right)^{p/2} \quad . \tag{52}$$

The gain G when b=1 can be obtained at any frequency from Eq. (35) using the value of D from Eq. (49). Thus,

$$\ln G = \ln \frac{k_2^2}{k_1\sqrt{p+2}} - \frac{1}{(p+2)} \tag{53}$$

From Eqs. (30) and (29), we have

$$\frac{k_2^2}{k_1} = \frac{3\eta\pi}{4c}\, 10^{15} F \quad . \tag{54}$$

Substituting Eq. (54) into Eq. (53), we obtain

$$G_{dB} = 10 \log\left[\frac{3\eta\pi}{4c}\, 10^{15} \frac{1}{\sqrt{p+2}}\right] + 10 \log F - \frac{4.34}{p+2} \quad . \tag{55}$$

The change in gain of points b=1 at various frequencies relative to the gain at F=1 is then given by

$$\Delta G_{dB} = 10 \log F \quad . \tag{56}$$

Using Eqs. (52), (56), (55), and (51), we can compute the values of G and C corresponding to points b=1 with the results shown in Table II.

Let us now make an assumption that for values of gain smaller than those indicated in Table II, the rms surface tolerance can be represented by its "basic value" -- i.e., $d = 4D^2 \times 10^{-6}$. This implies that we can achieve the required gain by variations of antenna diameter only, while the surface tolerance varies according to Eq. (18).

Since the assumption means that b=1, the cost will be given by Eq. (22):

$$C = nD^p \quad . \tag{22}$$

The general formula for gain is from Eq. (28):

$$\ln G = \ln(k_2 D)^2 - \left(\frac{k_1}{b} D^2\right)^2$$

and when b becomes unity,

$$\ln G = \ln(k_2 D)^2 - (k_1 D^2)^2 \tag{57}$$

or

$$G_{dB} = 10 \log (k_2 D)^2 - 4.34 (k_1 D^2)^2 \quad . \tag{58}$$

Table II

VALUES OF GAIN G AND COST C WHEN b = 1

Freq. (Gc)	Change in Cost Relative to Cost at F=1	Change in Gain Relative to Gain at F=1 (dB)	Absolute Gain, G (dB)	Absolute Cost (Millions of Dollars)
1	1	0	57.37	36.751
2	$\frac{1}{2.3} = .435$	3	60.37	15.898
3	$\frac{1}{3.8} = .263$	4.8	62.17	9.737
4	$\frac{1}{5.31} = .188$	6	63.37	6.876
5	$\frac{1}{7} = .143$	7	64.37	5.250
6	$\frac{1}{8.8} = .114$	7.8	65.17	4.211
7	$\frac{1}{10.7} = .0935$	8.5	65.87	3.349
8	$\frac{1}{12.3} = .0814$	9	66.37	2.974
9	$\frac{1}{14.1} = .071$	9.5	66.87	2.579
10	$\frac{1}{16.2} = .0616$	10.0	67.37	2.270

Since, from this point on, the value of b is kept at unity, the changes in gain are

$$\Delta G_{dB} = 10 \log\left(\frac{D}{D_\alpha}\right)^2 - 4.34 (k_1 D^2)^2 \left[1 - \left(\frac{D_\alpha}{D}\right)^4\right] . \quad (59)$$

Let

$$\beta = \frac{D_\alpha}{D} . \quad (60)$$

represent the change in diameter over the original value D . If we assume as a reference point the value of D corresponding to the case when b has originally reached unity, we can use Eq. (36), obtaining

$$k_1 D^2 = \frac{1}{\sqrt{p+2}} . \quad (61)$$

Substituting Eqs. (60) and (61) into (59) and observing that β is always less than one for the case under investigation,

$$\Delta G_{dB} = 10 \log \beta^2 - \frac{4.34}{(p+2)} (\beta^4 - 1) . \quad (62)$$

Equation (62) will now yield the proper sign for ΔG, and represents changes in gain relative to the gain at the point where b first reached unity (b=1) at any frequency.

The cost at this point at any frequency is from Eq. (22):

$$C = nD^p$$

When the diameter changes to D_α the cost becomes [from Eq. (60)]

$$C = nD^p \beta^p . \quad (63)$$

Therefore, change in cost corresponding to change in diameter of β is

$$\Delta C = \beta^p \quad (64)$$

or

$$\beta = \Delta C^{1/p} . \quad (65)$$

Comparing Eqs. (63) and (26),

$$\Delta C = \beta^p = b . \quad (66)$$

Note that for the case we are investigating, β and consequently ΔC must be less than 1.

Substituting Eq. (65) into Eq. (62),

$$\Delta G_{dB} = \frac{2}{p} (10 \log \Delta C) - \frac{4.34}{(p+2)} (\Delta C^{4/p} - 1) \quad . \tag{67}$$

Equation (67) relates the changes in gain (in dB) and cost relative to point b=1 for any given F. Using constants shown in Eq. (48), the absolute gain of a point at which b first reaches unity was found from Eq. (55) to be at any frequency F:

$$G_{dB} = 57.37 + 10 \log F \quad .$$

The absolute cost of the point b=1 at any frequency F was found from Eq. (51) to be

$$C = 36.751 \times \left(\frac{1}{F}\right)^{p/2} \times 10^6 \text{ dollars} \tag{68}$$

$$C_{dB} = 75.6534 - \frac{p}{2} (10 \log F) \quad . \tag{69}$$

The changes in gain relative to gain at point b=1 will always be negative (in dB) since we are considering only the case of gains lower than those at point b=1.

Thus,

$$\Delta G_{dB} = \left(G_{dB} \text{ required}\right) - 57.37_{dB} - 10 \log F \tag{70}$$

$$\Delta C = \frac{C_{new} \times F^{p/2}}{36.751 \times 10^6} \tag{71}$$

$$\Delta C_{dB} = \left(\text{Cost new}\right)_{dB} - 75.6534 + (p/2) (10 \log F) \quad . \tag{72}$$

Substituting Eqs. (70), (71), and (72) into (67), we obtain a general expression relating gain in dB and cost:

$$G_{req_{dB}} = 57.37 + 10 \log F + \frac{2}{p}\left(Cost_{dB} - 75.6534 + \frac{p}{2}\, 10 \log F\right) - \frac{4.34}{p+2}\left[\left(\frac{Cost \times F^{p/2}}{36.751 \times 10^{6}}\right)^{4/p} - 1\right] \quad (73)$$

$$G_{req_{dB}} = 57.37 + 20 \log F + \frac{2}{p}\left(\Delta C_1{}_{dB}\right) - \frac{4.34}{p+2}\left[\Delta C_1^{4/p} \times F^2 - 1\right] \quad (74)$$

where ΔC_1 represents the change in cost relative to \$36.751 million, and

$$\Delta C_1 = \Delta C / F^{p/2} \quad . \quad (75)$$

The results obtained from Eq. (74) are shown in Table IV and show the cost of required gain under the conditions that the "basic value" of rms surface tolerance is given by $d = 4D^2 \times 10^{-6}$ (i.e., b = 1 = a).

Comparing these results to those in Table III, which shows the cost of gain when the tolerances are held fixed regardless of diameter (i.e., b is unrestricted) as computed from Eq. (45), it appears that more realistic costs are given by formula 74 as shown in Table IV. Note that these results apply only to the values of gain that are less than those shown in Table II (corresponding to b=1). For higher values of gain, Eq. (46) is always applicable.

Table V was assembled using the data from Table IV for values of gain smaller than those shown in Table II and Eq. (46) for higher ones. It represents the minimum cost in millions of dollars which will have to be paid to obtain a required gain and shows the optimum diameter and surface tolerance corresponding to the minimum cost.

E. Approximate Expression for the Cost of Antenna Gain

Equation (74) is not suitable for general use because it does not directly relate the cost of the antenna for any given gain.

An approximation was therefore developed using Eq. (67). If the negative term of Eq. (67) is ignored, the relationship between G_{dB} and C_{dB} becomes a straight line with a slope equal to $\frac{p}{2}$ or 1.21 for our case.

$$\therefore \Delta C_{dB} = 1.21 \quad G_{dB}$$

We already know that for values of gain higher than those shown in Table II the relationship between C_{dB} and G_{dB} is also a straight line with a slope of 2.21 [Eq. (47)].

We can therefore attempt to approximate the total curve relating ΔG and ΔC by two straight lines

$$\Delta C = 2.21 \ (\Delta G_{dB}) \tag{76}$$

$$\Delta C = 1.21 \ (\Delta G) + g \tag{77}$$

where g is the intercept on ΔC axis (when $\Delta G = 0$)

Subtracting these two equations we find that the intersection of the two lines occurs at the points

$$\Delta G = g$$

$$\Delta C = 2.21g$$

Now, from Eq. (67) when $\Delta C = -13.25$ dB the value of ΔG can be found to be -10 dB.

$$\therefore -13.25 = 1.21(-10) + g$$

$$\text{or } g = -1.15$$

Thus, intersection of the two curves is at the point

$$\Delta G = -1.15$$

$$\Delta C = -2.54$$

This is shown in Fig. 3.

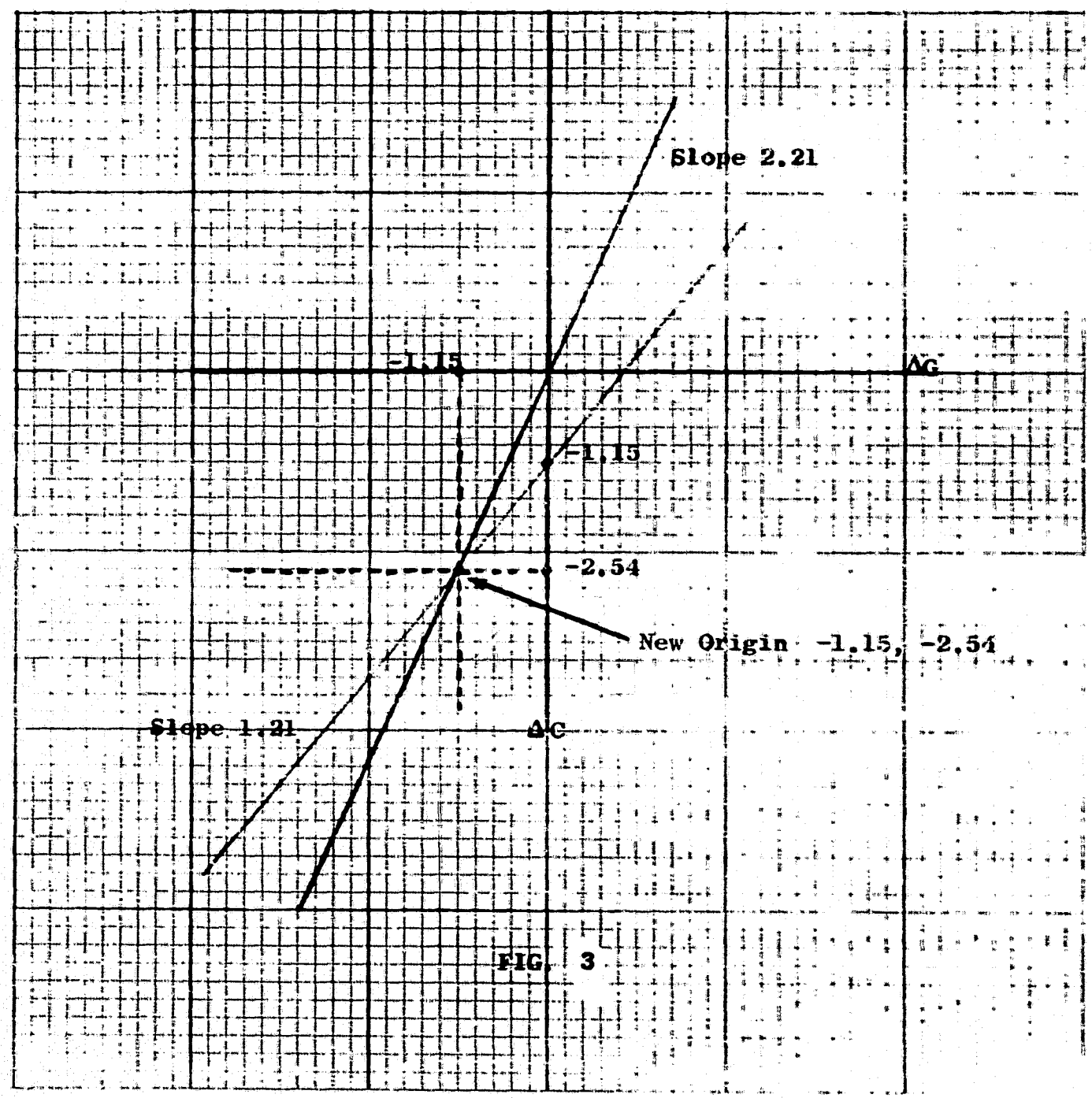


FIG. 3

Changing the origin to this point

$$\Delta G_{new} = \Delta G_{old} + 1.15$$

$$\Delta C_{new} = \Delta C_{old} + 2.54$$

Substituting into Eqs. (70) and (72)

$$\Delta C_{new} = Cost_{dB} - 75.65 + \frac{p}{2}(10 \log F) + 2.54$$

$$= C_{dB} - 73.11 + \frac{p}{2}(10 \log F) \qquad (78)$$

$$\Delta G_{new} = (Grequired)_{dB} - 57.37 - 10 \log F + 1.15 =$$

$$= G_{dB} - 56.22 - (10 \log F) \qquad (79)$$

Thus, with respect to the new origin

$$\Delta C_{new} = 2.21 \Delta G_{new}$$

when the required gain exceeds (56.22 + 10 log F)dB

and $\Delta C = 1.21 \Delta G_{new}$

when the required gain is below that value

The general expression is therefore

$$\Delta C = A \Delta G \qquad (80)$$

where A has one of the above values

Substituting Eq. (78) into (80) we obtain

$$Cost_{dB} = 73.11 - \frac{p}{2}(10 \log F) + A\,[G_{req} - 56.22 - 10 \log F]$$

$$= 73.11 - (\frac{p}{2} + A)(10 \log F) + A\,[G_{req} - 56.22]$$

For p = 2.42

Gain (dB)	F = 1 GC			Gain (dB)	F = 2 GC			F = 3 GC			
	Cost ($ millions)	Dia. (ft)	Toler. (inches)		Cost ($ millions)	Dia. (ft)	Toler. (inches)	Cost ($ millions)	Dia. (ft)	Toler. (inches)	($
57	30.5	320	0.446	66							
56	18.3	285	0.446	65							
55	11.0	254	0.446	64							
54	6.6	227	0.446	63							
53	4.0	202	0.446	62				9.1	190	0.149	
52	2.4	180	0.446	61				5.5	169	0.149	
51	1.4	160	0.446	60	13.1	226	0.223	3.3	151	0.149	
50	0.9	143	0.446	59	7.9	202	0.223	2.0	134	0.149	
49	0.5	127	0.446	58	4.7	180	0.223	1.2	120	0.149	
48	0.3	114	0.446	57	2.9	160	0.223	0.71	107	0.149	
				56	1.7	143	0.223				
				55	1.0	127	0.223				
				54	0.62	113	0.223				

	F = 8 GC				F = 9 GC			F = 10 GC		
67								1.9	101	0.045
66	2.4	113	0.057		1.62	100	0.050	1.10	91	0.045
65	1.5	101	0.057		0.98	90	0.050	0.7	81	0.045
64	0.88	90	0.057		0.59	80	0.050			

Table III

TENNAS WITH FIXED, RMS SURFACE TOLERANCE (b < 1)

F = 4 GC			F = 5 GC			F = 6 GC			F = 7 GC		
Cost ($ millions)	Dia. (ft)	Toler. (inches)	Cost ($ millions)	Dia. (ft)	Toler. (inches)	Cost ($ millions)	Dia. (ft)	Toler. (inches	Cost ($ millions)	Dia. (ft)	Toler. (inches)
						3.9	134	0.074	2.3	115	0.064
			4.4	144	0.089	2.4	120	0.074	1.4	103	0.064
5.7	160	0.112	2.6	128	0.089	1.4	107	0.074	0.83	91	0.064
3.4	142	0.112	1.6	114	0.089	0.85	95	0.074	0.5	81	0.064
2.0	127	0.112	0.96	102	0.089	0.51	85	0.074			
1.2	113	0.112	0.57	91	0.089						
0.8	101	0.112									
0.5	90	0.112									

TABLE VI
MINIMUM COST OF GAIN AT SPECIFIED FREQUENC
($ millions)

Gain (dB)	F = 1 GC		F = 2 GC		F = 3 GC		F = 4 GC	
	Exact*	Approximate**	Exact	Approximate	Exact	Approximate	Exact	Approximat
71								
70								
69								
68							71.9	71.9
67							43.2	43.2
66					69.5	69.4	26.0	25.9
65					41.8	41.7	15.6	15.6
64			100.4	100.3	25.1	25.1	9.4	9.3
63			60.4	60.3	15.1	15.0	5.8	5.6
62			36.3	36.2	9.2	9.0	3.9	3.5
61			21.8	21.8	6.1	5.4	2.9	2.7
60	140.1	140.0	13.4	13.1	4.4	4.1	2.1	2.0
59	84.3	84.2	9.2	8.3	3.3	3.1	1.6	1.5
58	50.6	50.6	6.7	6.2	2.4	2.3	1.2	1.1
57	30.9	30.4	4.9	4.7	1.8	1.7		
56	21.2	19.2	3.7	3.6	1.3	1.3		
55	15.5	14.5	2.8	2.7	1.1	1.0		
54	11.3	11.0	2.1	2.0				
53	8.5	8.3	1.6	1.5				
52	6.3	6.3	1.2	1.1				
51	4.8	4.7						
50	3.6	3.6						
49	2.7	2.7						
48	2.1	2.0						
47	1.6	1.5						

	F = 7 GC		F = 7.25 GC		F = 8 GC		F = 9 GC	
73					85.7	85.6	57.3	85.6
72	81.3	81.3	72.1	72.1	51.5	51.5	34.5	51.5
71	48.9	48.8	43.4	43.3	31.0	30.9	20.7	30.9
70	29.4	29.3	26.1	26.0	18.6	18.6	12.5	18.6
69	17.7	17.6	15.7	15.6	11.2	11.1	7.5	11.1
68	10.6	10.6	9.4	9.4	6.7	6.7	4.5	6.7
67	6.4	6.3	5.7	5.6	4.0	4.0	2.7	4.0
66	3.8	3.8	3.4	3.4	2.5	2.4	1.8	2.4
65	2.5	2.3	2.3	2.0	1.7	1.5	1.2	1.5
64	1.8	1.6			1.2	1.1	0.9	1.1
63	1.3	1.2						
62	0.9	.9						

TABLE VI
AIN AT SPECIFIED FREQUENCY
millions)

*Eqs. (46) & (74)
**Eq. (81)

F = 4 GC		F = 5 GC		F = 6 GC		Gain (dB)
ate	Exact	Approximate	Exact	Approximate	Exact	Approximate	
					82.8	82.7	71
			92.8	92.7	49.8	49.7	70
			55.8	55.7	29.9	29.9	69
	71.9	71.9	33.6	33.5	18.0	17.9	68
	43.2	43.2	20.2	20.1	10.8	10.8	67
	26.0	25.9	12.1	12.1	6.5	6.5	66
	15.6	15.6	7.3	7.2	3.9	3.9	65
	9.4	9.3	4.4	4.3	2.6	2.3	64
	5.8	5.6	3.0	2.7	1.9	1.7	63
	3.9	3.5	2.2	2.0	1.4	1.3	62
	2.9	2.7	1.6	1.5	1.0	1.0	61
	2.1	2.0	1.2	1.1			60
	1.6	1.5					59
	1.2	1.1					58
							57
							56
							55
							54
							53
							52
							51
							50
							49
							48
							47
F = 9 GC			F = 10 GC			
57.3		85.6	40.0	39.9			73
34.5		51.5	24.0	24.0			72
20.7		30.9	14.5	14.4			71
12.5		18.6	8.7	8.6			70
7.5		11.1	5.2	5.2			69
4.5		6.7	3.1	3.1			68
2.7		4.0	1.9	1.8			67
1.8		2.4	1.3	1.1			66
1.2		1.5	1.0	.9			65
0.9		1.1					64
							63
							62

F36B

Table

MINIMUM COST OF GAIN FOR ANTENNAS WITH RMS SUR

Gain (dB)	F = 1 GC			Gain (dB)	F = 2 GC			F = 3 GC			F
	Cost ($ millions)	Dia. (ft)	Toler. (inches)		Cost ($ millions)	Dia. (ft)	Toler. (inches)	Cost ($ millions)	Dia. (ft)	Toler. (inches)	Cost ($ millions
57	30.9	311	0.445	66							
56	21.2	266	0.384	65							
55	15.5	233	0.199	64							
54	11.3	205	0.168	63							5.8
53	8.5	182	0.133	62				9.2	188	0.140	3.9
52	6.3	161	0.105	61				6.1	159	0.102	2.9
51	4.8	144	0.082	60	13.4	214	0.193	4.4	138	0.078	2.1
50	3.6	128	0.067	59	9.2	188	0.140	3.3	123	0.060	1.6
49	2.7	114	0.052	58	6.7	165	0.109	2.4	108	0.048	1.2
48	2.1	102	0.041	57	4.9	146	0.083	1.8	96	0.038	
47	1.6	91	0.033	56	3.7	130	0.065	1.3	85	0.029	
46	1.2	80	0.026	55	2.8	115	0.052	1.1	76	0.023	
				54	2.1	101	0.041				
				53	1.6	91	0.035				
				52	1.2	81	0.26				
	F = 8 GC				F = 9 GC			F = 10 GC			
67								1.9	98	0.038	
66	2.5	110	1.049		1.8	96	0.036	1.3	85	0.028	
65	1.7	95	0.037		1.2	82	0.027	0.96	74	0.022	
64	1.2	82	0.027		0.9	72	0.021				

A

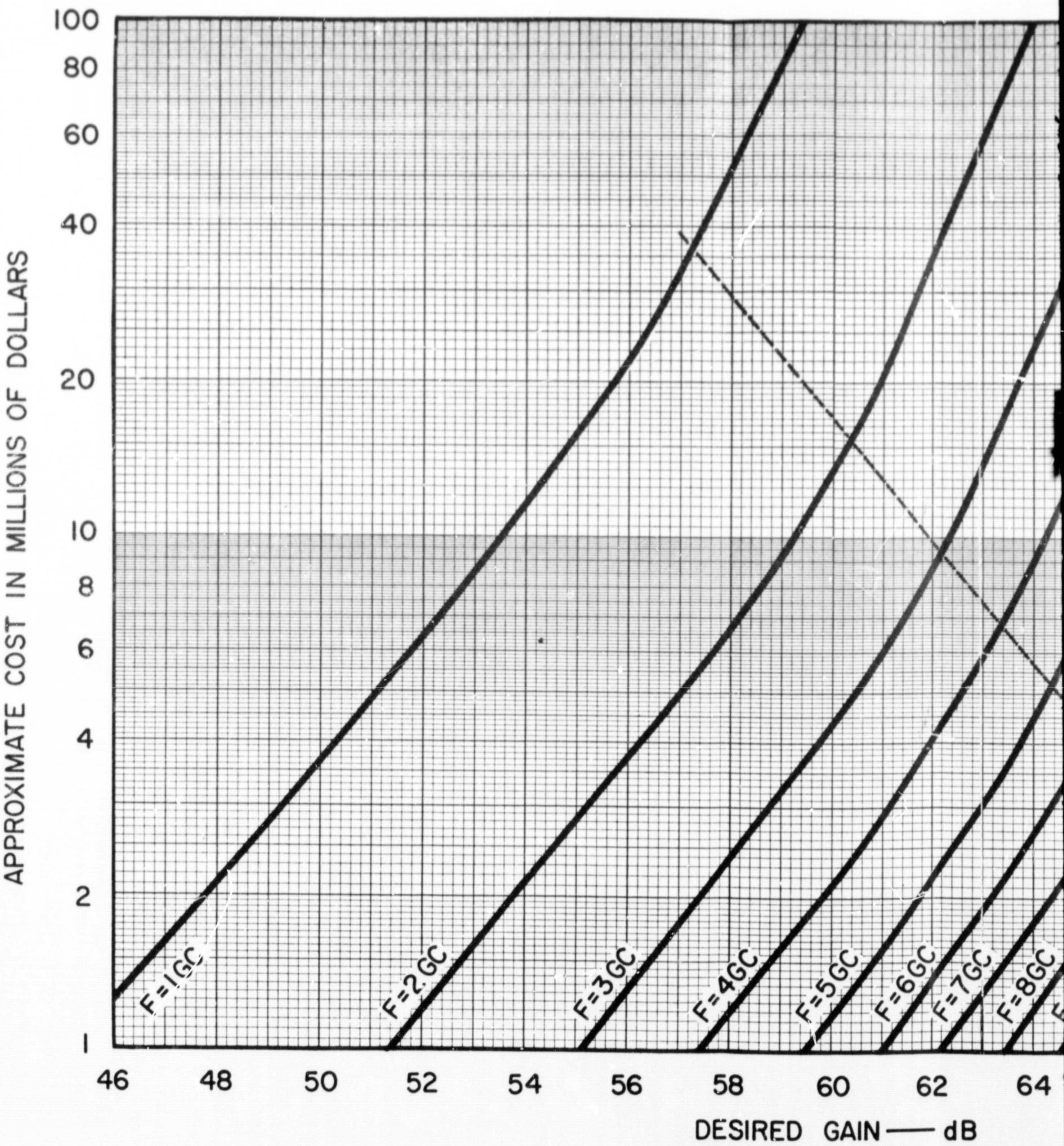
IV

FACE TOLERANCE EQUAL TO $4D^2 \times 10^{-6}$ (b = 1)

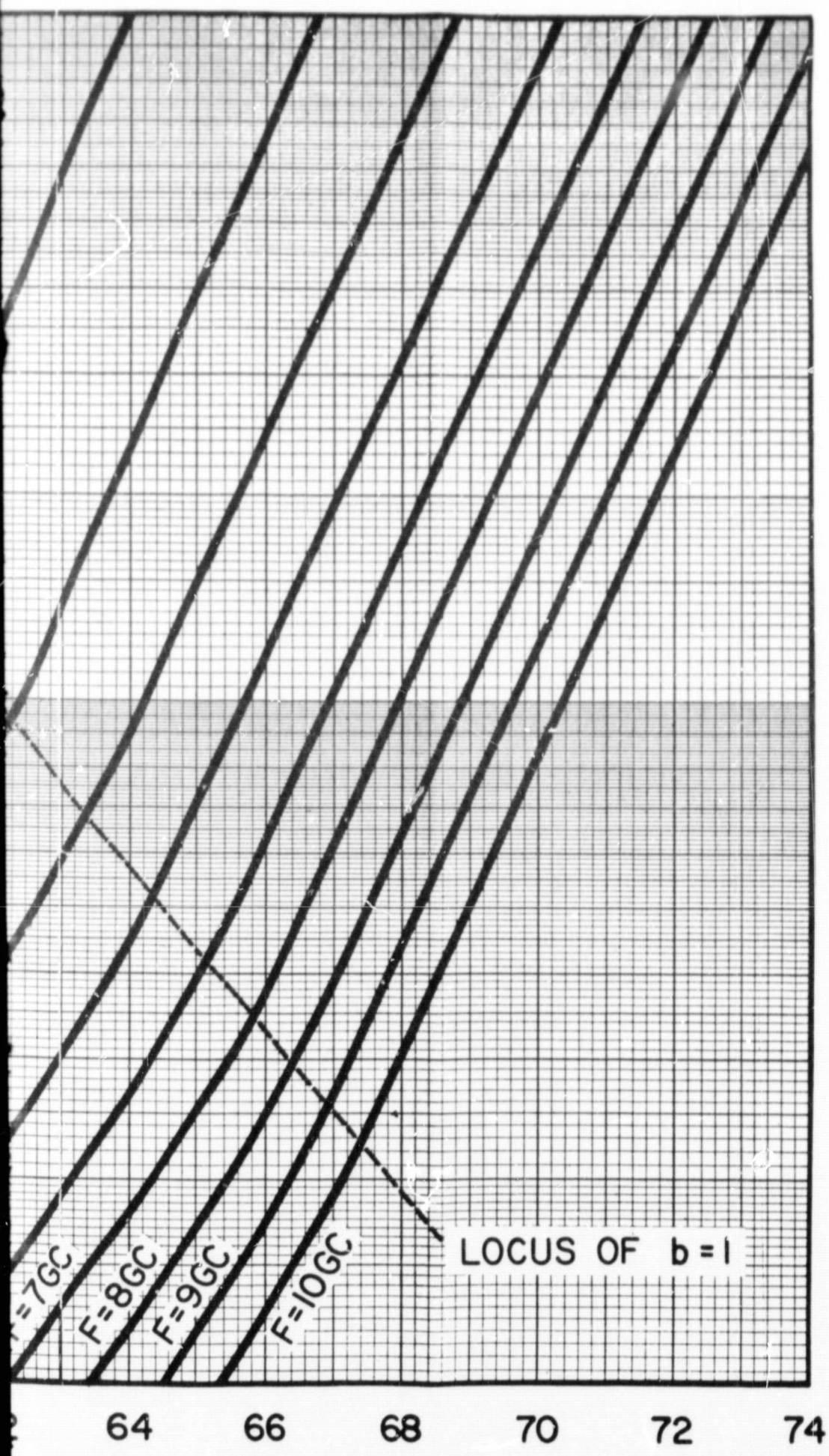
- 4 GC		F = 5 GC			F = 6 GC			F = 7 GC		
Dia. (ft)	Toler. (inches)	Cost ($ millions)	Dia. (ft)	Toler. (inches)	Cost ($ millions)	Dia. (ft)	Toler. (inches)	Cost ($ millions)	Dia. (ft)	Toler. (inches)
					3.9	133	0.070	2.5	109	0.048
		4.4	139	0.078	2.6	113	0.051	1.8	95	0.037
155	0.098	3.0	119	0.058	1.9	98	0.39	1.3	84	0.028
132	0.072	2.2	104	0.044	1.4	86	0.030	0.93	73	0.022
117	0.055	1.6	92	0.033	1.0	76	0.024			
102	0.042	1.2	81	0.026						
91	0.033									
81	0.026									

III CONCLUSIONS

The results of this study are tabulated in Table V and are plotted in Fig. 4 which shows the cost-gain relationship for large parabolic antennas. The dotted line shows the locus of point b=1 which represents the condition of maximum gain obtainable with "basic rms surface tolerance" corresponding to $4D^2 \times 10^{-6}$ inches. In that sense, it also represents the maximum gain obtainable for reasonable costs. The costs of these gains are computed from Eq. (74). To achieve gains higher than those corresponding to b=1, an improvement in tolerance is required beyond that given by Eq. (18).


APPROXIMATE COST IN MILLIONS OF DOLLARS
100
80
60
40
20
10
8
6
4
2
1
F=1GC
F=2GC
F=3GC
F=4GC
F=5GC
F=6GC
F=7GC
F=8GC
46
48
50
52
54
56
58
60
62
64
DESIRED GAIN — dB

A



TC - 188531-74

FIG. 4. MINIMUM COST OF GAIN FOR LARGE PARABOLIC ANTENNAS

B

GLOSSARY

---

a	= Multiplying factor for rms surface tolerance of antenna reflector
b	= Multiplying factor for the cost of the antenna
c	= Speed of light in miles/sec.
C	= Cost
d	= State-of-the-art rms deviation of antenna reflector from ideal parabolic profile
D	= Antenna diameter
η	= Efficiency of a parabolic antenna
F	= Frequency
G	= Gain
ln x	= Natural logarithm of x
log x	= Logarithm of x to base 10
β	= Ratio of diameters
ΔC	= Fractional change in cost
ΔG	= Fractional change in gain

REFERENCES

1. J. Ruze, "Antenna Tolerance Theory--A Review," Proc. IEEE (April 1966).

2. "A Large Radio-Radar Telescope," MIT Lincoln Laboratory, (January 1967).

3. P. D. Potter, et al., "Big Antenna Systems for Deep Space Communications," Astronautics and Aeronautics (October 1966).

APPENDIX G

PROBLEMS OF RADOME USE FOR VERY LARGE ANTENNAS

PROBLEMS OF RADOME USE FOR VERY LARGE ANTENNAS

I INTRODUCTION

Radomes have been used on several large communication antenna systems in recent years. Notably among these are the Haystack system at Lincoln Laboratory (using a 150-foot rigid space-frame radome) and the Andover Communication Satellite Earth Station (using a 210-foot air-inflated radome) built by BTL (now owned by Communication Satellite Corp.). There are two principal advantages to using a radome. These are the simplification of design made possible by the elimination of wind and weather effects on the antenna, and the ease of maintenance and operation made possible by the elimination of environmental effects.[1] Countering this of course are several disadvantages. First of all there is extra noise radiated and reflected from the radome which may enter the station receiver or be radiated into other adjacent receivers such as nearby point to point microwave relay. Secondly, there is direct signal loss due to attenuation of the received (and transmitted) signal by the radome, which may be particularly bad when the radome is wet.

Many radome installations in the past, for both communication and other electronic systems, have been required because of severe climate conditions which made the relatively benign environment inside the radome necessary for successful operation. This has been particularly true for various military systems. The bulk of radome experience over the past twenty years has been with fabric, air-supported radomes, which have been costly, particularly in large sizes, and are subject to deterioration with

---

1 J. S. Cook and A. J. Giger, "All-Weather Earth Station Satellite Communication Antennas," Bell System Technical Journal, XLIV (September, 1965), pp. 1225-1228.

time due to weather and sun. There has been a general tendency, wherever possible, to avoid the use of radomes in operational systems. For example, all Communication Satellite Corporation's ground stations (85-foot antennas) are being built without radomes. On the other hand, the Army, in designing the AN/MSC-46 transportable earth station, found that the use of an air-supported radome resulted in less antenna weight and permitted greater flexibility in operation. While no specific data on cost trade-off studies is known, it is probable that the Comsat Corporation's decision not to use a radome stems from the fact that construction techniques necessary to build an environmentally satisfactory 85-foot antenna exist at a cost low enough to negate the cost advantages of using a radome, when one also considers the other radome disadvantages, particularly in rain loss and increase in system noise temperature. The increase in cost and mechanical complexity of larger high-precision antennas appears to make the use of radomes much more cost competitive, particularly since much of the poor results stems from the experience obtained on the Andover antenna which uses an air-inflated, rubber-covered fabric radome. More recent work with a metal frame, rigid radome indicates the effects may not be as bad as previosuly anticipated.

II TECHNICAL DISCUSSION

D. Gibble of the Bell Telephone Laboratories has developed a formula for calculating the water film thickness, t, on a radome as a function of the rain rate.[2] The formula is:

---

[2] D. Gibble, "Effects of Rain on Transmission Performance of a Satellite Communications System," presented at 1964 IEEE International Convention. The full paper was not presented in the Convention Record, but the paper was quoted in: A. Cohen and A. Smolski, "The Effect of Rain on Satellite Communications Earth Terminal Rigid Radomes," Microwave Journal, 9 (September, 1966), p. 111. Actual transmission loss can be estimated by using the Gibble formula to determine the water film thickness and by data on the transmission loss through this film of water such as that found in: B. C. Blevis, "Losses Due to Rain on Radomes and Antenna Reflecting Surfaces," IEEE Transactions on Antennas and Propagation, AP-13 (January 1965) pp. 175-176.

$$t = 71.88(QR)^{1/3}$$

where: t = water film thickness in mils

Q = rain rate in millimeters per hour

R = radome radius in feet.

Experimental data using the Andover Earth Station has been gathered on transmission loss versus rain rate and has been plotted in Fig. 1.[3] As Cohen and Smolski have pointed out, this compares closely with corresponding data calculated from the Gibble formula, also plotted in Fig. 1.[4] This would lead one to believe that the Gibble formula is an accurate representation of the actual water films on the radome. However, the Gibble formula is based on classical laminar flow and there are several structural aspects of the radome design which would lend one to expect something other than laminar flow.[5] There is also reason to suspect that the fabric coated material used in the Andover radome absorbs some moisture since it was noted that transmission loss measurements took about 30 minutes to return to normal after the rain had stopped.[6] These results lead the BTL personnel to conclude that: "...worthwhile improvement in the earth station receiver sensitivity could be obtained by elimination of the antenna radome..."[7]

---

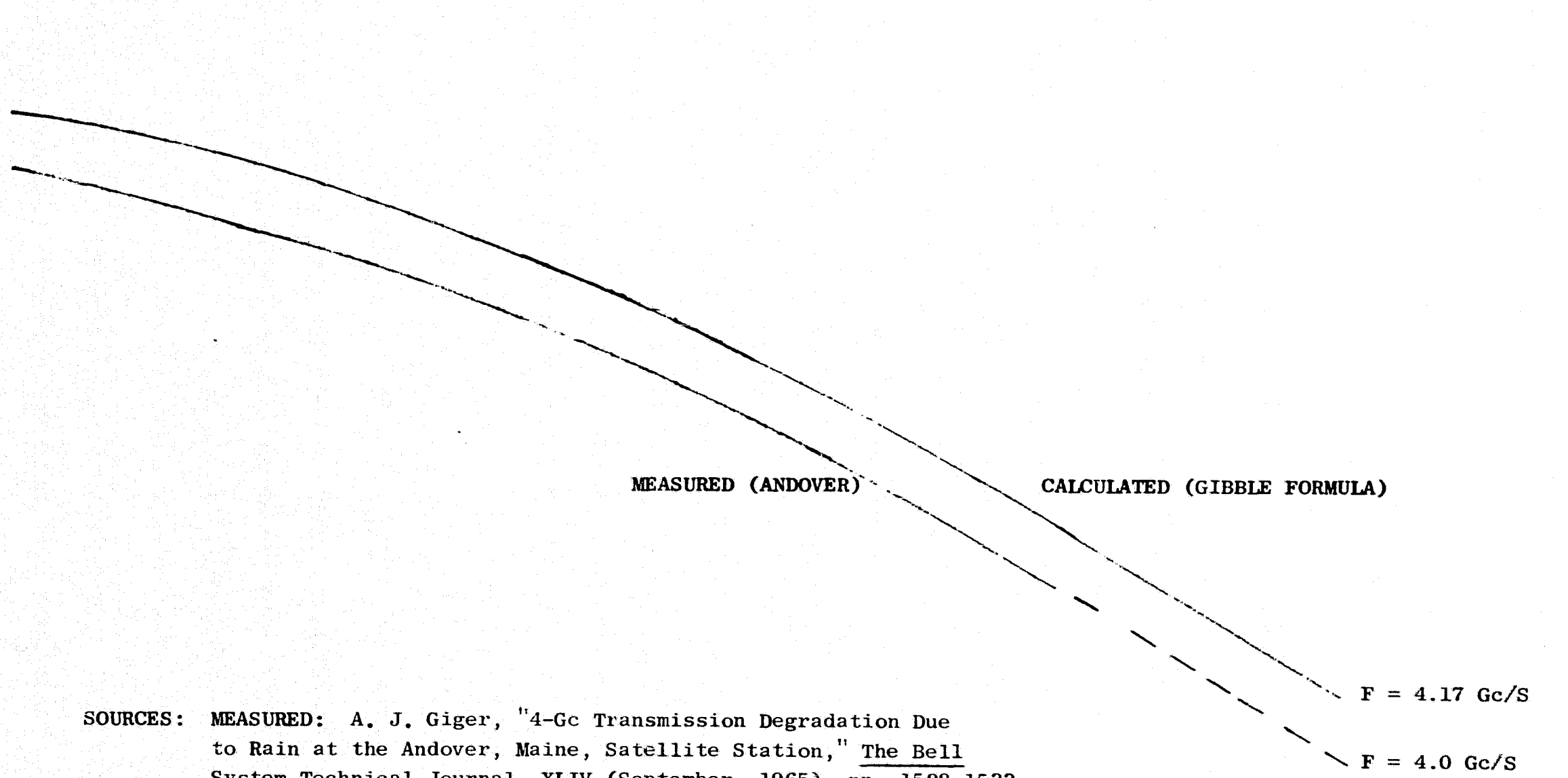
3 A. J. Giger, "4-gc Transmission Degradation Due to Rain at the Andover, Maine, Satellite Station," The Bell System Technical Journal, XLIV (September, 1965) pp. 1528-1533.

4 Cohen and Smolski, Op Cit, p. 111.

5 Ibid, pp. 111-112.

6 Giger, Op Cit, p. 1531.

7 Cook and Giger, Op Cit, p. 1225.



SOURCES: **MEASURED:** A. J. Giger, "4-Gc Transmission Degradation Due to Rain at the Andover, Maine, Satellite Station," The Bell System Technical Journal, XLIV (September, 1965), pp. 1528-1533.

CALCULATED: A. Cohen and A. Smolski, "The Effect of Rain on Satellite Communications Earth Terminal Rigid Radomes," Microwave Journal, 9 (September, 1966) pp. 111-121.

Fig. 1: TRANSMISSION LOSS IN AN ANDOVER-TYPE RADOME

However, it does not appear that these conclusions are valid for a rigid radome. A measurement program using a 55-foot diameter metal space frame radome has been reported by Cohen and Smolski.[8] A unique part of this test was the ability to artificially create various rain rates and to measure the thickness of the water film on the surface of the radome. These studies indicated greatly reduced losses, even at high rain rates. These are also plotted in Fig. 2. This can be compared with data for a 55-foot Andover-type radome, as calculated by the Gibble formula, shown in Fig. 2. The nominal 1.5 dB loss (actually two values measured at 1.0 and 1.7 dB) would compare with a value of approximately 4.3 dB for the Andover measurements extended to 40 mm/hr. (Fig. 1).[9] Cohen and Smolski noted that "...it appeared that a pattern of rivulets, streaks and various water run-off paths developed."[10] When the radome surface was treated to reduce these effects, even lower losses were observed at 40 mm/hr., as shown in Fig. 2. Thus, it appears that the rain effects on a rigid, metal frame radome are not nearly as severe as had been generally believed based on Andover data, at least for radomes of the general diameter of 50 feet.

In an attempt to better understand this phenomenon, Professor C. C. Mei of the MIT Civil Engineering Department modified the Gibble formula to account for the turbulent flow of the water.[11] The modified formula is:

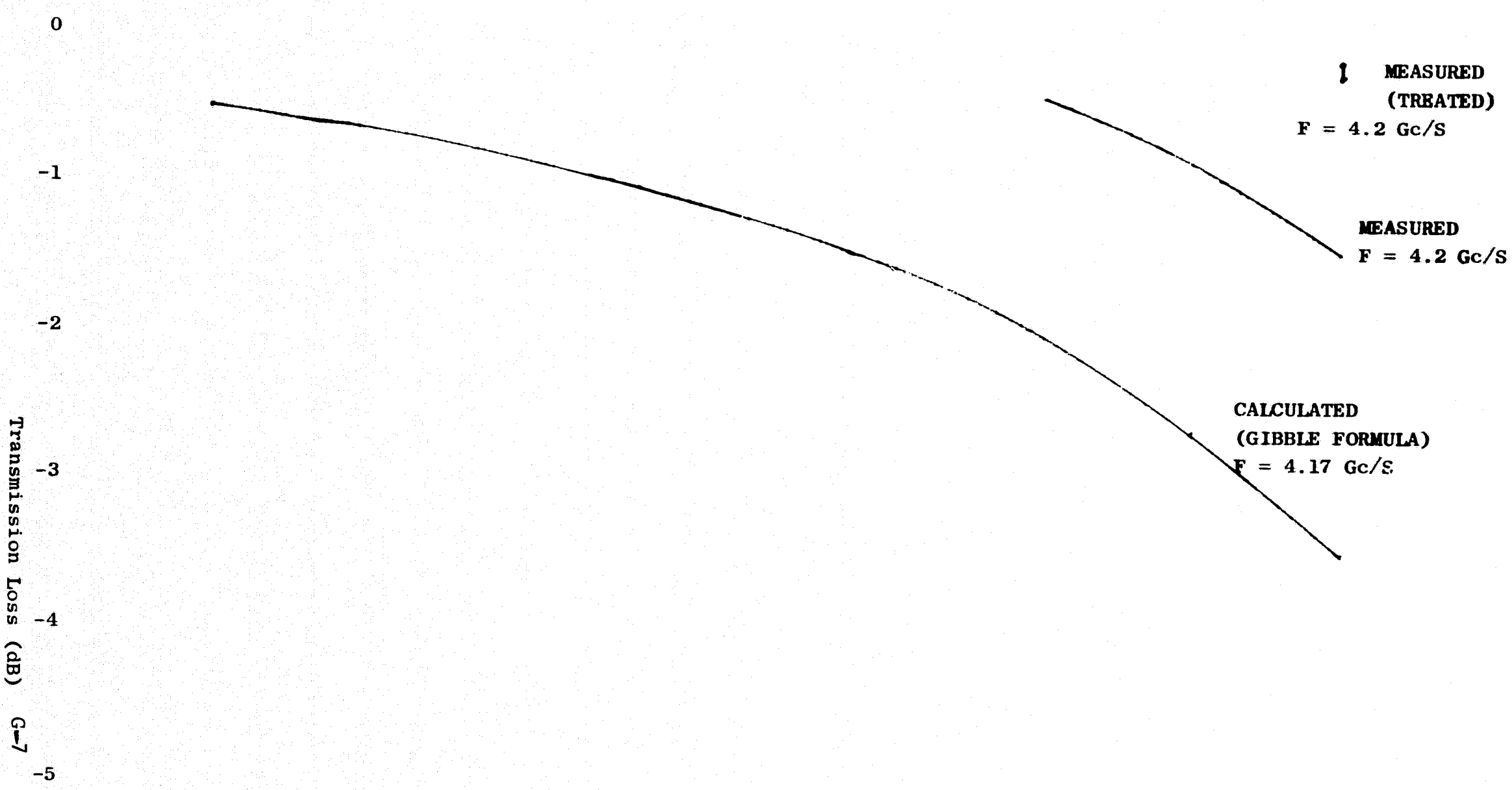
---

8 Cohen and Smolski, Op Cit, pp. 111-121.

9 Ibid, p. 120.

10 Ibid, p. 121.

11 John Ruze, "Effect of Rain on Radome Performance," in A Large Radio-Radar Telescope: CAMROC Design Concepts, 2 volumes (Cambridge, Mass: Cambridge Radio Observatory Committee, 15 January 1967), Volume II, pp. 2-1 to 2-10.



SOURCE: A. Cohen and A. Smolski, "The Effect of Rain on Satellite Communications Earth Terminal Rigid Radomes," Microwave Journal, 9 (September, 1966), pp 111-121.

Fig. 2: TRANSMISSION LOSS IN A RIGID 55-FOOT RADOME

$$t = 14.83(QR)^{7/12}$$

where: t = water film thickness in mils

Q = rain rate in millimeters per hour

R = radome radius in feet.

Values for t for radomes of a size of interest using both formulas are shown in Fig. 3. It should be noted that both formulas tend to converge for high rain rates. In the range of maximum rates to be expected for most geographical locations, 10-40 mm/hr, this is particularly true of large radomes. The Mei formula agrees with the Cohen and Smolski data for a 55-foot radome better than does the Gibble formula.[12] However, comparable data for a large rigid radome, such as the 150-foot Haystack radome, does not exist. As Ruze has pointed out, this type of data would help to clarify the situation for very large radomes.[13] Because of the complexity of the water flow and the lack of experimental data, it does not appear possible at this time to predict what the loss would be for very large radomes with any degree of precision. However, it is obvious that methods of radome treatment and construction do exist which will tend to minimize these losses.

The use of a radome is particularly attractive for very large antennas where structural problems add greatly to their cost. The use of a radome permits a much simpler antenna structure since unpredictable environmental loadings, such as ice and wind, do not need to be compensated for by a heavy back structure. It also permits a considerable reduction in the feed support structure reducing blockage and permitting a corresponding increase in antenna gain. Since, for large antennas (400-500 feet), the cost of structure to maintain high surface tolerance is very high, the advantages

---

12 Ibid, p. 2-9.

13 Ibid, pp. 2-9 to 2-10.

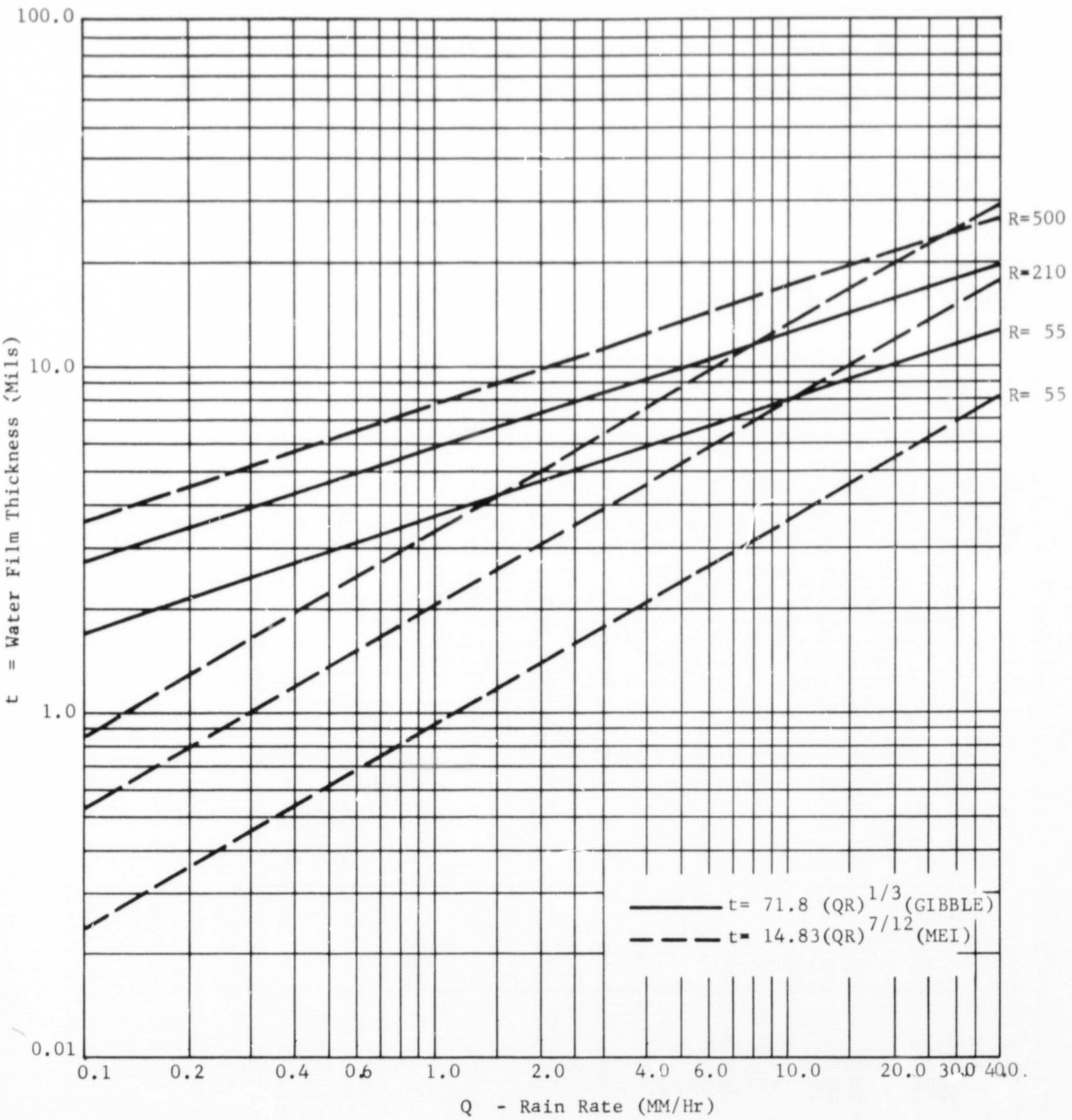


Figure 3. Two Estimates of Water Film Thickness on Large Radomes

of a rigid radome outweigh the disadvantages. The CAMROC study has shown the potential savings in this technique. This study concluded that an increase in antenna diameter of approximately 10% can fully compensate for the radome aperture blockage and the increased noise temperature.[14]

The cost reductions made possible by the use of a radome, however, are so great that the cost of the increased size necessary to make up for radome losses is more than compensated for by the use of the radome. For example, the CAMROC study found that:

> Subsequent studies, which were able to take full advantage of greater design freedom permitted by the radome, have revealed that the comparative weights of an exposed 400-foot antenna and its radome-enclosed equivalent will differ by about 15:1.[15]

Specifically, the estimated costs for both enclosed and exposed antennas as estimated by CAMROC, are as shown in Table I.[16] It must be remembered

Table I: COSTS OF ENCLOSED AND EXPOSED ANTENNAS

ANTENNA TYPE	COST	
	Antenna Size	
	400 Ft. Dia.	500 Ft. Dia.
	Radome Size	
	550 Ft. Dia.	688 Ft. Dia.
Enclosed		
Antenna	$ 8.9M	$12.6M
Radome	8.4M	13.5M
Total	$17.3M	$26.1M
Exposed (Range of Extrapolated Costs)	$92-137M	$155M Up

14 CAMROC, Op Cit, Volume I, p. 2-9.

15 Ibid, p. 2-8.

16 Ibid, Volume I, p. 6-6. Costs are adapted from Fig. 6.2.

that this design was for a fully steerable paraboloid having a surface tolerance of 0.1 inches and a pointing accuracy of 15 arcseconds. To extend the highest operating frequency to 10 GHz would require a surface tolerance of approximately .06 inches, with some increased cost. However, the figures in Table I do indicate the dramatic cost savings possible with the use of a radome for such an antenna design.

III CONCLUSIONS

Several attempts have been made to predict the effects of rain on transmission losses of large radomes. To date conflicting results have been obtained with the limited experimental data available on the various types of large radomes.

At this point in time it does not appear possible to predict with any degree of accuracy what the losses will be for a radome of the size of 400-600 feet in diameter. However, it is apparent that the use of a rigid radome, designed with water run-off in mind will minimize these losses. Further experimental work using the Haystack 150-foot radome as a vehicle could clarify this situation.

It does appear obvious however that the use of a rigid radome for high performance antennas over 200 feet in diameter permits a reduction in the cost of the antenna structure which more than offsets the cost of the radome. This effect appears to increase greatly with antenna diameter.

Thus it appears that large, steerable, high performance antennas built in the foreseeable future should consider the use of a rigid radome designed to maximize water run-off.

APPENDIX H

A SURVEY OF VERY HIGH POWER MICROWAVE TRANSMITTER

A SURVEY OF VERY HIGH POWER MICROWAVE TRANSMITTERS

1.0 Microwave Power Amplifier Types

The ability to produce very high power at microwave frequencies is primarily dependent on the type of power amplifier that is used. Klystrons, traveling wave tubes (TWTs), and cross-field amplifiers are used to generate power at microwave frequencies. The klystron amplifier has the highest power handling capability at a reasonably high efficiency. It is estimated that an average power of up to 30 megawatts can be achieved in a single tube if sufficient funds are provided to develop a tube of this power. The bandwidth of the klystron amplifier becomes its limiting parameters. Tuneable bandwidths are large but operating bandwidths are normally on the order of 1 percent. As the power capability is decreased higher bandwidths of up to about 5 percent become available. The TWT amplifier provides the greatest bandwidth capability. Between 20 and 25 percent bandwidths are readily achievable. Maximum power and efficiency are the limitations of TWTs. Cross-field amplifiers, also known as amplitrons, fall midway between klystrons and TWTs. The advantage of amplitrons is in their power efficiency which can be as high as 80 percent. Comparison of these major characteristics is shown in Table 1. It can be concluded that for powers of 1 megawatt or more, only klystrons can be considered to achieve these power levels.

1.1 Available Klystrons

A listing of available high power klystrons are shown in Tables 2 and 3. Table 2 is a summary of those available tubes able to deliver 100 KW or more. The list in Table 3 is more inclusive and shows the commerically produced tubes having outputs in excess of 20 KW when operating between 1 and 10 GHz. The relationships between output, operating frequency band, and tube cost are shown in Fig. 1. Power output is seen to be independent

Table 1

COMPARISON OF MICROWAVE TRANSMITTERS

Parameters	Klystron	TWT	Cross-Field Amplifier
Available Power-KW	1000	10	375
Estimated Maximum Power-KW	30,000	30	375
Bandwidth	0.5%-5%	20-30%	10%
Efficiency	60%	47%	80%

Table 2

AVAILABLE HIGH POWER KLYSTRONS 100 KW AND ABOVE

Power Output- KW	Operating Frequency KHz	Manufacturer and Designation	High Voltage Supply KV	Unit Price	
100	7.1-8.5	Varian VA 879 A	45	$35,000	
100	-8.0-	Eimac X 3066	36	----	
100	7.1-9.0	General Electric ZM 6602	17	----	Westford
250	-8.0-	Varian VA 949	45	$60,000	Haystack
400	1.2-1.4	Litton L 3874	--	----	
400	-2-	Eimac Developmental	--	$70,000-$100,000	
500-1000	X-band	Eimac Developmental	--		

Table 3

COMMERCIALLY PRODUCED TUBES
20 KW CW and ABOVE--1 to 10 GHZ

	Power Output KW	Operating Frequency GHZ	Designation	High Voltage Supply KV	Manufacturer	Unit Price $	Beam or Anode Efficiency %	Note
Klystron	20	1.7-1.8	5KM70SF	21	Eimac		34	
	21	1.7-1.8	LD659	18	Nippon Elec.		42	
	20	1.7-2.4	5KM70SF	20	Eimac	17,500	35	
	20	1.7-2.4	4KM70SJ	21	"	15,000	40	
	20	2.0-2.2	5K70SI	21	"		39	
	24	2.09-2.12	5K70SG	23	"	17,000	55	
	25	2.4-2.5	X812B	22	"		45	
	20	2.6-2.7	4KM70SK	21	"		38	
	20	5.2-5.3	SAC406	20	Sperry		35	
	27	5.4-5.9	SAC47	20	"		16	
	20	5.7-6.2	X3052	20	Eimac		35	
	20	5.9-6.4	VA884A	20	Varian	10,000	29	
	22	5.9-6.5	VA860	22	Varian	12,500	22	
	25	7.1-9.5	VA849	26	Varian	10,000	40- 50	
	20	7.2-8.4	X-3050	20	Eimac		33	
Magnetrons								
	20	8.8-10	MxM41	930V	Meteom		39	
	25	-9.0-	EM15LS	2.3	Eimac	2300	87	
Amplitron	21	3.0-3.2	9KS1110		Raytheon		?	
TWT	20	5.0-8.0	X1014	3.0	Eimac		11.5	
Tetwde	25	-1.0	TH491	6.0	Thomp-Varian		?	
	25	-1.0	2029	9.0	RCA		55	
Klystron	60	1.2-1.4	4K200LX	25	Eimac	30,000	35	
	60	7.1-8.5	VA873	28	Eimac	30,000	43	
	50	7.1-9	ZM6601	13	G.E.		32	
Magnetron	35	9.0-9.8	QK1169		Raytheon		?	
	50	9.0-9.1	MAG14	14	G.E. Ltd.		30	

	Power Output KW	Operating Frequency KHZ	Designation	High Voltage Supply KV	Manufacturer	Unit Price $	Beam or Anode Efficiency %	Note
Amplitron	50	x-band	QK1225		Raytheon		?	
Pentode	65	-1.2	7214	10	RCA		36	
Totrode	50	-1.5	ZP1045	8.0	G.E.		65	
Klystron	122	1.7-2.0	VA858A	35	Varian		35	No longer available
	122	2.0-2.4	VA858B	35	Varian		35	" "
	100	2.1-2.4	5KM30031	38	Eimac	35,000	45	
	100	7.1-8.5	VA879A	45	Varian	35,000	22	
	100	7.1-9.0	ZM6602	17	G.E.		33	
	100	8.0	X3066	36	Eimac		41	
Klystron	400	1.2-1.4	L3876		Litton		31	
	400	2	Development		Eimac	70-100,000	?	Developmental tube
	250	8	VA949	45	Varian	60,000	40-50	
	500-1000	x-band	Development		Eimac		40-50	500 KW achieved -1000 in development

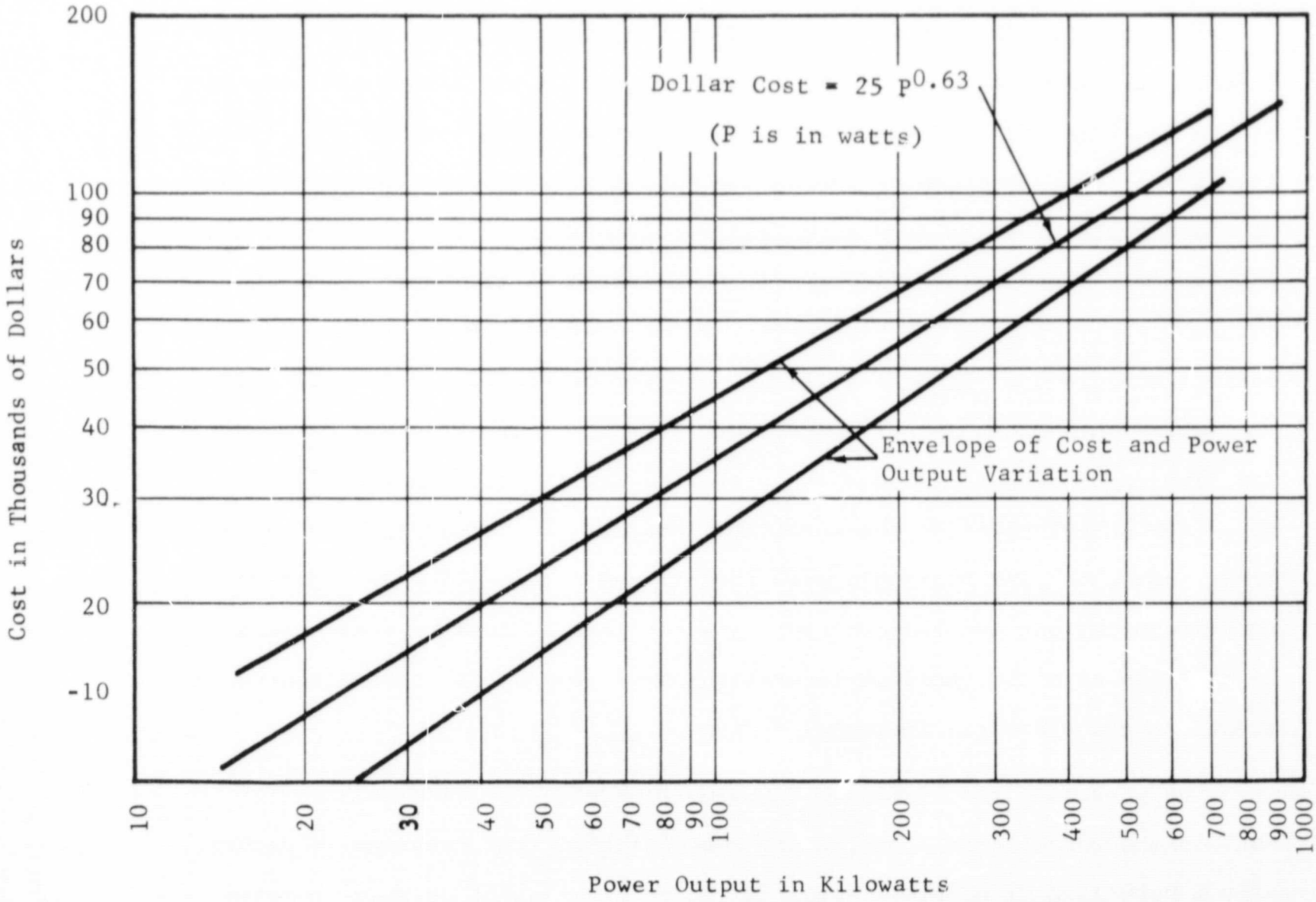


Figure 1. Variation of Frequency and Cost with Power Output for Klystron Power Amplifiers.

of operating frequency band; however, costs increase exponentially with increased power. The best fit for the exponent appears to be 0.63 so that the cost equation for transmitter power amplifiers has been taken to be:

$$\text{Cost} = 25P^{.63}$$

1.2 Power Output Limitations

Available power output is limited by two factors; first, the temperature at the extremities of the resonant cavities in the tubes, and secondly, by the breakage limit of windows in the output waveguide feeds. The first limitation is most severe as far as the tube itself is concerned. Heating of the cavities results from circulating currents induced by the resonance phenomenon. The heating effects are concentrated at the junction of the resonant cavities with the waveguide. Unfortunately, these points of high current density are the most difficult portion of the cavity to cool. If the temperature at these extremities or the temperature gradient between the tips and the body, becomes too high, the cavity distorts and either drops the output power or regenerately increases the temperature and destroys the tube. The available area for a tuned cavity will vary inversely with frequency and temperature rise is a function of related area. Thus, as might be expected, maximum theoretical power output is inversely proportional to the operating frequency.

The window is the nonconducting membranes which provides a hermetic seal in the output feed. In the high power tubes, this membrane is generally a beryllium oxide plate which is sealed by means of ceramic-to-metal techniques to the surrounding output waveguide. Properly matched, these windows have been tested up to 1 megawatt for 7 minutes and at 250KW for long periods; however, comparatively small mismatches can result in excessive heating or dielectric stress and cause rupture. This can occur very rapidly and, to prevent such occurences, in addition to preventing other tube damage, elaborate control systems are usually provided in the output

network to remove high voltage and drive in the presence of a mismatch.

This is done by providing sensors in the output network to detect the mismatch. These sensors are generally either photo-electric devices which detect ionization in any one of 2 or more places in the guide and at the surface of the window, or reflected power measuring devices which detect an increase in reflected power above a preset limit.

The sensors are used to trigger an electronic switch which removes drive power and a crowbar device which short circuits the high voltage supply. The spark gap crowbar is described in the section on power supplies. This device provides a very rapid response, but, after the arc is quenched sufficient energy may still remain in the power supply filter to damage the tube. Therefore, a hydrogen thyratron type switch and a mechanical switch are paralleled with the spark gap. The spark gap responds within 1 microsecond. The thyratron fires within about 10 microseconds, thus before the spark gap quenches, and the mechanical switch operates within a few milliseconds, assuring a short circuit in the event of thyratron failure.

Some trouble has been encountered in the field with the thyratrons, largely due to cathode sputtering making the glass envelope opaque and preventing visual inspection of thyratron operation, thus preventing detection of faulty tubes.

The output feed limitation may be ameliorated by sharing the power among two or more output feeds, but this device requires some means for recombining the output at some point in the system, and the recombination must be phase coherent. Since the output feed limitation is still present, even if the window problems can be overcome by use of quartz, the recombination cannot take place, anywhere in the waveguide feeds but must occur in the output load, usually an antenna feed. Thus, the antenna feed must be capable of handling the full power output in a fashion that does not

cause phase front distortions and still acts as a matching device between the power feed and the antenna.

1.3 Paralleling of Amplifiers

Some successful attempts have been made in paralleling two or more tubes to achieve higher powers. In this case, it is possible to achieve output phase coherence by applying phase correction between the inputs to the power tubes and a common driver; however, modulation bandwidth may be severely reduced unless the output tubes are closely matched.

Up to eight 50 megawatt (peak) pulse tubes have been operated in parallel at S band at a low duty cycle, each tube averaging about 6.25 KW.

Ohio State has operated eight 10 KW C.W. tubes and four 20 KW C.W. tubes in parallel at S band and very recently Lincoln Labs has operated two 250 KW tubes in parallel at X band.

1.4 Mechanical Characteristics

All of the larger tubes are liquid cooled, the liquid generally being water unless the tube is to be operated in a situation where ambient temperatures go below freezing in which case the addition of ethelyene glycol (anti-freeze) is recommended. Because of the mechanical problem of transferring the heat out from the inside of the tube, it is presently considered impossible to air cool tubes having dissipations much in excess of 10 KW.

Although the greater part of the heat is dissipated at the anode, several other parts of the structure must also be cooled to eliminate local hot spots and strains on the seals. The external surfaces surrounding the cathode is usually air cooled, and water cooling is provided in the body and to the electromagnet. The section containing the output window is also water cooled and water cooling is generaly required along the output waveguide feeding the load, particularly that section closest to the tube.

The anode coolant jackets are permanently assembled around the cooling fins that are fabricated as part of the tube structure. The coolant capacity of the anode jacket typically holds 1/2 to 1 quart of water for a 25 KW tube, and the 250 KW tube holds about 1 gallon. A 25 KW tube typically requires a total of 10 to 11 gallons of water per minute at 100 psi and the 250 KW tube required 110 gallons per minute of 100 psi.

The physical length of the tubes is primarily controlled by the power output and secondarily by the operating wavelength, and the diameter is controlled primarily by the operating wavelength.

The size and weight of the electromagnet is controlled primarily by the operating wavelength, since its function is to provide an essentially uniform magnetic field around the beam, and the area that the field must encompass is governed by the tube diameter for an externally mounted magnet. The cost of the electromagnet assembly runs between approximately $2500 and $5000 for tubes of interest here.

For anode voltages below 42KV, X-rays present negligible problems, since the number of electrons exceeding the 85KV velocity are small, and a small amount of lead shielding built into the cathode section provides adequate shielding. Even for the 250 KW tube whose operating potential is 45KV, this shielding plus that inherent in the tube structure provides sufficient shielding to ensure radiation levels well below those requiring any special precautions.

1.5 Electrical Characteristics of Power Tubes*

Modulation Bandwidth. Modulation bandwidth of high power klystrons operating at X band are partially dependent on the tuning range of the tube. With tuning ranges of approximately 500 MHz bandwidths of up to 1.5% of the operating frequencies can be considered as catalog items. For narrower tuning ranges, 2% is achievable. Discussions with leading manufacturers have indicated that with additional R&D of approximately $350000 modulation bandwidth for high power tubes of 3 to 4% could be achieved.

Output Power. 250 KW tubes have been built and higher powers are quite feasible. For the amount of additional R&D mentioned above, a tube with rated output of 500 to 700 KW could be developed in 12 months exhibiting bandwidth in excess of 3% of operating frequency.

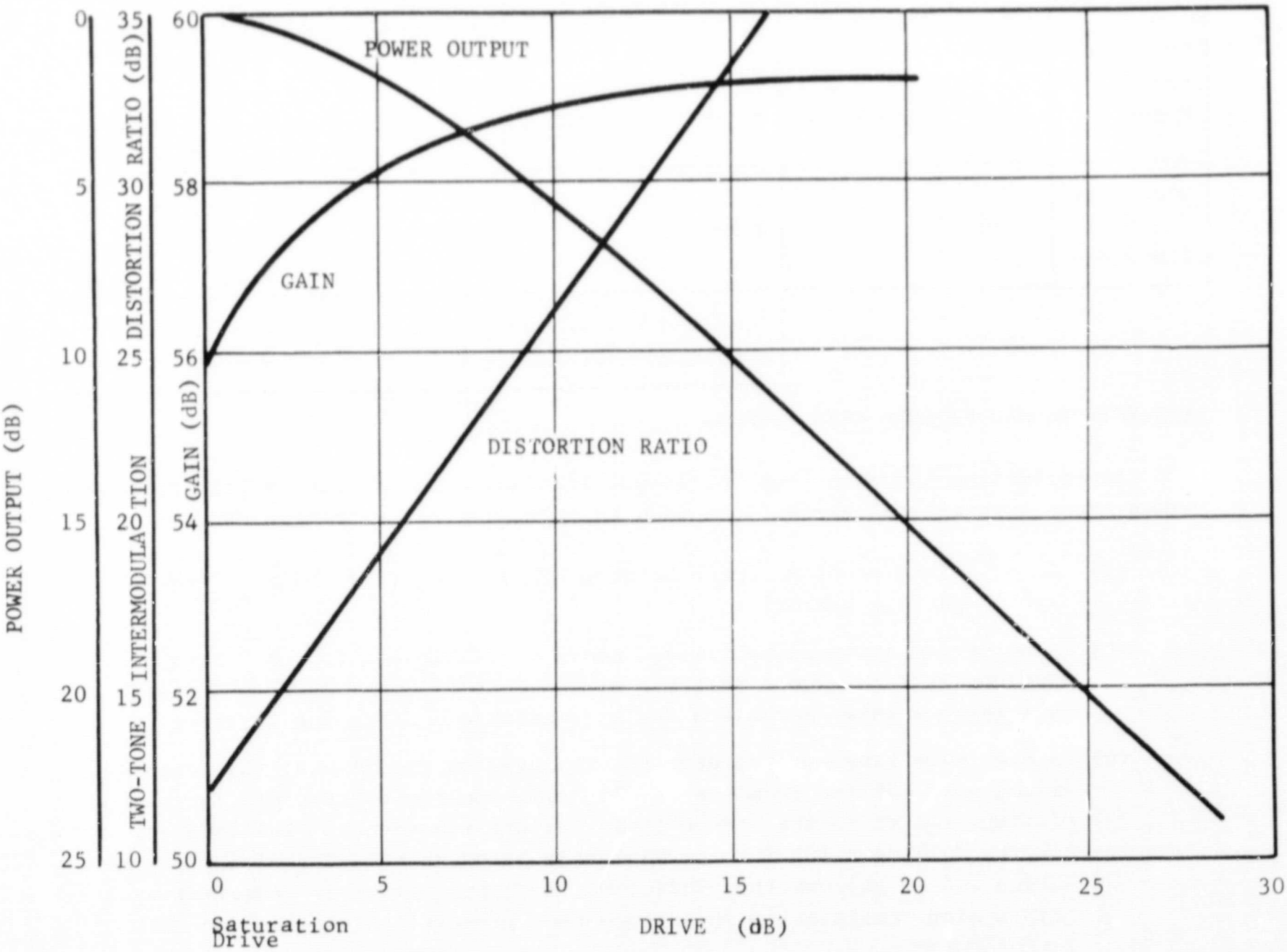
Distortion. All klystrons exhibit basically similar saturation characteristics which are shown in Fig. 2. It can be seen that reducing the drive 3 dB below saturation point reduces the output power by approximately 1 dB with the corresponding distortion products ratio of approximately 16 dB. We will assume therefore for the purposes of our study that a power tube will be operated at an output of 1 dB below rated value resulting in negli-
ble distortion.

Klystron Reliability. The estimate of reliability of X band klystron power amplifiers has been obtained from Varian Associates for their VA-922 and VA-856 tubes and is shown in Table 4 together with the assumptions on which it is based. Repairability data are also provided.

Conclusion. As a result of the data presented in this memo, we will assume that by 1970 a power klystron with the following characteristics

---

* This paragraph was written by B. R. Stack



Source: Varian Associates

Figure 2. Klystron Performance Data

Table 4

Klystron Reliability Data

Module	Gun Assembly	Body Assembly	Collector Assembly	Overall Assembly
Principal Failure Modes	Open or shorted heater Loss of emission	Cracked window Melted drift tubes	Clogged or melted collector Low water flow	Vacuum leaks Mechanical defects
Occurrence Per 1,000 Hrs	3.6%	0.2%	0.7%	0.4%
		Combined Failure Rate, per 1000 hours = 4.9% Estimated MTTF at 90% C.L. = 20,400 Hours		

ASSUMPTIONS AND FAILURE RATE SOURCES

In estimating the mean time to failure for the proposed tube, Varian Associates makes three conventional assumptions used in such feasibility estimates:

(a) No interface problems occur between man and tube; all human elements are completely reliable.

(b) None of the anticipated failure modes and estimated failure rates include system-induced failures or unnecessary removals from socket. All failure rates described are attributable only to the klystron.

(c) Since there have not yet been any failures on the VA-922, the failure modes were derived from the VA-856, relating the hazard rate for each failure reason to the VA-856 field failure experience. The accuracy of the failure rates for the VA-856 is based on reliable field information and we believe the prediction to be appropriately conservative. It is also consistent with failure mode proportions experienced with other tubes.

REPAIRABILITY

(a) Klystrons are typically repairable 3 to 4 times. The cost, to the user, for repair typically runs 50 to 60 percent of new tube unit cost (in comparable quantities).

(b) Repair tubes produce life directly comparable with new production units.

Source: "Broadband X-Band Klystrons for Advanced Low Noise Amplifier Klystrons," Varian Associates, 1967.

could be made available at the cost of $350,000 in additional R&D.

Additional R&D Cost

Nominal output power (8 GHz) = P_{max} = 630 KW

Operating output power (8 GHz) = P_o = 500 KW

Bandwidth at P_o = W = 300 MC

Intermodulation product ratio at P_o = I => 16 dB

It will also be assumed that the bandwidth can be doubled by utilizing two physically separate transmitters driven by the same driver TWT. The high power outputs of these transmitted will be radiated by separate feed horns utilizing the same antenna reflector.

1.6 Trends

The cost of tubes has decreased in the past few years and the efficiency has gone up largely due to the employment of computer in design of the electron gun. This technique has made electron gun operation more predictable and has extended the predictability to account for higher order effects. Coupled with the time-acquired experience in fabrication, this has led to more reliable, efficient designs for the entire tube. As the quantity, of a particular type or design, increases and as operating experience pinpoints design or fabrication weaknesses, costs tend to decrease. It has been estimated that costs of the very high power types could be expected to decrease between 30 and 50 per cent for quantities in the order of hundreds.

1.7 Transmitter Costs

The cost of output power amplifiers has been shown to be approximately as follows:

$$\text{Cost} = 25P^{0.63}$$

As pointed out by Feldman,* the output power amplifier "is only one of the

---

* N. E. Feldman, "High Power Microwave Transmitters," Appendix C to "A Study of Passive Communication Satellites," S. H. Reiger, Rand Corp. R-415-NASA, Feb. 1963.

many expensive items in a transmitter." Aside from the D.C. power supply and the cost of prime power which are considered later in this report, other basic items comprising a typical transmitter procurement are: (1) magnet, (2) heat exchanger, (3) dummy load, (4) remote control panel, (5) exciter, (6) racks and other structural elements, (7) instruction manuals, sketches and manufacturing drawings, and (8) assembly and integration costs.

Transmitter design and fabrication costs are likely to have large variations which are primarily dependent on application, e.g., commercial, military or experimental use. The only direct way of determining costs would be to define a specific application and then design transmitters with varying power levels to meet that application. Even if available, use of historical data from different laboratories would usually lead to erroneous results because of different design applications. The approach taken in estimating transmitter costs is to use a cost allocation method which groups all elements into approximately equal cost groups and then relate these groups directly to the cost of a power amplifier. The accuracy of this approach is admittedly coarse but appears to provide reasonably accurate indications of the costs for the major elements of high power transmitters. The major elements and assumed relationships are shown in Table 5. The cost of a transmitter, not including the D.C. power supply can be taken to be:

$$\text{Cost} = 100P^{0.63}$$

A preliminary analysis of possible variance in this equation has shown that the constant may vary from 10 to 880 and the exponent from 0.8 to 0.5 in respective order, i.e., the higher constant is associated with the smaller exponent. An example of the possible range of variation is shown in Figure 3. A one megawatt transmitter is likely to cost between 600 and 900 thousand dollars.

Table 5

Transmitter Costs
(Not Including D.C. Power Supply)

Major Transmitter Elements	% of Total Cost	Cost Equation
Power Amplifier	25	$C = 25P^{0.63}$
Magnet, Heat Exchanger, Dummy Load and associated waveguide parts	25	$C = 25P^{0.63}$
Exciter, Remote Control Panel, Racks and other structural members	25	$C = 25P^{0.63}$
Instruction Manuals, Sketches and Manufacturing Drawings	25	$C = 25P^{0.63}$
Transmitter	100	$C = 100P^{0.63}$

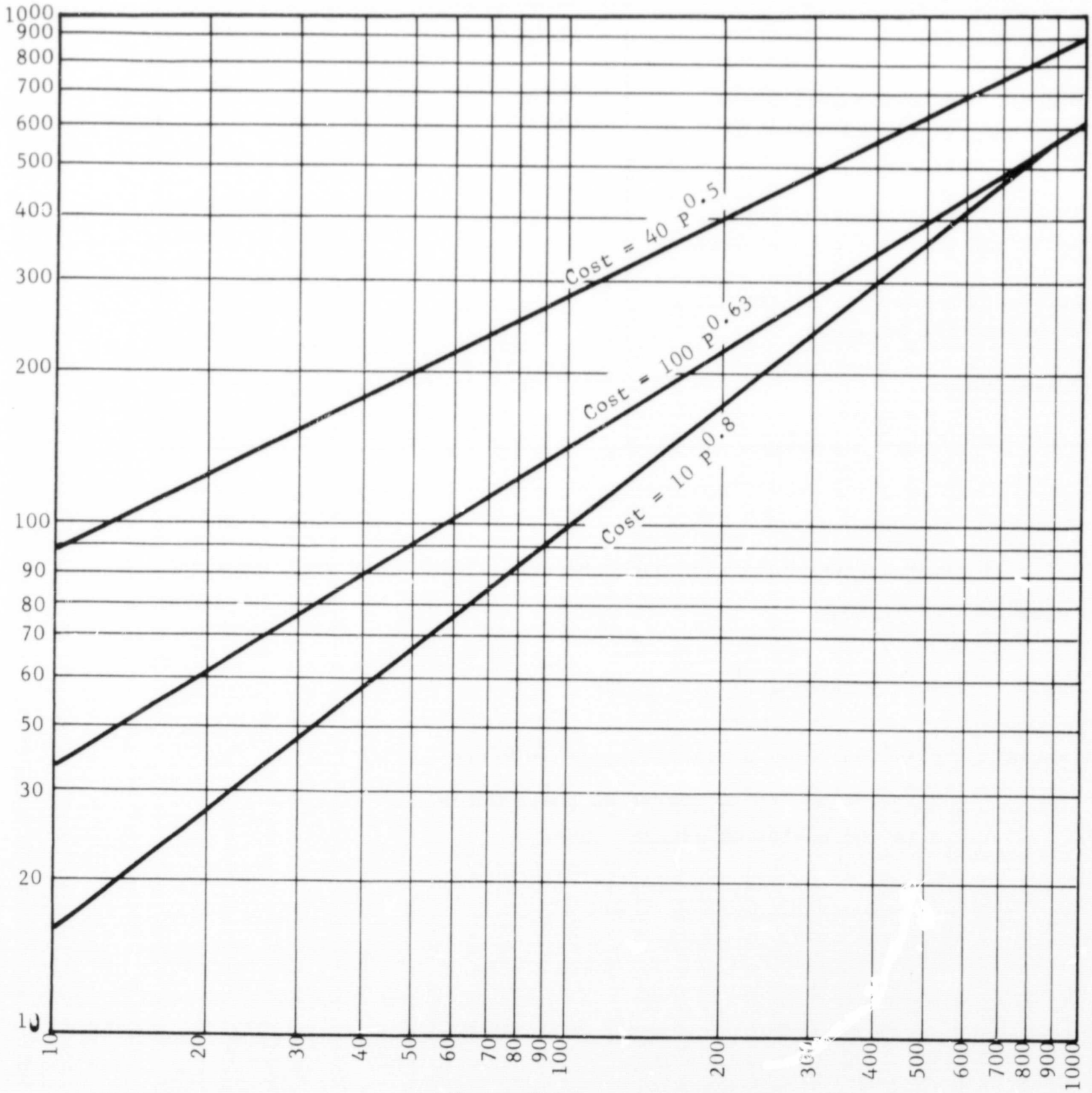
If several power tubes are used in parallel the cost would then be expressed as follows:

$$\text{Cost} = 75(m+k)\left(\frac{P}{k}\right)^{0.63} + 25P^{0.63}$$

where P is the total delivered power in watts

k is the number of operating power tubes.

m is the number of standby tubes



Note: (Cost of D.C. Power Supplies are not included.)

Figure 3. Possible Cost Equations of Transmitter Power Output

2.0 Direct Current High-Power Power Supplies

2.1 Electrical Characteristics

In high power D.C. supplies, rectifier cells are used in series and parallel combinations to achieve desired capacity. In general, high power rectifiers are almost completely solid state. Each cell has R-C networks to limit peak surges and assure correct voltage distribution among cells. The reactance is usually built into the transformer to provide for peak current protection. There are no apparent maximum current limitations in a practical design. However, voltage limitations exist and are generally associated with the external circuit-corona problems. Efficiency of a rectifier-transformer combination is generally about 90 percent. Additionally 5 percent is lost in primary control giving an overall efficiency of approximately 85 percent.

2.2 Mechanical Characteristics

Rectifier units are constructed both dry and oil filled. Dry types are generally used below approximately 25 KV, oil filled are used above. Water cooling of oil filled types is sometimes employed. Where high reliability is required, double walled water tubes with conducting fins between the walls are used to assure that water leakage from tube will not contaminate the oil. The transformer rectifier is generally contained within a single enclosure. If a bleeder is used, it is also in the same enclosure, as are any chokes or capacitors. Standard rectifier stacks are used for economy and mechanical flexibility and are placed in series or parallel to get the desire capacity.

2.3 Reliability

In general, D.C. power supplies are built with access plates to allow removal of the rectifier assembly for maintenance. Sufficient safety factors are allowed - usually 2 to 2-1/2 times above limiting rating-- to assure long life. Because of these allowances, there are usually an excess (above nominal rating) number of rectifier cells in series. If a cell fails, it fails in the short circuit condition. If it were to fail in the open condition, the full secondary voltage would appear across it and cause it to short. The excess number of cells allows the supply to continue uninterrupted operation. Therefore, catastrophic failures are practically unknown. There is no simple method of determining if one or more cells have failed. The rectifier assembly must be removed and each individual cell checked. It will be assumed that with proper maintenance a mean time to failure at 90 percent C.L. will be approximately 44000 hours or 5 years.

2.4 Regulation

Unless very tight, high speed regulation is required, normal regulation is usually provided by means of servo-driven Variac or Powertrol (variable auto transformer) type on the primary side. Because of mechanical operation, the rate at which voltage correction takes place is in the order of 1 to 5 seconds. Regulation of this type covers the 2 to 10 percent range. If the output voltage must be varied, an overriding arrangement is provided on the variable transformer control. Output voltage variations in excess of 2 to 1 become expensive, and physically large.

Regulation requirements at less than 50 percent load also increase costs, and at less than 10 percent load usually require a bleeder and possibly, to account for bleeder loss, increased ratings of transformer and/or rectifiers. In addition, size and cooling requirements are increased.

SCR (silicon controlled rectifier) power control is not widely used for two reasons; first, power handling capacities may not be available, and second, they increase the output ripple problem.

Where tight regulation or fast transient response are required, hard tube secondary regulation can be provided. The arrangement used is the familiar series pass tube. This arrangement requires very large tubes and reduces efficiency appreciably besides increasing size, weight, cooling requirements, and costs, and decreasing reliability and life.

2.5 Total Cost of Transmitter Power

The total cost of obtaining very high power at microwave frequencies must consider the cost of the transmitter, the D.C. power supply with control equipment and the cost of prime power. The capital investment cost of the D.C. power supply plus controls is estimated to vary with power in

approximately the same manner as the power amplifier. This is partially supported by the data shown in Table 5. Using this assumption the total investment cost of a transmitter will be:

$$\text{Cost in Dollars} = 125P^{0.63}$$

where P is the transmit power in watts.

2.6 Prime Power

The preferred prime power source is 3 phase at 480V for lower power (approximately 25 KW or less) supplies and 4160V for the higher power supplies. The secondary arrangement is sometimes arranged for 6 phase rectification. This reduces ripple, stored-energy in filters, and--for a given output ripple--may allow size reduction.

The power required by the transmitter can be roughly computed as follows:

Power tube efficiency	39%
Power supply efficiency	85%
Combined efficiency	33%

Required prime power for 500 KW rf output $\approx$ 1.5 megawatts

Table 5

Power	Voltage	Type	Description	Price
400 KW	20 KV	Dry Type	Full magnetic primary control, secondary filter approx. 5'x8'x7' high est. wt. 10,000 lbs	$40,000 *
400 KW	40 KV			$50,000 est.
65 KW	180 KV	Oil filled water cooled	Less primary switch-gear--tank size 40" x 50" x 82"--add ¼ to ½ for estimated primary switch gear volumes. This package was de-signed for minimum volume	
1,100 KW	32 KV	Oil filled	Including 50 Mfd of output-filter & 50% output volrage control -add 15% to 20% to cost for full output control	$85,000 *
45 KW	180 KV	Oil filled	Convection cooled	Little difference in price for this change in output current (250 Ma to 350 Ma)
63 KW	180 KV	Oil filled	Water cooling necessary to dissipate bleeder heat	

* Since high power units of this type are not built in large quantities and each requirement is slightly different, each design is generally a custom design and price includes some engineering costs. The maximum production run for power supplies of this type built by Energy Systems, Inc., to date is approximately 20.

3.0 Summary

On the basis of data presented in this technical note, the following limiting characteristics will be assumed in our studies for a high power transmitter.

Operating frequency - 8 GHz

Modulation bandwidth - 300 MHz

Rated output power - 625 KW

Operating output power - 500 KW

Signal to distortion rate > 16 dB

Tube mean time to failure at 90% C.L. - 20400 hours

$\approx$ 2.3 years of continuous operation

Power tube cost in dollars $\approx 25P^{0.63}$ (P in watts)

M.T.T.F. of transmitter (except power tube) at 90% C.L. $\approx$ 44000 hours

$\approx$ 5 years

Prime power required $\approx$ 1.5 megawatts

Total cost of a complete power subsystem (supply and transmitter)

$$C = 75(m+k)\left(\frac{P}{k}\right)^{0.63} + 50P^{0.63}$$

where k is the number of operating power tubes

m is the number of standby power tubes.

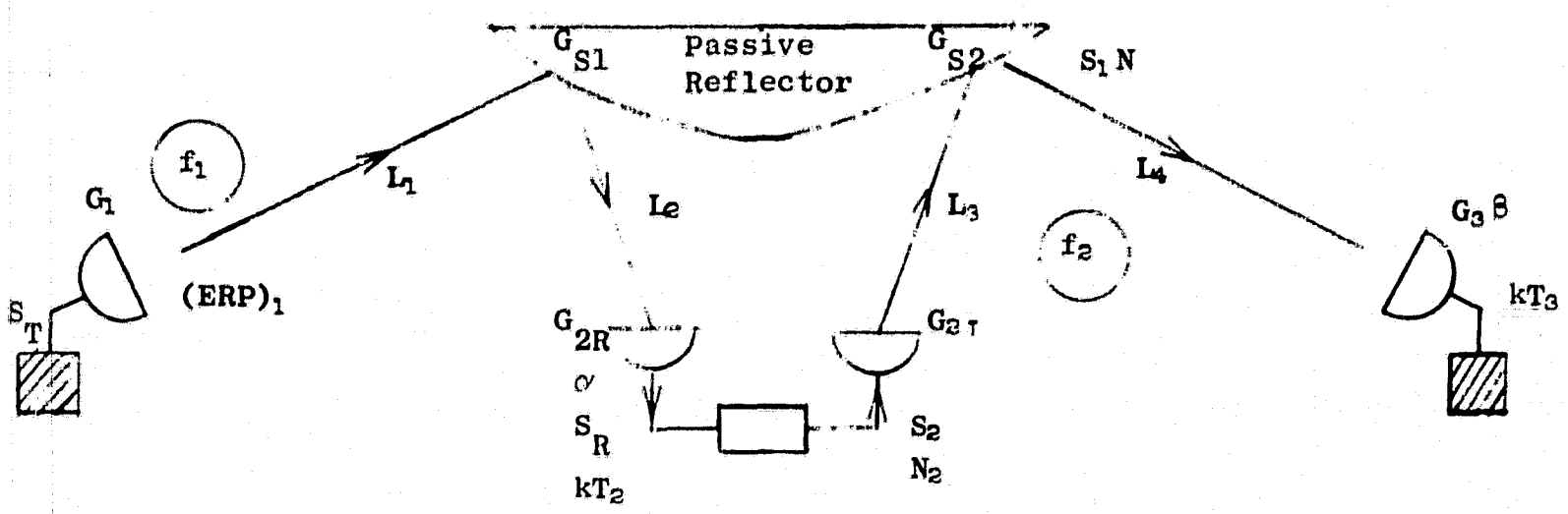
APPENDIX I

DERIVATION OF EXPRESSION FOR THE SYSTEM GAIN OF A DOUBLE-HOP PASSIVE SATELLITE SYSTEM

DERIVATION OF EXPRESSION FOR THE SYSTEM GAIN OF A DOUBLE-HOP PASSIVE SATELLITE SYSTEM (B1)

The configuration of the system under study is shown in Fig. 1. It is assumed that repeater R2 is linear.

Fig. 1



Transmitter R1 — Repeater R2 — Receiver R3

G represents antenna gains

L represents free space losses

S represents transmitter power output

S_R represents received power

N represents noise per cycle

α, β represent miscellaneous losses (margins, equipment, etc.)

R = required carrier to noise density ratio

$$R = \frac{S}{N + \frac{kT_3 L_4 \beta}{G_3}}$$

Referred to satellite output ..... (1)

$$R = \frac{S_2}{N_2 + \frac{kT_3 L_4 \beta L_3}{G_3 G_{S2} G_{2T}}}$$ Referred to transmitter output of R2 ..... (2)

but $$N_2 = kT_2 \frac{S_2}{S_R}$$ ..... (3)

and $$S_R = \frac{(ERP)_1 . G_{S1} . G_{2R}}{L_1 L_2 \alpha}$$ ..... (4)

$$\therefore \quad N_2 = k \frac{T_2}{G_{2R}} \frac{S_2 L_1 L_2 \alpha}{(ERP)_1 . G_{S1}}$$ ..... (5)

From (2)

$$\frac{1}{R} = \frac{N_2}{S_2} + \frac{kT_3 L_3 L_4 \beta}{S_2 G_{2T} G_{S2} G_3}$$ ..... (6)

Substituting (5) into (6)

$$\frac{1}{R} = \left[\frac{kL_1 L_2 \alpha T_2}{(ERP)_1 G_{S1} G_{2R}} + \frac{kL_3 L_4 \beta T_3}{S_2 G_{S2} G_{2T} G_3}\right]$$ ..... (7)

Define

$$x = \frac{G_{2R}}{G_{2T}} \text{ and } y = \frac{G_{S1}}{G_{S2}}$$ ..... (8)

Then

$$G_{2T} . G_{S2} = R\left[\frac{kL_1 L_2 \alpha T_2}{(ERP)_1 \; xy} + \frac{kL_3 L_4 \beta T_3}{S_2 G_3}\right]$$ ..... (9)

or $$G_{2R} . G_{S1} = R\left[\frac{kL_1 L_2 \alpha T_2}{(ERP)_1} + \frac{kL_3 L_4 \beta T_3}{S_2 G_3} \; xy\right]$$ ..... (10)

Let $$a_1 = k \frac{T_3}{G_3} L_3 L_4 \beta xy$$ ..... (11)

$$a_2 = k \frac{T_2 \alpha L_1 L_e}{(ERP)_1} \qquad \text{..... (12)}$$

$$Z = G_{2R} \cdot G_{S1}$$

From (10)

$$Z = G_{2R} \cdot G_{S1} = R\left[a_2 + \frac{a_1}{S_2}\right] \qquad \text{..... (13)}$$

Now, the total transmitted power per access is equal to

$$P_A = S_2 + N_2 B \qquad \text{..... (14)}$$

B = Receiver Bandwidth

and $$N_2 = kT_2 \frac{S_2}{S_R} \qquad \text{..... (15)}$$

and $$S_R = \frac{(ERP)_1 . G_{S1} . G_{2R}}{L_1 L_e \alpha} \qquad \text{..... (16)}$$

Combining (14), (15) and (16)

$$P_A = S_2\left[1 + \frac{kT_2 B L_1 L_e \alpha}{(ERP)_1 G_{S1} . G_{2R}}\right] \qquad \text{..... (17)}$$

or $$S_2 = \frac{P_A}{1 + \frac{kT_2 B L_1 L_2 \alpha}{(ERP)_1} \cdot \frac{1}{G_{S1} . G_{2R}}} \qquad \text{..... (18)}$$

Using (12)

$$S_2 = \frac{P_A}{1 + \left(a_2 B \cdot \frac{1}{Z}\right)} \qquad \text{..... (19)}$$

Substituting (19) into (13)

$$Z = R\left[a_2 + \frac{a_1\left(1 + a_2 B.\frac{1}{Z}\right)}{P_A}\right] \qquad \text{..... (20)}$$

Rearranging

$$Z = R\left[a_2 + \frac{a_1}{P_A} + \frac{a_1 a_2 B}{Z P_A}\right]$$

$$Z^2 - ZR\left[a_2 + \frac{a_1}{P_A}\right] - \frac{R\, a_1 a_2 B}{P_A} = 0 \qquad \text{..... (21)}$$

Solving Equation (20) for Z

$$Z = G_{2R}.G_{S1} = \frac{R}{2}\left[a_2 + \frac{a_1}{P_A}\right] + \sqrt{\left[\frac{R}{2}\left(a_2+\frac{a_1}{P_A}\right)\right]^2 + \frac{Ra_1 a_2 B}{P_A}} \qquad \text{..... (22)}$$

$$Z = G_{2R}.G_{S1} = R\left[\frac{1}{2}\left(a_2 + \frac{a_1}{P_A}\right) + \sqrt{\left[\frac{1}{2}\left(a_2+\frac{a_1}{P_A}\right)\right]^2 + \frac{a_1 a_2 B}{R.P_A}}\right] \qquad \text{..... (23)}$$

Since the expression under the square root is always greater than $\frac{1}{2}(a_2+\frac{a_1}{P_A})$, the solution of equation (21) involving the negative sign in front of the square root is disregarded, since it would result in a negative answer.

Equation (22) determines the value of the product of passive reflector gain (G_{S1}) and receiving antenna gain (G_{2R}) of the repeater station which is required to meet the performance requirement R. This value is dependent upon the transmitted power per channel (P_A) and upon transmission constants and equipment characteristics described by constants a_1 and a_2.

If the value of Z is known, (P_A) can be calculated by rearranging Eq. (20) as follows

$$P_A = \frac{Ra_1(Z+a_2 B)}{Z(Z-Ra_2)} \qquad \text{..... (24)}$$

Calculation of constants for the case of stationary satellite (operating frequencies 8 GC and 7.25 GC):

$$a_1 = k \frac{T_3}{G_3} L_3 L_4 \beta xy$$

k = Boltzman's constant = 1.38×10^{-23} = -228.6 dB

L = free space loss = $\left(\frac{4\pi df}{c}\right)^2$

d = slant range to satellite (miles)

c = speed of light (miles/sec.)

$$a_1 = 1.38 \times 10^{-23} \left(\frac{4\pi}{c}\right)^4 (d_3 d_4)^2 \ (f_2)^4 \ \beta \cdot x \cdot y \cdot \frac{T_3}{G_3}$$

$$a_1 = 0.28753 \times 10^{-3} (d_3 d_4)^2 \ f_2^4 \ \beta xy \ \frac{T_3}{G_3}$$

where d's are expressed in miles

f's are expressed in gigahertz

For stationary satellite orbit of d = 22300 miles, we can assume $d_3 = d_4$

$$a_1 = 7.1101 \times 10^{13} \ f_2^4 \ \beta.x.y \ \frac{T_3}{G_3} \qquad \ldots\ldots\ldots\ldots\ldots \qquad (25)$$

If f_2 = 7.25 GC

$$a_1 = 1.9645 \times 10^{17} \beta xy \frac{T_3}{G_3} \qquad \ldots\ldots\ldots\ldots\ldots \qquad (26)$$

or in dB

$$a_1 = 172.93 + \beta_{dB} + x_{dB} + y_{dB} - \left(\frac{G_3}{T_3}\right)_{db} \qquad \ldots\ldots\ldots\ldots\ldots \qquad (27)$$

$$a_2 = kL_1 L_2 \alpha \frac{T_2}{(ERP)_1}$$

$$= 1.38 \times 10^{-23} \cdot \left(\frac{4\pi}{c}\right)^4 (d_1 . d_2)^2 f_1^4 \alpha \frac{T_2}{(ERP)_1}$$

$$= 0.28753 \cdot 10^{-3} (d_1 . d_2)^2 f_1^4 \alpha \frac{T_2}{(ERP)_1} \quad \ldots\ldots\ldots\ldots \quad (28)$$

For stationary orbit $d = d_1 = d_2 = 22{,}300$ miles

$$a_2 = 7.1101 \times 10^{13} f_1^4 \cdot \alpha \cdot \frac{T_2}{(ERP)_1} \quad \ldots\ldots\ldots\ldots \quad (29)$$

If $f_1 = 8$ GC

$$a_2 = 2.9125 \times 10^{17} \alpha \frac{T_2}{(ERP)_1} \quad \ldots\ldots\ldots\ldots \quad (30)$$

or in dB

$$(a_2)\text{dB} = 174.64 + \alpha \text{ dB} + (T_2) \text{ dB} - (ERP)_1 \text{ dB} \quad \ldots\ldots\ldots\ldots \quad (31)$$

Therefore for stationary orbit and $f_1 = 8$ GC and $f_2 = 7.25$ GC

$$a_1 . a_2 = 5.721 \times 10^{34} \alpha\beta xy \frac{T_3}{G_3} \cdot \frac{T_2}{(ERP)_1} \quad \ldots\ldots\ldots\ldots \quad (32)$$

or in dB

$$(a_1 a_2)\text{dB} = 347.57 + \alpha \text{ dB} + \beta \text{ dB} + x \text{ dB} + y \text{ dB} + (T_2)\text{dB} - \left(\frac{G_3}{T_3}\right)\text{dB} - (ERP)_1 \text{ dB}$$

$$\ldots\ldots\ldots\ldots \quad (33)$$

To yield a physical meaning to these equations, consider one side of the link of the double-hop.

If the transmitter transmits a power S_T in the direction of the satellite, the power per unit area at the range of the satellite L_1 can be given as:

$$\frac{S_T}{A_1}$$

If the satellite occupies an area of space given by A_{S1} then it intercepts a portion of the power transmitted. This is given by:

$$\frac{S_T}{A_{S1}} \cdot A_{S2} = S_i \text{ (power intercepted)}$$

If it is assumed that this reflector has a reflection coefficient very near unity (a reasonable assumption), then the power reflected is equal to the power incident. This reflected power is confined in a cone of apex angle θ_S where θ_S is determined by the satellite (reflector) geometry.

The power per unit area back at the Earth, assuming the satellite is directed toward the Earth, is thus

$$\frac{S_i}{A_2}$$

If the receive antenna occupies an area given by A_a and is directed toward the satellite, then the power received is

$$S_R = \frac{S_i}{A_2} A_a$$

or, substituting for S_i

$$S_R = S_T \frac{A_S A_a}{A_1 A_2}$$

From the figure it is easily seen that

$$A_1 = \frac{\pi R_1^2 \theta_T^2}{4} \quad (\theta \text{ is in radians})$$

$$A_S = \frac{\pi D_S^2}{4}$$

$$A_2 = \frac{\pi R_2^2 \theta_S^2}{4} \qquad (\theta \text{ is in radians})$$

$$A_a = \frac{\pi D_R^2}{4}$$

Substituting

$$S_R = S_T \frac{D_S^2 D_R^2}{R_1^2 R_2^2 \theta_T^2 \theta_S^2}$$

So far it has been assumed that each antenna is 100 percent efficient. If this is not true, then

$$S_R = \frac{S_T D_S^2 D_R^2 \eta_T \eta_R}{R_1^2 R_2^2 \theta_T^2 \theta_S^2}$$

where η_T and η_R are the transmit and receive antenna efficiencies respectively.

If it is assumed that the noise-power received is primarily due to the receiver, then

$$N_R = KT_2 B$$

where

N_R = noise power received

T_2 = noise temperature of receiver in degrees Kelvin

K = Boltzman's constant

B = Receiver bandwidth

Thus, the signal-to-noise ratio at the input of the receiver is given as

$$\frac{S_R}{N_R} = \frac{S_T D_S^2 D_R^2 \eta_T \eta_R}{R_1^2 R_2^2 \theta_T^2 \theta_S^2 KT_2 B}$$

To show that the above is equivalent to the equations used in this report is easily done

$$\frac{S_R}{N_R} = S_T + G_1 - L_1 + G_{S1} - L_2 + G_{2R} - KT_2 B \quad [\text{in dB}]$$

or

$$\frac{S_R}{N_R} = \frac{S_T G_1 G_{S1} G_{2R}}{L_1 L_2 KT_2 B}$$

where

$$L = \left[\frac{4\pi R}{\lambda}\right]^2 = \text{the path loss between isotropic antennas}$$

$$G_T = \eta_T \frac{4\pi A_T}{\lambda 2} = \eta T \frac{\pi^2 D_T^2}{\lambda 2} = \frac{4\pi}{\theta_T^2} \eta_T \quad (\theta \text{ in radians})$$

= power gain due to directivity with respect to isotropic.

It should be noted that in using the last portion of the above definition, it is assumed that the antenna beamwidth is square. If a circular beamwidth is considered as usually is the case

$$G_T = \eta_T \frac{4\pi}{\theta_T^2} \cdot \frac{4}{\pi} = \eta_T \frac{16}{\theta_T^2}$$

$$G_R = \eta_R \frac{\pi^2 D_R^2}{\lambda^2} \quad \text{(receive antenna power gain)}$$

G_s = satellite gain = $\left[G_{S1}\right]\left[G_{S2}\right]$

The satellite gain can be broken up into a receive gain, G_{S1}, and a transmit gain, G_{S2}, where

$$G_{S1} = \frac{\pi^2 D_S^2}{\lambda^2}$$

$$G_{S2} = \frac{4\pi}{\theta_S^2} \quad \text{but, as before, for a circular beam}$$

$$G_{S2} = \frac{16}{\theta_S^2}$$

Substituting these definitions into the equation for the signal-to-noise ratio

$$\frac{S_R}{N_R} = \frac{S_T \left[\eta_T \frac{16}{\theta_T^2}\right] \left[\frac{\pi^2 D_S^2}{\lambda^2} \cdot \frac{16}{\theta_S^2}\right] \left[\eta_R \frac{\pi^2 D_R^2}{\lambda^2}\right]}{\frac{4\pi R_1}{\lambda}^2 \quad \frac{4\pi R_2}{\lambda}^2, \quad K T_2 B}$$

or,

$$\frac{S_R}{N_R} = \frac{S_T\ D_S^{\,2}\ D_R^{\,2}\ \eta_T\ \eta_R}{R_1^{\,2}\ R_2^{\,2}\ \theta_T^{\,2}\ \theta_S^{\,2}\ KT_2\ B}$$

From the reflection characteristics of the saddle satellite and the expression for satellite gain derived above

$$G_S = G_{S1}\ G_{S2}$$

$$G_S = \frac{\pi^2\ D_S^{\,2}}{\lambda^2} \quad \frac{16}{\theta_S^{\,2}}$$

for the saddle the reflection geometry is such that

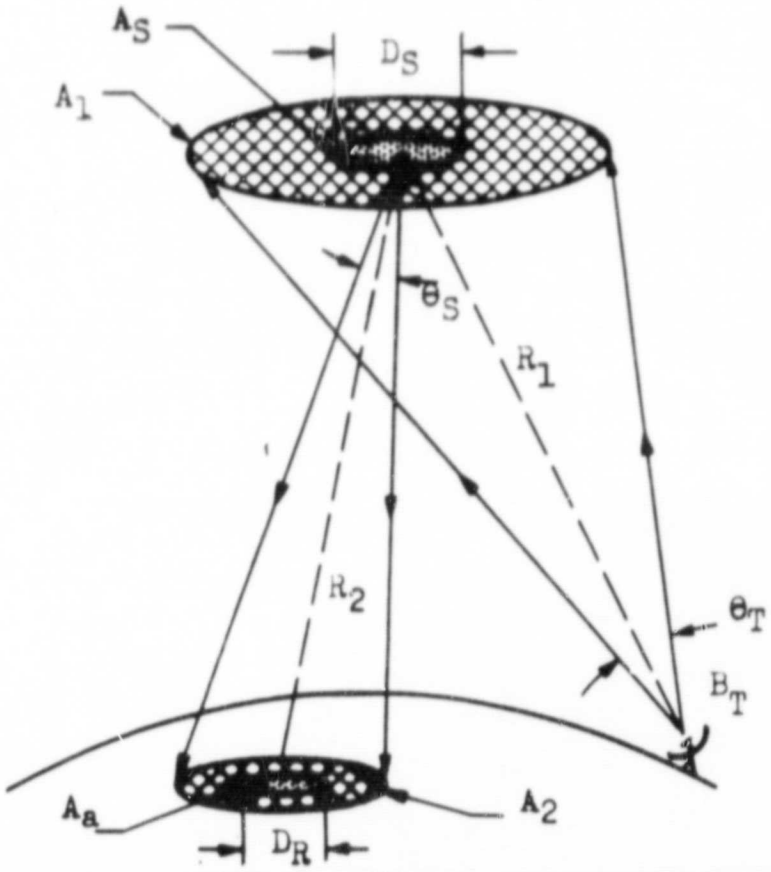
$$\theta_S = \frac{2\ D_S}{\rho}$$

where ρ is the radius of curvature of the satellite

Thus,

$$G_S = \frac{\pi^2\ D_S^{\,2}}{\lambda 2} \quad \frac{16\ \rho^2}{4D_2^{\,2}}$$

$$G_S = \frac{4\pi^2\ \rho 2}{\lambda^2}$$



Link Calculation (Master Terminal to ST-1)

D_S	325 ft
D_R	6 ft (ST-1)
η_R	.55
θ_T	$.775 \times 10^{-3}$ radians
η_T	.60
θ_S	.0174 radians (1°)
R_1 (worst case)	22,300 n.mi.
R_2 (worst case)	22,300 n.mi.
T_2	315° K (ST-1)
B	30 KHz
K	1.38×10^{-23} joules/^{o}K
S_R/N_R (Receiver Threshold)	7.1 dB
S_T (Minimum required)	30 watts
Margin	~ 3 dB
S_T (per voice channel)	60 watts

APPENDIX J

POTENTIAL ACTIVE SATELLITE IMPROVEMENT AREAS

POTENTIAL ACTIVE SATELLITE IMPROVEMENT AREAS

General

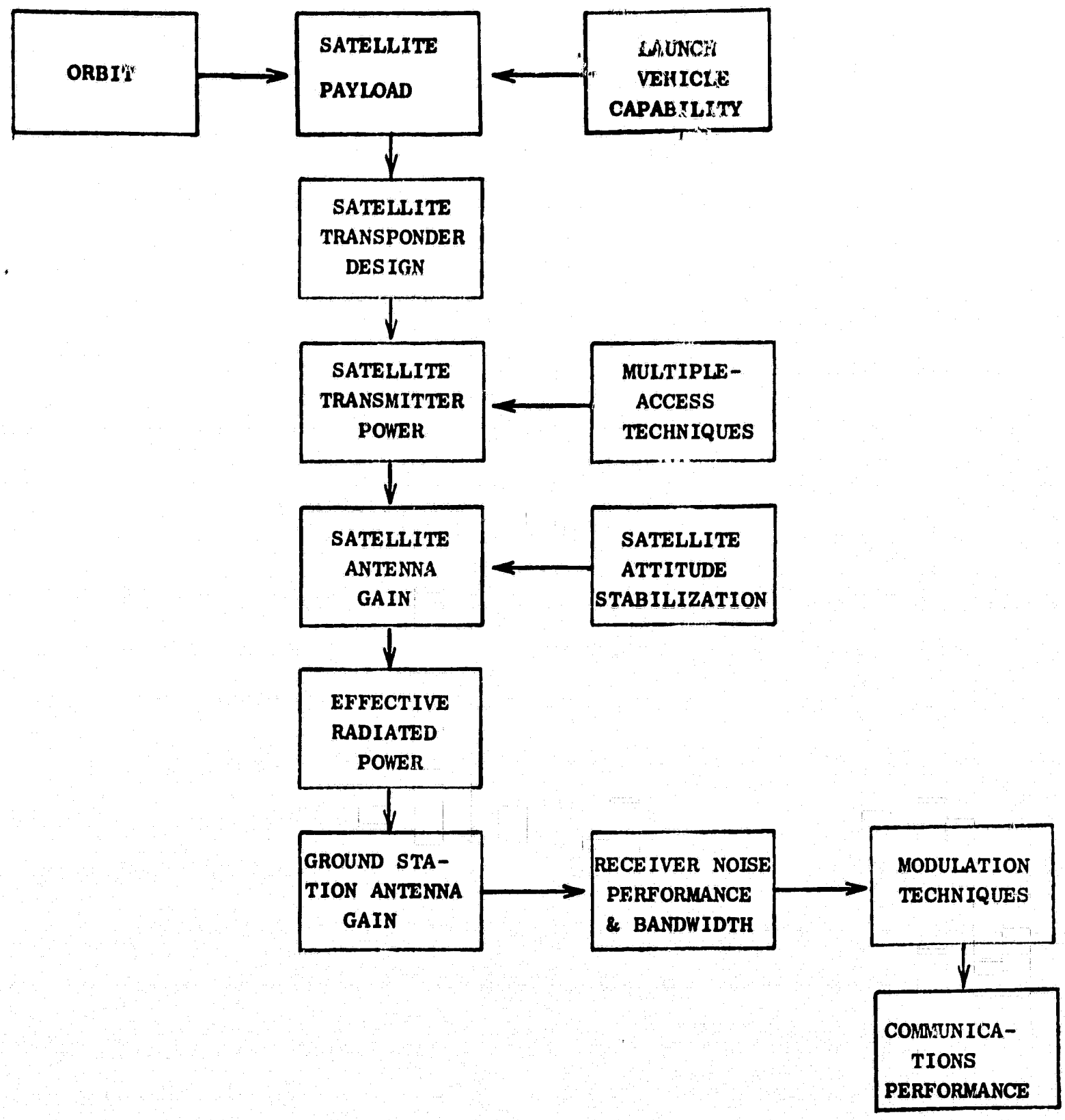
For the immediate future, the capacity of communications satellites will be limited by the amount of power they can radiate toward the earth. This so called "down-link" limitation is largely due to the economic cost of orbiting high power transmitters in space, with their attendant large and heavy spacecraft structures and solar power supplies. However, the ability to orbit large steerable antennas (preferably with multiple beams) will ease this transmitter power problem and permit a much higher ERP through the passive antenna gain. At this point satellite capacity will probably become limited more by repeater instantaneous bandwidth than power.

Thus, three prime areas for future satellite communication improvement exist: (1) satellite transponder design, (2) satellite transmitter power output device, and (3) satellite antenna gain. The critical items for down-link performance are shown in Fig. 1. Actually, of course, the total system performance must be looked at for an optimized solution since down-link performance reflects back on up-link performance in terms of many of the same type of parameters shown in Fig. 1; e.g., the satellite ERP and the satellite front end noise temperature are inversely proportional given a fixed allowable up-link noise contribution.

The above selection of critical areas depends on several assumptions: (1) frequency allocations will be such that available bandwidth will be no limitation, (2) the ability to economically produce d.c. power up to several kilowatts will exist, and (3) the cost and technical capability of producing ERP on the ground will be such that despite improved down-link performance, the up-link will not become limiting.

Figure 1.

SATELLITE DOWN-LINK COMMUNICATIONS PERFORMANCE



SOURCE: Stanford Research Institute

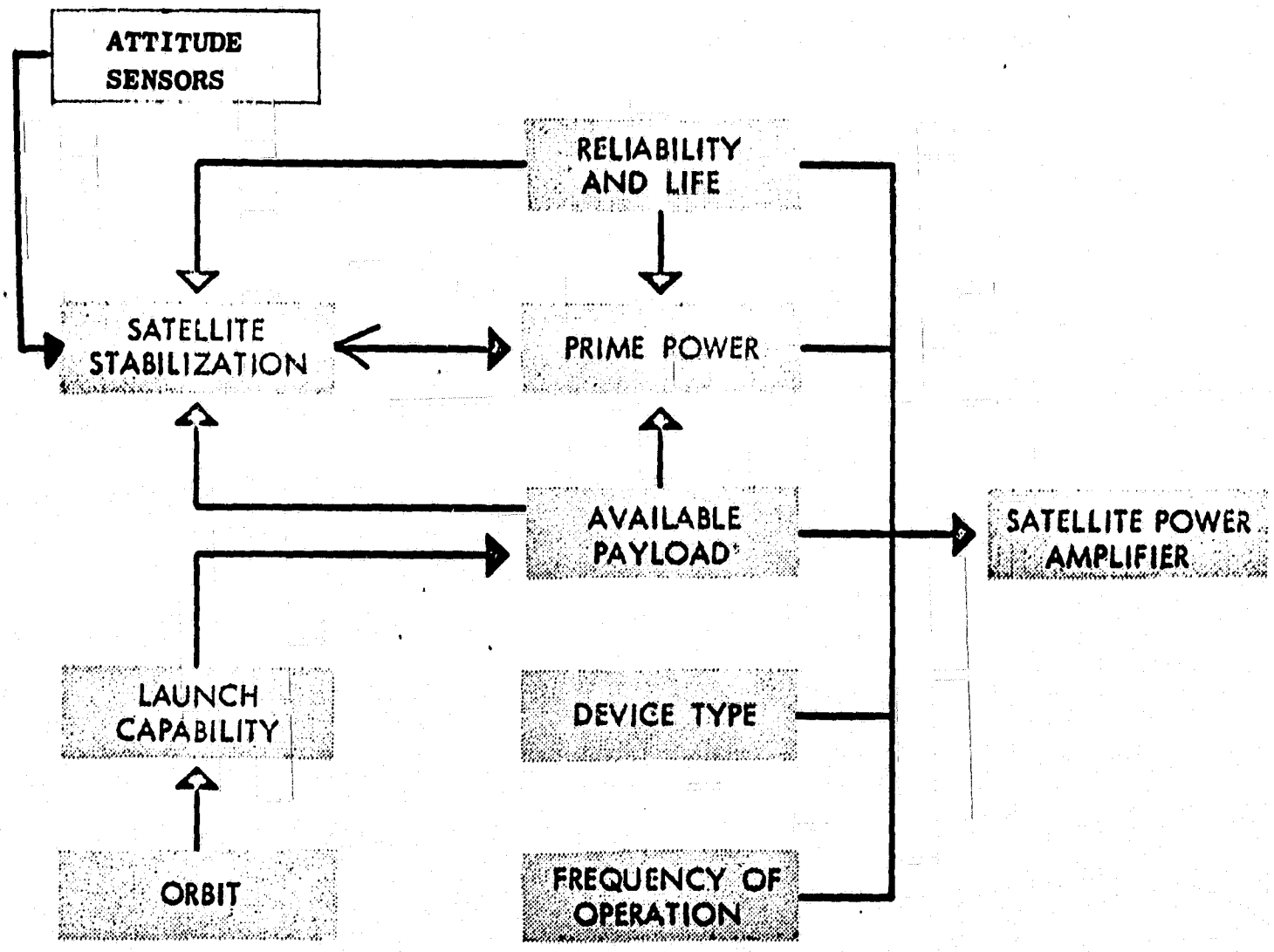
Improvement of a given down-link or satellite parameter is not a simple task that can be treated in isolation. Each relates to several other satellite or system design parameters, and improvement is usually related to improvement in these other parameters. In some cases, the steps necessary to achieve an improvement in one area may cause a decrease in capability in another area. For example, as in any system, an increase in performance may be achieved through an increase in equipment complexity that causes a decrease in system reliability. The implementation of such a system improvement depends on whether the system performance increase caused by the new capability is greater than the system performance decrease caused by the lower reliability. Such an analysis often is reduced to cost terms as a common denominator for decision purposes. Figures 2 and 3 show some of the interactions involved in considering the important parameters that hold promise for improving down-link performance through technological change. Obviously, there are interactions between the same parameter in the figures, so one cannot be considered separate from the other. There also are many second- and third-order interactions between elements that, while subtle, may influence the system design.

The Present Status

The basic spin-stabilized communication satellite design, so successfully demonstrated with Syncom in 1963, has now evolved through several design modifications to become the standard commercial communication satellite (Intelsat III) for use during the 1968-72 time period. Major design changes evolving during the transition from Syncom through Early Bird (Intelsat I) and Intelsat II, to Intelsat III include larger size, higher power amplifiers, and higher gain antennas. The pertinent parameters of these satellites are shown in Table I. As may be seen, both the power level of the final amplifier and the gain of the antenna have been increasing over the five-year period. With increased satellite size, higher RF

FIGURE 2

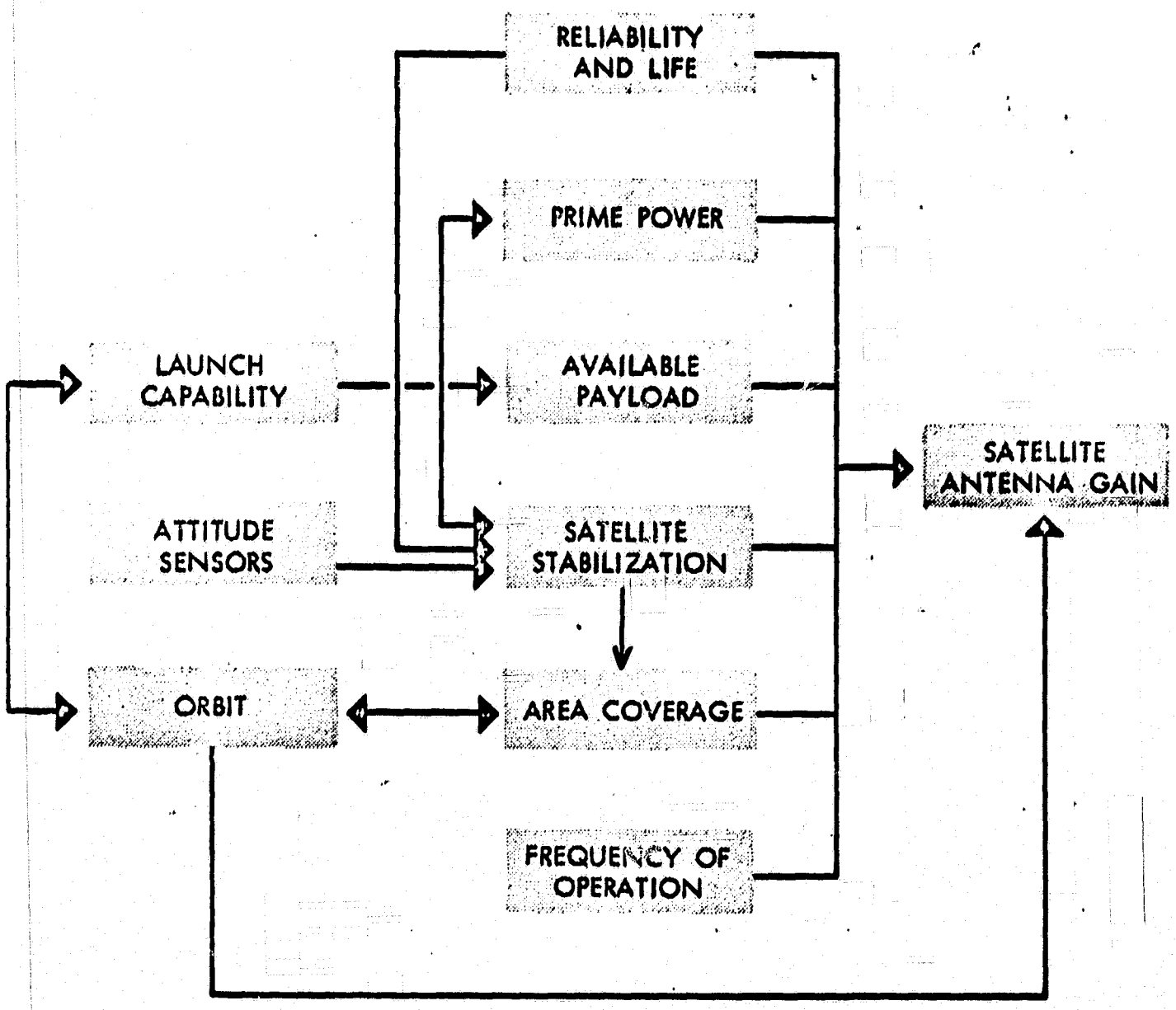
SATELLITE POWER AMPLIFIER INTERACTIONS



SOURCE: Stanford Research Institute.

FIGURE 3

SATELLITE ANTENNA GAIN INTERACTIONS



SOURCE: Stanford Research Institute.

Table I

DESIGN PARAMETERS FOR INTELSAT I, II, AND III

Parameter	SYNCOM	INTELSAT I (Early Bird)	INTELSAT II	INTELSAT III
SIZE				
Solar array diameter	72 cm	72 cm	142 cm	141 cm
Solar array length	40 cm	59 cm	67 cm	104 cm
WEIGHT				
At launch	66.5 kg	68 kg	175 kg	269 kg
Postapogee motor fire	35.4 kg	38.5 kg	87 kg	136 kg
COMMUNICATIONS				
Repeater	Two redundant, selectable, frequency translation repeaters, with bandwidths of a single 5 MC or 2 each 0.5 MC channel respectively	Two independent frequency translation repeaters, each with 25 MHz bandwidth	Two redundant linear repeaters, each with 126 MHz bandwidth	Two independent repeaters, each with 225 MHz bandwidth
Power amplifier	Two 2-watt TWT's, one operating and one spare	Two 6-watt TWT's, one operating and one spare	Four 6-watt TWT's; one, two, three, or four operating at one time	Two 10-watt TWT's, one in each band
Antenna	Receiver, omni; transmit, coaxial slot array; 25° beam-centered at equator	Receiver, omni; transmit, collinear slot array; 11° beam centered at $+7^{o}$ aspect angle	Receiver, omni; transmit, multiple-element biconical horn; 12° beam--entered at equator	
EIRP	9 dBW	10 dBW/repeater	14 dBW	22 dBW/repeater

Table I (cont'd)

Parameter	SYNCOM	INTELSAT I (Early Bird)	INTELSAT II	INTELSAT III
FREQUENCIES				
Up-link	7361, 7363 MHz	6301 ± 13 MHz, 6390 ± 13 MHz	6345 ± 63 MHz	Repeater I 5930 to 6155 MHz
Down-link	1815, 1814 MHz	4081 ± 13 MHz, 4161 ± 13 MHz	4120 ± 63 MHz	3705 to 3930 MHz Repeater II 6195 to 6420 MHz 3970 to 4195 MHz

SOURCE: Intelsat I, II, and III data from Robert C. Barthle and Robert D. Briskman, "Trends in Design of Communications Satellites Earth Stations." Microwave Journal, 10, (October, 1967) p. 28.

Syncom data from Syncom-Engineering Report, NASA Goddard Space Flight Center, Greenbelt, Md., NASA TR R-233; March 1966.

powers can be supported by the increased solar panel area available and with increased confidence in satellite attitude stabilization and attitude measurement, higher gain antennas may be used. For practical purposes, for for global communication systems, antenna beamwidth is limited to earth coverage plus some overlap for satellite attitude errors. Intelsat I has demonstrated the ability to "squint" the antenna off axis and limit the beam to less than earth coverage in a north-south direction. Up through Intelsat II all transmit beams had been donut shaped because of the spin stabilization of the vehicle. However, on Intelsat III a mechanically despun antenna will permit essentially earth coverage beamwidth.

Improvement Areas

Satellite Power Amplifier

At the present time, traveling wave tubes (TWT) are used almost exclusively for active communications satellites, and these range in RF power output from 2-10 w.* The advantages of the TWT are its broad bandwidth, relatively high efficiency, and long life. It has many of the disadvantages of electron beam devices, but by careful design, manufacturing, and testing, many of these have been minimized. TWTs produced by five different manufacturers have been flown in U.S. communications satellites to date. At the present time, the highest power TWT built specifically for space communications has a power output of 35 watts and is designed to operate in the 7-8 GHz range. Other tubes flown to date are designed for the 2-4 Gc/s range.

Other electron beam devices, such as the electrostatically focused klystron and amplitron, have been considered for satellite use, but the particular characteristics of the TWT, especially its wide bandwidth and

---

* All RF power outputs refer to saturated power.

demonstrated reliability, have made the TWT most popular.[1] Since bandwidth requirements tend to increase because of higher capacity and multiple-access operation, the requirement for TWTs will probably continue, even though other devices may have somewhat higher efficiencies. As the reliability of other devices is demonstrated and their characteristics are optimized for space applications, they will undoubtedly see more use. Solid state devices have also been given serious consideration for specific applications. Considerable work is now going on to extend the power-frequency curve of such devices and to advance the efficiency of operation, which, at powers and microwave frequencies currently in use for space communications, is considerably less than that of TWTs.[2] At the present time, the only satellite flying that uses an all solid state microwave repeater is the MIT/Lincoln Laboratory Lincoln experimental satellite (LES); however, LES is designed as a low power, limited bandwidth satellite to try out ideas for military systems. Quite a bit of work currently is under way at Lincoln Laboratories with considerable success in improving overall circuit efficiencies and adapting new devices as they become available.

On the basis of recent device and circuit advances, it is entirely possible that the next several years will produce solid state circuits with efficiencies approximately equal to present TWT/power supply efficiencies at microwave frequencies and with some potential increase in reliability and life. However, recent work on TWT designs promises substantial increases in efficiency in the next few years if sufficient effort is applied.[3,4] Tests have shown efficiencies over 50 percent

---

1 Comparison of Electrostatically Focused Klystrons, Helix Travelling Wave Tubes, and Amplitrons for Space Communication Applications, Litton Industries, Electron Tube Division, June 17, 1964.

2 N. E. Feldman, Communication Satellite Output Devices, Paper P-2997-1, The Rand Corporation, June 1965.

3 New Concepts for Achieving High Efficiency in Traveling Wave Tubes Contract DA 28-043AMC-00076(E), Watkins-Johnson Company, Palo Alto, California.

4 Applied Research on Efficiency Improvement in O Type TWTs, Contract AF-33(615)-1951, Hughes Aircraft Company, Culver City, California.

(measured at the input frequency and neglecting heater power) on a laboratory tube set-up.[1] As power increases, focusing problems become greater and weight increases. However, advances in magnetic materials and design techniques are improving this situation. Looking to the 1975 time frame, we can expect TWTs to continue to predominate in communications satellite design, but with the added capability of generating powers up to about 1,000 w with reliability and life comparable to designs in existence today, i.e., a $\geq$ 90 percent probability of 50,000-100,000 hours life. Both power efficiency and power output per pound will be considerably higher than possible today--perhaps reaching as high as 60 percent power efficiency, about twice the present capability.

Powers beyond 1000 watts are also possible and may be required for applications such as space broadcasting. Present CW TWTs have been built with power levels up to 12.5 KW at X-band.[2] Power levels beyond 1 KW greatly increase the problems discussed below, particularly heat removal and high voltage operation in space. Also cost becomes an important factor in both the tube and the associated power supply. It is always more costly to develop and produce a high power tube than a tube having much lower power but other similar characteristics. In most cases in the past where high power devices have been produced, quantities required have been sufficiently large to permit spreading the development cost and to result in a reduced production cost because of production economies. The situation will probably not be the same for a space designed tube. Unless other applications are found, only a limited number of tubes would be required and the cost would be proportionately higher. Based on discussions with various tube manufacturers. estimates of the

---

[1] New Concepts, op. cit.

[2] Microwave Tube Characteristics Tabulation, (Orange, New Jersey: Derivation and Tabulation Associates, Inc., November 1966 - April 1967.)

development and production costs of X-band TWTs are shown in Table II .

Despite the fact that a large number of high power TWTs have been produced for various applications, a number of significant problem areas exist in their design for space applications. It has generally been assumed that the limiting failure mode for a well designed and built TWT is cathode wear-out. To minimize this cathode current densities have been kept very low in space designed tubes. In higher power tubes, despite larger cathodes, the current densities generally run higher. However, tests run by cathode manufacturers on their high power cathodes in a diode configuration indicate lives in excess of 50,000 hours. However, it is now necessary to design these cathodes into tubes where great care has been taken to assure proper gun design with a potential barrier to prevent ion bombardment of the cathode and to minimize outgassing caused by heating due to beam interception in the interaction circuit.[1] In order to assure that appropriate life characteristics have been designed into these tubes, a fairly extensive life test program will be necessary. Because of the cost of the tubes, this type of program should be started as soon as possible in order to minimize the number of tubes put on test to achieve a given confidence of minimum life. However, it appears apparent that TWTs up to a kilowatt can be made available for space application with a minimum development and evaluation program. TWTs beyond 1 kilowatt will require further development work in terms of reliability and heat removal as well as associated problems such as high voltage operation in space.

---

1 John T. Mendel, "High-Powered Traveling-Wave Tubes for Space Transmitters," Communication Satellite Systems Technology, Richard B. Marsten (Ed.). (New York: Academic Press, 1966).

Table II

High Power TWT Development and
Production Cost Estimates

Power Range	Development Costs [a]	Production Cost/Tube [b]
35 - 100 watts	$250 K	$10 K
100 - 500 watts	450 K	15 K
500 - 1,000 watts	700 K	25 K
1,000 - 10,000 watts	2.0 M	75 K

a Only a very limited life test program is implied in these cost estimates (about 3 prototype tubes on indefinite life test). For a more stringent life test program of 20 tubes on indefinite life test assume an initial cost equal to 70% of the development cost plus 5% per year continuing cost.

b In production lots of 5 tubes, space qualified.

Satellite Antenna Gain

Experimental satellites to date have used antenna designs which result in a considerable amount of power being radiated into space. This is largely because spin stabilization has been used with antenna beams that radiate in a toroidal pattern with the earth intercepting only a small part of the beam. At synchronous altitudes, this results in a gain of from 6 to 8 dB. At the present time, designs have been completed for conical earth coverage antenna beams and have been flown on the NASA ATS program.[1] For spin-stabilized vehicles, these designs in essence form a narrow beam just encompassing the earth, with some spill-over for satellite attitude error. The beam is spun at the same rate but opposite to the satellite spin rate to maintain the beam pointing at the earth.[2] The spinning can be accomplished both mechanically and electrically. If other stabilization techniques are used, such as gravity-gradient stabilization, fixed antennas can be attached to the satellite body and designed with the appropriate beamwidth to intercept the earth. The degree of excess beamwidth required to compensate for satellite attitude instabilities depends on the stabilization technique used. It is quite small (1°-2°) for spin-stabilized vehicles that can be corrected in attitude (and largely dependent on the active attitude-sensing devices used in positioning the satellite), such as Intelsat III, but becomes larger for passive gravity-gradient-stabilized vehicles at synchronous altitudes that may have libration angles on the order of $\pm 3^{o}$.

There are a number of problems involved in any attempt to increase the gain of a satellite antenna resulting in beamwidths less than earth

---

1 Applications Technology Satellite-Experimental Communications System - Description and Requirements, GSFC-S11-012-00, Goddard Space Flight Center, February 28, 1965.

2 H. R. Erhardt and D. C. Mead, Advanced Syncom-Phased Array Antenna System, NASA Contract 5-2797, Hughes Aircraft Company, October 1963.

coverage. Some are technological and some are operational. A few of the subsystem interactions are shown in Fig. 3. Particularly important to the determination of satellite antenna gain are the factors of desired area coverage, orbital altitude and inclination, frequency of operation, and satellite-stabilization technique. As shown, there are many secondary interactions with other system parameters, all of which must be given careful consideration. Most of the operational problems evolve from the requirements for a given area of coverage. In those cases where communications satellites are used to span intercontinental or large continental distances, and single antenna beams are to be used, they must be wide enough to encompass both the transmit and receiver earth stations on any anticipated link in either a north-south or east-west direction. Some specialized beam shapes may be used, such as in Early Bird, where the antenna pattern is "squinted" to narrow it in the north-south direction such that areas of the Southern Hemisphere are excluded from the beam and the North Atlantic path is emphasized. However, the gain enhancements that can be achieved by this technique are relatively limited if long path lengths are required, such as in a true global system. Using multiple antenna feeds on a single high gain reflector, even if the reflector is stationary, is not a particularly easy task.

There are a number of techniques currently under investigation that would provide the capability of achieving very high antenna gains, e.g., > 35 dB. Conceptually, the simplest approach, of course, is to fly a large fixed or steerable antenna on the order of a 30-ft diameter parabola which would provide 49-dB gain at 4 Gc/s. However, with parabolic antennas, the generation of multiple beams, even with limited separation, is a difficult and complicated matter, and, at high gains, the beamwidth of a single beam is so narrow that only a limited distance on the earth would be encompassed within the beam. Also, it is obvious that such an antenna would have to be mounted on a very stable satellite or would have to move

counter to the satellite motion in order to prevent wide excursions of the illuminated area on the earth. NASA is currently considering such a development for the post 1970 time frame on the ATS F or G series, where a 30-ft parabolic antenna with steering capability would be erected after the satellite is injected into orbit. A 30-ft antenna would have considerable interest for applications like direct broadcasting and limited area, limited bandwidth telecommunications. It would appear to be somewhat limited in its application to international telecommunications because of the difficulty in forming multiple beams.

A more amenable approach for long-haul communications is one of the several designs suggested for electronically steerable antenna arrays.[1,2] These can be designed to meet the three prime antenna requirements for communication satellites:

1. High antenna gain.
2. Multiple, independent, simultaneous beams.
3. Antenna beam steering with "no mass" movement capable of compensating for satellite attitude movements or to cover different geographical areas.

The complexities involved in the erection and mechanical design of such antennas should be emphasized. The basic component design and device reliability problems are extremely severe as the gain and operating frequency of antenna arrays increase. However, considerable work has already been done to demonstrate the feasibility of techniques which, with further refinement and experimentation, could find application in the 1970s.[3,4,5]

---

1 D. L. Backus, "Electronically Steerable Antennas for Communication Satellites," IEEE International Convention Record, Vol. 13, Part 2, March 22-26, 1965.

2 L. J. Ricardi, Array Beam-Forming Networks, Technical Note 1965-12, MIT/Lincoln Laboratory, Lexington, Massachusetts, April 13, 1965.

3 C. C. Cutler, et al, "A Self-Steering Array Repeater," BSTJ, Vol. XLII, No. 5, September 1963, p. 2013.

4 Pseudo Passive Satellite Technique Study, RADC-TDR-64-157, Contract AF 30(602)-2957, Sylvania Electronic Systems, Central, Williamsville, New York, October 1964.

5 Final Report on Electronically Steerable Antenna Systems, Signal Corps Contract No. DA-036-039-SC-85198, Sanders Associates, Inc., June 1960 to June 1962.

An attempt at a flight experiment of a high gain, 40-50 dB, phased-array antenna capable of multiple beam formation may also be made by NASA on ATS F or G about 1970.

It is highly probable that by 1975 the capability will exist to achieve antenna gains on the order of 35 dB or higher. Where very small area coverage is required (or permissible) fixed or steerable reflectors with single or multiple feeds will probably be used, which would require a three axis stabilized satellite or an advanced spin stabilized vehicle. Work now going on for the DoD tactical satellite communication satellite program holds out the hope of adapting spin stabilized satellites to large antennas, on the order of 3 to 8 feet. Again sensing and holding the attitude of the satellite and the relative position of the antenna beam are severe problems, since the beam width is very small for such large reflectors, and slight satellite movement will cause considerable shift in the area coverage on the earth.

Where a wide area coverage is required, for services like international telecommunications, some form of phased array will be required in the long run if very high gains are simultaneously required. Equipment complexities will undoubtedly increase to achieve this; reliability, as such, may not be significantly affected because of increases in individual component reliability and increases in redundancy through the substitution of multiple solid state devices feeding individual antenna elements rather than depending on a single power amplifier device. While it is conceivable that a group of fixed high gain antennas could be used, each covering a limited area, the complexities of interconnecting between antennas to achieve a random access capability would be severe. Thus in the long run, for this type of operation, individual, high gain beams will probably be formed as required to illuminate an individual earth station or geopolitical area. Thus, the concept fits in with the idea of a worldwide system having a form of random or controlled-access operation.

RF Power Capability

The state-of-the-art in the generation of DC power (and as a result of RF power) in space with solar cell technology is advancing at a rapid pace. Discussions with manufacturers indicate that approximately 35 watts of RF power at X band can be considered as state-of-the-art with flight qualified components.

The estimates of future capability of active satellite to general RF power vary rather widely with manufacturers. The following figures are based on data obtained from Comsat Corporation[1] and represent the best estimate available at this time.

r_s = Specific power (watts/lb) = 9 w/lb 1972 technology
18 w/lb 1975 technology

p = DC to RF conversion efficiency at 8 GC = 0.25

m = Functional allocation of payload to power supply = 0.35

n = Fraction of DC power allocated to spacecraft electronics and batteries = 0.5

W_T = Spacecraft payload

Therefore, the RF power can be estimated from $P_{rf} = mpr_s W_T (1 - n)$, and using the above figures with r_s based on 1972 technology, $P_{RF} = 0.4 W_T$; thus, for satellites with different weights the RF power can be estimated as follows. The costs of R&D associated with the development of these satellites and the estimated satellite unit cost based on Comsat Corporation estimates are also shown.

---

[1] Satellite broadcasting - March 1967 (Revision B - July 1967) by Communication Satellite Corporation.

TABLE 3

Payload wgt.(lbs)	DC power kw	RF Power Watts	RF Power dB	Cost of R & D ($M)	Unit cost of Satellite
1000	3.2	400	26	27.4	5.1
2000	6.4	800	20	35.0	9.0
3000	9.6	1200	31	42.0	11.5

The ERP which can be produced by these satellites can be calculated from the formula

$$\text{ERP} = \text{RF power} + \text{antenna gain}$$

$$\text{Antenna gain} = \frac{1}{1 - \cos(\theta/2)}$$

where θ = half power beamwidth in degrees

We also assume that approximately 3 dB loss is incurred as a result of problems associated with stabilization pointing accuracy, antenna despinning, etc.

Accordingly, the ERP capability of these satellites can be calculated from the above relationships.

The pertinent data is summarized in Table 4. We have listed four types of satellites representative of existing and future state-of-the-art, which are designated as follows:

Low-power SAT-1 represents existing state-of-the-art and is assumed to have a payload weight of 1000 lbs.

High-power SAT-2, SAT-3, SAT-4 represent future state-of-the-art in high power satellites and their payload weight is assumed to be 1000, 2000, and 3000 lbs. respectively.

The resulting ERP's are shown in Table 4 for various antenna beamwidths.

TABLE 4

EFFECTIVE RADIATED POWER FROM SATELLITES

	SAT-1	SAT-2	SAT-3	SAT-4
Satellites weight (pounds)	1000	1000	2000	3000
RF power (dB)	15	26	29	31
Antenna gain (1° beamwidth) dB	44	44	44	44
Losses - dB	3	3	3	3
ERP 1° beamwidth	56	67	70	72
2° beamwidth	50	61	64	66
4° beamwidth	44	55	58	60
8° beamwidth	38	49	52	54
16° beamwidth	32	43	46	48

Satellite Transponder Design

At the present time the bulk of satellite transponder designs have consisted of double conversion frequency translators using transistorized i.f. amplifiers for the bulk of the gain and a TWT for power amplification. Bandwidths on the order of 100-150 MHz have been obtained using this technique. However, as bandwidths become larger, it becomes increasingly difficult to obtain these bandwidths in the relatively low frequency i.f. amplifier and higher frequency solid state i.f. amplifiers become increasingly difficult to design.

More recent transponder designs have used a single conversion design consisting of a tunnel diode amplifier (TDA), a broad band mixer, a low power TWT, and a high power TWT as shown in Fig. 4. The Intelsat III

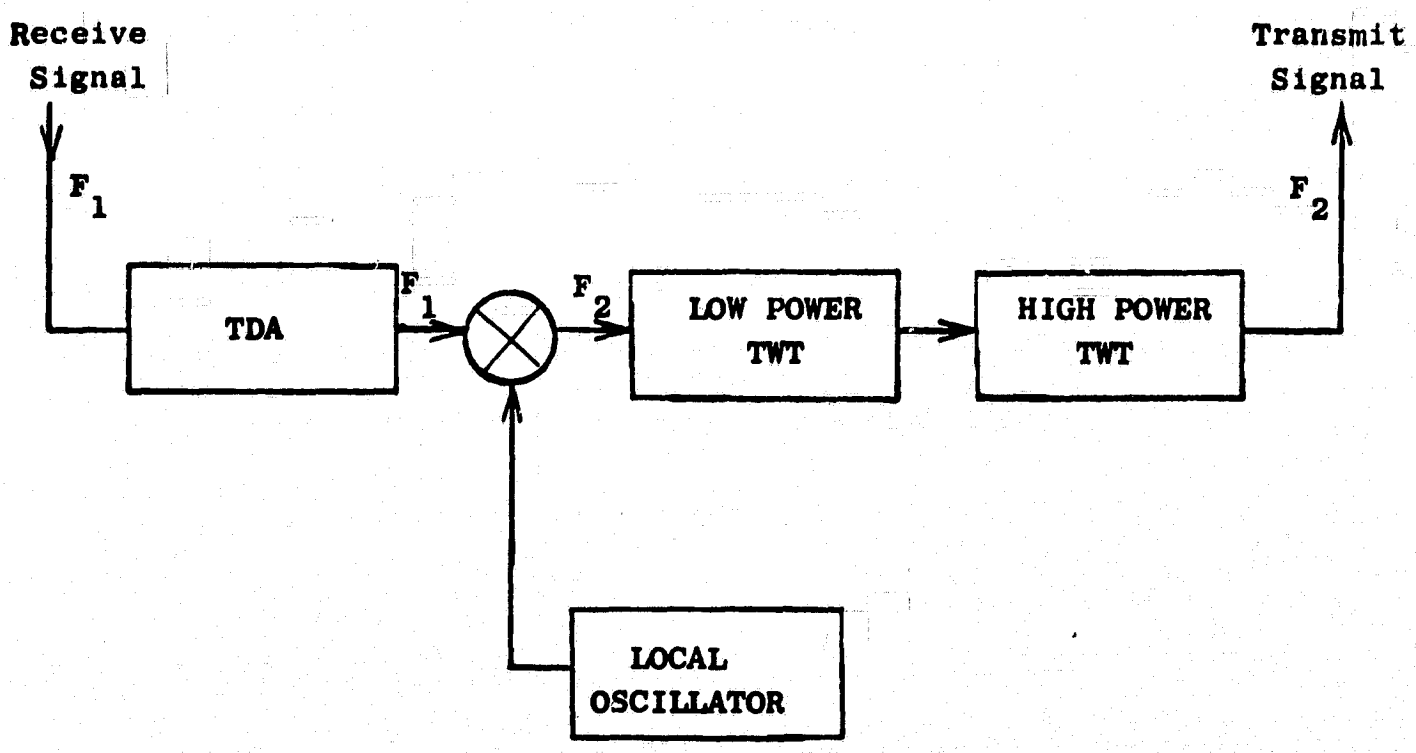


Figure 4

Single Conversion Transponder

satellite design uses this technique to achieve a transponder design having a bandwidth of 225 MHz.[1] Experimental re-entrant mode transponders have been built with bandwidths up to 500 MHz.[2] Bandwidths beyond this could probably be achieved if required. In the re-entrant mode the low power TWT is used to amplify both the receive frequency and the converted transmit frequency as shown in Figure 5. Because of the wide bandwidth and inherent linearity of the TWT when operated below saturation, this type of operation is possible. This eliminates the requirements for very high gain in both the low and high power TWTs as is required for the conventional single conversion transponder. However, re-entrant operation does aggravate nonlinearities inherent in the TWT.[3] Using this type of design might make it possible to eliminate the TDA if a low noise, high gain TWT were used as the re-entrant device. In this case the basic bandwidth limiting device would be the broadband down converter. Based on the above, it appears that bandwidths on the order of 500 to 1000 MHz can be designed into future communication satellite transponders. For the purposes of our study, 500 MHz will be assumed.

---

1 Morris Feigen, Neville J. Barten and R. G. Slaughter, "Description of the Global Communications Satellite," presented at the AIAA Communications Satellite Systems Conference, Washington, D. C., May 2-4, 1966.

2 Ronald R. Cagnon and Scott D. McCaskey, "Spacecraft Transponder with Re-entrant Mode TWT Amplifier," The Microwave Journal, 9 (March 1966), p. 120.

3 Ibid, p. 122.

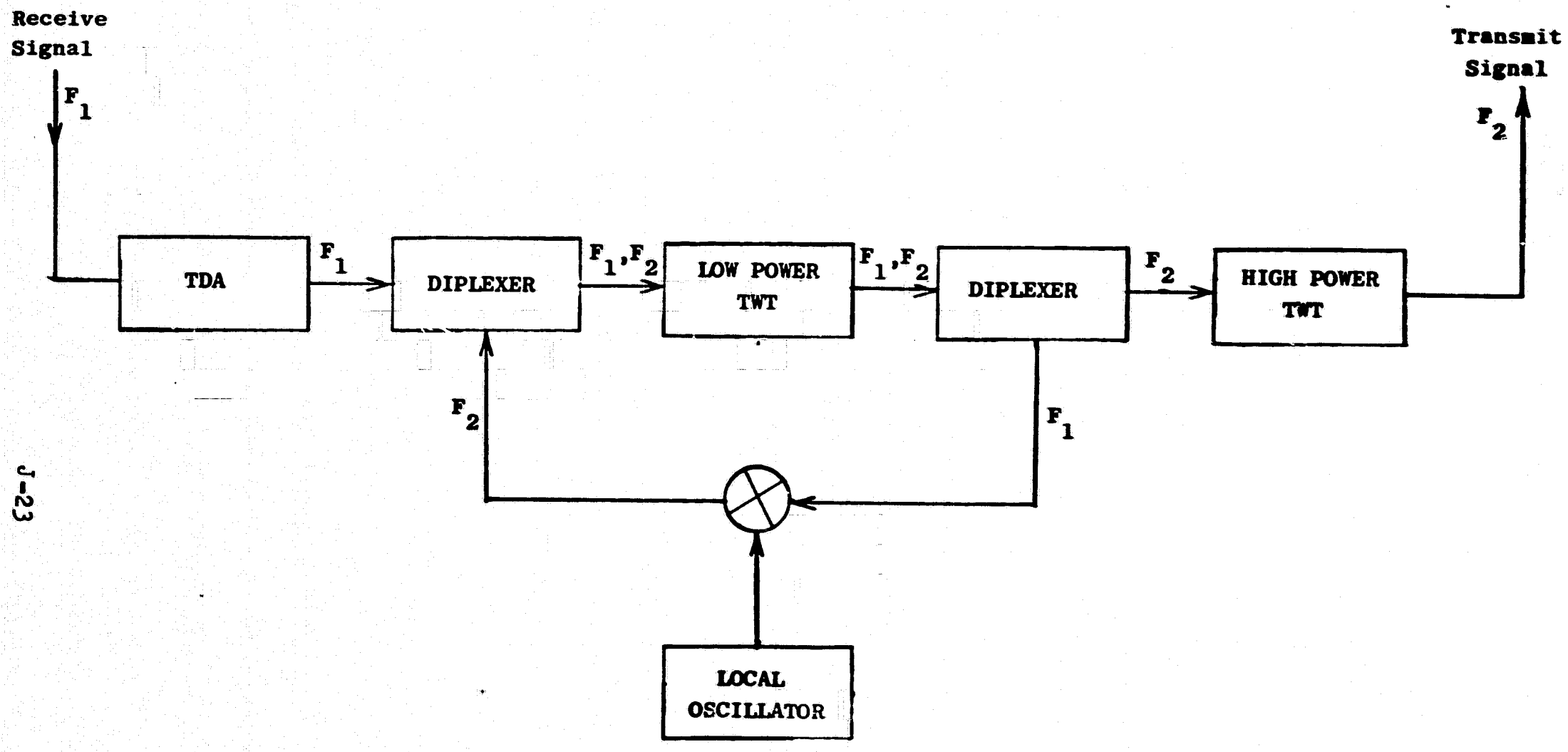


Figure 5

Re-Entrant Mode Transponder

The Cost of R&D

The total cost of R&D includes the development of new designs required to produce high RF powers, the development of new antennas with very narrow beamwidth and flight qualification tests.

In case of the low power satellite SAT-1 which represents the existing state-of-the-art, the principal R&D costs required are those associated with development of narrow beam antennas.

Because of the wide divergence of views between various manufacturers concerning the R&D costs of developing antennas with 1 and 2 degree beamwidth, and meeting the associated pointing accuracy and stabilization requirements a compromise figure of $10 million has been adopted.

For 4 and 8 degrees (at 8 GC) it is assumed that only minor modifications are required. In case of high power satellites these costs are absorbed in the total R&D costs estimated by Comsat Corporation and are listed in Table 3. These costs do not include a flight test which is considered necessary before any new designs may become flight qualified. Accordingly, the total cost of the R&D program can be presented by the following equation

$$C_T = C_{RD} + NC_S + 1.1C_L \qquad (1)$$

where

C_T = total R&D program cost

C_{RD} = R&D cost

C_S = flight satellite unit cost

C_L = cost of launch

N = number of flight qualified satellites required

It is assumed that launch vehicles required to lift various payloads into stationary orbit and their respect cost are as follows:

Payload Wt.	Booster	Launch Cost
1000	Atlas-Agena	$ 8.4 Million
2000	Titan IIIC	$15.9 Million
3000	Titan IIIC & BII	$18.1 Million

It is also assumed that two flight qualified satellites are manufactured as part of the R&D program. Thus, N=2 in Eq. (1). Using this data, total R&D costs have been computed and are shown in Table 5.

Table 5

ACTIVE SATELLITE R&D COSTS ($Million)

Beam-width Degrees	Satell. ERP (DBW)	Satellite Wt. (lb.)	Booster required	C_{LS} Launch cost ($M)	+ C_s Satellite unit cost ($M)	= C_x Cost per Launch	Total Cost/ Launch ($1.1C_x$)	R&D Costs to develop ($M) Power Capabil.	Antenna & Stabiliz.	Flight Test Costs ($M) 2 flt. Satell.	Launch 1.1 Cl	Total R&D
1°	56	1000	Atlas/Agena	8.4	4.5	12.9	14.1	-	10	9	9.2	28.2
	67	1000	Atlas/Agena	8.4	6.0	14.4	15.8	27	10	12	9.2	58.2
	70	2000	Titan IIIC	15.9	10.0	25.9	28.5	35	10	20	17.5	82.5
	72	3000	Titan IIIC + BII	18.1	12.0	30.1	33.1	45	10	24	20	99.0
2°	50	1000	Atlas/Agena	8.4	4.0	12.0	13.2	-	10	8	9.2	27.2
	61	1000	Atlas/Agena	8.4	5.5	13.9	15.3	27	10	11	9.2	57.2
	64	2000	Titan IIIC	15.9	9.5	24.5	27.0	35	10	19	17.5	81.5
	66	3000	Titan IIIC + BII	18.1	12.0	30.1	33.1	45	10	24	20	99.0
4°	44	1000	Atlas/Agena	8.4	3.5	11.9	13.1	-	2.	0	0	2.0
	55	1000	Atlas/Agena	8.4	5.0	13.4	14.7	27.	0	10	9.2	46.2
	58	2000	Titan IIIC	15.9	9.0	24.9	27.4	35.	0	18	17.5	70.5
	60	3000	Titan IIIC + BII	18.1	12.0	30.1	33.1	45.	0	24	20	89.0
8°	38	1000	Atlas/Agena	8.4	3.0	11.4	12.5	--	0.5	0	0	0.5
	49	1000	Atlas/Agena	8.4	5.0	13.4	14.7	27.	0	10	9.2	46.2
	52	2000	Titan IIIC	15.9	9.0	24.9	27.4	35.	0	18	17.5	70.5
	54	3000	Titan IIIC + BII	18.1	12.0	30.1	33.1	45.	0	24	20	89.0
16°	32	1000	Atlas/Agena	8.4	3.0	11.4	12.5	--	0	0	0	0
	41	1000	Atlas/Agena	8.4	5.0	13.4	14.7	27.	0	10	9.2	46.2
	46	2000	Titan IIIC	15.9	9.0	24.9	27.4	35.	0	18	17.5	70.5
	48	3000	Titan IIIC + BII	18.1	12.0	30.1	33.1	45.	0	24	20	89.0

APPENDIX K

CRITERIA FOR COMPARISON OF PERFORMANCE OF ACTIVE AND PASSIVE COMMUNICATION SATELLITE SYSTEMS

The development of criteria for comparison of active and passive satellite systems will be based on the determination of the performance requirements for various modes of information transmission. The modes selected for study are:

a. Analog voice
b. Digital transmission through analog channel
c. Vocoded voice
d. Teletype
e. High speed data
f. Facsimile
g. Television

The approach will consist in determining the basic requirement for acceptable SNR and a very brief consideration of modulation techniques and receiver configurations in order to determine maximum permissible noise limits at the input to the receiver.

1. Analog Voice

The exchange of voice communications traffic over any type of a system requires an allocation of frequency, power, and time. These three quantities are of a great economic importance in the communications world and the effectiveness of the communications system is often judged by how efficiently they are used. For a long time, signal-to-noise-ratio has been accepted as a general criterion for expressing the quality of the communication circuit. More recently, however, greater emphasis has been placed on the determination of intelligibility to any substantial extent.

---

* This technical note is based to a large degree on work performed under author's supervision by P. Shaft and H. Shaver while with Philco Corp. and reported in Communication Sciences Tech. Memo. No. 82. Figs. 1,2, 5,7,8,9, and Table 5 are taken from this Tech. Memo. with permission.

This fact has been utilized in normal commercial telephone radio communications in which the speech spectrum which normally extends from below 100 cycles to above 7000 cycles is usually transmitted in the band of 250 to 3000 cycles per second. It has also been shown[1*] that peak clipping of speech does not result in loss of speech intelligibility in noise and that, as an example, 24 dB peak clipping permits one to achieve a specified level of intelligibility with about 13 dB less peak signal power than would be required for distortionless transmission. This result implies that a one watt peak clipping amplifier could be used in place of a 20 watt linear amplifier.[2] It has also been demonstrated that high degree of intelligibility can be preserved in speech which is interrupted at a low rate in such a way that it is on only half the time. As a result, by alternating between two conversations, it is possible to provide two-way communications in a single channel thereby achieving double use of the facility. These examples indicate that economies in the use of bandwidth, power, and time can be achieved with appropriate techniques of speech processing.

There exist other speech processing methods which take advantage of various properties of speech. One of these methods identifies the zero crossings of the speech wave and transmits only this information to the far end. Another method identifies the maxima and minima of the speech wave and transmits this information. In both cases, the reconstructed speech wave at the receiver is intelligible but lacks the naturalness and quality of the original speech. A controversy exists on the relative importance of preserving the attributes of speech other than intelligibility. It appears that psychologically, particularly in cases of emergency, the emotional content of a message may in many cases be important.

---

* References are listed at the end of this appendix.

It is felt, therefore, that the incorporation of new speech processing techniques which would result in the loss of speech attributes other than intelligibility may not necessarily be advisable. Since, as mentioned previously, the criterion for the specification of the quality of speech communication links has been the signal to noise ratio, the relationship between SNR and the intelligibility is of importance. An extensive experimental program has been performed at RADC.[3] This study derived a relationship between word intelligibility as measured with phonetically balanced word lists (Harvard PB-50 Word Lists) and the SNR. The noise was gaussian and white in a bandwidth of 6100 cycles. In order to relate these results to a standard voice bandwidth of 4 kc (3 dB points at 300 and 3500 cycles per second), the following approximation was accepted: Since the effect of band limiting of speech signal to the 300-3500 cycles reduces the PB word intelligibility to approximately 95 percent,[4] each point on the RADC curve of intelligibility vs. SNR has been lowered by 5 percent to make the resultant curve asymptotically approach 95 percent intelligibility rather than 100 percent for very high SNR. The result is shown in Fig. 1. Keeping in mind the approximations involved, it tells us that approximately 9 dB signal to noise ratio is required to achieve 90 percent word intelligibility. A different result may be obtained if noise is other than gaussian. However, the figure quoted represents an acceptable result.

To establish the minimum SNR permissible, another parameter must be added to this figure. This parameter represents the dynamic variations of the volume level of a speaker. For a large number of speakers, the total dynamic range of the system must encompass the variations in their average level and in addition the range over which the level of any

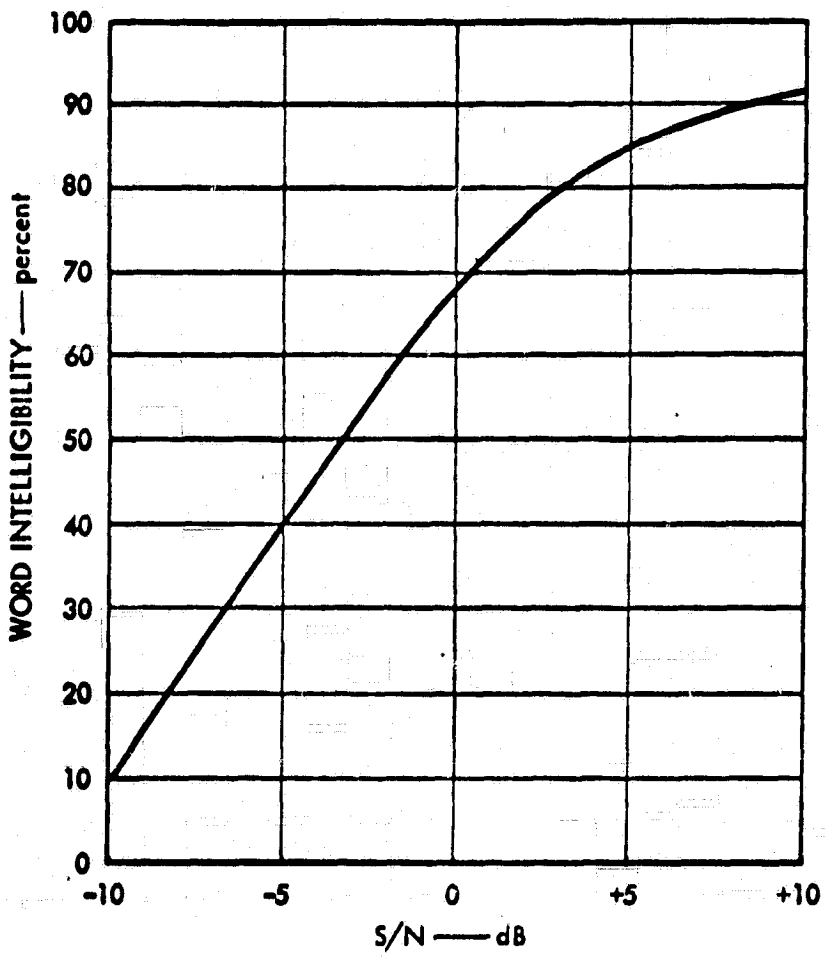


FIG. 1 - HARVARD PB WORD INTELLIGIBILITY AS A FUNCTION OF SIGNAL-TO-NOISE RATIO FOR OPTIMUM SPEECH LEVEL SETTING

individual speaker may vary. McAdoo[5] has performed a large number of measurements intended to establish the average VU level and the distribution around that level for a large number of typical telephone connections. The results of this study showing the distribution of levels are given in Fig. 2. These results may not be directly applicable to all types of analog voice service. For example, many military communications applications would be restricted to male voices only and accordingly the average volume (represented by 0 in the X-axis of Fig. 2) would probably be higher than for the Bell System However, the form of the distribution would probably remain the same. Fig. 2 indicates that 99 percent of speech volume measurements were contained in the range of approximately 24 dB. If we assume, without attempting to defend this assumption, that for many communications applications, the total variations in speech volume are contained in the range of 15 dB (representing almost 90% of cases) then the total signal-to-noise-ratio necessary for satisfactory service is given by the minimum SNR of 9 dB previously derived plus the volume range of 15 dB for a total of 24 dB.

The above discussion has been presented for the purpose of indicating the procedure to be followed in establishing the necessary performance criteria for analog voice systems. These criteria will in turn affect the design specifications of the hardware and the cost of the system. It should be pointed out that recent experiments indicate that various processing schemes intended to reduce the speech bandwidth and which essentially consist of the removal of redundancy, render the voice transmission substantially more vulnerable to noise and interference. Thus in evaluating the advantages of such schemes, experimental results for performance in noise environment, representative of conditions to be found in actual environment, are required.

For the purposes of this study a figure of 24 dB SNR for analog voice transmission will be used as minimum acceptable criterion which will yield speech intelligibility of 90% or more for most users.

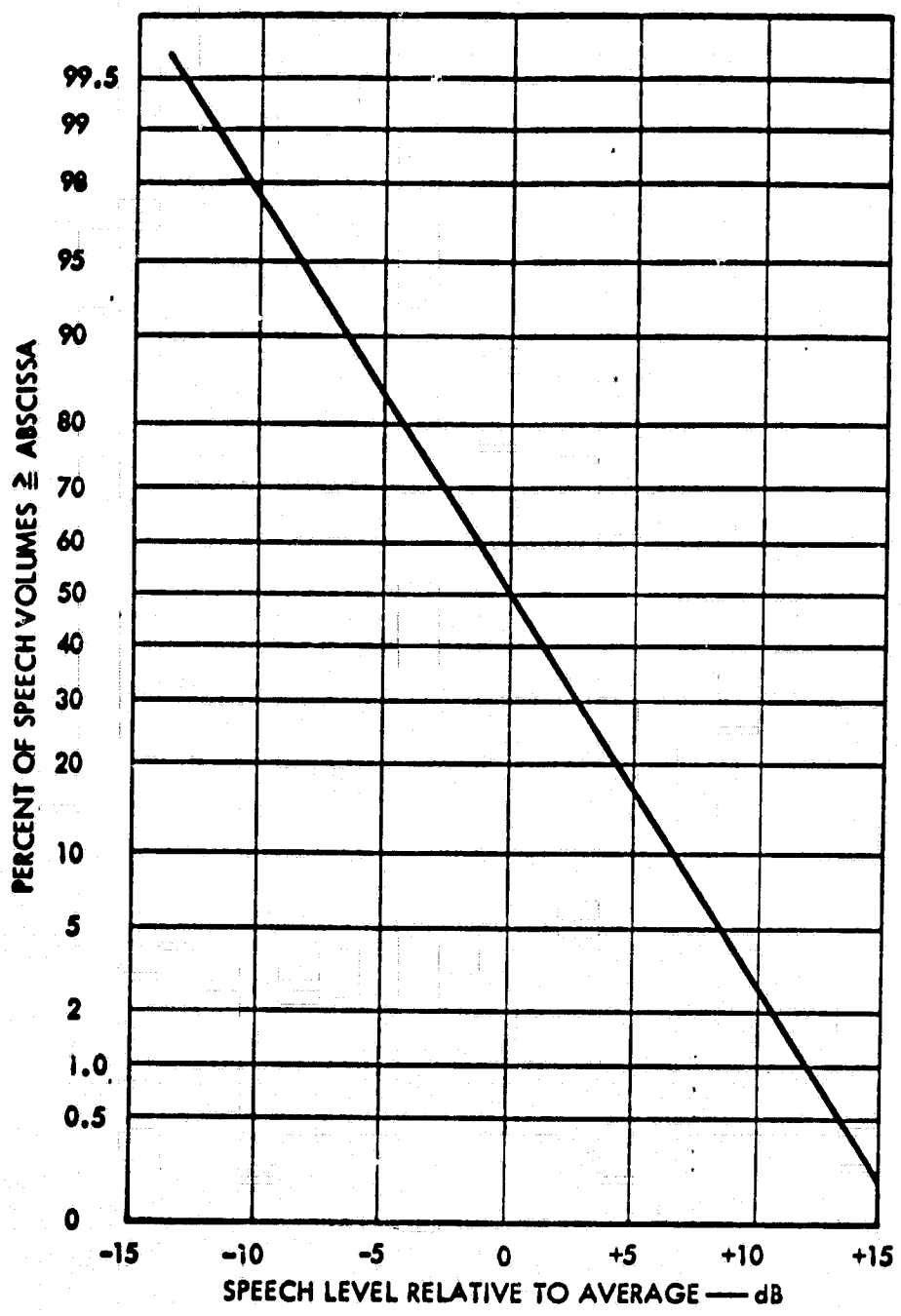


FIG. 2 - THE DISTRIBUTION OF AVERAGE TELEPHONE SPEAKING LEVELS FOR A LARGE NUMBER OF DIFFERENT SPEAKERS - FROM MC AD006

1.1 Determination of the Required SNR and Bandwidth at the Input to the FMFB Receiver

Let $(SNR)_{out}$ represent the required output SNR in bandwidth b. It is desired to determine the $(SNR)_{in}$ and the rf bandwidth B at the input to the FMFB receiver as shown below.



From conventional f-m receiver theory, we know that the SNR improvement between the input and output SNRs is approximately given by $3m^2(m+1)$ when the input bandwidth is determined by Carson's rule.

Thus $$(SNR)_{in} = (SNR)_{out} \cdot \frac{1}{3m^2(m+1)} \qquad \text{.....} \qquad (1)$$

or in dB

$$(SNR)_{dB} = (SNR)_{out\text{-}dB} - 4.8 - 10 \log m^2(m+1) \qquad \text{.....} \qquad (2)$$

The required rf bandwidth is determined from Carson's rule as

$$B = 2b(m+1) \qquad \text{.....} \qquad (3)$$

where m is the fm deviation ratio.

It is evident from (1) and (3) that B and $(SNR)_{in}$ are both determined by the selected value of m and consequently cannot be chosen independently.

There exists a restriction on the value of m which is imposed by the requirement that in FMFB systems $(SNR)_{in}$ must be above threshold. To find the limits on m therefore, the threshold SNR must be known.

The determination of threshold, particularly when FM feedback receivers are used represents a difficult problem which still has no definite solution. The threshold varies depending on the amount of feedback and on the modulation index.

In order to determine the threshold value the results of a recent study[6] have been selected. Fig. 3, which is taken from reference 6, shows the variations of the threshold (in dB) as a function of the feedback factor F and modulation index "m". The threshold value shown is measured in approximately twice the information bandwidth (2b).

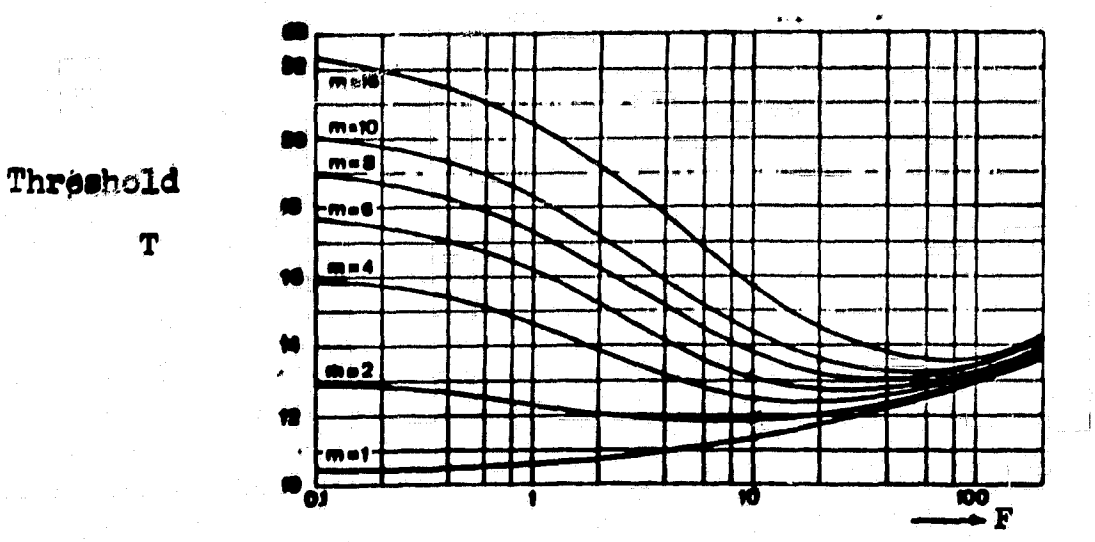


Fig. 3
Threshold T as a Function of
F (Feedback Factor) and m (Deviation Ratio)

Taking as an example the case of receivers with a feedback factor of 20, we obtain from Fig. 3 the following values.

Table 1

Relationship Between m and T

Value of Deviation Ratio m	Threshold SNR Value dB in Bandwidth 2b
m = 2	12
m = 4	12.5
m = 6	12.8
m = 8	13.2

Assume that threshold value T can be represented by formula

$$\text{Threshold}_{dB} = X_{dB} + a \log(m+1) \qquad \ldots\ldots\ldots\ldots\ldots \quad (4)$$

Using values from Table 1,

$$\text{Threshold}_{dB} = 12 = X + a \log(3)$$

$$\underline{12.5 = X + a \log(5)}$$

$$0.5 = a(\log(5)-\log(3))$$

$$a = \frac{0.5}{.222} = 2.25$$

Therefore

$$X = 12 - 2.25\ (0.477)$$

$$= 12 - 1.04$$

$$\approx 11 \text{ dB}$$

Therefore, approximately

$$\text{Threshold}_{dB} = 11 + 2.3 \log(m+1) \qquad \ldots\ldots\ldots\ldots\ldots \quad (5)$$

measured in bandwidth 2b.

Converting to bandwidth B = 2b(m+1)

$$\text{Threshold SNR} = 11 + 2.3 \log(m+1) - 10 \log(m+1)$$

$$T_{dB} = 11 - 7.7 \log(m+1) \qquad \ldots\ldots\ldots\ldots\ldots \quad (6)$$

Converting to a fraction, the threshold SNR in bandwidth B is

$$T = \frac{12.6}{(m+1)^{0.77}} \qquad \ldots\ldots\ldots\ldots\ldots \quad (7)$$

The limiting value of m can now be derived by substituting T from (6) in place of $(SNR)_{in}$ in (2). Thus at threshold

$$11 - 7.7 \log(m+1) = (SNR)_{out} - 4.8 - 10 \log m^2(m+1)$$

$$(SNR)_{out\text{-}dB} = 15.8 + 20 \log m + 2.3 \log(m+1) \qquad \ldots\ldots\ldots\ldots \quad (8)$$

from which we can plot a curve of $(SNR)_{out}$ versus m for threshold operation. The various results obtained so far are shown in Fig. 4.

Fig. 4 shows that for any desired output SNR a value of m can be found which will result in $(SNR)_{in}$ being at threshold. This is shown by the upper curve (1). The lower curve (2) shows the value of threshold SNR in bandwidth 2b(m+1) and the difference between the two curves is plotted as curve (3) and represents the improvement factor ($=3m^2(m+1)$). The values of m determined in this manner are the optimum values. If a larger value of m is selected, $(SNR)_{in}$ will be below threshold. As a result, additional signal power will be required to reach threshold. The selection of a lower value of m will result in the value of $(SNR)_{in}$ being higher than threshold which is equivalent to saying that signal power is more than needed when optimum m is chosen. It can easily be shown from equations (1) and (3) that as m departs from optimum value the ratio of needed signal power to optimum signal power varies as

$$\frac{S}{S_{opt}} = \left[\frac{\overline{m}_{opt}}{\overline{m}}\right]^2 \quad \text{for } m < m_{opt} \qquad \ldots\ldots\ldots\ldots \qquad (9)$$

If m is larger than m optimum, the additional signal power needed to reach threshold depends on the amount of feedback in the fm receiver and on the value of m. Since in conventional fm terminology the magnitude of the feedback factor is numerically equal to the reduction in deviation ratio m which it produces

$$F = \frac{m}{m_1} \quad \text{or} \quad m_1 = \frac{m}{F}$$

Thus threshold SNR in bandwidth 2b is specified by the equation

$$\frac{S}{2b\left(\frac{m}{F} + 1\right) N_o}$$

DEV RATIO m	SNR-OUT dB	THRESHOLD dB	IMPROVEMENT FACTOR	dB
.5	10.1	9.6	1.1	.5
1.0	16.4	8.6	6.0	7.8
1.5	20.2	7.9	16.8	12.2
2.0	22.9	7.3	36.0	15.5
2.5	25.0	6.8	65.6	18.1
3.0	26.7	6.3	108.0	20.3
3.5	28.1	5.9	165.3	22.2
4.0	29.4	5.6	240.0	23.8
4.5	30.5	5.3	334.1	25.2
5.0	31.5	5.0	450.0	26.5
5.5	32.4	4.7	589.8	27.7
6.0	33.2	4.4	756.0	28.7
6.5	34.0	4.2	950.6	29.7
7.0	34.7	4.0	1176.0	30.7
7.5	35.4	3.8	1434.3	31.5
8.0	36.0	3.6	1728.0	32.3
8.5	36.6	3.4	2059.1	33.1
9.0	37.1	3.3	2430.0	33.8
9.5	37.6	3.1	2842.8	34.5
10.0	38.1	2.9	3300.0	35.1

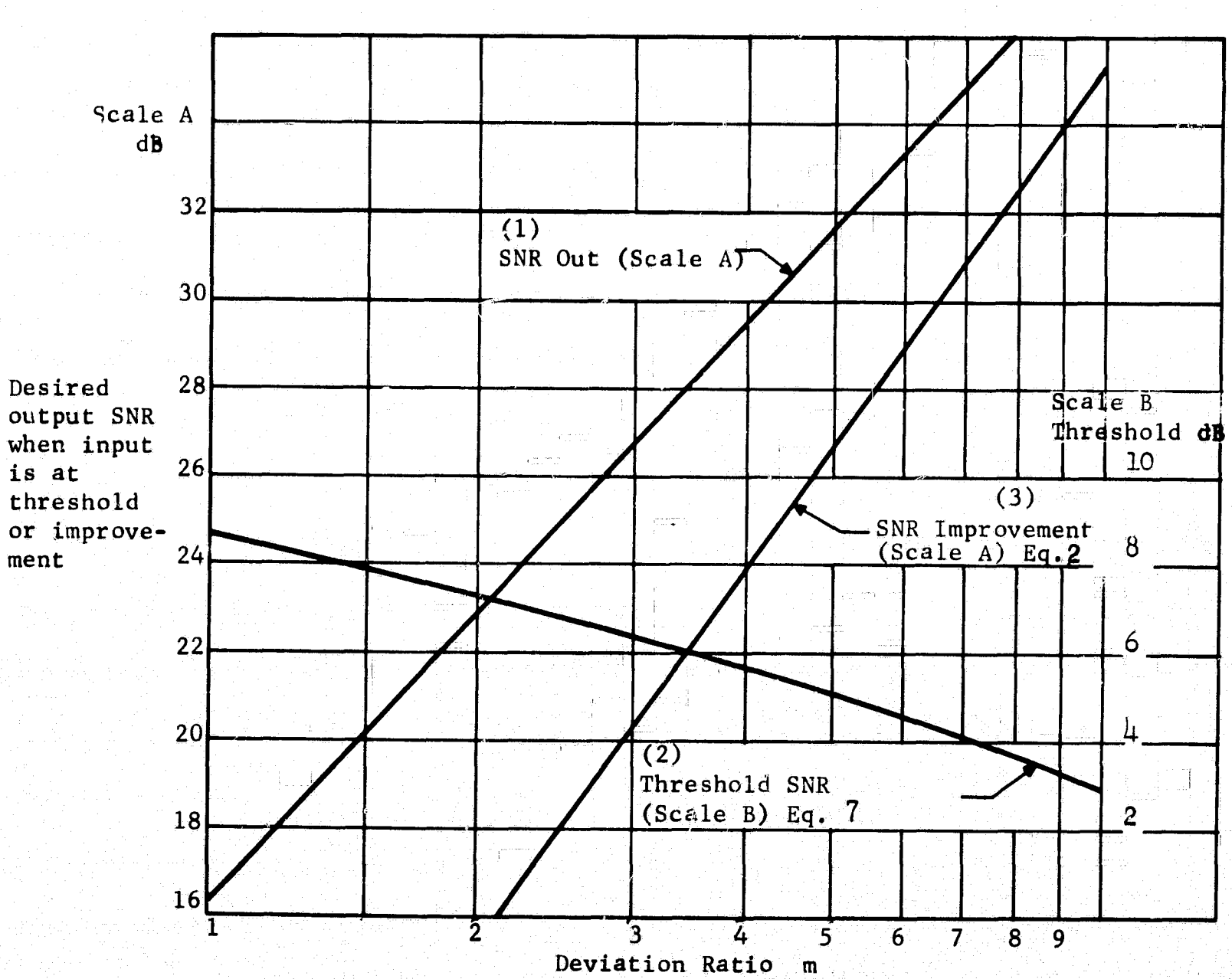


Figure 4. Performance Characteristics of FMFB Receivers

To reach this threshold the original value of m must be reduced from m to m_{opt}; thus

$$\frac{S}{S_{opt}} = \frac{m + F}{m_{opt} + F} \qquad \text{.....} \qquad (10)$$

Equations (9) and (10) are plotted in Fig. 5.

Optimum values of m as shown in Fig. 4 specify the rf operating bandwidth B=2b(m+1) while yielding the minimum required power from the satellite. In that sense, Fig. 4 represents the best design from the power minimization point of view. However, in certain cases when bandwidth is important a trade-off between power and bandwidth may be desirable.

When operating above threshold with substantial feedback (more than 10 dB), the variations in bandwidth are expressed by

$$\frac{B}{B_o} = \frac{m + 1}{m_o + 1}$$

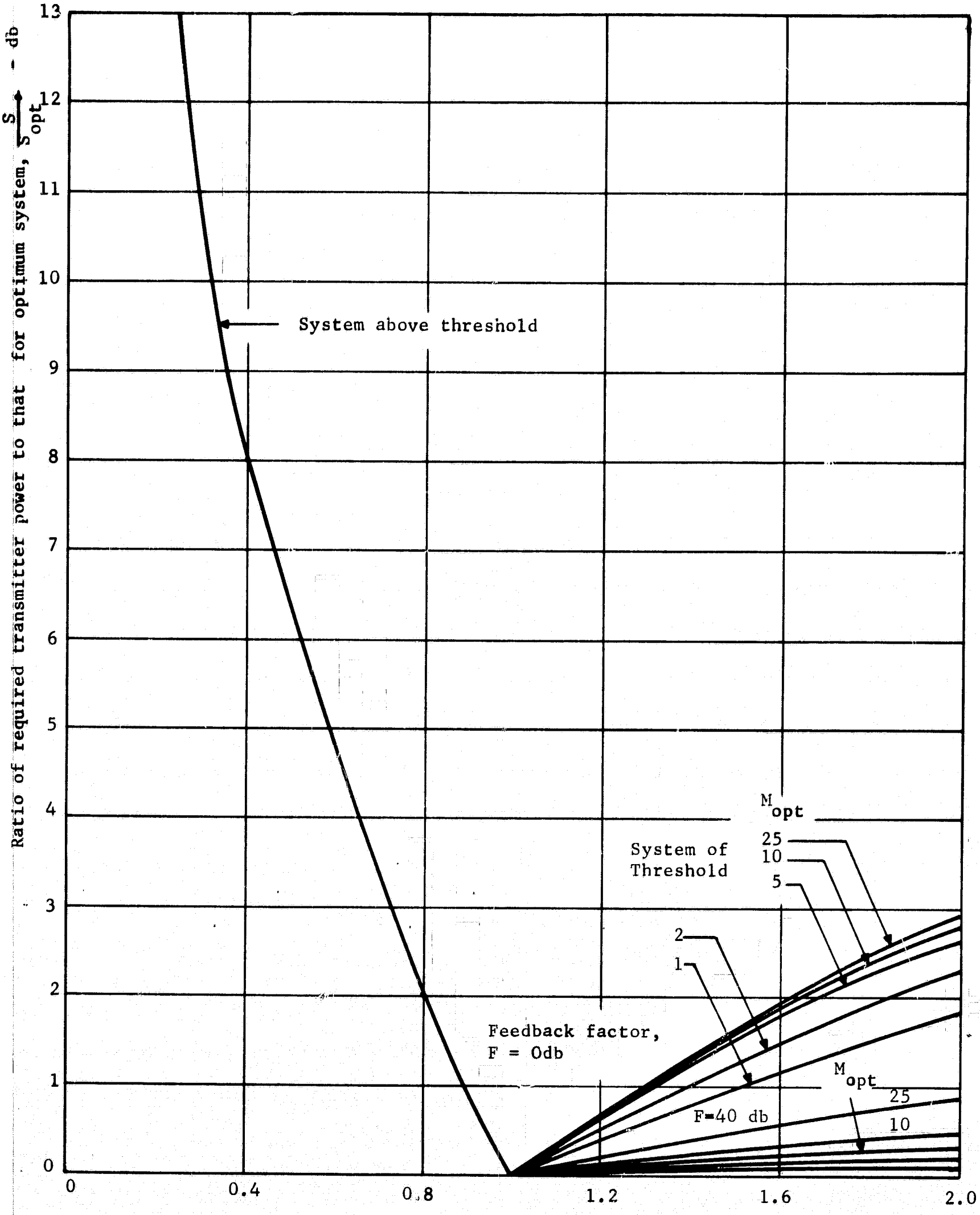
and variations in signal power are expressed by equation (9)

$$\frac{S}{S_o} = \left(\frac{m_o}{m}\right)^2$$

Knowing the optimum values, Fig. 5 can be used to estimate the trade-off penalties. The trade-off is also shown in Fig. 6 which indicates input-output relations.

The values of input SNR which are equal to threshold are shown by dotted line (for various m's). Thus for any given $(SNR)_{out}$ the largest value of m that can be selected is at the intersection of the threshold curve with the desired $(SNR)_{out}$.

Fig. 6 clearly shows possible trade-offs. Thus for required output SNR of 30 dB, the highest permissible value of m is approximately 4.3 resulting in operation at threshold value of 5.4 dB. However should we select m=3 for example, the required value of $(SNR)_{in}$ would be at 7.1 dB (which is

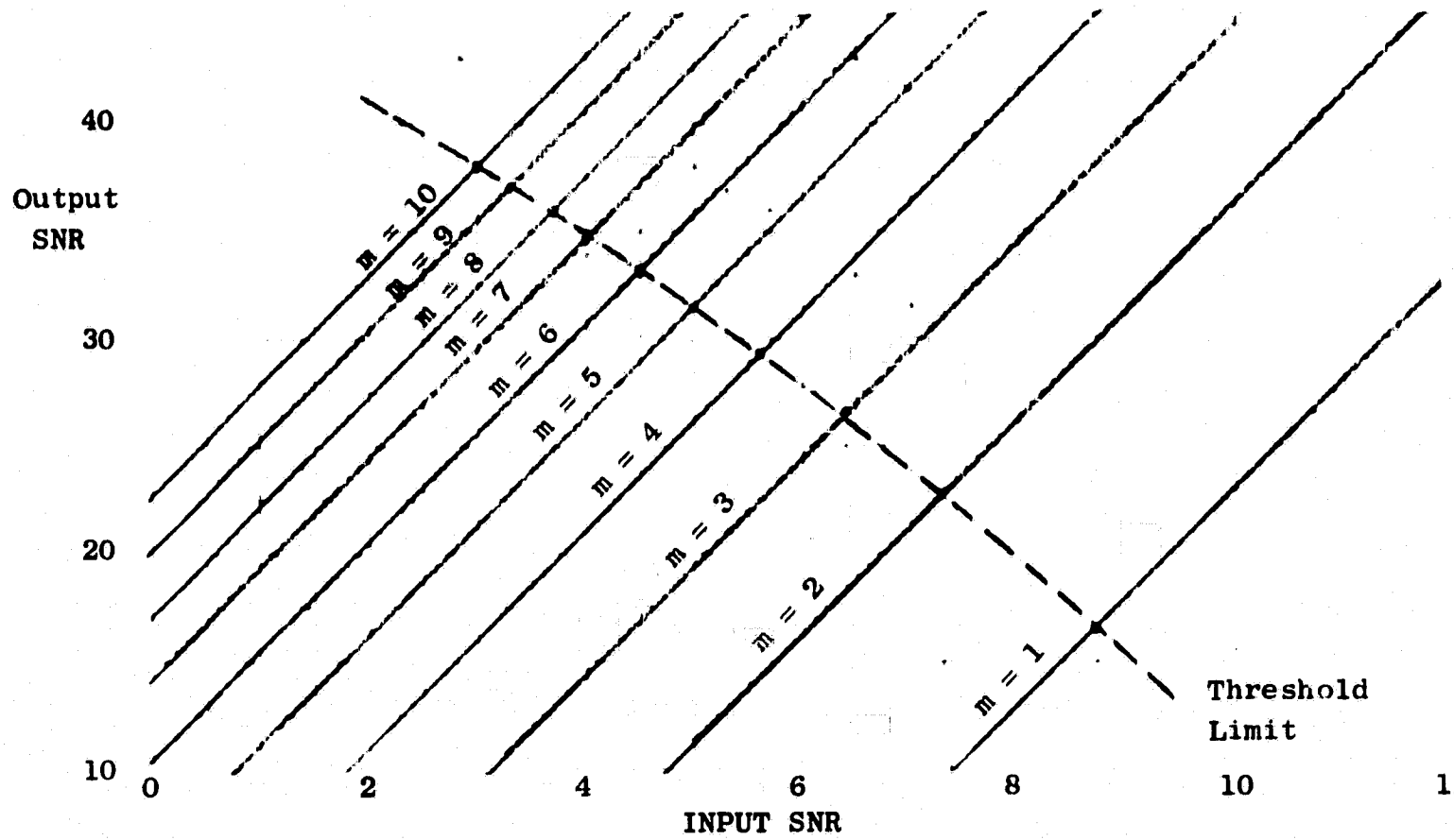


(from Rand Corp., RM-2787-NASA)

Figure 5. Power Penalties for Non-Optimum System Design

Fig. 6

Input-Outputs SNR Relationship
in Frequency-Feedback Receivers



above threshold). Now, since the rf bandwidth B = 2b(m+1) the selection of m specifies both B and $(SNR)_{in}$. Note that operation at threshold requires the least $(SNR)_{in}$ and therefore the lowest power from the satellite but at the same time requires the widest bandwidth. Operation above threshold requires more power but less bandwidth. Thus a power bandwidth trade-off is possible and is specified by the selection of deviation ratio m.

For the case of voice transmission where 24 dB SNR is required at the output of the receiver, the corresponding minimum values of the other constants can be now determined. Thus:

for (SNR) = 24 dB in bandwidth 4 KC

m = 2.25

$(SNR)_{in}$ = 7.1 dB (in bandwidth 2b(m+1)) = 5.14

B = 2b(m+1) = 26 KC.

To provide for separation between channels additional 15% will be added to the RF bandwidth yielding B ≈ 30,000 cps.

These values will be used in our study.

2. Television

The signal to noise ratio at the output of the receiving ground station, when television signals are transmitted, depends on the desired quality of TV picture and on the noise generated in the distribution facilities connecting the output of the ground receiving station and the user's receiver. To obtain the required values, we will use the results summarized in reference (7).

If subjective approval of the quality of a 625-line 5 MC monochrome television signal as reported by viewers is expressed by the factor Q, the following absolute scale can be established:

Q = 1 defect imperceptible
Q = 2 defect just perceptible
Q = 3 defect clearly perceptible, but not disturbing
Q = 4 defect slightly disturbing
Q = 5 defect distinctly disturbing
Q = 6 pictures unusable.

According to reference (2), the relationship between Q and the output signal to weighted white noise ratio can be represented by a straight line. Rearranging these results, we obtain

$$Q = 11.30 - 0.196 \left(\frac{S}{N}\right)_{\text{dB, 6 MC}} \qquad \text{.....} \qquad (11)$$

Equation (11) can be modified for other bandwidths by assuming a constant spectral density of noise. Thus a relationship between the subjective quality Q and the output SNR is established. We now assume that the television signal is distributed to the local broadcasting station via an fm microwave relay which conforms to CCIR recommendation 421 yielding a weighted signal to noise ratio of 57 dB. Assuming the weighting filter described in CCIR recommendation 421, the weighting of the de-emphasized triangular noise over the band of 0 to 6 MC introduces a loss of 15.7 dB. Accordingly the unweighted SNR is 41.3 dB. The limit of the broadcast transmitter range can be defined by the recommended field strength figures (CCIR recommenda-

tion 417 for example) at various frequencies, assuming the values of the signal to weighted noise ratio at the output of the television receiver of approximately 47 dB has been obtained (see reference (7)). The unweighted ratio can be obtained by subtracting the loss due to weighting of white noise, i.e., 9.3 dB.

We now have the SNR contributions from the microwave relay (57 dB) and from the local distribution network (47 dB) as well as the total signal to noise ratio for desired quality Q which can be computed from equation (11). Thus for any given SNR at the output of the satellite ground terminal a corresponding value of Q can be determined, since

$$\left(\frac{N}{S}\right)_{final} = \left(\frac{N}{S}\right)_{ground\ station} + \left(\frac{N}{S}\right)_{microwave\ relay} + \left(\frac{N}{S}\right)_{local\ distribution}$$

where all ratios are weighted SNRs and

$$Q = f\left(\frac{N}{S}\right)_{final}$$

Using the values given above, the following results have been obtained based on data in reference (7) for a 6 MC signal.

Table 2

Overall signal-to-weighted-noise ratio S/N' and subjective quality Q of the pictures, as functions of the signal-to-weighted-noise ratio S_n/N'_1 of the satellite/Earth-station circuit

$\frac{S_n}{N'_1}$ dB	High field-strength			Low field-strength		
	$\frac{S}{N'}$ dB	Q monochrome	Q colour	$\frac{S}{N'}$ dB	Q monochrome	Q colour
43	42.8	2.9	3.2	41.4	3.2	3.5
45	44.7	2.55	2.85	42.7	2.9	3.2
47	46.6	2.15	2.45	43.8	2.7	3.0
49	48.4	1.8	2.1	44.6	2.55	2.85
51	50.0	1.5	1.8	45.2	2.45	2.75
53	51.5	1.2	1.5	45.7	2.35	2.65
55	52.9	$\approx$ 1.0	1.25	46.0	2.30	2.6
57	54.0	$<<$ 1	$\approx$ 1.0	46.2	2.25	2.55
59	54.9	$<<$ 1	$<<$ 1	46.4	2.2	2.5
∞	57.0	$<$ 1	$<$ 1	46.6	2.15	2.45

The results in Table 2 correspond to a 625-line 6 MC TV system. If we want to convert to a 4 MC system, we note that equation (11) gives the relationship between Q and the output SNR assuming a 6 MC bandwidth.

Since to the first approximation we can assume that noise spectral density remains constant a change to a 4 MC bandwidth would be equivalent of increasing the given SNR by 1.75 dB with the corresponding reduction in Q by a factor of 0.343 (from equation (11)).

Conversely if in a 4 MC system the SNR specified for a 6 MC system is used Q will increase by 0.343. Since the SNR of the local broadcasting network is much lower than that of the microwave relay, the variations of the ground station SNR will, to the first approximation, follow the same pattern. Thus if the values in column 1 of Table 2 are increased by 1.75 dB and assumed to apply to a 4 MC bandwidth the table can be used without changes. This approximation is justified by the fact that the entire derivation is highly theoretical and does not take into account any other sources of possible degradation of transmission except noise and that Q itself is highly subjective.

The weighted values of SNR given in Table 2 can be converted to unweighted SNR by subtracting the insertion-loss corresponding to the weighting of de-emphasized triangular noise. This loss approximates 15.7 dB for a 6 MC 625-line system. (See CCIR recommendation 421 for weighting network characteristics.)

As a result of these modifications, the values in Table 3 have been calculated and can be used in our study. As a general guideline, the SNR of approximately 33 dB in a 4 MC bandwidth will be assumed for TV channels.

Using Fig. 4, we can select the best deviation ratio m = 5.75. The corresponding threshold SNR is approximately 5 dB and the rf bandwidth required is

$$B = 2 \cdot 4\ MC(6.75) = 54.2\ MC$$

and the required signal-to-noise density ratio is 82.3 dB

$$S/N_o = 82.3\ dB$$

Table 3

Picture Quality vs SNR

Picture Quality Factor Q	SNR in 4 MC Bandwidth Required at the Output of Ground Station			
	High Field Strength		Low Field Strength	
	Monochrome	Color	Monochrome	Color
1 - Excellent	41 dB	43	-	-
2 - Very good	34 dB	35	50	-
2.5 - Good	31 dB	33	35	44
3 - Acceptable	29 dB	30	31	34

Note that if we decide to reduce the rf bandwidth to 26 MHz, the corresponding values would be

SNR_{out} = 33 dB

SNR_{in} = 16 dB

m = 2.25

B_{RF} = 26 MHz

S/N_o = 90.4 dB

and if we selected m = 3,

SNR_{out} = 33 dB

SNR_{in} = 13 dB

m = 3

B_{RF} = 32 MHz

S/N_o = 88.2 dB

(This case corresponds to the Bell System Proposal to FCC for "An Integrated Space/Earth Communications System," 1967, and will be used in our study.)

3. Vocoded Voice

The application of a channel vocoder permits transmission of a 4 KC analog voice wave in digital manner at a rate of 2400 bits/sec. The limitations of vocoder voice links should be noted at this point:

a. Conference calls (more than two subscribers on the same circuit cannot be accomplished).

b. Channel vocoders cannot be operated in tandem. This means that once a vocoded speech has been reconstituted it cannot be vocoded again. This restriction results from the fact that the basic pitch information is not available in reconstituted analog wave form.

c. Due to the vocoder requirement that fundamental pitch be extracted, vocoders cannot be operated from the output of most telephone circuits (which do not transmit frequencies below 200 cps). This makes it impossible to transmit analog voice over standard telephone lines and then vocoderize it at some central station. It also implies that vocoder equipment must be located next to the users telephone and that all telephone sets in the network must be equipped with vocoders.

These limitations may represent severe problems in many applications; for the purposes of our analysis, however, it will be assumed that this mode of communications is useful.

It has been shown[8] that because of great redundancy of voice, the intelligibility and speaker recognition of a 2400 bit vocoded voice is

preserved quite well at high bit error rates. The results of experiments indicate that intelligibility remains in excess of 90% even at bit error rates of one in a hundred (10^{-2}). Subjective listening tests in which the writer participated further support this conclusion. We will therefore accept the 10^{-2} bit error rate as acceptable to yield good grade vocoded voice communication link.

4. Teletypewriter

The standard military teletype format consisting of a signalling code of 7.42 unit start-stop code (unit length start pulse, five unit length information pulses and a 1.42 unit stop pulse) will be used in this analysis. Nominal teletypewriter operating speeds are 60, 66, 75, and 100 words per minute.

It will be assumed that the standard teletype code is converted before transmission to a 75 bit/sec data stream of uniform bit length and that a standard teletype page represents roughly 20000 binary digits (40 lines at 72 letters, each letter 7 bits).

On the assumption that a single character error is caused by a single bit error, the following relationship between bit error rate and letter errors is obtained.

Bit Error Rate	Number of Letter Errors Per Page
10^{-2}	200
10^{-3}	20
10^{-4}	2
10^{-5}	0.2

Subjective ratings[9] by teletype operations are shown in Table 4.

Table 4

Quality of Teletype Copy for
Different Error Rates

RATING	ERROR RATE
Good (almost no errors)	less than 5×10^{-4}
Fair (readable)	2×10^{-2} to 5×10^{-4}
Poor (unreadable)	greater than 2×10^{-2}

Roughly speaking - for conversational text - the operators have judged about 10 errors or less per page as "good."

For encrypted material where no correlation between letters exists, the error rate of 10^{-5} or better would be required.

5. High Speed Data

The analysis of this type of service will be restricted to 2400 bit/sec data circuits.

The permissible error rates will normally be dependent on the nature of data being transmitted. It is generally accepted that a 10^{-5} bit error rate constitutes a satisfactory criterion.[10] Data can be additionally protected by the insertion of controlled redundancy (error correction coding) or by multiple transmissions. For the purposes of our analyses, a 10^{-5} bit error rate for all high speed data will be accepted.

6. Facsimile

Standard facsimile equipments described in MIL-STD-188A (25 April 1958) transmits 8 x 10 copy with line advance of 96 lines per inch at rates of 180, 90 or 45 lines per seconds to transmit a page. To digitalize this

transmission, it will be assumed that reasonably acceptable results are obtained when 120 lines per second facsimile signal is converted into a two-level (black and white) signal which is transmitted at 2400 bits/sec. Similarly for a 45-line per second system, 1200 samples/sec would be satisfactory.

In Table 5 bit rates and bit error rates for several levels of quantization are specified. These are given as a function of the three different drum rotation rates which determine the time required to transmit a picture. The bit error rates are given in a general form, assuming an average of "n" errors per picture line (96 lines per inch) and, for a specific illustrative case, assuming an average of four errors per line. It should be recognized that it has been assumed that there is a one-to-one correspondence between bit errors and picture element errors. This correspondence is not true, of course, as the number of bits representing each picture element (sample) is greater than one. In Table 5, 16-level quantization represents 4 bits per sample and, for values of n less than 4, the use of the one-to-one correspondence between bit errors and picture element errors provides a good estimate of the effect of errors. It is worth noting that the allowable bit error rate as given in Table 5 is independent of the drum rotation rate. If one were to accept an average of four errors per line, the allowable bit error rates would range from 2.5×10^{-3} to 6.67×10^{-4}, depending upon the number of levels into which each picture sample is quantized. For our purposes an error rate of 10^{-3} will be used.

7. Transmission of Digital Information

In order to transmit digital data in a system with frequency division multiple access, two methods can be used depending on the design of the receivers.

1. Data can be transmitted through the analog channel optimized for transmission of voice;

Drum Roation Rate (lines per min.)		45	90	180
Picture Transmission Time (8 x 10) in sec.		1280	640	320
Sampling Rate (samples/sec.)		1200	2400	4800
2-level Quantization	Bit Rate	1200	2400	4800
	Bit Error Rate (n errors per line)	$(\frac{n}{1600})$	$(\frac{n}{1600})$	$(\frac{n}{1600})$
	Bit Error Rate (4 errors per line)	2.5×10^{-3}	2.5×10^{-3}	2.5×10^{-3}
4-level Quantization	Bit Rate	2400	4800	9600
	Bit Error Rate (n errors per line)	$(\frac{n}{3200})$	$(\frac{n}{3200})$	$(\frac{n}{3200})$
	Bit Error Rate (4 errors per line)	1.25×10^{-3}	1.25×10^{-3}	1.25×10^{-3}
8-level Quantization	Bit Rate	3600	7200	14,400
	Bit Error Rate (n errors per line)	$(\frac{n}{4800})$	$(\frac{n}{4800})$	$(\frac{n}{4800})$
	Bit Error Rate (4 errors per line)	8.3×10^{-4}	8.3×10^{-4}	8.3×10^{-4}
16-level Quantization	Bit Rate	4800	9600	19,200
	Bit Error Rate (n errors per line)	$(\frac{n}{6400})$	$(\frac{n}{6400})$	$(\frac{n}{6400})$
	Bit Error Rate (4 errors per line)	6.25×10^{-4}	6.25×10^{-4}	6.25×10^{-4}

Table 5 Summary of facsimile analog-to-digital conversion analysis.

(From WDL-Tech Memo 82 - by permission)

2. Special receivers for digital transmission are used.

In the first case the threshold of the FMFB receiver will dictate the required (SNR)in in the same manner as was discussed for voice transmission.

In the second case however various combinations of modulation schemes and receivers can be used and these result in different requirements for (SNR) corresponding to the bit error rate requirements. This problem is discussed below.

Conversion of Bit Error Rates into an Equivalent Signal to Noise Ratio

The signal to noise ratio at the output of a digital transmission channel which is required to yield a specified probability of error can be computed from the relationship between power and energy. Thus the energy to noise power density ratio can be expressed as

$$\frac{E}{N_o} = \frac{EB}{N} = \left(\frac{S}{N}\right)TB$$

where B = noise bandwidth

E = energy per bit

T = integration time (pulse duration)

N = noise power

N_o = noise power density

S = signal power

Thus when $B = \frac{1}{T}$ the signal to noise ratio equals the energy to noise density ratio. Since T represents the duration of one bit, this condition states that E/N_o is equal to the received signal to noise ratio measured in a bandwidth equal to the reciprocal of pulse duration. Thus, for example, if the bit rate is 2400 bits/second, each bit is $\frac{1}{2400}$ second

long and the bandwidth B is taken as 2400 cps. The selection of the bandwidth allows a relatively low pulse distortion.

It is therefore necessary to find the relationship between the probability of error and the enrgy per bit-to-noise density ratio (E/N_o). It is apparent that the choice of the modulation-demodulation technique will strongly influence the results.

Many techniques can be used and the results for some of them are summarized in Figs. 7 and 8.[11] Fig. 7 refers to cases when the rf carrier is directly modulated by the binary data stream while Fig. 8 shows the results when the data stream first modulates a subcarrier which in turn modulates an rf carrier. The choice of the modulation technique will be dictated by the overall system considerations. For example, subcarrier modulation techniques have been very popular, particularly when relatively slow data rates are involved. A typical modulation scheme consists of two stages. First a binary data stream bi-phase modulates a subcarrier which in turn phase modulates an rf carrier. At the receiver the modulated subcarrier is first recovered by a narrow band phase lock loop and the data is then recovered by conventional biphase detectors. Note the following advantage of this technique. The phase lock loop which recovers the subcarrier at the receiver requires a noise bandwidth which is substantially smaller than the data bandwidth. As a result an almost noiseless reference signal can be established. This statement is valid for most of the data rates of interest except possibly for the case of a single teletype channel which remains to be investigated.

If we now assume that the noise at the input to the phase lock loop is white and gaussian and that the bit timing and the phases of the two signals at the input of the biphase detector have been derived and are known exactly, the probability of error can be computed from the following formula.

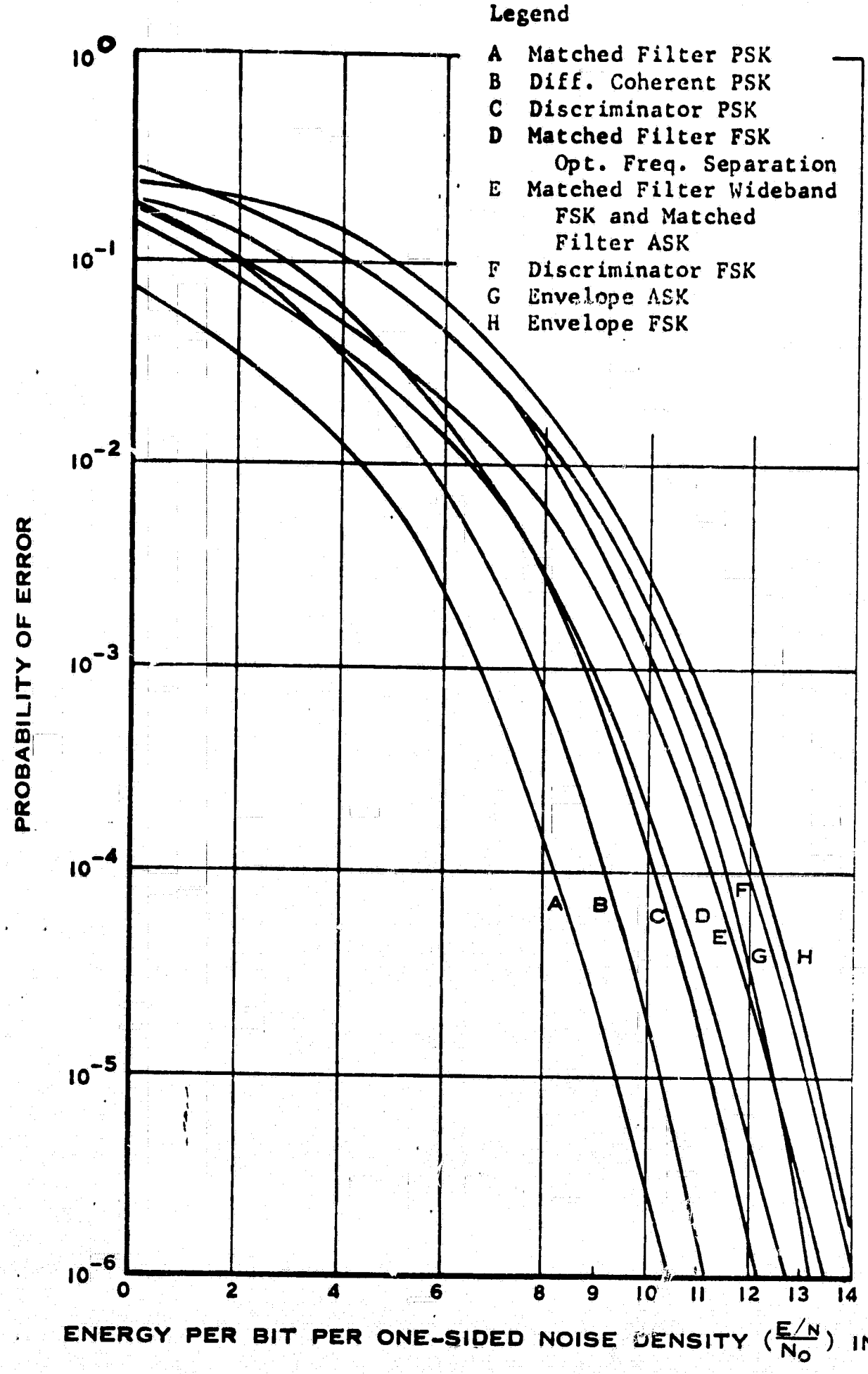


Figure 7 Probability of Error for Non-Subcarrier Binary Systems

Source: Philco W.D.L. Tech Memo No. 82

Legend

A Matched Filter PSK
B Matched Filter PSK-PM
FSK-PM, and ASK-PM
C Sine φ-Matched Filter
PSK-PM
D Sine φ-Diff. Coherent
PSK-PM
E Sine φ-Discriminator PSK-PM
F Sine φ-Matched Filter FSK-PM
Opt. Freq. Separation
G Sine φ-Matched Filter Wide-
band FSK-PM
H Sine φ-Discriminator FSK-PM
I Sine φ-Envelope FSK-PM
J Sine φ-Matched Filter ASK-PM
K Sine φ-Envelope ASK-PM

Note: All systems are PM and/or FM

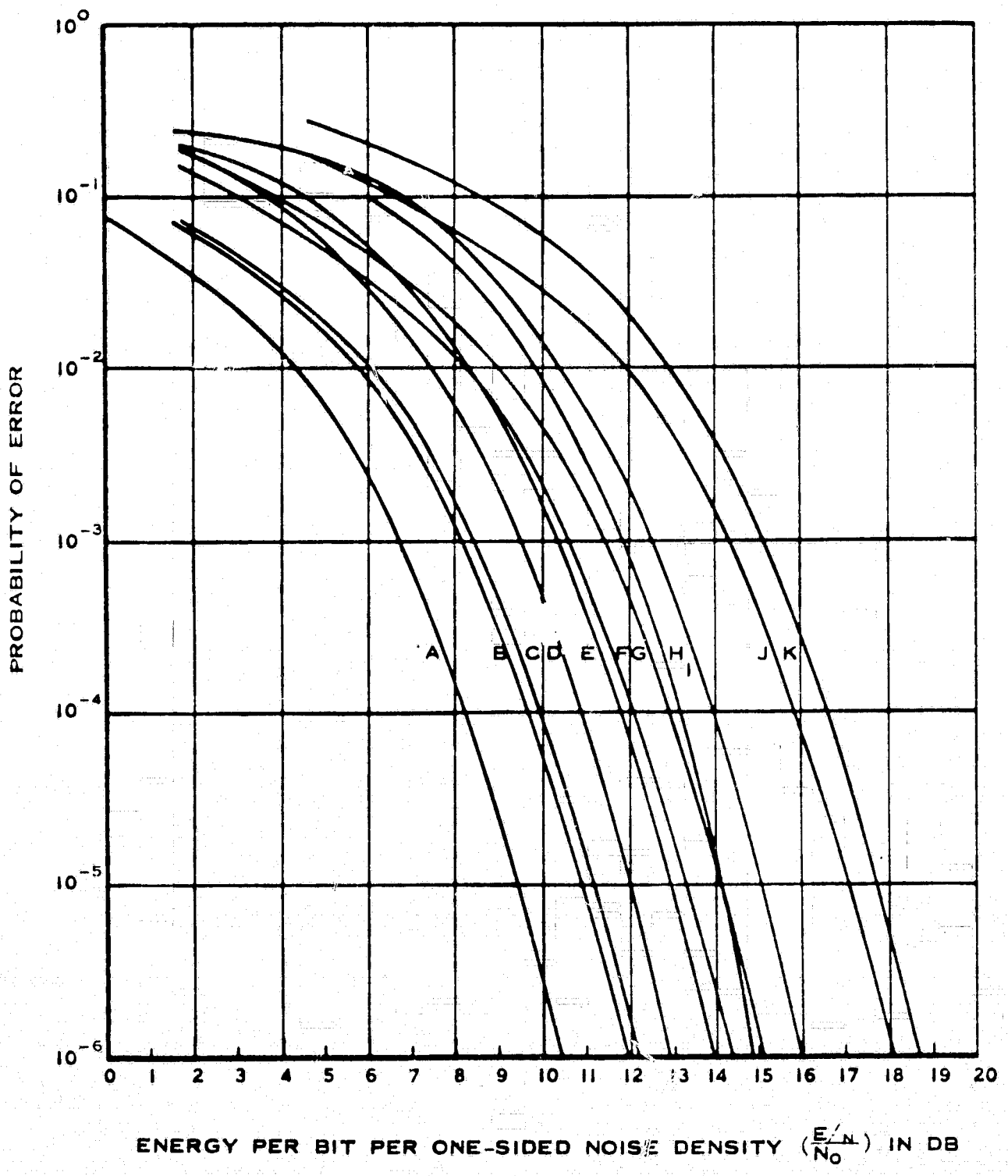


Figure 8 Probability of Error for Subcarrier Binary Systems

$$P_e = \frac{1}{\sqrt{2}} \int_{\sqrt{\frac{2J_1^2(B)\,E(1-\rho)}{N_o}}}^{\infty} \mathrm{Exp}\left(-\frac{x^2}{2}\right) dx \qquad \text{..... (12)}$$

where $J_1(B)$ is the first-order Bessel function of the first kind with argument B.

B is the modulation index for the phase modulation.

E is the energy in one bit of signal, i.e., the average signal power times the bit length, T.

ρ is the correlation between the two alternative signals subject to detection in the correlation detector.

N_o is the one-sided noise-power spectral density.

If we now assume that phase reversal (180°) is used to modulate the subcarrier and that the modulation index of the main carrier is B = 1.4, we obtain $\rho = -1$ and formula (12) becomes:

$$P_e = \frac{1}{2\pi} \int_{\sqrt{\frac{1.175E}{N_o}}}^{\infty} \exp\left(-\frac{x^2}{2}\right) dx \qquad \text{..... (13)}$$

Equation (13) is plotted in Fig. 9 from which the energy to noise density ratio for various required probabilities of error can be computed. As explained previously, the E/N_o equals the required SNR measured in the bandwidth which is the reciprocal of the bit rate.

It is rather difficult to precisely define the rf bandwidth which is required to maintain satisfactory operation. We will assume for our study

that a sinusoid of frequency f_o of duration T requires a bandwidth of approximately 1.0/T centered around f_o for the distortion to be acceptably small. Thus the subcarrier whose phase is reversed at the rate of 2400 reversals/sec requires an output bandwidth of 2400 cps. The bandwidth on the output of the rf modulator however will depend on the subcarrier frequency. With a modulation index of approximately 1.4 radians, the minimum permissible bandwidth at the output will be twice the input bandwidth or $2 \times (f_o + \frac{0.5}{T})$. Thus to minimize the bandwidth f_o should be low. Assuming that $f_o = \frac{4}{T}$ (four times the bit rate) for example, the total rf bandwidth required is approximately $\frac{9.0}{T}$ (nine times the bit rate). Thus for bit rates of 2400 cps we require an rf bandwidth of approximately 21.6 KC under the most optimistic conditions. From Fig. 9, for an error rate of 10^{-5}, we would require approximately 11.8 dB SNR in 2400 cps. Assuming that no SNR improvements occur in the receiver, this is equivalent to about 2.8 dB in the rf bandwidth of 21.6 K or a carrier to noise density ratio of approximately 46 dB.

It can be seen from Figs. 8 and 9 that the subcarrier modulation requires a slightly higher SNR than the direct carrier methods to achieve the same error rate. This penalty is sometimes accepted for reasons of ease of manufacture and practical implementation. If the rf carrier is directly modulated by the data stream, substantial savings in rf bandwidth are possible. In this case the subcarrier of the previous example can be considered as the final carrier. Thus the output rf bandwidth under most optimistic assumptions would be equal to the bit rate.

In actual practice, this is not practical and the rf bandwidth approximates 1 5T while the baseband filler is approximately 1 1T. This technique is limited by practical consideration of equipment design to the cases where the bit rate constitutes a reasonable percentage of the carrier frequency.

If operation is at i.f. and a second step of modulation (other than AM) is added, we are back to the subcarrier case. Since our study concerns

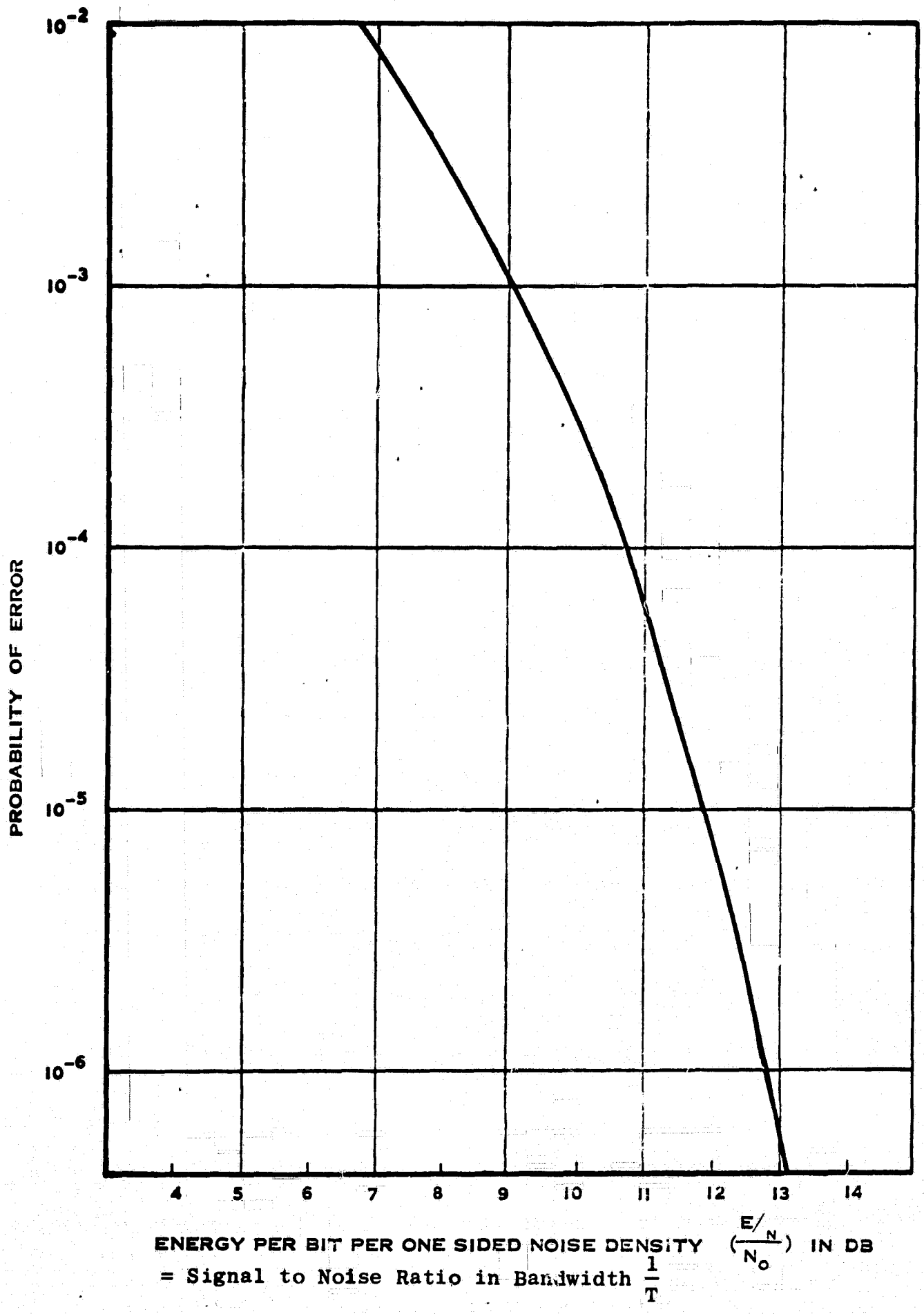


Figure 9 Probability of Error for PSK-PM Modulation-Demodulation Technique (Assuming mod index = 1.4 and bi-phase modulation)

carriers in the X-band range and relatively low bit rates direct modulation of carrier is not practically feasible. As a result we will use Fig. 9 to determine the SNR requirements and assume that the minimum rf bandwidth required is

$$B_{rf} = 9 \times (\text{bit rate}) \text{ cps}$$

Summary of Performance Requirements and Combined System

The results of the preceding sections are summarized in Table 6. A special digital systems receiver for PSK-PM modulation scheme has been assumed in case of digital transmission and a frequency feedback receiver has been assumed to receive analog signals which are frequency modulated with modulation index m.

For analog transmission, operation at threshold is assumed and corresponding figures are given for SNR and B. If SNR at input to the receiver is higher than threshold, different values of bandwidth and modulation index would result.

Table 6

SUMMARY OF REQUIRED PERFORMANCE CRITERIA

Modulation Technique		Performance Requirements: Information bandwidth b KHTz	Performance Requirements: Output SNR in information bandwidth	Performance Requirements: Bit Error Rate	Performance Requirements: $\frac{E}{N_o}$	Nominal RF Bandwidth KHz	Required SNR in Nominal RF Bandwidth (dB)	Required Signal-to-Noise Density Ratio (C/N_o)
FM (Operation at FMFB Threshold)	Analog Voice 90% to 95% Intelligibility	4	24	-	-	30	7.1	51
	Digital Transmission Optimized for Analog Voice	4	24	-	-			
	Television from Satellite	4000	33	-		{54200 {32000	{5 {13	{82 {88.2
For PSK-PM Modulation Scheme	Vocoded Voice (2400 bits/sec)	2.4	-	10^{-2}	6.5	21.6	-2	41
	Teletype (75 bits/sec)	0.075	-	10^{-4}	10.5	0.675	+1	29
	High-Speed Data (2400 bits/sec)	2.4	-	10^{-5}	11.7	21.6	+2	46
	Facsimile	2.4	-	10^{-3}	9.0	21.6	0	43

The values of RF bandwidth and required input SNR have been computed for operation at threshold, thereby resulting in minimum power requirements and relatively large bandwidth. If smaller bandwidths are required, operation above threshold is necessary and the required values can be computed from equations (1), (3), (7), and (8).

References

1 "Intelligibility of Peak Clipped Speech at High Noise Levels," by Irwin Pollack and J. M. Pickett, Journal of Acoustical Society of America, Vol. 31, No. 1, January 1959.

2 "Handbook of Experimental Psychology," by S. S. Stevens, p. 1064.

3 R. J. Christman, G. E. Renaud, and A. Rubin, "The Effects of Speech and Noise Level and Masking of Speech by Pure Tones in Random Noise," RADC Tehcnical Note 60-97, July 1960 (AD 241096).

4 N. R. French and J. C. Steinberg, "Factors Governing the Intelligibility of Speech Sounds," Journal of Acoustical Society of America, Vol. 19, p. 102, January 1947.

5 Transactions AIEE, March 1962, p. 8213, "Speech Volumes on Bell System Message Circuits."

6 P. Frutiger, "Noise in FM Receivers with Negative Frequency Feedback," Proceedings of the IEEE Vol. 54, No. 11, Nov 1966.

7 H. Mertens, "Method of Specifying the Signal-to-Noise Ratio for a Satellite Television-Distribution System," European Broadcasting Union Review No. 103-A.

8 R. W. Steele, "Performance of Vocoder Equipments...," 1964 International Symposium on Global Communications, Philadelphia, June 4, 1964.

9 "Analysis of IOS-STC Interstation Communication Problems," prepared for USAF-SSD by Philco WDL.

10 P. A. Baker, "Phase Modulation Data Sets for Serial Transmission at 2000 and 2400 Bits Per Second," Communications and Electronics #61, July 1962.

11 Philco WDL Communication Sciences Tech Memo No. 82, P. D. Shaft and H. N. Shaver, June 1964.

12 Final report "Technical and Cost Factors that Affect Television Reception from a Synchronous Satellite", Atlantic Research Corp. - Contract NASW-1305 June 1966.

References (cont'd)

W.K.E. Geddes, "A Meter for the Assessment of Dropouts in Video Tape Recording," E.B.U. Review, No. 78-A, April 1963.

"Record of Investigations Undertaken by the E.B.U. Ad-hoc Group on Colour Television", published by the E.B.U. Tehcnical Centre, October 1963, pp. 26 and 110.

APPENDIX L

SPACE SEGMENT ESTABLISHMENT AND MAINTENANCE ANALYSIS

SYSTEM ESTABLISHMENT AND MAINTENANCE ANALYSIS

I INTRODUCTION

The objective of this study is to derive expressions for the number of launches required to establish and to maintain a system of n satellites in orbit.

It is assumed that the satellite life time is a negative exponential function and the launches occur at uniform time intervals. The conventional approach, based on a Markov process, is used with transition probabilities being derived in terms of moment generating functions.

Computer runs for this study have been performed by TRW Corporation, Redondo Beach, California, using their programs.

II MATHEMATICAL APPROACH

The development which follows is based on the simplifying assumption that failures of orbiting satellites occur at discrete time intervals T and that all launches occur at the end of the interval. Accordingly we can define the conditional probability P_{in} which denotes the state of the satellite system at the beginning of the time interval T. More specifically P_{in} represents the probability of transition from exactly i satellites functioning in orbit in the T's period of time to exactly n satellites functioning in orbit in the (T + 1)th period of time. If the time pericd T is chosen to correspond to the launch interval, the transition probability matrix will be identical for all time intervals.

We assume that the satellite life time is a negative exponential function

$$P = \exp -\left(\frac{t}{m}\right) = \exp\ (-T) \qquad \ldots\ldots\ldots\ldots \qquad (1)$$

where m is the satellite mean life, and

t is the interval between launches.

T = t/m represents the interval between launches where the unit of time is one mean lifetime of the satellite, then

$$Q = (1 - P) \qquad \ldots\ldots\ldots\ldots \qquad (2)$$

denotes the probability that a satellite fails during the interval T. Thus the probability that exactly n satellites survive the time interval T if i satellites are in orbit at the beginning of T is given by the binomial distribution

$$b(n;i,P) = \frac{i!}{n!(i-n)!} P^{n} Q^{(i-n)} \qquad \ldots\ldots\ldots\ldots \qquad (3)$$

The moment generating function[1,*] f(x,i) for the bionomial is

$$(Px + Q)^{i} \qquad \ldots\ldots\ldots\ldots \qquad (4)$$

or from (1)

$$\left[\exp(-T) \cdot x + (1-\exp(-T)\right]^{i} \qquad \ldots\ldots\ldots\ldots \qquad (5)$$

which represents the probability that i satellites will survive the time interval T. Similarly since the outcome of a launch is independent of the behavior of the satellite in orbit the generating function for a successful launch is

$$(px + q) \qquad \ldots\ldots\ldots\ldots \qquad (6)$$

where p is the combined booster and deployment reliability and

$$q = (1 - p) \qquad \ldots\ldots\ldots\ldots \qquad (7)$$

represents the probability of launch failure.

There are two ways in which a transition from i satellites at the beginning of period T to n satellites at the beginning of period (T + 1) can occur.

---

* All references are listed on the end of this report.

1. Either (n-k) satellites survive period T (which is equivalent to saying that (i-n+k) satellites fail during period T) and then a successful launch of k satellites occurs;

or

2. n satellites survive period T (i.e., (i-n) satellites fail) followed by a launch failure.

The transition probability therefore is the sum of two probabilities corresponding to the above two cases and can be calculated from the product of generating functions (4) and (6).

$$(Px + Q)^i (px + q) \qquad \ldots\ldots\ldots\ldots \qquad (8)$$

or

$$\overline{\exp(-T)x + (1-\exp(-T)}^{\,i} \qquad \ldots\ldots\ldots\ldots \qquad (9)$$

Equation (8) can be expressed in matrix form to permit the calculation of probabilities P_{in} from the coefficients of x^n. The general term of the transition probability matrix can be shown to be

$$P_{in} = \binom{i}{n} P^n Q^{i-n} q + \binom{i}{n-k} P^{(n-k)} Q^{i-n+k} p \qquad \ldots\ldots\ldots\ldots \qquad (10)$$

where k represents the number of satellites launched with one booster and $\binom{i}{n}$ represents the number of combinations of i things taken n at a time. Note that for $n > i$, $\binom{i}{n}$ automatically goes to 0

and for $n > (i+k)$, $\binom{i}{n-k}$ automatically goes to 0.

Thus we have the special cases

$$P_{in} = Q^i q \text{ for } n = 0$$

$$= P^i p \text{ for } n = i+k$$

$$= 0 \text{ for } n > i+k$$

The P_{in}'s form an infinite matrix A assuming an unlimited number of satellites can be launched.

$$A = \begin{bmatrix} P_{00} & P_{01} & 0 & 0 & 0 & \cdot & \cdot \\ P_{10} & P_{11} & P_{12} & 0 & 0 & \cdot & \cdot \\ P_{20} & P_{21} & P_{22} & P_{23} & 0 & \cdot & \cdot \\ \cdot & \cdot & \cdot & \cdot & \cdot & \cdot & \cdot \\ \cdot & \cdot & \cdot & \cdot & \cdot & \cdot & \cdot \\ \cdot & \cdot & \cdot & \cdot & \cdot & \cdot & \cdot \end{bmatrix} \quad \ldots.(11)$$

Using (10), A can be written

$$A = \begin{bmatrix} q & p & 0 & 0 & & \\ Qq & Pq+Qp & Pp & 0 & \cdot & \cdot \\ Q_q^2 & Q(2Pq+Qp) & 3PQ(Pq+Qp) & P_p^2 & \cdot & \cdot \\ \cdot & \cdot & \cdot & \cdot & \cdot & \cdot \\ \cdot & \cdot & \cdot & \cdot & \cdot & \cdot \end{bmatrix} \quad \ldots.(12)$$

More explicitly using (1), (2), and (7)

$$A = \begin{bmatrix} (1-p) & p & 0 & \cdot\ \cdot\ \cdot \\ (1-p)(1-\exp(-T)) & p+\exp(-T)-2p\,\exp(-T) & p\,\exp(-T) & \cdot\ \cdot\ \cdot \\ \cdot & \cdot & \cdot & \cdot\ \cdot\ \cdot \\ \cdot & \cdot & \cdot & \cdot\ \cdot\ \cdot \end{bmatrix} \quad \ldots(13)$$

Let $F_{0,k}^{y}$ denote the probability of having precisely k satellites in orbit at the yth launch, given no satellites were in orbit at time zero.

Define a row vector $F_0^y = (F_{0,0}^y, F_{0,1}^y \ldots F_{0,n}^y \quad 0, \ldots)$ ....(14)

which represents a discrete probability density function described by $F_{0,k}^{y}$.

It can be shown[2] that given a row vector F_0^y and matrix A

$$F_0^{y+1} = F_0^y \cdot A \qquad \ldots\ldots\ldots\ldots \quad (15)$$

To define the initial probability density function F_0^0, we assume that at zeroth launch (which represents no launch at all) the probability that we have no satellite in orbit is unity ($p = 1$). Hence from (15)

$$F_0^0 = (1, 0, \ldots .)$$

$$F_0^1 = F_0^0 A = (q, p, 0, \ldots .)$$

$$F_0^2 = F_0^1 A = ((q^2 + Qpq), (qp + Pqp + Qp^2), Pp^2, 0, \ldots),$$

$$\text{etc.} \qquad \ldots\ldots\ldots\ldots \qquad (16)$$

The initial vector F_0^0 and the matrix A completely define a Markov chain. It can also be shown[3] that

$$F_0^{y+1} = F_0^y A = F_0^0 A^{y+1} \qquad \ldots\ldots\ldots\ldots \qquad (17) .$$

A. Systems Establishment

Using the above expressions, it is possible to derive a table of probabilities of establishing a system of n satellites with a given number y of launches.

The infinite matrix A is now reduced to a finite (n+1) x (n+1) square matrix A_1 by replacing the last row by (0, 0, 0 ..... 0, 1). This restricts the calculations to satellite failures occurring before all n satellites are established. Hence

$$A_1 = \begin{matrix} \overline{P_{00}} & P_{01} & 0 & \ldots\ldots & 0 \\ P_{10} & P_{11} & P_{12} & \ldots\ldots & 0 \\ \cdot & \cdot & \cdot & & \\ \cdot & \cdot & \cdot & & \\ \cdot & \cdot & \cdot & & \\ P_{n-1,0} & P_{n-1,1} & P_{n-1,2} & \ldots\ldots & P_{n-1,n} \\ \underline{0} & 0 & 0 & \ldots\ldots & 1 \end{matrix} \qquad \ldots\ldots(18)$$

Let the row vector associated with A_1 be denoted by

$$X_0^y = (X_{0,0}^y, X_{0,1}^y \ldots\ldots, X_{0,n}^y) \qquad \ldots\ldots\ldots\ldots\ldots \quad (19)$$

The last element $X_{0,n}^y$ denotes the probability of having n satellites in orbit for the first time in y launches or less.

Similarly if the last row of the matrix A is replaced by (0,0....0,0), we obtain a transition matrix A_2.

$$A_2 = \begin{bmatrix} P_{00} & P_{01} & 0 & \ldots\ldots & 0 \\ P_{10} & P_{11} & P_{12} & \ldots\ldots & 0 \\ \cdot & \cdot & \cdot & & \\ \cdot & \cdot & \cdot & & \\ P_{n-1,0} & P_{n-1,1} & P_{n-1,2} & \ldots\ldots & P_{n-1,n} \\ 0 & 0 & 0 & \ldots\ldots & 0 \end{bmatrix} \qquad \ldots\ldots(20)$$

with an associated row vector

$$K_0^y = (K_{0,0}^y, K_{0,1}^y \ldots\ldots K_{0,n}^y) \qquad \ldots\ldots\ldots\ldots\ldots \quad (21)$$

The last element $K_{0,n}^y$ defines the probability of having precisely n satellites in orbit at the yth launch.

Since $X_{0,n}^y$ represents a cumulative probability

$$X_{0,n}^y = \sum_{k=n}^{y} K_{0,k}^y \qquad \ldots\ldots\ldots\ldots\ldots \quad (22)$$

or $$K_{0,n}^y = X_{0,n}^y - X_{0,n}^{y-1} \qquad \ldots\ldots\ldots\ldots\ldots \quad (22)$$

The expected number of launches E(y) required to establish the system of n satellites for the first time can now be obtained from

$$E(y) = \sum_{y=n}^{\infty} y \cdot K_{0,n}^y \qquad \ldots\ldots\ldots\ldots\ldots \quad (23)$$

The cumulative density $X^{y}_{0,n}$ can be used to determine the confidence level for a particular launch sequence.

Example: As an example of the application of the approach described above, the number of launches required to establish a system of 2 satellites is computed below for the following parameters:

T = launching time interval = 1 mo.

m = satellite mean life = 12 mos.

P = exp(- 1/12) = 0.92

Q = 1 - P = 0.08

p = 0.7

q = 1 - p = 0.3

The results are shown in Table 1.

Table 1

Probabilities of Establishing the System of Two Satellites Launched One at a Time

(1) Launch Number y	(2) Cumulative Density $X^{y}_{0,2}$	(3) Density $K^{y}_{0,2}$	(4) Expected Number of Launches $\sum_{y=2}^{\infty} y.K^{y}_{0,2} = \sum_{y=2}^{\infty}$ Col(1)xCol(3)
2	.44183	.44183	.88366
3	.72676	.28493	1.73844
4	.87219	.14543	2.32017
5	.94127	.06908	2.66558
6	.97321	.03194	2.85721
7	.98782	.01461	2.95945
8	.99447	.00665	3.01266
9	.99749	.00302	3.03985
10	.99886	.00137	3.05358
11	.99948	.00062	3.06043

The second column shows that one could establish the system with 5 launches with a 94.127% confidence factor. By interpolating the number of launches corresponding to a 90% confidence level is found to be approximately 4.4.

The expected number of launches to establish the system is shown by the last entry in Col. 4, i.e., 3.06 launches.

B. System Restoration

This problem relates to the situation in which the first satellite failure occurs after n satellites are established. It is assumed that the delay from the time the satellite fails to the time of restoration launching is T_2. Since more satellites could fail during this time lag, the probable state of the system after launch is represented by the generating function

$$(P_1 x + Q_1)^{n-1} (px + q) \qquad \ldots\ldots\ldots\ldots\ldots \quad (24)$$

where $P_1 = \exp(-\frac{t_2}{m}) = \exp(-T_2)$

$Q = (1 - P)$

The same transition matrices, as those developed previously, can be used provided the first launch occurs at time zero.

The probable states of the system after the first restoration launch are determined in the same manner as previously described, i.e.,

$$X^2_{n-1} = X^1_{n-1} A_1 \qquad \ldots\ldots\ldots\ldots\ldots \quad (25)$$

and in general

$$X^{y+1}_{n-1} = X^y_{n-1} A_1 \qquad \ldots\ldots\ldots\ldots\ldots \quad (26)$$

where A_1 is the transition matrix and X is the row vector associated with A_1.

Example 2: For the same system described in the previous example, the probabilities of restoration are shown in Table 2.

Table 2

Probabilities of Restoring a System of Two Satellites

(1) Launch Number y	(2) Cumulative Density $X^{y}_{1,2}$	(3) Density $K^{y}_{1,2}$	(4) Expected Number of Launches $\sum_{y} \cdot K^{y}_{1,2}$
1	.63756	.63756	.63756
2	.85298	.21542	1.0684
3	.93662	.08363	1.3193
4	.97187	.03525	1.4603
5	.98735	.01548	1.5378
6	.99429	.00692	1.5793
7	.99741	.00312	1.6012
8	.99882	.00141	1.6125
9	.99947	.00064	1.6183

It can be seen that the expected number of launches to restore the system is approximately 1.62 as shown by the last entry of column 4 and that approximately 2.6 launches are necessary to restore the system with a 90% confidence. (Interpolation between the figures in column 2).

C. System Maintenance

The approximate relation used to derive the annual number of maintenance launches is

$$\text{Annual launches} = \frac{12}{\frac{m}{nL} + t_2}$$

where m is the satellite mean life (months)

n is the number of satellites in the system

L is the number of restoration launches required

t_2 is the time delay from satellite failure to first restoration launch (months).

Note that only L is considered as a stochastic variable. The derivation of equations considering m and L as variables is rather complex and was considered outside the scope of this study. Thus the expected value of the number R of annual launches to maintain the system is

$$E(R) = \frac{12}{\frac{m}{n} \cdot \frac{1}{E(L)} + 1}$$

and the 90% confidence value is

$$(R)_{90} = \frac{12}{\frac{m}{n} \cdot \frac{1}{L_{0.9}} + 1}$$

where E(L) and $L_{0.9}$ are respectively the expected number of restoration launches and the number of restoration launches required to attain 90% confidence level.

D. Tables of Launch Requirements

The summary of results presented in this section is based on calculations which have been made using the various relationships developed in the preceding paragraphs for the following set of system parameters.

n = number of satellites in system	= 1,2,3,4,5,6,7,8,9,10
k = number of satellites launched per launch vehicle	= 1,2,3*
p = booster reliability	= 0.7, 0.8, 0.9
r = satellite deployment reliability	= 0.99
m = satellite mean-time-to-failure	= 3 yrs, 5 yrs, 1 yr.
t = interval between launches	= 1 month

t_2 = interval to first launch after restoration decision is made = 1 month

c = EXP (-t/m) = EXP (-T) = 0.9726, 0.9834, 0.9200

d = EXP ($-t_2/m$) = EXP ($-T_2$) = 0.9726, 0.9834, 0.9200

g = number of satellites which must fail to require replenishment action = 1

* for replenishment, only k = 1 was considered.

Computer runs utilizing programs developed by TRW Corporation (Redondo Beach, California) have been used and the results are summarized in Tables 1 through 11 as follows.

1. Establishment Statistics: Number of expected launches to establish a system of n satellites -

Table 1	one satellite per launch
Table 2	two satellites per launch
Table 3	three satellites per launch

Number of launches to establish a system of n satellites with 90% confidence -

Table 4	one satellite per launch
Table 5	two satellites per launch
Table 6	three satellites per launch

2. Replenishment Statistics: Number of launches to restore a system of n satellites (one satellite per launch) -

Table 7	expected number of launches
Table 8	number of launches for 90% confidence level

Annual number of launches to maintain a system of n satellites (one satellite per launch)

Table 9	expected number of launches
Table 10	number of launches for 90% confidence level

Number of launches required for 5 years to maintain a system of n satellites

Table 11	number of launches for 90% confidence level

Table 1

NUMBER OF EXPECTED LAUNCHES TO ESTABLISH A SYSTEM OF N SATELLITES

k = 1

Satellite Mean Time to Failure	Launch Success Probability	Minimum Number of Satellites in Orbit (n)									
		1	2	3	4	5	6	7	8	9	10
m = 1	0.7	1.4	3.1	4.9	7.1	9.6	12.7	16.6	21.6	28.4	38.5
	0.8	1.3	2.7	4.2	6.0	8.1	10.5	13.4	17.0	21.7	27.9
	0.9	1.1	2.4	3.7	5.2	7.0	9.0	11.2	14.1	17.5	21.8
m = 3	0.7	1.4	2.9	4.5	6.1	7.8	9.6	11.5	13.5	15.6	17.8
	0.8	1.3	2.6	3.9	5.3	6.8	8.3	9.9	11.5	13.3	15.1
	0.9	1.1	2.3	3.5	4.7	6.0	7.3	8.7	10.1	11.6	13.1
m = 5	0.7	1.4	2.9	4.4	6.0	7.6	9.2	10.9	12.6	14.4	16.2
	0.8	1.3	2.6	3.9	5.2	6.6	8.0	9.5	10.9	12.4	14.0
	0.9	1.1	2.3	3.4	4.6	5.8	7.1	8.3	9.6	10.9	12.3

Table 2

NUMBER OF EXPECTED LAUNCHES TO ESTABLISH A SYSTEM OF N SATELLITES

k = 2

Satellite Mean Time to Failure	Launch Success Probability	Minimum Number of Satellites in Orbit (n)									
		1	2	3	4	5	6	7	8	9	10
m = 1	0.7	1.4	1.5	2.9	3.2	4.5	5.2	6.5	7.5	8.9	10.2
	0.8	1.3	1.3	2.5	2.8	3.9	4.5	5.5	6.4	7.5	8.6
	0.9	1.1	1.1	2.2	2.5	3.5	3.9	4.8	5.5	6.5	7.4
m = 3	0.7	1.4	1.5	2.9	3.0	4.3	4.7	5.8	6.4	7.5	8.1
	0.8	1.3	1.3	2.5	2.6	3.8	4.1	5.1	5.5	6.5	7.0
	0.9	1.1	1.1	2.2	2.3	3.4	3.6	4.5	4.9	5.7	6.2
m = 5	0.7	1.4	1.5	2.9	3.0	4.3	4.6	5.8	6.2	7.3	7.8
	0.8	1.3	1.3	2.5	2.6	3.8	4.0	5.1	5.4	6.4	6.8
	0.9	1.1	1.1	2.2	2.3	3.3	3.5	4.5	4.7	5.6	6.0

Table 3

NUMBER OF EXPECTED LAUNCHES TO ESTABLISH A SYSTEM OF N SATELLITES

k = 3

Satellite Mean Time to Failure	Launch Success Probability	Minimum Number of Satellites in Orbit (n)									
		1	2	3	4	5	6	7	8	9	10
m = 1	0.7	1.4	1.4	1.5	2.9	2.9	3.3	4.4	4.7	5.4	6.3
	0.8	1.3	1.3	1.3	2.5	2.6	2.9	3.8	4.1	4.7	5.4
	0.9	1.1	1.1	1.1	2.2	2.3	2.5	3.4	3.6	4.1	4.7
m = 3	0.7	1.4	1.4	1.5	2.9	2.9	3.1	4.3	4.4	4.8	5.8
	0.8	1.3	1.3	1.3	2.5	2.7	2.7	3.8	3.8	4.2	5.0
	0.9	1.1	1.1	1.1	2.2	2.3	2.4	3.3	3.4	3.7	4.5
m = 5	0.7	1.4	1.4	1.5	2.9	2.9	3.0	4.3	4.3	4.7	5.7
	0.8	1.3	1.3	1.3	2.5	2.6	2.6	3.8	3.8	4.1	5.0
	0.9	1.1	1.1	1.1	2.2	2.2	2.3	3.3	3.4	3.6	4.5

Table 4

NUMBER OF LAUNCHES TO ESTABLISH A SYSTEM OF N SATELLITES WITH 90% CONFIDENCE

k = 1

Satellite Mean Time to Failure	Launch Success Probability	Minimum Number of Satellites in Orbit (n)									
		1	2	3	4	5	6	7	8	9	10
m = 1	0.7	2.0	4.5	7.0	10.2	14.1	19.0	25.3	34.0	46.6	65.9
	0.8	1.7	3.6	5.7	8.2	11.2	15.0	19.4	25.2	33.2	44.4
	0.9	1.1	2.8	4.7	6.7	9.1	11.9	15.4	19.7	25.1	32.4
m = 3	0.7	2.0	4.1	6.1	8.2	10.5	12.9	15.1	17.7	20.5	23.3
	0.8	1.7	3.3	5.0	6.8	8.6	10.5	12.5	14.6	16.7	19.0
	0.9	1.1	2.7	4.0	5.6	7.1	8.7	10.4	12.1	14.0	15.8
m = 5	0.7	2.0	4.0	6.0	7.9	9.9	11.9	14.0	16.1	18.3	20.5
	0.8	1.7	3.3	4.9	6.5	8.1	9.8	11.6	13.3	15.1	17.0
	0.9	1.1	2.7	3.9	5.4	6.8	8.2	9.7	11.1	12.7	14.3

Table 5

NUMBER OF LAUNCHES TO ESTABLISH A SYSTEM OF N SATELLITES WITH 90% CONFIDENCE

k = 2

Satellite Mean Time to Failure	Launch Success Probability	Minimum Number of Satellites in Orbit (n)									
		1	2	3	4	5	6	7	8	9	10
m = 1	0.7	2.0	2.0	3.9	4.7	6.2	7.5	9.0	10.6	12.5	14.6
	0.8	1.6	1.7	3.1	3.8	5.0	6.0	7.2	8.5	9.9	11.5
	0.9	1.0	1.2	2.6	3.0	4.0	4.8	5.8	6.9	8.0	9.2
m = 3	0.7	2.0	2.0	3.9	4.2	5.8	6.4	7.7	8.6	9.7	10.8
	0.8	1.6	1.7	3.1	3.5	4.7	5.2	6.3	7.0	8.0	8.8
	0.9	1.0	1.1	2.6	2.8	3.8	4.3	5.1	5.8	6.6	7.3
m = 5	0.7	2.0	2.0	3.9	4.1	5.7	6.2	7.6	8.2	9.4	10.2
	0.8	1.6	1.7	3.1	3.4	4.7	5.0	6.1	6.8	7.8	8.4
	0.9	1.0	1.2	2.6	2.7	3.8	4.1	5.0	5.6	6.4	6.9

Table 6

NUMBER OF LAUNCHES TO ESTABLISH A SYSTEM OF N SATELLITES WITH 90% CONFIDENCE

k = 3

Satellite Mean Time to Failure	Launch Success Probability	Minimum Number of Satellites in Orbit (n)									
		1	2	3	4	5	6	7	8	9	10
m = 1	0.7	2.0	2.0	2.1	3.9	4.1	4.9	6.0	6.6	7.6	8.6
	0.8	1.6	1.6	1.7	3.1	3.3	3.9	4.8	5.3	6.1	6.9
	0.9	1.0	1.1	1.2	2.6	2.7	3.1	3.9	4.3	4.9	5.6
m = 3	0.7	2.0	2.0	2.1	3.9	3.9	4.4	5.7	5.9	6.7	7.5
	0.8	1.6	1.6	1.7	3.1	3.1	3.6	4.7	4.8	5.4	6.1
	0.9	1.0	1.1	1.2	2.6	2.6	2.9	3.8	3.9	4.4	5.0
m = 5	0.7	2.0	2.0	2.1	3.9	3.9	4.3	5.7	5.8	6.4	7.4
	0.8	1.6	1.6	1.7	3.1	3.1	3.5	4.7	4.7	5.2	6.1
	0.9	1.0	1.0	1.2	2.6	2.6	2.8	3.8	3.9	4.3	4.9

Table 7

NUMBER OF EXPECTED LAUNCHES TO RESTORE A SYSTEM OF N SATELLITES

k = 1

Satellite Mean Time to Failure	Launch Success Probability	Minimum Number of Satellites in Orbit (n)									
		1	2	3	4	5	6	7	8	9	10
m = 1	0.7	1.4	1.6	1.8	2.1	2.5	3.1	3.8	5.0	6.8	9.9
	0.8	1.3	1.4	1.6	1.8	2.0	2.4	2.9	3.6	4.6	6.2
	0.9	1.1	1.2	1.4	1.5	1.7	2.0	2.3	2.7	3.4	4.3
m = 3	0.7	1.4	1.5	1.6	1.6	1.7	1.8	1.9	2.0	2.1	2.2
	0.8	1.3	1.3	1.4	1.4	1.5	1.5	1.6	1.7	1.7	1.8
	0.9	1.1	1.2	1.2	1.2	1.3	1.3	1.4	1.4	1.5	1.5
m = 5	0.7	1.4	1.5	1.5	1.6	1.6	1.6	1.7	1.7	1.8	1.8
	0.8	1.3	1.3	1.3	1.3	1.4	1.4	1.4	1.5	1.5	1.5
	0.9	1.1	1.1	1.2	1.2	1.2	1.2	1.3	1.3	1.3	1.3

Table 8

NUMBER OF LAUNCHES TO RESTORE A SYSTEM OF N SATELLITES WITH 90% CONFIDENCE

k = 1

Satellite Mean Time to Failure	Launch Success Probability	Minimum Number of Satellites in Orbit (n)									
		1	2	3	4	5	6	7	8	9	10
m = 1	0.7	2.0	2.6	3.1	4.0	5.1	6.7	9.0	12.6	18.4	28.5
	0.8	1.7	1.9	2.4	3.0	3.8	4.8	6.2	8.3	11.4	16.4
	0.9	1.1	1.6	1.9	2.3	2.9	3.6	4.5	5.8	7.7	10.4
m = 3	0.7	2.0	2.2	2.4	2.6	2.8	3.0	3.2	3.5	3.8	4.1
	0.8	1.7	1.8	1.9	1.9	2.1	2.3	2.5	2.7	2.9	3.1
	0.9	1.1	1.3	1.5	1.6	1.7	1.8	1.9	2.0	2.1	2.4
m = 5	0.7	2.0	2.1	2.2	2.3	2.4	2.6	2.7	2.8	2.9	3.9
	0.8	1.7	1.7	1.8	1.8	1.9	1.9	2.0	2.1	2.2	2.4
	0.9	1.1	1.2	1.3	1.4	1.5	1.6	1.7	1.7	1.8	1.8

Table 9

EXPECTED NUMBER OF ANNUAL LAUNCHES TO MAINTAIN A SYSTEM OF N SATELLITES

k = 1

Satellite Mean Time to Failure	Launch Success Probability	Minimum Number of Satellites in Orbit (n)									
		1	2	3	4	5	6	7	8	9	10
m = 1	0.7	1.3	2.6	3.8	5.0	6.2	7.3	8.3	9.2	10.1	10.7
	0.8	1.1	2.3	3.4	4.5	5.5	6.6	7.5	8.5	9.4	10.1
	0.9	1.0	2.0	3.0	4.0	5.0	6.0	6.9	7.8	8.6	9.4
m = 3	0.7	.5	.9	1.4	1.8	2.3	2.7	3.2	3.7	4.1	4.5
	0.8	.4	.8	1.2	1.6	2.0	2.4	2.8	3.2	3.6	4.0
	0.9	.4	.7	1.1	1.4	1.8	2.2	2.5	2.9	3.2	3.6
m = 5	0.7	.3	.6	.8	1.1	1.4	1.7	2.0	2.2	2.5	2.8
	0.8	.2	.5	.7	1.0	1.2	1.5	1.7	2.0	2.2	2.5
	0.9	.2	.4	.7	.9	1.1	1.3	1.5	1.8	2.0	2.2

Table 10

ANNUAL NUMBER OF LAUNCHES REQUIRED TO MAINTAIN A SYSTEM OF N SATELLITES WITH 90% CONFIDENCE

k = 1

Satellite Mean Time to Failure	Launch Success Probability	Minimum Number of Satellites in Orbit (n)									
		1	2	3	4	5	6	7	8	9	10
m = 1	0.7	1.71	3.63	5.24	6.86	8.16	9.24	10.08	10.72	11.19	11.51
	0.8	1.49	2.89	4.5	6.0	7.35	8.47	9.4	10.16	10.74	11.28
	0.9	1.01	2.53	3.86	5.21	6.57	7.71	8.69	9.53	10.23	10.76
m = 3	0.7	.63	1.31	2.0	2.69	3.36	4.0	4.6	5.25	5.85	6.39
	0.8	.54	1.09	1.64	2.09	2.71	3.32	3.92	4.5	5.04	5.55
	0.9	.36	.81	1.33	1.81	2.29	2.77	3.24	3.69	4.13	4.8
m = 5	0.7	.39	.78	1.19	1.59	2.0	2.48	2.87	3.26	3.64	4.0
	0.8	.33	.64	.99	1.29	1.64	1.92	2.27	2.62	2.98	3.43
	0.9	.22	.46	.73	1.02	1.33	1.65	1.99	2.22	2.55	2.77

Table 11
NUMBER OF LAUNCHES REQUIRED TO MAINTAIN A SYSTEM
OF N SATELLITES FOR 5 YEARS WITH 90% CONFIDENCE

k = 1

Satellite Mean Time to Failure	Launch Success Probability	Minimum Number of Satellites in Orbit (n)									
		1	2	3	4	5	6	7	8	9	10
m = 1	0.7	8.55	18.15	26.2	34.3	40.8	46.2	50.4	53.6	55.95	57.55
	0.8	7.45	14.45	22.5	30.0	36.75	42.35	47.0	50.8	53.7	55.9
	0.9	5.05	12.65	19.3	26.05	32.85	38.55	43.45	47.65	51.15	53.8
m = 3	0.7	3.15	6.55	10.0	13.45	16.8	20.0	23.0	26.25	29.25	31.95
	0.8	2.7	5.45	8.2	10.45	13.55	16.6	19.6	22.5	25.2	27.75
	0.9	1.8	4.05	6.65	9.05	11.45	13.85	16.2	18.45	20.65	24.0
m = 5	0.7	1.95	3.9	5.95	7.95	10.0	12.4	14.35	16.3	18.2	20.0
	0.8	1.65	3.2	4.95	6.45	8.2	9.6	11.35	13.1	14.9	17.15
	0.9	1.1	2.3	3.65	5.1	6.65	8.25	9.95	11.1	12.75	13.85

References

1 See for example "Probability Theory and Its Applications," W. Feller, J. Wiley & Sons, Inc., Chapter 11.

2 Ibid.

3 Ibid.

APPENDIX M

DETERMINATION OF CHANNEL CAPACITY OF AN ACTIVE SATELLITE

DETERMINATION OF CHANNEL CAPACITY OF AN ACTIVE SATELLITE

I INTRODUCTION

The objective of this technical note is to derive an expression for the total number of communication channels which an active satellite can accommodate when operating in a frequency-division-multiple access mode. The two cases considered are: (a) when a hard limiting transponder is used in the satellite, and (b) when a linear transponder is used.

The effects of intermodulation due to hard limiting are first reviewed and discussed. The equations for the channel capacity of the satellite are then derived for a general case of a hard limiting satellite. The capacity of a satellite with a linear transponder is then deduced from these equations.

II ASSUMPTIONS

It is well known that when several signals are passed through a hard limiting amplifier distortion products due to intermodulation between signals are generated which substantially reduce the signal-to-noise ratio at the output of the limiter. Several mathematical analyses of this problem have been performed over the past few years.* All have been based on a set of simplifying assumptions which do not always hold under actual operating conditions. The results, however, are useful since they indicate

---

* This section is based primarily on the following reports:

M. Gyi, "Some Topics on Limiters and FM Demodulators," Stanford University Report SEL-65-056, July 1965.

P. D. Shaft, "Intermodulation Interference in Frequency Division Multiple Access," Stanford Research Institute paper, 1966.

L. Schuchman, T. T. Jones, Philco Ford Report TM-115, Contract AF 30(602)-4392, Feb. 1967, "Error Rate Analysis of M'ary Transmitted Reference Systems.....," Appendices D and E.

the general behavior of the system and can be interpreted for various conditions where the assumptions may not be entirely valid.

Two cases of importance will be considered. One where the channel spacing within the allowable bandwidth is random and the other where channel spacing is uniform: The mathematical analysis of both of these cases have been reported in the technical literature and the results are summarized below. The assumptions that have been made for the sake of simplification are as follows:

1. No noise at the input to the limiter
2. Hard rather than soft limiting
3. Equal amplitude signals at the input to the limiter
4. Equal bandwidth signals at the input to the limiter
5. Phase shift through the limiter is independent of the amplitude of the input.

The first two assumptions represent the worst possible situation from the point of view of generation of intermodulation products and establishes therefore the lower bound for signal-to-intermodulation (SIR). Calculations for various amounts of input noise have been made and results are available. For our purposes however the worst case condition will be used.

The assumption of equal amplitude of input signals is made to avoid consideration of "signal suppression" effects. This situation would result in unequal amplitudes of intermodulation products of particular type and as a result SIR in various channels would change. Although signal suppression effects have been calculated for small numbers of signals, no generalized solution exists.

For our purposes, it will be assumed that all signals entering the hard limiter are roughly equal in power and consequently suppression effects on individual signals arising from power inequalities will not be considered. This assumption is justified on the basis that we are considering a system where all ground stations are identical and located

within a relative small geographical area. In addition, ground stations can be equipped with a closed or open loop power equalizing device if required.

The equal bandwidth assumption results in the spectrum of total intermodulation power being fairly uniformly distributed across the signal bandwidth. With "rectangular" input spectra the extent of cross products is always bounded by rectangles with power density greatest at the carrier frequency and falling off to zero at the limit set by the rectangles. (This assumes uniform carrier spacing.) Thus, for this case the worst case condition is again obtained and actual results in the field could be better than indicated by analytical results. The last assumption concerning the independence of the amplitude and the phase shift through the limiter is the most restrictive one from a practical point of view. It assumes that no AM to PM conversion occurs and as a consequence no intelligible crosstalk between the channels is generated. The magnitude of such crosstalk depends in a complicated manner on the signal design of the system and on the AM-PM dependence characteristics. Since in a well designed system crosstalk from this source would normally be within acceptable limits, it is assumed for the purposes of this study that no dependence between amplitude variations and phase shifts exist.

An additional consideration in our study is the fact that we are talking about a system with a large number of accesses. It has been shown[1] that a careful selection of carrier frequencies can result in a substantial improvement in the signal to intermodulation crossproduct ratio. This, however, is accomplished at the expense of bandwidth utilization. In our case, since we are interested in accommodating the largest possible number of accesses through one transponder, the economy of bandwidth is important. Accordingly bandwidth utilization must be maximized consistent with the required channel performance. We will therefore attempt to develop an expression relating the total number of accesses to the bandwidth utilization for a given set of system operating parameters.

We are also assuming in this study that the signal-to-noise ratios of individual communication channels are such as to permit operation of frequency modulated equipment with f-m feedback receivers. This means that the threshold SNR value of the FMFB receiver is exceeded in all cases.

Cahn[2] and others[3] have estimated that when a large number of signals uniformly spaced and contiguous is transmitted through a hard limiter, the resulting signal-to-intermodulation power density is approximately 9 dB. This result has been generally accepted and used in the literature and will constitute the starting consideration in our work. It assumes that the intermodulation crossproduct spectrum across the transponder is uniform.

III EXPRESSIONS FOR SIR AT THE OUTPUT OF THE HARD LIMITER

Notation

S/I = total signal to intermodulation power density

SIR = signal-to-intermodulation products ratio in bandwidth B $\frac{S}{IB}$

W = total bandwidth of hard limiting satellite transponder

B = receiver noise bandwidth

p_{max} = W/B maximum possible number of accesses in system

p = actual number of active accesses in system

$Q = \frac{pB}{W}$ = bandwidth utilization factor ($Q<1$) = $\frac{p}{p_{max}}$

$a = \frac{1}{Q} = \frac{W}{pB}$ = bandwidth "wastage" factor ($a>1$)

When all channels are uniformly spaced, the above relationships also hold for each individual access.

$a \cdot B = A$ represents carrier spacing or total bandwidth of one access ..... (1)

$p = \frac{W}{A} = \frac{W}{aB}$ ..... (2)

$a = \frac{W}{pB}$ = bandwidth "wastage" factor ($a>1$) ..... (3)

(reciprocal of bandwidth "utilization" factor)

A. SIR When Access Allocations are Randomly Selected

This case assumes that out of the total possible number of accesses $p_{max} = \frac{W}{B}$, only a certain number $p = Qp_{max}$ (randomly selected) is used at any one time. The ratio $Q = \frac{p}{p_{max}}$ (less than 1) represents the bandwidth utilization factor when equal bandwidth channels are used $Q = \frac{PB}{W} = \frac{1}{a}$.

Gyi[4] and Shaft[5] have shown that for a large number of accesses in an FDM multiple access system, if the accesses to be used are randomly selected from a uniform distribution (across the total number of accesses that can be accommodated by the transponder bandwidth), the signal-to-intermodulation density ratio is inversely proportional to the bandwidth utilization.* Shaft's formula for this case (using our symbols) is

$$SIR_{db} \simeq 9.0 + 10 \log \frac{W}{pB}$$

$$\simeq 9.0 + 10 \log a \qquad \ldots\ldots\ldots\ldots \qquad (4)$$

or expressed as a fraction

$$SIR = 8a \qquad \ldots\ldots\ldots\ldots \qquad (5)$$

Note that because of the assumptions explained previously, formula (5) represents the worst value for SIR.

This formula assumes that each access to be utilized is independently selected at random from a uniform distribution. In practice, because the total number of accesses that can be contained within the transponder bandwidth is finite, the probability distribution from which accesses succeeding the first one are selected will no longer be uniform unless the total number is very large.

As a result this formula becomes less accurate as W/B decreases. We will use it in our study with the understanding that it is applicable only in cases of systems capable of supporting a very large number of active accesses.

---

* SIR expresses the signal-to-intermodulation ratio in one cycle of bandwidth. Thus, it also represents SIR within bandwidth of the signal spectrum.

In actual practice a situation corresponding to the case under discussion would occur if out of p_{max} possible accesses only p were used because of duty factor of ground transmitters being less than 100%. Q would then represent the average fractional number of transmitters on the air. However due to the statistical nature of the traffic, the value of Q would vary continuously and as a result the SIR would also vary.

Accordingly, in order to guarantee a minimum value of SIR, only a specified maximum number of accesses can be allowed to operate at any one time. The imposition of such a maximum does not appear to represent a very practical solution unless a central switching terminal is used to control the traffic.

B. Accesses Uniformly Distributed Throughout the Transponder Bandwidth

The second possible system arrangement is one whereby individual access carriers are uniformly separated from each other. In this case, Q represents the ratio of signal bandwidth B to the carrier separation bandwidth A (access bandwidth).

Thus $$Q = \frac{B}{A} = \frac{pB}{pA} = \frac{pB}{W} \qquad (Q<1)$$

or $$a = \frac{W}{pB} \qquad (a>1) \qquad \ldots\ldots\ldots\ldots \qquad (3)$$

This case corresponds to the practical situation when more than the necessary bandwidth is assigned to each access, and all transmitters are active all the time. Such a situation could arise when each ground station handles a large volume of traffic and schedules it in such a manner as to insure continuous operation.

This case has been investigated by Schuchman and Jones[6] and their conclusions indicated that as the uniformly spaced carriers are separated further apart, the SIR rises from the original value of 9.0 dB to an estimated value of approximately 14.5 dB for a = 2 (twice the spacing) and

becomes asymptotic to approximately 16 dB as the carrier spacing "a" becomes very large. This result is shown in Fig. 1 below:

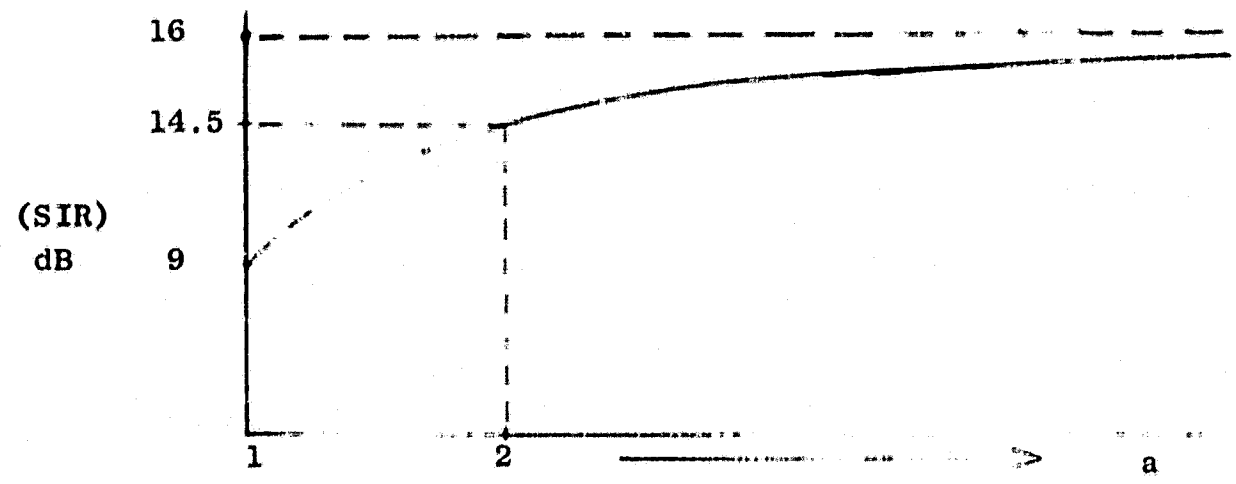


Fig. 1
SIR as a Function of a

The curve in Fig. 1 can be expressed by an equation

$$(SIR)_{dB} = 16 - \frac{7}{a^{2.3}}$$

or expressing SIR as a fraction

$$SIR = \frac{40}{10^{(0.7/a^{2.3})}} \qquad \ldots\ldots\ldots\ldots\ldots \quad (6)$$

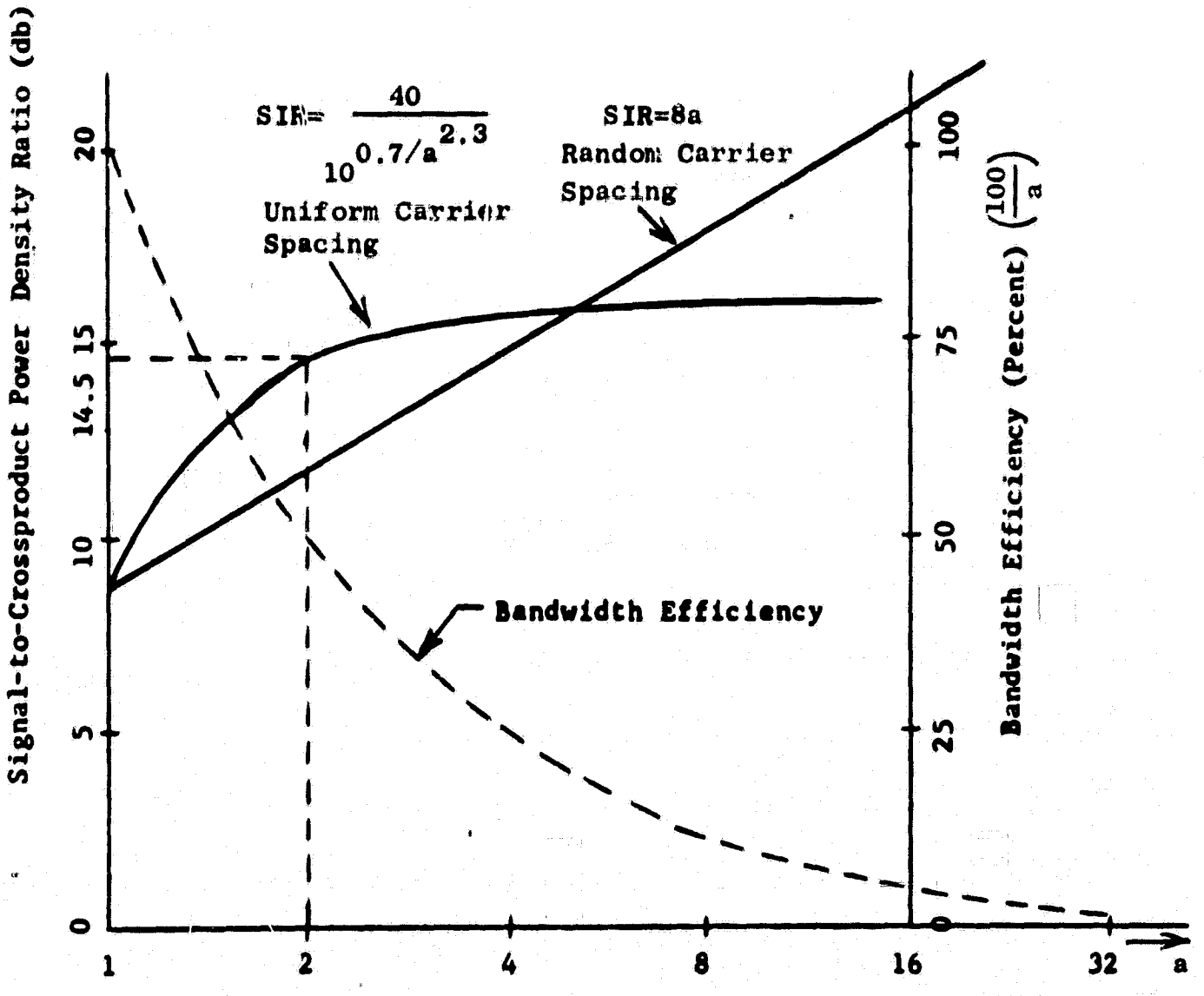
The two equations for the signal-to-intermodulation product density ratio viz

$$SIR = 8a \text{ -- corresponding to random access selection} \qquad \ldots\ldots\ldots\ldots\ldots \quad (5)$$

and

$$SIR = \frac{40}{10^{0.7/a^{2.3}}} \text{ -- corresponding to uniform channel spacing} \qquad \ldots\ldots\ldots\ldots\ldots \quad (6)$$

are plotted in Fig. 2. It can be seen that in the range of a between 1 and 5 which represents a bandwidth utilization of 100% to 20%, it is preferable to space the carriers uniformly (eq(6)). At lower bandwidth utilization factors ($a > 5$) a random distribution of carriers appears preferable.



Parameter "a"
Representing carrier spacing factor when spacing is uniform or total bandwidth wastage when spacing is random.

Fig. 2. Summary of signal-to-crossproduct power density ratio estimates and bandwidth efficiency as a function of the carrier spacing parameter (bandwidth wastage parameter) "a".

C. Peak to Average Signal Power Ratio

The peak-to-average power ratios for various waveforms are shown in Table 1.[7]

Table 1

WAVEFORM PEAK-TO-AVERAGE POWER CHARACTERISTICS

Distribution	Waveform	Peak-to-Average Power Ratio		Peak Definition
		Value	db	
Delta	Square wave	1	0	Natural
Sinusoid	Sine wave test tone	2	3	Natural
Uniform	Carefully companded	3	4.8	Natural
Gaussian	Gaussian noise, Multichannel baseband	10.9	10.4	Exceeded 0.1 percent
Speech	Single talker	63	18	Exceeded 0.1 percent

Of particular interest in our study is the case of a single speech channel since one of the applications of interest is a small satellite ground station which serves one user only.

As can be seen from Table 1, speech is characterized by very high peak to average ratio. We will assume in our study that by means of instantaneous companding a uniform distribution is approached and will accept a peak to average ratio of 6 dB for individual speech channels.

Where more than one speech channels are combined in the baseband, the multi-channel peak factor varies depending on the number of channels. Values of approximately 10 to 13 dB have been used in practice.

The significance of the peak factor in our study relates primarily to the problem of bandwidth occupancy by the transmitted rf signal. We have

shown in the preceding section that with FDM access and hard limiting transponders, the signal-to-intermodulation power density ratio depends on the separation of carriers.

In an fm system the rf bandwidth of the channel must be engineered to accommodate signal peaks which occur rather infrequently. Hence, on the average the portion of rf bandwidth occupied by the signal spectrum will be substantially smaller than the total allocated bandwidth. However, the intermodulation products and noise are assumed to be uniformly distributed throughout the transponder bandwidth. Accordingly the signal to intermodulation product ratio in the channel bandwidth will be degraded by the ratio of "peak-to-rms bandwidth' which is equal to the peak factor of the modulating waveform.

For example, if we assume a 6 dB peak factor for the instantaneously companded speech, the rms rf signal spectrum will occupy only 1/4 of the total bandwidth provided and the rms signal-to-intermodulation noise ratio will be 6 dB below the peak value.

Thus for fm speech transmission through a frequency-division-multiple access system utilizing hard limiters, the SIR as expressed by equations (5) and (6) has to be modified to read

$$SIR = 8a \cdot \frac{1}{(PF)} \qquad \text{.....} \qquad (5a)$$

$$SIR = \frac{40}{10^{0.7/a^{2.3}}} \cdot \frac{1}{(PF)} = 10 \left[1.6 - \left(\frac{0.7}{a^{2.3}}\right)\right] \cdot \frac{1}{(PF)} \qquad (6a)$$

where (PF) represents the peak factor of the information waveform and its value depends upon the characteristics of the information transmitted, the modulating techniques, and equipment design.

IV DETERMINATION OF THE ACCESS CAPACITY OF AN ACTIVE SATELLITE SYSTEM WITH A HARD LIMITING TRANSPONDER

A general formula for the channel capacity of an active satellite system when frequency division multiple access to the satellite is used will now be derived.

The formula is applicable to linear and hard limiting transponders and permits the determination of the total number of individual accesses that can be handled by the system.

The value of signal-to-noise ratio in bandwidth B at the input to the receiver (referred to the output of the satellite antenna) is given by

$$(SNR)_S = \frac{S}{(I + N + N_3 L)\ B} \qquad \ldots\ldots\ldots\ldots \qquad (7)$$

This value must exceed or at least be equal to the (SNR) specified by system operating requirements.

$$\therefore \quad (SNR)_S \geq (SNR)$$

$$\therefore \quad \frac{1}{(SNR)} \geq B\left(\frac{I}{S} + \frac{N}{S} + \frac{N_3 L}{S}\right) \qquad \ldots\ldots\ldots\ldots \qquad (8)$$

where I is the intermodulation power density

N is the retransmitted uplink noise density

N_3 is the ground receiver noise density ($=kT_3$)

L is the net loss from the output of the satellite transmitting antenna to the input of ground station front end

$L=L_D/G_3$ (L_D is the free space down link loss and G_3 is the gain of the receiving antenna)

B is the receiver rf bandwidth

S is the effective radiated signal power per access from the satellite

SNR is the required signal-to-noise ratio at the input to the receiver.

Now

$$(SNR)B \leq \frac{S}{(I + N + N_3 L)} \qquad \ldots\ldots\ldots\ldots \qquad (9)$$

Let the carrier-to-noise density ratio be

$$R = (SNR)B \qquad \text{..... (10)}$$

Inverting (9) and (10), we obtain

$$\frac{1}{R} \geq \frac{I}{S} + \frac{N}{S} + \frac{N_3 L}{S} \qquad \text{..... (11)}$$

The value of $\frac{S}{I}$ represents the total signal-to-cross modulation power density and can be computed from equation (5) or (6) using the relation

$$\frac{S}{I} = B \cdot SIR \qquad \text{..... (12)}$$

The value of $\frac{S}{N}$ which represents the ratio of signal power-to-retransmitted noise density can be calculated from the fact that N arises from the noise temperature of the satellite receiver kT_2. Further, it has been shown in the literature that for a reasonable number of carriers of approximately equal power the signal to noise ratio of each signal at the output of a hard limiter is reduced by approximately 1 dB from that at the input while the signal-to-signal ratios are preserved.*

Thus $$\left(\frac{S}{N}\right)_{out} = \left(\frac{S}{N}\right)_{in} \cdot \frac{1}{1.26} \qquad \text{..... (13)}$$

Let $$X = \frac{S}{(I + N)B} \qquad \text{..... (14)}$$

represent the output SNR from satellite. Hence from (9)

$$\frac{1}{SNR} \geq \frac{1}{X} + \frac{N_3 LB}{S} \qquad \text{..... (15)}$$

Transposing

$$\frac{N_3 LB}{S} < \frac{1}{SNR} - \frac{1}{X} \qquad \text{..... (16)}$$

---

* This result is the same as in the case of strong noise controlling the limiter and one signal, since to any one signal the other signal powers can be considered as noise. It is of interest to consider the situation when one of the p carriers at the input to the limiter is substantially stronger than the others and controls the limiter. This may be representative of a jamming situation. It has been shown that under limiting conditions ($S/N_m \rightarrow \infty$) the strong signal to noise ratio at the output increases by 3 dB while the output signal-to-noise ratio of the remaining (p-1) weak signals decreases by 3 dB.

Now X, the ratio of signal power output to the sum of the intermodulation power plus the internal noise power is independent of the absolute value of signal power S since it is determined prior to power amplification and is fixed by the design of the transponder. Also, the value of SNR at the input to the receiver is specified as a requirement. Thus, only in the term $\frac{N_3LB}{S}$ of (16) must the absolute value of S be known.

Note that X represents the total interference power and includes the power (I) generated internally in the satellite, due to nonlinearities of the transponder, and the power (N) picked up by the satellite receiver (input SNR). Thus by proper choice of the form of equations for I and N, X can be made to include the effects of up-link jamming and can also represent any case of FDM access even when the input signals are not equal in power. In such a case the output signal S will include the effects of suppression of each individual signal and will therefore be represented by the sum

$$S_{out} = \sum_{j=1}^{m} S_j \alpha_j$$

where α_j represents the reduction of the power in jth signal relative to that at the input to the satellite. In a similar manner, the intermodulation crossproduct total power ratio S/I may be computed by selecting a proper formula for I. Accordingly, equation (16) represents the general case.

Since from (14),

$$\frac{1}{X} = \frac{(I + N)B}{S}$$

we can rearrange equation (16) as follows:

$$\frac{IB}{S} \leq \frac{1}{SNR} - \frac{NB}{S} - \frac{N_3LB}{S} \qquad \text{.....} \qquad (17)$$

or $$S \geq \frac{N_3 LB}{\frac{1}{SNR} - \frac{NB}{S} - \frac{IB}{S}} \qquad \text{..... (18)}$$

where $\frac{S}{IB}$ is a function of "a" given by either equations (5) or (6) or any other appropriate relationship

$\frac{S}{NB}$ represents the ratio of the signal-to-reradiated noise power (which is a function of the uplink SNR)

$\frac{S}{N_3 LB}$ represents the down-link signal to noise ratio for the case that all satellite transmitted power is in the signal (ideal case)

SNR represents the required signal to noise ratio at the input to the receiver and is specified.

From the discussion in the preceding paragraph, we know that $\frac{IB}{S}$ is a function of the bandwidth utilization factor "a" (given by equations (5) or (6)). Thus from equation (17), we can calculate the relationship between "a" and S under the constraint of operation above threshold. Similarly if the value of "a" is given, the required signal power can be computed from (18). Since the factor "a" is a measure of the required bandwidth, equation (18) represents a trade-off between bandwidth and power requirements. To illustrate this point, assume that equation (5) is used.

$$\frac{S}{IB} = 8a$$

Also from (1), $a = \frac{A}{B}$

where A is the required bandwidth per access.

$$\therefore \quad \frac{S}{IB} = \frac{8A}{B}$$

Substituting into (18)

$$S \geq \frac{N_3 LB}{\left(\frac{1}{SNR} - \frac{NB}{S}\right) - \frac{B}{8A}} \qquad \text{..... (19)}$$

or $$\frac{1}{S} \leq \frac{\left(\frac{1}{SNR} - \frac{NB}{S}\right)}{N_3LB} - \frac{B}{8N_3LBA} \qquad \text{..... (20)}$$

$$\frac{1}{S} + \frac{1}{AK_1} \leq K_2 \qquad \text{..... (21)}$$

where $K_1 = 8N_3L$

$$K_2 = \frac{\left(\frac{1}{SNR} - \frac{NB}{S}\right)}{N_3LB} \qquad \text{..... (22)}$$

Multiplying by S

$$1 + \frac{S}{AK_1} \leq SK_2 \qquad \text{..... (23)}$$

$$SK_2 - \frac{S}{AK_1} \geq 1 \qquad \text{..... (24)}$$

$$S\left[K_2 - \frac{1}{AK_1}\right] \geq 1 \qquad \text{..... (25)}$$

Thus as the bandwidth A increases, the power S increases. If the cost of power S and the cost of bandwidth could be independently established, it would then be possible to optimize the relationship between S and A by minimizing the total cost functions. From the corresponding value of A, the optimum value of the factor "a" could be deduced, since

$$a_{opt} = \frac{A_{opt}}{B} \qquad \text{..... (26)}$$

If we now look at the total power per access (P_T) which the satellite must radiate rather than on the signal power per access (S), we have the following:

The total radiated power per access P_A is

$$P_A = S + (I + N)Ba$$

but $\frac{S}{(I + N)B} = X$ by definition

$$\therefore \quad P_A = S\left(1 + \frac{a}{X}\right) \qquad \text{.....} \qquad (27)$$

Substituting the minimum value of S from (18) into (27), we obtain

$$P_A = N_3 LB\left(1 + \frac{a}{X}\right)\left(\frac{1}{\frac{1}{SNR} - \frac{1}{X}}\right) \qquad \text{.....} \qquad (28)$$

Thus for any value of "a", equation (28) represents the minimum required total satellite ERP per access. The minimum required bandwidth per access for this value of "a" is from equation (1):

$$A = aB \qquad \text{.....} \qquad (29)$$

Thus the minimum value of total ERP per cycle of access bandwidth is

$$\gamma = \frac{P_A}{A} = N_3 L\left(\frac{1}{a} + \frac{1}{X}\right)\left(\frac{1}{\frac{1}{SNR} - \frac{1}{X}}\right) \qquad \text{.....} \qquad (30)$$

Equation (30) requires that (SNR)$<$X to obtain positive values of γ. The optimum value of γ could be obtained by substitution of a_{opt} from equation (26) into (3), remembering that X is a function of a.

$$\gamma = \frac{P_A}{A} = \frac{pP_A}{pA} = \frac{P_T}{W^*} \qquad \text{.....} \qquad (31)$$

where P_T is the total satellite ERP and W* is the minimum total transponder bandwidth required.

Let p = total number of accesses

W = available transponder bandwidth

$$p = \frac{W}{aB} = \frac{W}{P_T} \cdot \frac{P_T}{aB} = \frac{P_T}{\gamma aB} \qquad \text{.....} \qquad (32)$$

Also

$$p = \frac{P_T}{P_A} = \frac{P_T}{W} \cdot \frac{W}{P_A} = \gamma \frac{W}{P_A} \qquad \text{.....} \qquad (33)$$

Thus the total number of accesses can be calculated in terms of γ when P_T is specified, (equation 32), or when W and P_A is specified (equation 33).

To complete formula (23), let us now substitute system parameters.

We had $$\frac{1}{X} = \frac{IB}{S} + \frac{NB}{S} \qquad \ldots\ldots\ldots\ldots \qquad (34)$$

$\frac{S}{BI}$ can be calculated from any appropriate formula for the intermodulation power in a hard limiting satellite transponder.

$\frac{S}{NB}$ represents the retransmitted uplink SNR and is assumed to be one dB less than the input SNR. (See equation (13) for an explanation.)

But in terms of system parameters

$$(SNR)_{in} = \frac{(ERP)_1 \cdot G_{2R}}{L_u \cdot \propto} \cdot \frac{1}{kT_2B} \qquad \ldots\ldots\ldots\ldots \qquad (35)$$

$$(SNR)_{in} = \frac{(ERP_1)}{B} \cdot \frac{1}{M} \qquad \ldots\ldots\ldots\ldots \qquad (36)$$

where $$M = \frac{T_2}{G_{2R}} \cdot kL_u \propto \qquad \ldots\ldots\ldots\ldots \qquad (37)$$

and L_u is the net uplink space loss (between transmitting and receiving antennas).

The constant M is therefore determined by the design of the satellite receiving system and the uplink space loss. The term $\frac{(ERP_1)}{B}$ represents the total effective power radiated by the transmitting ground terminal per cycle of rf signal bandwidth and can therefore be used as a parameter.

Let $$P_1 = \frac{(ERP)_1}{B} = \frac{(ERP)_1}{2b(m+1)} \qquad \ldots\ldots\ldots\ldots \qquad (38)$$

Thus $$\frac{1}{X} = \frac{IB}{S} + 1.26 \frac{M}{P_1} \qquad \ldots\ldots\ldots\ldots \qquad (39)$$

Substituting into (30), we obtain

$$\gamma = \frac{kT_3 L_D \beta}{G_3} \left[\frac{I}{a} + \left(\frac{IB}{S} + 1.26\,\frac{M}{P_1}\right)\right] \left[\frac{1}{\frac{1}{(SNR)_{in}} - \left(\frac{IB}{S} + 1.26\frac{M}{P_1}\right)}\right] \quad \ldots (40)$$

Now substituting (40) into (32) or (33), the total number of accesses can be computed depending on whether the power or the bandwidth are the limiting considerations.

An alternative approach for the power limited case (which is the predominant case with today's state-of-the-art) is to substitute equation (28) into

$$p = \frac{P_T}{P_A}$$

Hence

$$p = \frac{P_T}{BLN_3} \left[\frac{\frac{1}{SNR} - \frac{1}{X}}{1 + \frac{a}{X}}\right] \quad \ldots\ldots\ldots\ldots \quad (41)$$

Substituting (38) and (39) into (41), we obtain

$$p = \frac{P_T}{B} \cdot \frac{G_3}{T_3} \cdot \frac{1}{kL_D\beta} \left[\frac{\frac{1}{SNR} - \left(\frac{IB}{S} + 1.26\,\frac{M}{P_1}\right)}{1 + a\left(\frac{IB}{S} + 1.26\,\frac{M}{P_1}\right)}\right] \quad \ldots\ldots\ldots\ldots \quad (42)$$

where

p = total number of accesses

P_T = total satellite ERP

SIR = signal to intermodulation power ratio in bandwidth B

a = bandwidth wastage factor $\frac{W}{pB}$

M is defined by (37)

P_1 is defined by (38)

$\frac{G_3}{T_3}$ is the gain to system noise temperature of the receiving ground station

G_{2R} is the gain of the satellite receiving antenna

L_D is the net down-link loss (between antennas) = $L \cdot G_3$

β represents miscellaneous losses associated with the receiving system.

B = rf signal bandwidth per access.

Equation (42) represents a general case. For the case of fm modulation of analog signals and FMFB receivers, we have from conventional fm theory

$$B = 2b(m+1)$$

In Appendix K we have decided, for practical reasons, to increase this bandwidth to

$$B = 2.3b(m+1) \qquad \ldots\ldots\ldots\ldots \qquad (43)$$

$$(SNR)_{in} = (SNR)_{out} \frac{1}{3m^2(m+1)} \qquad \ldots\ldots\ldots\ldots \qquad (44)$$

Substituting into (36), we obtain

$$p = \frac{P_T}{B} \cdot \frac{G_3}{T_3} \cdot \frac{1}{kL_D\beta} \left[\frac{\frac{3m^2(m+1)}{(SNR)_{out}} - \left(\frac{1}{SIR} + 1.26 \frac{M}{P_1} \right)}{1 + a\left(\frac{1}{SIR} + 1.26 \frac{M}{P_1} \right)} \right] \qquad \ldots\ldots\ldots\ldots \qquad (45)$$

Also from (29)

$$p = \frac{W}{aB} = \frac{W}{2ab(m+1)} \qquad \ldots\ldots\ldots\ldots \qquad (46)$$

where m is the fm deviation ratio (chosen to ensure that FMFB threshold is exceeded as discussed in Appendix K).

$(SNR)_{out}$ is the required SNR at the output of the receiver in bandwidth b.

V ACCESS CAPACITY OF AN ACTIVE SATELLITE WITH LINEAR TRANSPONDER

All equations derived in the previous section are valid provided the signal-to-intermodulation distortion ratio SIR or $\left(\frac{S}{IB}\right)$ approaches infinity or the intermodulation power density I approaches 0.

Thus $\frac{S}{I} \longrightarrow \infty$

$\frac{I}{S} \longrightarrow 0$

$I \longrightarrow 0$

also in all equations for total power a=1.

Thus the pertinent formulae are as follows:

(13) becomes $\left(\frac{S}{N}\right)_{out} = \left(\frac{S}{N}\right)_{in}$ ..... (47)

(18) becomes $S \geq \frac{N_3 LB}{\frac{1}{SNR} - \frac{NB}{S}}$ ..... (48)

(28) becomes $P_A = \frac{N_3 LB}{\frac{1}{SNR} - \frac{NB}{S}}$ ..... (49)

(29) becomes $A = B$ ..... (50)

The total number of accesses is

$$p = \frac{P_T}{B} \cdot \frac{G_3}{T_3} \cdot \frac{G_{2T}}{kL_D\beta} \left[\frac{\frac{1}{SNR} - \frac{M}{P_1}}{1 + \frac{M}{P_1}}\right] \quad \text{..... (51)}$$

References

1 See, for example, J. L. Sevy, "The Effect of Multiple CW and FM Signals Varied Through a Hard Limiter on TWT," IEEE Transactions on Communication Theory, Vol. COM-14, No. 5, Oct. 1966.

2 C. R. Cahn, "Crosstalk Due to Finite Limiting of Frequency Multiplexed Signals," Proceedings IRE, Jan 1960.

3 J. J. Lows, "Output Signal to Crossproduct Ratio for Hard Limited Equal Strength Signals," Philco Ford Communication Sciences Dept., Tech Memo, Dec 20, 1966.

4 M. Gyi, "Some Topics on Limiters and FM Demodulators," Stanford University Report SEL-65-056, July 1965.

5 P. D. Shaft, "Intermodulation Interference in Frequency Division Multiple Access," Stanford Research Institute paper, 1966.

6 L. Schuchman, T. T. Jones, Philco Ford Report TM-115, Contract AF 30(602)-4392, Feb 1967, "Error Rate Analysis of M'ary Transmitted Reference Systems.....," Appendices D and E.

7 Table 1 was taken from Rand Corp. Memo RM-4997-NASA (NASr-21(02)), p. 71.

APPENDIX N

APPROXIMATE COST OF LARGE GROUND BASED REPEATER STATION

APPROXIMATE COST OF LARGE GROUND BASED REPEATER STATION

The objective of this study is to determine the approximate cost of ground based repeater used with a double-hop passive satellite system. The repeater receives the communication signals generated by various users and reflected by the passive reflector in orbit. The entire band containing these signals is amplified by low noise parametric amplifiers, translated in frequency into the transmitting frequency band and retransmitted by high power klystron amplifiers. The individual signals are not demodulated during this process, the repeater simply acting as a frequency changing amplifier. This implies that no system management functions such as switching, supervision, etc., are performed at the repeater. The reason for this assumption was to maintain a fair basis of comparison with an active system, which does not utilize a ground repeater and cannot therefore perform such functions.

Since we are primarily interested in the power and bandwidth capabilities of the ground repeater, we will consider four major subsystems.

a) antenna subsystem

b) low noise front end

c) electronics

d) power amplifier

These subsystems are discussed below.

1. Antenna Subsystem

The antenna subsystem was considered in detail in Appendices D, E, F, and G. These studies have resulted in the estimates of antenna performance and costs which are summarized respectively in Table 10 of Technical Note D and Fig. 3 of Appendix F. Accordingly these results will be used and no further discussion of antennas will be undertaken.

2. Low Noise Front Ends

The state of the art of low noise front ends is advancing rapidly and relevant data has been published in technical literature. Discussions with several manufacturers, who in most cases wished to remain unidentified, have resulted in the general agreement that presently achievable bandwidth with parametric amplifiers of 500 MHz in the X band range could be extended up to 1 KMHz by 1970. The noise temperature of these amplifiers will be maintained at approximately 25°K which is presently obtainable. Additional R&D on maser front ends would permit the extension of presently achievable bandwidth of 150 MHz to possibly 500 MHz with the presently achievable noise temperature of 10° being maintained.

We will assume therefore for purposes of our study that parametric preamplifiers with a bandwidth of 500 MHz and noise temperatures of approximately 25° can be made available for use with the ground repeater station without additional R&D.

A survey of literature and additional discussions with manufacturers indicate that the cost of parametric amplifiers is approximately $50000 to $60000 for a 50° temperature. Using estimates supplied by Comsat Corporation[1] and a graph of cost versus noise temperature published in a recent study for NASA[2], we have developed the following relation for the cost of parametric amplifiers as a function of noise temperature.

$$\$ \text{ of single unit} = \frac{1800000}{T^{0.9}} \qquad \ldots\ldots\ldots\ldots \qquad (1)$$

where T is the receiver noise temperature in degrees Kelvin. This formula yields the following values which appear to reasonably represent the existing situation.

Temp ^{o}K	Approx Cost of Single Unit
25	$98,000
50	$53,000
100	$20,000

The bandwidth provided by these paramps is estimated at 500 MHz.

3. Electronics

Under this group of equipment are included all subsystems other than front ends and high power transmitters (such as tracking electronics, frequency supply, modulator/exciters and boresight facilities including test equipment). Our cost estimates are based on data supplied by Comsat Corp., RCA Victor Ltd and other manufacturers of stations in 85 to 100 ft range, and on the published data for Goldstone 210-foot antenna installation. For small stations the first costs of electronics supplied by various manufacturers are in fairly good agreement with Comsat Corporation's estimates and are shown below.

Table 1

Item	Estimated Costs in Thousands $		
	High	Low	Average
Tracking electronics and drive system	400	300	350
Receivers, modulators, demodulators, etc.	600	400	500
Boresight facility	150	75	112
Test equipment	400	200	300
TOTAL	1550	975	1212

The published cost of "electronics" at the Goldstone facility[3] (210-foot antenna) is $3.1 million. Since this overall figure was not itemized, no breakdown comparable to that in Table 1 was available. However, since the Goldstone figures included the cost of preamplifiers and power transmitter, we can compare it to the costs of 85-foot stations by adding the estimated costs of these two items to the totals in Table 1. The range of estimates for these two items in a commercial 85-foot station was:

	High	Low	Average
Paramps and power amplifiers	$700K	$500K	$600K

Since for comparable power output and paramp temperature the cost of these items is not dependent upon the size of the station, we could assume that the cost of electronics at Goldstone excluding these two items is approxi ately 2.5 million dollars (3.1 - 0.6).

Again to the first approximation it could be assumed that only one half of the total cost of items listed in Table 1 should be dependent upon the size of the antenna. This implies that approximately $600K could be considered as a constant cost regardless of the antenna size. Consequently variable costs are

In 85-foot station = 0.6 million

210-foot station = 1.9 million (2.5 - 0.6)

Thus the following approximate formula can be adopted:

Cost of electronics = $0.63(1+D/100)$ million dollars ..... (2)

It is evident that equation (2) is only an approximate indicator. However, because of the fact that for large installations this item constitutes only a relatively small percentage of the total cost, it is sufficient for our purposes. To obtain a more accurate estimate would be very difficult because of the scarcity of cost data on large antenna installations and because of the "custom made" aspect of such costs which often result in expenditures substantially above what could be considered reasonable. (example--Greenbank)

4. Facilities

In a similar manner we can compare the published cost of "facilities" at Goldstone of $2.5 million and the average figure for the cost of buildings and site improvements for 85-foot installations, which averages approximately 0.95 million dollars. Relating the cost ratio to the size of antenna to obtain an indicator, we get

$$\text{Cost of facilities} = \left(\frac{D}{100}\right)^{1.25} \text{ millions of dollars} \quad \ldots\ldots\ldots \quad (3)$$

The cost of land is not included in this equation.

5. Start-up Costs

The remaining items relate to costs of all items associated with getting the station operational. These costs include the items listed below together with the high and low estimates used by Comsat Corporation for 85-foot stations.

Item	High Cost	Low Cost	Average
Site surveys and improvements	$ 550	$210	
Architect and engineering	225	20	
Spares	360	160	
Technician training	150	75	
Documentation	100	50	
Initial program mangement and engineering	300	10	
Total in thousands	$1685	$525	$1105

We will assume that these costs remain relatively constant with the size of the installation and will use

$$\text{Start-up Cost} = \$1.1 \text{ million} \qquad \ldots\ldots\ldots\ldots \qquad (4)$$

as an indicator.

6. Summary

Using expressions (1), (2), (3), and (4) and the expression derived in Appendix H for the cost of power transmitter, we obtain the expression for the total cost of station C_T in millions of dollars

$$C_T = C_A + n\left(\frac{1.8}{T^{0.9}}\right) + 0.63\left(1 + \frac{D}{100}\right) + \left(\frac{D}{100}\right)^{1.25} + 1.1 + \left[75(m+k)\left(\frac{P}{k}\right)^{0.63} + 50(P)^{0.63}\right]10^{-6} + C_L \qquad \ldots\ldots\ldots\ldots \qquad (5)$$

where

1st item (C_A) represents the antenna cost (see Appendix F, Fig. 3))

2nd item represents the cost of n paramps with noise temperature $T^{\circ}K$

3rd item represents the cost of electronics

4th item represents the cost of facilities

5th item represents the start-up costs

6th item (bracket) represents the total cost of the power subsystem of P watts composed of k power amplifiers. (The first item is the cost of klystrons, the second item is the cost of the D.C. supply and start-up cost.) m represents the number of klystrons provided for each operating unit (hot standby, etc.).

7th item (C_L) represents the cost of land.

It is apparent that only a gross estimate can be obtained from the above formula since the actual costs will depend on the geographical locations, climatic environment, operating environment, etc., and similar factors which cannot be accurately predicted. However, because of the limitations on the scope of our study, expression (5) will be used in our work.

7. Annual Operations and Maintenance Cost

The annual operating and maintenance costs are dependent on many items such as number of personnel operating the station, utility bills, spares, inventory replacements, factors associated with the geographical location (transportation, recreation, etc.) repairs, etc.

Comsat Corporation assumes the following values[4] for operations and maintenance costs for receiving stations.

	% Per Year of Initial Cost
Antennas	5
Buildings	5
Cooled paramps	25
Other electronic devices	20

We will accept these figures and extend them as follows.

Table 2

Annual Operating and Maintenance Costs

Item	% Per Year of Initial Cost
Antenna	5%
Facilities	5%
Cooled paramps	25%
Power amplifier tubes	20%
Other electronic devices	20%

Thus the annual O&M costs can be expressed as follows:

$$C_{OM} = .05\ C_A + 0.05\left(\frac{D}{100}\right)^{1.25} + 0.25\left[\frac{1.8n}{T^{0.9}}\right] + 0.20\left[0.63\left(1 + \frac{D}{100}\right) + \frac{75}{10^6}\,(m+k)\left(\frac{P}{k}\right)^{0.63} + \frac{50}{10^6}\,p^{0.63}\right] \qquad (6)$$

Equation (6) will be used in our study to represent the annual cost of operation and maintenance of the ground-based repeater.

References

1 Comsat Corp. Tech Memo SAD-9-66.

2 "Technical and Cost Factors that Affect Television Reception from a Synchronous Satellite,' by Atlantic Research Corp., Contract NASW-1305, June 1966, Fig. 3.3.3.

3 P.D. Potter, et al, "Big Antenna Systems for Deep Space Communications," Aeronautics and Astronautics, Oct 1966.

4 "Economic Comparison of Alternative Domestic Satellite TV Distribution Systems," by R. Swensen, et al, Report SAD-9-66, Dec 1966.